UNION CARBIDE CORPORATION
CHEMICALS AND PLASTICS
RIVER ROAD, BOUND BROOK, N. J. 08805 · TELEPHONE (201) 356-8000

August 30, 1979

Dr. James E. McGrath
Department of Chemistry
Virginia Polytechnic Institute
and State University
Blacksburg, Virginia 24060

Dear Jim:

My apologies for missing the Ph.D. dissertation committee for Andy Wnuk but, as you know, my flight was grounded for more than three hours at Newark thus making it impossible to attend even part of the session.

I've read the entire Ph.D. thesis of Andy's and consider it to be of excellent quality. The conclusions reached in his thesis were concise and correct to the best of my ability to judge. The quantity of work was more than adequate for a Ph.D. research project; in fact, would be the equivalent of two thesis projects at many universities. His work in constructing a unique impact tester and correlating the impact characteristics of various polymers was an outstanding piece of work, demonstrating an ability not commonly found even in Ph.D.'s.

As I had stated previously, the questions I had submitted as part of Andy's doctoral examination were answered better than I had expected; and the personnel I shared the results with here at UCC were quite impressed.

In summary, Andy had done a super job in preparing for a doctoral both in obtaining basic knowledge in polymer science and in reducing it to practice in his thesis work. I extend my congratulations to him and wish him well in his future career. Obviously, the polymer science program you have assembled at VPI contributed significantly to that; and, if the quality of work demonstrated by Andy continues, the polymer science program at VPI will be quickly rated as the best available.

Sincerely,

L. M. Robeson

LMR/tcr

ENGINEERING PROPERTIES OF MULTIPHASE BLOCK COPOLYMERS

by

Andrew J. Wnuk

Dissertation submitted to the Graduate Faculty of the

Virginia Polytechnic Institute and State University

in partial fulfillment of the requirements for the degree of

DOCTOR OF PHILOSOPHY

in

Materials Engineering Science

APPROVED:

James E. McGrath, Chairman

Thomas C. Ward

James P. Wightman

Lloyd M. Robeson

Walter R. Hibbard, Jr.

August 29, 1979

Blacksburg, Virginia

TO MY PARENTS

Acknowledgements

The author is pleased to express his appreciation to Dr. James E. McGrath for his friendship and guidance during the past three years. He is also grateful to Dr. McGrath for reviewing and strengthening this dissertation. Special thanks are due to Dr. Thomas C. Ward who worked closely with the author on much of the work presented here. Appreciation is also extended to Drs. James P. Wightman, Walter R. Hibbard, Jr., and Lloyd M. Robeson for their willingness to serve on the graduate committee.

Several members of the VPI & SU staff made essential contributions to this research. The aid of and with the electronic and mechanical aspects of the falling weight impact tester is gratefully acknowledged. The author would also like to recognize the efforts of who patiently spent many hours of his time at the Rheovibron and Rheogoniometer. Finally, the author wishes to thank for typing the rough draft and for typing the final manuscript.

Table of Contents

List of Figures

List of Tables

I. Introduction

Multiphase polymer systems have received widespread attention in recent years, especially since the rate of appearance of new polymer types has diminished considerably. The new multiphase materials may be obtained in the form of blends, block and graft copolymers, or 'interpenetrating' networks, all of which are characterized by the presence of two or more polymeric phases in the solid state. Such materials are, therefore, distinguished from composite materials which include fiber and particulate filled thermoplastics and thermosets. The considerable number of recent collective works[1-5], dealing with multiphase polymer systems, attests to their growing impact on current materials technology.

Within the last decade, the poor economics of new polymer and copolymer production, coupled to the need for new cost effective materials for specific applications, has generated wide interest in polymer blends or alloys.[6] Unfortunately, most homopolymer pairs are immiscible with one another and give rise to low strength materials due to the lack of interfacial adhesion between the separate phases. Block and graft copolymers, while being more expensive than simple blends and certainly more restricted in their range of composition, do offer several advantages over blends. First, the different segments are covalently bonded together, thereby eliminating the interface problem. Second, the molecular architecture can be accurately controlled, especially in the case of anionically prepared systems. Third, block or graft copolymers can be used to strengthen blends of immiscible polymers by serving as physical connections between the phases, thus

improving the interfacial adhesion and load transferring capability of the components.[7]

Block and graft copolymers themselves undergo phase separation under certain conditions, but on a much smaller scale than that which occurs in heterogeneous blends. The term microphase separation has been used to describe this phenomena. Microphase separation has been exploited commercially in the form of impact modified thermoplastics and thermoplastic elastomers. The impact thermoplastics such as ABS or impact polystyrene contain graft copolymers, whereas the thermoplastic elastomers are usually linear block copolymers. More will be said about these materials in a later section. Both types consist of either amorphous or semicrystalline segments coupled to elastomeric segments, the ultimate properties depending upon the weight fractions of the components, their distribution in the solid state, and, of course, the individual chain properties.

Very little attention has been paid to block copolymers consisting of two rigid amorphous components, probably since no exciting phenomena can be predicted for such systems. However, the fact that synergetic effects have been observed in certain blends, for example those of poly (phenylene oxide) (PPO) and polystyrene,[8] makes such a study more intriguing.

In this study, multiblock copolymers of bisphenol-A polycarbonate (I) and several aromatic polysulfones (II) were prepared from previously synthesized oligomers. The structure of bisphenol-A polysulfone is depicted when x in II is replaced by the isopropylidene group.

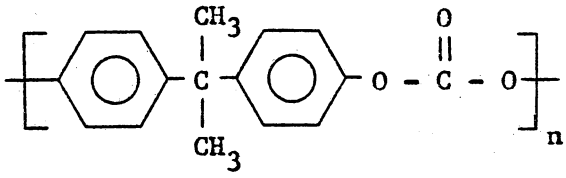

(I)

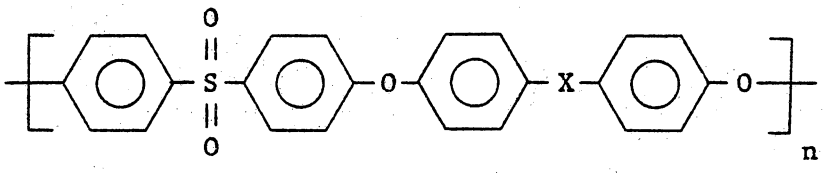

(II)

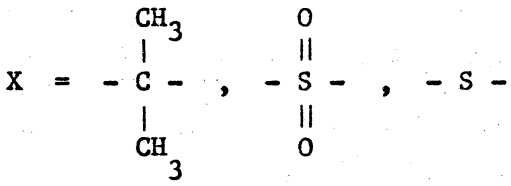

Bisphenol-S and bisphenol-T polysulfone are represented when x is replaced by the sulfone and thio groups respectively. The two polymer types were chosen for the reasons provided below.

a. Both homopolymers are important commercial materials. They are the leading examples of tough, ductile, amorphous thermoplastics.

b. Both homopolymers can be prepared with phenolic end groups which facilitate copolymerization.

c. Both homopolymers are amorphous and dissolve in similar solvents. Thus, solution characterization of the oligomers and block copolymers is possible in the same solvents.

d. The bisphenol units in each homopolymer can be the same or varied to provide a range of properties and solubility characteristics.

e. No interchange reactions occur between the components at high temperatures, thereby allowing the copolymers to be molded using the same techniques required for the homopolymers.

The overall goal of preparing, characterizing, and testing polysulfone/polycarbonate block copolymers was carried out with the following two questions in mind:

(1) What chemical and physical parameters govern microphase separation in the polysulfone/polycarbonate system and how can they be assessed?

(2) How do the properties of these block copolymers change as the morphology procedes from a single phase to a multiphase system?

A wide variety of existing characterization tools were employed to obtain answers to the above questions. In addition, a new technique for analyzing the phenolic end groups of polysulfone was developed during the course of this investigation. Also, a novel type of falling weight impact tester was designed and constructed in order to evaluate the toughness of the new copolymers. Both of these developments will be described in detail in subsequent sections.

II. Literature Review

The scope of this investigation was broad and involved many aspects of polymer synthesis and characterization. In order to acquaint the reader with many of the terms to be used in subsequent sections, this review begins with a general discussion of copolymer types and properties followed by brief descriptions of the prominent theories of polymer-polymer compatibility and microphase separation. Since this study is concerned with rigid amorphous block copolymers, a section covering previous work in this area is also included followed by a detailed review of the synthesis, properties, and various block copolymers of polycarbonate and polysulfone.

A major portion of this writer's efforts were directed towards the design and application of an instrumented falling weight impact tester. For this reason, a discussion of conventional and instrumented impact test methods is also included in the final section of this review.

A. General Aspects of Copolymers

1. Random Copolymers. Random copolymers represent the simplest means of combining two chemically different monomers into one macromolecule. Such materials are characterized by a random or statistical coupling of the monomer units which is dependent upon the relative rates of reaction of the two components. Virtually all commercial random copolymers are derived from vinyl monomers and/or conjugated dienes.[9] The properties of random copolymers are intermediate to those of the corresponding homopolymers depending, of course, on the weight fraction of each specie. For example, random copolymers of styrene and acrylonitrile containing 20 to 30% of the latter component display better heat resistance, impact strength, and solvent resistance than polystyrene alone. The copolymers retain the transparency and good processability usually associated with polystyrene.

2. Alternating Copolymers. Copolymers of this type are relatively few in number due to the fact that suitable monomers are rarely available. The end unit of a growing chain must have no tendency to react with its own monomer type, yet be able to react with the comonomer. A well known example is the alternating copolymer of styrene and maleic anhydride.[10] Like random copolymers, the properties can usually be represented by a weighted average of the individual homopolymer properties.

3. Graft Copolymers. Graft copolymers consist of a main backbone chain (A segments for example) onto which a series of branches or grafts of a second polymer type (B) are bound as shown below. These copolymers

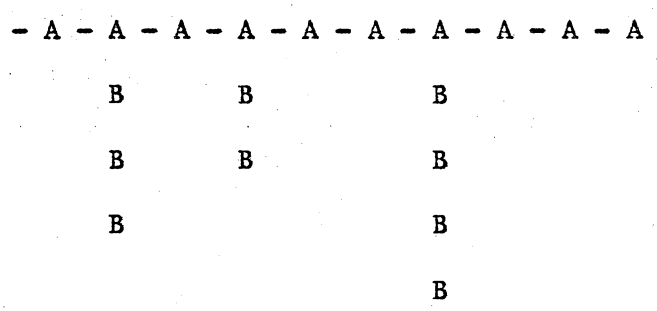

have been prepared in a variety of ways, but free radical techniques have been the most important commercially. Two basic means of forming graft copolymers exist. One method involves the formation of grafts through initiation and propagation of the second monomer specie from reactive groups, such as radicals, along the backbone chain. The second method entails the grafting of preformed side chains onto reactive sites along the main chain. The synthesis of graft copolymers has been reviewed in detail by Kennedy[11] and others.[12,13]

The lack of structural regularity, which can be accurately controlled in the case of block copolymers, is perhaps the most significant limitation of graft copolymers. In addition to homopolymer contamination, the number, length, spacing, and molecular weight distribution of the grafts cannot be defined with certainty. Nevertheless, graft copolymers have found important commercial applications as impact modified thermoplastics.

Impact grade polystyrenes have been prepared via the free radical reaction of polybutadiene with styrene.[14] The allylic hydrogens on the butadiene chains are susceptible to removal by free radicals, thus creating radical sites along the rubber molecules which are capable of initiating styrene polymerization. The final product, containing 5-15%

rubber, usually consists of a mixture of polystyrene, polybutadiene, and the graft copolymer. The morphology of the solid material consists of spherical rubber particles dispersed within a polystyrene matrix.[15] The proposed function of rubber particles is to lower the craze initiation stress relative to the fracture stress of the matrix. The prolonged crazing during deformation provides an additional means of energy dissipation and, therefore, improves the impact strength markedly.[15] However, the gain in impact strength is somewhat offset by reduced clarity, softening point, and tensile strength.[14]

One type of acrylonitrile-butadiene-styrene resin is prepared by the free radical reaction of acrylonitrile and styrene in the presence of a polybutadiene latex.[16] As in the preceding example, the product is usually a mixture, consisting of graft copolymer, styrene-acrylonitrile random copolymer and butadiene homopolymer. Some crosslinking of the graft copolymer also occurs, an essential aspect of high strength ABS plastics.

4. Block Copolymers. Block copolymer technology has grown rapidly during the past 20 years. More than two thousand literature references have been identified with this topic between 1960 and 1976.[17] Correspondingly, there are numerous collective works[18,19,20] and monographs[17,21] dealing with the synthesis and properties of block copolymers available today. Noshay and McGrath[17] have provided the most current and certainly the most comprehensive treatise thus far.

In view of the enormous amount of previous work carried out on block copolymers, this section will be limited to a brief overview of structures, syntheses and properties of the same. The main purpose here

is to acquaint the reader with many of the terms to be used in later chapters.

(a) Block Copolymer Architecture. Four basic types of block copolymer structures can be identified. Using A's and B's to denote dissimilar chemical structures one may define an A-B diblock copolymer as:

A B

The addition of a third block produces an A-B-A or B-A-B triblock copolymer.

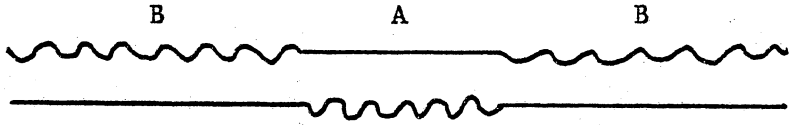

B A B

A B A

Coupling four or more blocks together gives rise to $[A-B]_n$ multiblock

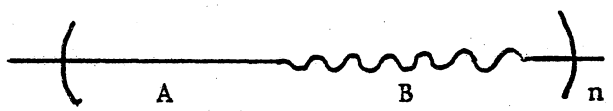

n=2,3,4.....

copolymers where n is greater than 1. Lastly, three or more diblock copolymers may be coupled at a single junction point to form radial or star block copolymers.

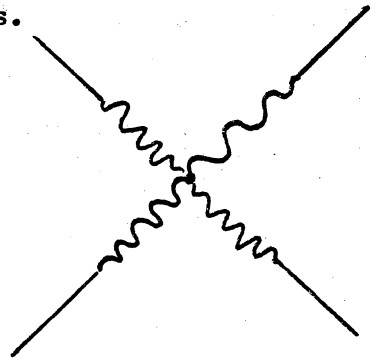

(b) Synthesis of Block Copolymers. The preparation of A-B and A-B-A block copolymers with well defined structures became possible with the development of non-terminating anionic polymerizations.[22] The simplest procedures involve the polymerization of a "living" A block followed by the addition and sequential polymerization of monomer B to form an A-B diblock copolymer. Monofunctional initiators such as alkyllithium compounds are widely used for such reactions. It is important that both A and B anions be able to initiate polymerization of the comonomer if triblock or multiblock systems are desired through further sequential reactions. Triblock copolymers may also be prepared through use of difunctional initiators such as sodium-naphthalene to prepare the center block with two "living" terminals. Sequential addition of the second monomer leads to the formation of two identical end blocks. Morton[23] and Janes[24] have discussed these techniques and others for preparing a variety of A-B and A-B-A materials. The anionic polymerization methods allow blocks with predictable molecular weights and narrow molecular weight distributions to be prepared. The reactants, initiators and solvents employed must be extremely pure in order to prevent premature termination of the "living" polymer chains.

Radial block copolymers have been prepared via the reaction of A-B block copolymers with "living" end groups and polyfunctional coupling agents such as $SiCl_4$ or divinyl benzene.[25] Difunctional coupling agents such as phosgene or diethyl terephthalate[26] can be used to prepare multiblock copolymers in the same manner.

The anionic polymerization schemes do not readily lend themselves

towards the preparation of multiblock copolymers due to the rigorous purification steps required. However, the step growth reactions used to prepare many important commercial polymers are particularly suited to the task. Since step growth reactions involve the condensation of two chemically different species, multiblock copolymers can be easily prepared from oligomers terminated with mutually reactive end groups. A wide range of block copolymers becomes possible since many anionically prepared oligomers can also be terminated with reactive functional groups.[24] Strictly alternating block copolymers result when the end groups of one oligomer type can react only with those of the second and not with each other. In cases where the end groups of each specie are identical and a difunctional coupling agent is employed, block copolymerization becomes statistical in nature. Preferential coupling may occur if the reactivities of the oligomer end groups differ appreciably from each other.

B. Effects of Microphase Separation

1. Morphology. Earlier, it was pointed out that the mutual incompatibility of block copolymer segments leads to the formation of extremely small microphases called domains. The consequences of domain size and shape are critical since these parameters ultimately govern the macroscopic bulk properties of the material. Five general morphological arrangements are illustrated in Figure 1 based on the volume fractions of the components. These structures have been confirmed in the case of styrene-diene block copolymers by transmission electron microscopy. Staining of the diene phase with OsO_4 to increase the electron density of the rubber allowed the necessary phase contrast to be obtained.[27]

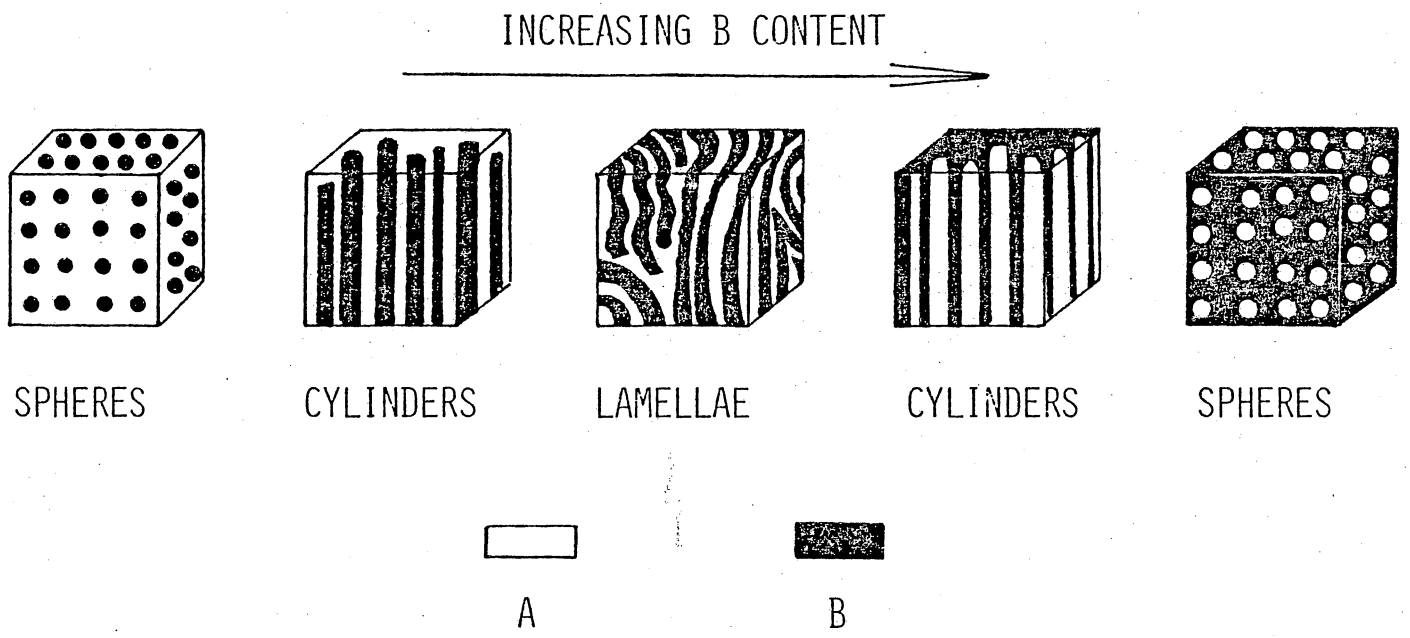

Figure 1. Block copolymer morphology (after Molau[7]).

Small angle X-ray scattering is also a powerful technique for establishing the size and spacing of the domains, especially where staining techniques are not applicable.[28]

Both the domain arrangement and the sharpness of the domain interface are subject to variations in fabrication conditions. Aggarwal[29] has reviewed the effects of solvent casting and processing on the morphologies of linear and radial styrene-diene block copolymers.

2. Transitional Properties. In phase separated block copolymers the glass transition temperatures and/or melting points of both components may be observed. The difference in modulus-temperature behavior between homogeneous and microphase separated systems is schematically illustrated in Figure 2. The reader should note the presence of the modulus plateau between the Tg's of the components in the latter case. The level of the modulus plateau is determined by the overall composition of the copolymer whereas its temperature sensitivity (slope) is governed by the degree of phase separation. In some types of thermoplastic elastomers a melting point (Tm_B), rather than Tg_B, defines the upper use temperature of the material.

3. Mechanical Properties. The tensile properties of single phase copolymers usually lie between those of the pure components. In phase separated block copolymers the tensile behavior is not only dependent on the composition and morphology, but also on the molecular architecture to a large extent. For example, in elastomeric styrene-butadiene diblock copolymers, domain formation takes place but the tensile properties differ little from those of random copolymers unless some crosslinking

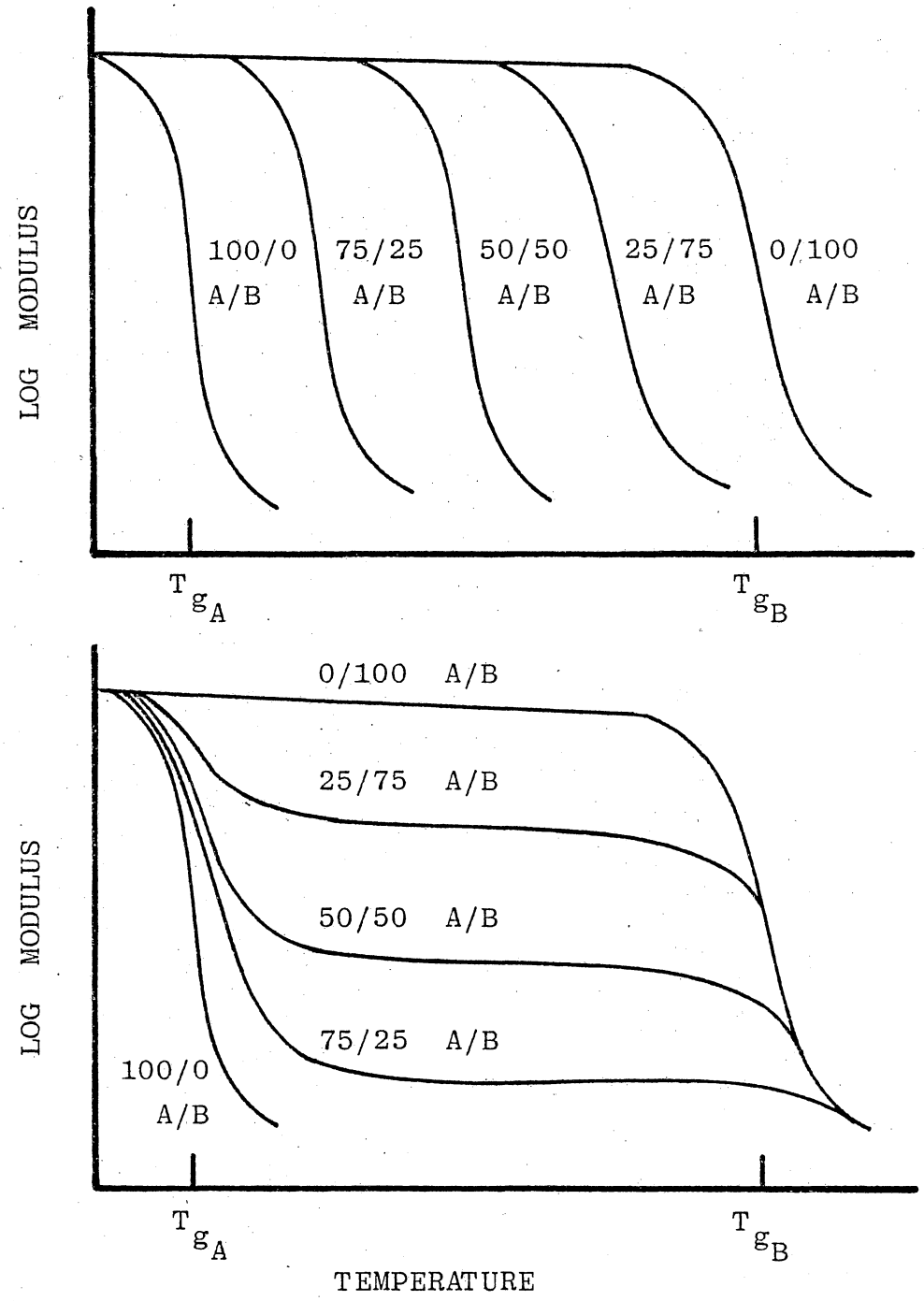

Figure 2. Generalized modulus-temperature behavior of homogeneous (top) and microheterogeneous (bottom) block copolymers (after McGrath (106)).

is present.[30] On the other hand, triblock S-B-S copolymers display excellent recovery properties similar to those of vulcanized rubbers. The critical difference between the S-B and S-B-S molecules rests with the "network" forming ability of the latter. One S-B-S chain is capable of connecting two styrene domains which serve then as physical rather than chemical crosslinks. This has been termed a macro-network. Network formation cannot occur in diblock copolymers as Milkovich[31] first pointed out in 1963. It follows that both radial and multiblock copolymers are also capable of network formation.

Block copolymers comprised of brittle or ductile segments coupled to a small fraction of elastomeric segments display improved toughness. Styrene-butadiene-styrene copolymers ranging from 10-30% rubber have been shown to have better transparency, impact strength and ultimate elongation than corresponding S-B or B-S-B copolymers of similar composition.[32]

The mechanical properties of selected glassy-glassy and glassy-crystalline block copolymers will be discussed in later sections.

4. Processability. The melt flow properties of many homopolymers and single phase copolymers follow the behavior suggested by the lower curve in Figure 3. At very low shear rates where little molecular alignment occurs the melt viscosity (η) remains constant with increasing shear rate ($\dot{\gamma}$) in accordance with Newton's law,

$$\eta_o = \tau/\dot{\gamma} = \text{constant}$$

where τ is the shear stress. The term η_o represents the lower limiting or zero shear viscosity. At somewhat higher values of $\dot{\gamma}$ the apparent

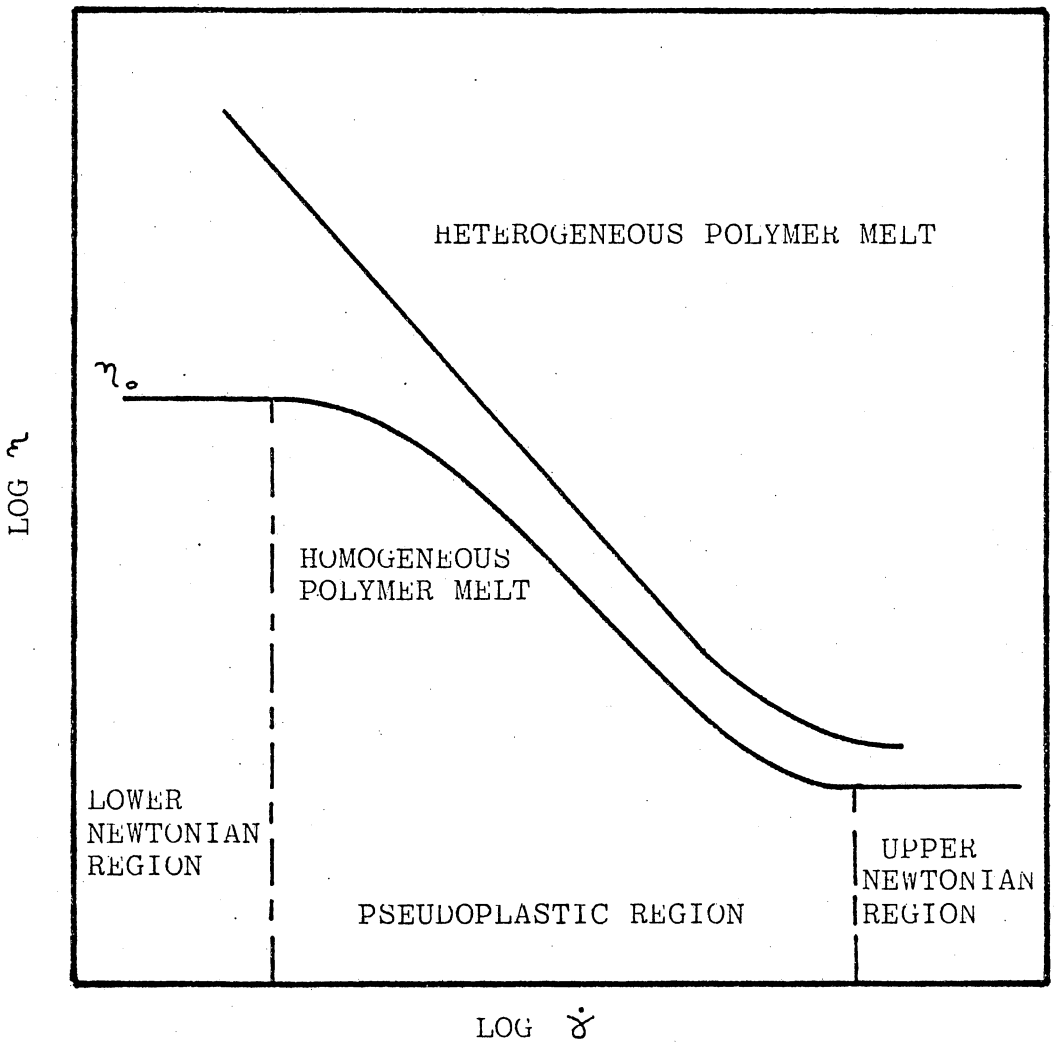

Figure 3. Melt rheology of homogeneous and heterogeneous block copolymers.

viscosity decreases with $\dot{\gamma}$ as the molecules begin to untangle and align with the shear field. This region is designated as the shear thinning or pseudoplastic region in the figure. At still greater values of $\dot{\gamma}$ the molecular alignment becomes maximized and another limiting viscosity (η_∞) or the upper Newtonian region is approached.[33]

The flow behavior of heterogeneous melts differs considerably from that of the homopolymer materials. Even at very low shear rates non-Newtonian behavior is observed due to the retention of the domain structure in the melt.[34] True thermoplastic behavior occurs only at high shear rates where the network is broken down.[35] The melt viscosities of two phase melts are much greater than those of either homopolymer at equal molecular weights and temperature.

B. Theories of Compatibility in Blends and Block Copolymers

1. Polymer-Polymer Compatibility. In order to achieve miscibility of two initially separated materials, basic thermodynamics requires that the total free energy of mixing (ΔG_M) be negative. Thus,

$$\Delta G_M = \Delta H_M - T\,\Delta S_M < 0$$

where ΔH_M and ΔS_M are the enthalpy and entropy of mixing respectively and T is the absolute temperature. It follows that the condition $\Delta G_M < 0$ can be realized only if $\Delta H_M < 0$ or $T\Delta S_M > \Delta H_M$. For most polymer pairs ΔH_M is positive, making miscibility the exception.

The earliest attempts at predicting the phase behavior of solid polymer mixtures originated with Scott[36] who applied the Flory-Huggins[37] theory of polymer solutions to the problem. Like Flory, Scott assumed a lattice model for the mixture and further assumed that the enthalpic

and entropic contributions to ΔG_M were independent of each other. The following relations for ΔH_M and ΔS_M were derived.

$$\Delta H_M = \frac{RTV}{V_r} v_A v_B \chi_{AB}$$

$$\Delta S_M = -\frac{RTV}{V_r} \left[\frac{v_A}{x_A} \ln v_A + \frac{v_B}{x_B} \ln v_B \right]$$

where v_A and v_B are the volume fractions of components 1 and 2, X_A and X_B are the degrees of polymerization, V is the total volume of the mixture, Vr is the volume of a lattice site (or repeat unit) and χ_{AB} is the interaction parameter between the polymers. The quantity RT retains its usual meaning. An equation for χ_{AB} due to Hildebrand[38] was written as

$$\chi_{AB} = \frac{Vr}{RT} (\delta_A - \delta_B)^2$$

where δ_A and δ_B are the solubility parameters or cohesive energy densities of the components. Although solubility parameters could be easily calculated for low molecular weight liquids from a knowledge of vaporization energy and density,[38] their application to polymers was an oversimplification of the problem. One dimensional solubility parameters for polymers have been estimated from swelling data,[39] intrinsic viscosities,[40] or group contributions[41] based on the solubility parameters of solvents. It has been generally acknowledged, however, that such values do not adequately describe the behavior of materials capable of interacting with one another through hydrogen bonding or other specific interactions. Other workers such as Hansen[42] and Crowley and

Teague[43] argued that a single parameter was inadequate and proposed three-dimensional parameters to account for dipole interactions, dispersion forces, and hydrogen bonding. More recently, Shaw[44] has proposed a two-dimensional solubility parameter approach to the problem of polymer compatibility. The interaction energy was assumed to be due only to dispersion and dipole (polar) interactions. Shaw found that this approach did improve the predictability of polymer miscibility and, like the original theory, correctly predicted that miscibility decreased with increasing molecular weight. The main drawbacks of the basic theory still remained however, those being the inability to predict negative values of ΔH_M and the incorrect prediction that solubility increased with temperature in contrast to actual observations. In other words, the concentration and temperature dependence of χ_{AB} could not be accounted for.

It is well known that many apparently miscible polymer blends and solutions display a cloud point or lower critical solution temperature (LCST) on heating. In 1964 Flory[45,46] proposed an equation-of-state theory for polymer solutions taking into account the free volume effects which arise from the disruption of the local liquid structure by the dissolved solute. McMaster[47,48] has since applied a modified equation-of-state theory to the problem of polymer-polymer miscibility. The approach is quite rigorous in its use of mathematics so only a brief overview will be presented here. Basically, an equation-of-state for the solid polymer was derived in terms of temperature, internal pressure and volume. The equation of state variables corresponding to T, P, and

V were obtained from expressions for the thermal expansion coefficient (α) and the thermal pressure coefficient (γ) shown below.

$$\alpha = \frac{1}{V}\left(\frac{\partial V}{\partial T}\right)_P$$

$$\gamma = \left(\frac{\partial P}{\partial T}\right)_V$$

Using the equation of state variables, McMaster derived an equation for the Helmholz free energy of mixing (ΔF_M) in terms of a combinatorial entropy of mixing identical to ΔS_M described earlier, an equation-of-state entropy due to free volume effects, and an interaction energy term which accounted for equation-of-state and segment contact effects. An expression for the interaction parameter (χ_{AB}) was obtained from equations for the chemical potential of one component in terms of the equation-of-state variables. Theoretical phase boundaries were calculated by substituting realistic values of the equation-of-state variables into the appropriate expressions for the binodal and spinodal curves and compared to those experimentally obtained for several polystyrene blends.

McMaster's work predicted that in mixtures of polymer pairs where $\chi_{AB} \leq 0$ LCST behavior should occur. Simultaneous LCST and upper critical solution temperature (UCST) behavior was predicted for mixtures with slightly positive values of χ_{AB}. Gross incompatibility should then occur where χ_{AB} takes on larger positive values. Surprisingly, the most important variable in determining miscibility via this treatment proved to be the thermal expansion coefficient (α). Even small differences

(<4%) in α were predicted to lead to complete immiscibility. The effects of molecular weight and polydispersity were also taken into account.

More recent efforts have confirmed some of McMaster's predictions. Paul and Barlow[6] estimate that more than fifty miscible polymer systems have been described in the literature. Of these, nearly all exhibit negative interaction parameters and, therefore, negative heats of mixing. Strong specific interactions such as hydrogen bonding or charge transfer interactions[49] have been considered responsible for such behavior. Paul and coworkers[6,50,51,52] at the University of Texas have extensively studied blends of poly(vinylidene fluoride) (PVF_2) with acrylic polymers and have demonstrated that the interaction parameters between PVF_2 and poly(methyl methacrylate), poly(ethyl methacrylate), poly(methyl acrylate), poly(ethyl acrylate), and poly(vinyl methyl ketone) are negative. The degree of miscibility could be related to the availability of the carbonyl group for interaction with the PVF_2 segments.[6] Moreover, nearly all the systems investigated displayed LCST behavior on heating. Recall that McMaster[47] predicted LCST behavior for negative values of χ_{AB}. Similar trends have been pointed out for binary mixtures of low molecular weight species.[53] It should be noted, however, that a comprehensive understanding and modeling of the details of polymer-polymer miscibility is still an area of active debate in the literature.

2. Microphase Separation. The same principles which govern the mutual solubility of two polymers must also apply when the polymers are linked as in a block or graft copolymer. However, the presence of

covalent bonds between the segments gives rise to a loss in the configurational entropy of the system which is not easily accounted for. A number of workers have proposed theories of microphase separation, several of which will be reviewed here.

Meier[54] provided the initial theoretical treatment of microphase separation in 1969. The theory was restricted to A-B diblock copolymers in which the A segments formed a dispersed phase of spherical domains. The copolymers in question were further assumed to be monodisperse, amorphous, and composed of equal sized A and B repeat groups. Realizing the difficulty in approaching the problem from a lattice-type model, Meier adopted a modified diffusion equation to generate the necessary random flight chain statistics. Additional constraints locating the A and B chains in essentially pure domains served as boundary values in the analysis. A further crucial assumption stipulated that the density of the domains was uniform, thereby limiting their size to some function of chain length.

Three contributions to the entropy of microphase separation were envisioned. The first accounted for the entropy difference between random placement of the A-B junction and the restriction that the junction was located on the domain surface. The second contribution accounted for the entropy restriction arising from placement of the remaining A and B segments in their respective domains, and the third accounted for the increase in chain dimensions over their unperturbed values.

In the equation for the free energy of microphase separation, Meier

considered the enthalpy as simply the negative of ΔH_M described by the Flory-Huggins theory, and introduced a term to account for the surface free energy at the domain surface. These assumptions allowed him to estimate that the critical block length for microphase separation in the case of a styrene-butadiene diblock copolymer was 2.5-5 times greater than that in the corresponding homopolymer mixture.

In subsequent publications Meier[55,56] extended his theory to predict the change in morphology with composition. The trend was correctly identified as proceeding from spherical to cylindrical to lamellar domains.

A second theoretical approach to microphase separation has been discussed by Krause[57] using assumptions similar to those of Meier. The main differences in Krause's work were the omission of morphological considerations as well as individual chain statistics, leaving the method purely thermodynamic in nature. In an early paper[58] Krause considered an expression for the demixing of a homogeneous copolymer which was just the negative of the familiar Flory-Huggins equation. This approach predicted that microphase separation would occur at lower block lengths in the copolymer than in the blend, just the opposite of what is actually observed. In later work,[57] terms were added to account for the immobilization of the AB junctions on the domain surface and the number of blocks in the copolymer. The expressions for ΔH and ΔS of microphase separation were given as below:

$$\Delta H = \frac{-kTV}{Vr} v_A v_B \left(1-\frac{2}{z}\right) \chi_{AB}$$

$$\Delta S = k[\ln (v_A)^{v_A} (v_B)^{v_B} - 2(m-1) (\frac{\Delta S_{dis}}{R}) + \ln (m-1)]$$

where V is the total volume, Vr is the volume of a lattice site, v_A and v_B are the volume fractions of the components A and B, Z is the lattice coordination number ($6<Z<8$), and χ_{AB} is the lattice interaction parameter. In the expression for ΔS, M is the number of blocks and $\Delta S_{dis}/R$ is the disorientation entropy lost when the junction segments are confined to the domain surface. The latter term had been presented earlier by Flory[37] who showed that

$$\frac{\Delta S_{dis}}{R} = \ln [\frac{z-1}{e}]$$

where e is the base of natural logarithims. Krause approximated that $\Delta S/R \tilde{=} 1.0$ by assuming Z=8. An expression for the critical interaction parameter was obtained by setting $\Delta G = \Delta H - T\Delta S = 0$ and solving for χ_{AB}. These corrections reversed the prediction stated earlier by Krause[58] and brought her theory into agreement with that of Meier. Krause has also adapted the theory to include terms allowing for crystallizable blocks and for the presence of homopolymer.[59]

Whereas Meier and Krause treated the microphase surfaces as sharp boundaries, other workers considered a mixed phase lying between the pure domains. Leary and Williams[60,61,62] rejected the concept of a surface energy contribution in favor of a solubility parameter expression to account for the mixed interfacial layer. Their approach was limited to A-B-A block copolymers only. Three entropic contributions similar to those of Meier were also considered. These authors also conceived of a

separation temperature T_s characterizing a first order transition involving the separation of a homogeneous melt into microphases upon cooling. The value of T_s could be approximated by

$$T_s \simeq (\Delta H/\Delta S)_{Demix}$$

assuming $\Delta G = 0$ and was, thus, proportional to the square of the solubility parameter differences $(\delta_A-\delta_B)^2$. The authors indicated that T_s should lie in the range of conventional processing temperatures when $(\delta_A-\delta_B)$ is small. They observed, through various techniques, that the values of T_s predicted for several S-B-S triblock copolymers were indeed in the range established by experiment. It was pointed out, however, that the success of the model depended greatly on the solubility parameters used in the calculation. Since only one dimensional solubility parameters were used, it was obvious that the model could only be applied in the absence of specific interactions between the components. The theories of Meier and Krause are also limited in this regard.

Another model, based on strict statistical thermodynamic principles, has been proposed by Helfand.[63,64] Like Meier,[54] Helfand employed modified diffusion equations to obtain the necessary chain statistics assuming a "narrow interphase approximation" or, in other words, that the interphase was much narrower than the domain size. Helfand's theories are typified by rigorous mathematics and statistical analysis, and it suffices to say that many of the same assumptions originating with Meier are employed.

Le Grand[65] adopted a micellar model for the structure of domains in

A-B and A-B-A type copolymers. An additional free energy term to account for elastic deformation of the domains was required to extend the model's applicability to $[A-B]_n$ multiblock systems.[66] The domain boundaries in S-B-S and polycarbonate-polydimethyl siloxane copolymers were found to be diffuse rather than sharp through analysis of small angle X-ray data.

Inoue and coworkers[67] found that the morphology of styrene-isoprene diblock copolymer films cast from solution varied with composition and solvent power. A transition from spherical to cylindrical to lamellar domains was observed directly by electron microscopy as the composition was varied from 20 to 70% styrene. Films cast from good solvents for one of the components typically showed that component to be the major or continuous phase. The authors proposed that a critical concentration existed in solution at which micellar aggregates formed and above which persisted until solid structures formed. A thermodynamic model was described taking into account solvent power, chain length, composition, and the degree of interaction between the polymer species involved.

The same authors[68] later extended their model to include studies of domain formation in the presence of residual homopolymers. It was found that as long as the molecular weight of the homopolymer was less than that of the corresponding block in the copolymer, the added homopolymer did not affect domain formation and was, in fact, incorporated into the domain. Results obtained for triblock S-I-S copolymers[69,70] were similar to those found for the diblock systems. Swelling and mechanical relaxation data indicated that in S-I-S systems two styrene domains could be

connected by a single molecule whereas the same was not possible in diblock systems. Five types of copolymer morphology were obtained leading the authors to conclude that five types of micelles existed in solution.

All of the thermodynamic models presented here, with that of Helfand excepted, are based on the traditional Flory-Huggins approach to polymer compatibility. It would seem that the next step would include equation of state principles based on the success of McMaster's[47] work. Such work has not been reported.

D. Glassy-Glassy Block Copolymers

Block copolymers with thermoplastic elastomeric properties have become important commercial materials and an enormous number of reports concerning their preparation and properties have appeared in the literature. In contrast, relatively few studies of block copolymers composed of glassy segments have been carried out. This section points out some of the earlier work on glassy block copolymers.

1. Styrene-α-Methyl Styrene (S-αMS). Baer[71] prepared copolymers of the type αMS-S-αMS and S-αMS-S anionically using Na-naphthalene as initiator. Both types of copolymers displayed single glass transitions which were intermediate to those of polystyrene (115°C) and poly(α-methyl styrene) (180°C). Simple blends of the two homopolymers were cloudy and exhibited two distinct damping maxima when studied by dynamic mechanical techniques. Annealing of the copolymers at 190°C did not induce microphase separation.

Robeson et al.[72] employed sec-butyl lithium initiator to prepare

S-αMS diblock copolymers by sequential polymerization in THF. Single phase behavior was observed at block lengths as high as 200,000 g/mole. Blending of the copolymers with styrene or α-methyl styrene homopolymers revealed results similar to those obtained by Inoue[68] described earlier for styrene-isoprene diblock copolymers. Two phase morphologies resulted when the molecular weight of the added homopolymer was greater than that of the corresponding block. The solubility of poly(α-methyl styrene) was found to be greater than that of polystyrene in the block copolymers.

The results of Robeson et al.[72] agreed favorably with the theoretical predictions of Krause[73,74] who pointed out that S-αMS diblock copolymers should be homogeneous up to block lengths of 8×10^5 g/mole. Krause also predicted that triblock copolymers would only experience microphase separation when the block lengths exceeded 10^6 g/mole. A value for the critical interaction parameter of S-αMS copolymers was estimated to lie in the range 0.0030-0.0036. Similar values were obtained for the triblock materials as well. The single phase nature of the di- and triblock copolymers were, thus, attributed to the near zero interaction parameter of the components.

2. Styrene-Methyl Methacrylate (S-MMA). Anionically prepared triblock copolymers of the type MMA-S-MMA were reported by Baer[71] in 1964. The corresponding S-MMA-S copolymers could not be prepared due to the inability of MMA anions to initiate styrene polymerization. Two phase behavior was noted in an unfractionated block copolymer consisting of a ~66,000 g/mole styrene midblock coupled to MMA endblocks of roughly

20,000 g/mole each. The copolymers were transparent indicating that the size of the microphases was smaller than the wavelength of light.

The glass transition behavior of random and triblock copolymers (MMA-S-MMA) have been studied by Beevers.[75] A minimum was noted in the Tg of random copolymers at about 70% styrene content. The Tg of the block copolymers was likewise depressed. All the polymers, however, had broad molecular weight distributions ($\bar{M}w/\bar{M}n > 3$) implying that the presence of low molecular weight species might be responsible for the lower than expected Tg values. The block lengths were evidently too small to promote microphase separation since only one Tg was observed for the copolymers.

Rempp[76] has reported the synthesis of block and graft copolymers of S and MMA. The block polymers were synthesized anionically in the presence of 1,1-diphenyl ethylene in order to overcome a side reaction of the "living" polystyrene anions with the carbonyl group of the MMA units. The reaction of styrene anions with the ester functions on PMMA backbones was utilized in the preparation of graft copolymers. No thermal or mechanical characterization was reported.

Several investigations of the solution properties of S-MMA and MMA-S-MMA copolymers have been carried out.[77,78,79,80] At low temperatures, the triblock copolymers remain in a segregated conformation[80] which changes to a pseudo-Gaussian form at higher temperatures. The transition was manifested by an abnormal change in the refractive index increment with temperature.

3. Methyl Methacrylate-αMethyl Styrene (MMA-αMS). The morphology

of MMA-αMS block copolymers has been studied by Hsiue et al.[81] as a function of composition. Electron microscopy revealed that the copolymers were two phase materials with spherical MMA domains in the range 2000-500 Å. The mechanical properties were shown to be dependent on the continuous αMS phase as expected. The modulus displayed a maximum at 84% αMS which was greater than that of the two homopolymers. This apparent stiffening was explained as a disturbance of the αMS chains by the MMA domains which acted as filler particles.

4. Styrene-Acrylonitrile (S-AN). Perry[82] prepared a series of S-AN blends and some random and block copolymers. Only block copolymers containing less than 15% AN proved to be wholly amorphous. At higher AN content crystallization of the AN segments occurred. A block copolymer composed of 14% AN was, however, a two phase system possessing AN domains less than 560 Å in average size.

5. Phenylene Oxide Block Copolymers. An amorphous diblock copolymer of poly(2,6-diphenylphenylene oxide) and poly(2,6-dimethyphenylene oxide) has been reported by Bennet et al.[83] Initially 2,6-diphenylphenol was polymerized by oxidative coupling[84] in the presence of an amine-CuBr catalyst. The second block was formed upon addition of 2,6-dimethylphenol to the reaction. Interestingly, the reverse procedure gave rise to a random copolymer which was attributed to a significant side reaction. The block copolymer displayed a single intermediate Tg at 227°C but upon heating to 290°C crystallized somewhat due to the semicrystalline nature of the diphenylphenylene ether block.

Rigid, amorphous block copolymers based on polysulfone or

polycarbonate segments have also been described. These materials will be dealt with in the following section.

E. Materials

1. Polysulfone

(a) Synthesis. The development of synthetic techniques, capable of producing high molecular weight polysulfones, has only evolved in recent years. Basically, only two synthetic routes to poly(aryl ether sulfones) are available, nucleophilic aromatic substitution and electrophilic aromatic substitution. Both methods permit a wide range of polymers to be prepared and will be reviewed in some detail here.

In 1967, Johnson et al.[85] described the synthesis of a large number of poly(aryl ethers) via condensation of dihydric phenols and activated aromatic dihalides. Their study pointed out the guidelines by which high molecular weight polymers could be prepared. An important consequence of this work was the synthesis of bisphenol-A polysulfone, derived from the disodium salt of bisphenol-A and 4,4'-dichlorodiphenyl sulfone as shown below. This polymer is currently marketed by Union Carbide Corp. under the tradename of Udel.

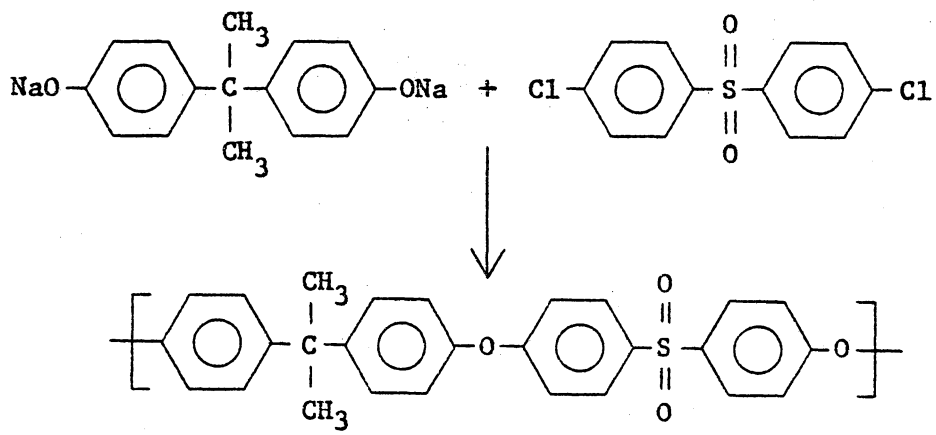

The sulfone group takes on an essential role in nucleophilic aromatic substitution. Its electron withdrawing ability activates the ring to attack at the ortho and para positions. Due to steric hinderance, ortho attack is not favored and polymers consisting of essentially all para links result.[86] Less activating groups such as $-\overset{O}{\overset{\|}{C}}-$ and $-N{\equiv}N-$ can also be employed but the reaction is sluggish.[85]

Besides being dependent upon the nature of the activating group, the reactivity of the dihalo compound is also governed by the halogen involved. For a given activated dihalide, the ease of displacement is generally F>>Cl>Br>I.[87] The more electronegative halogens are more effective in decreasing the electron density around the substrate carbon atom, allowing the nucleophile to attack more quickly.

Johnson et al.[85] reported that the reactivity of the bisphenols used in such syntheses varied inversely with their acidity. The more acidic biphenols required higher reaction temperatures or reaction with difluorodiphenyl sulfone to yield high molecular weight polymers.

Polysulfones containing substituted bisphenol A segments have been examined by Robeson et al.[88] The bisphenol reactivity followed the trend:

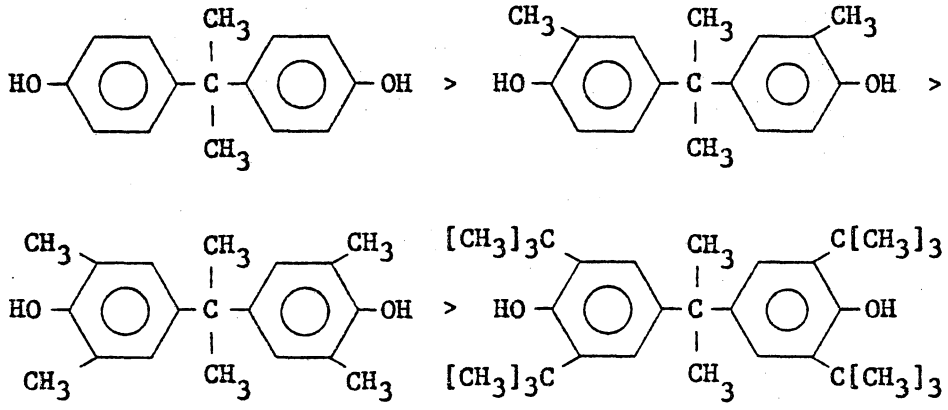

which was explained on the basis of increasing steric hinderance.

The choice of solvent is critical in obtaining high molecular weight polymer and dipolar aprotic solvents such as DMSO, DMAC, and sulfolane (tetrahydrothiophene-1,1-dioxide) appear to be the only viable candidates.[85] The solvent must be able to withstand high reaction temperatures without decomposing, be unreactive with both the starting materials and intermediates, and yet dissolve the reactants and polymer under anhydrous conditions.

As mentioned earlier, an additional material such as chlorobenzene is added to the reaction to facilitate the removal of water through azeotropic distillation. Both benzene and toluene may also serve in this function.[89]

Complete removal of water or any alcoholic impurity is important. Hydrolysis of the alkali metal phenate groups results in the formation of strong bases such as NaOH or KOH which are capable of attacking the activated halides.[85] The unreactive end groups thus formed disrupt the stoichiometry and lower the molecular weight. As in the case of other condensation polymerizations control of reaction stoichiometry is critical in achieving high molecular weights. The presence of even small amounts of excess alkali may cleave the polymer chains at the reaction temperatures employed.

High molecular weight poly(aryl ether sulfones) were synthesized by Cohen and Young[90] in 1965. Two different routes, involving electrophilic aromatic substitution, were employed to prepare bisphenol-S polysulfone as shown below.

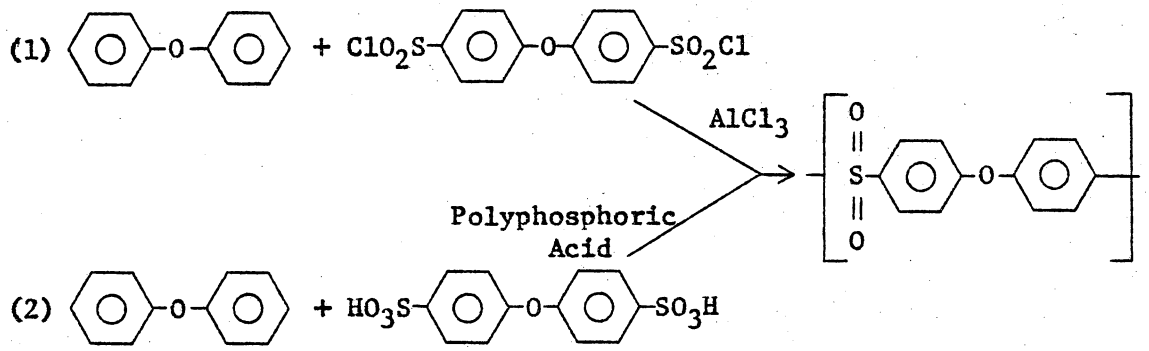

In the first process, diphenyl ether was reacted with 4,4'-dichlorosulfonyl diphenyl ether in a nitrobenzene solution containing a stoichiometric amount of $AlCl_3$. Analysis of the product revealed that substantial amounts of residual catalyst were chemically combined in the purified polymer. The residual catalyst also contributed to cross-linking at elevated temperatures.

The second synthesis involved the condensation of diphenyl ether with 4,4'-diphenyl ether disulfonic acid in an o-chlorobenzene-carbon tetrachloride mixture to form short oligomers. Dehydration was then carried out by heating in vacuo over P_2O_5. The dried oligomers were then polymerized in polyphosphoric acid at 240°C for four to either hours.

The synthesis of poly(aryl ethers) by melt condensation has been investigated by Cudby et al.[91] The polymers resulting from self-condensation of p-phenoxybenzene sulfonyl chloride (III) and the corresponding two reactant technique were compared as to their molecular weight and structure.

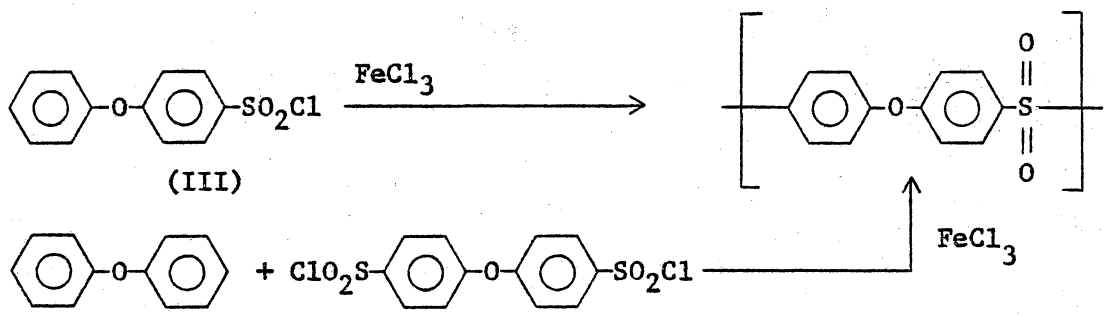

The self-condensation reaction yielded polymers of higher molecular weight since the difficulties associated with reaction stoichiometry were alleviated.

The choice of catalysts for electrophilic aromatic substitution reactions is limited to those compounds which are needed only in catalytic quantities. Thus, $FeCl_3$, $SbCl_5$, or $InCl_3$ appear to be the most widely used.[86] The low catalyst levels aid in eliminating side reactions and potential difficulties in purifying the polymer.

Because the attacking species carries a positive charge, the substrate ring cannot possess any electron withdrawing substituents. Thus, diphenyl ether and other similar molecules are acceptable comonomers while benzophenone and diphenylsulfone are not.[86]

As in the case of nucleophilic condensation reactions discussed earlier, the choice of available solvents is limited. Although melt condensations do not require a solvent, the high viscosities encountered in such processes render control of the reaction difficult. As an added benefit, the solvent also allows hydrogen chloride to escape more readily without foaming.[89] Solvents such as chlorinated biphenyl and nitrobenzene are the most effective in this regard.

(b) Properties of Polysulfones. The poly(aryl ether sulfones) form a class of tough, rigid polymers which are capable of extended use at temperatures above 150°C. Their high thermal and oxidative resistance[92] impart desirable thermoplastic processing properties which permits their use in conventional molding equipment. Objects molded from poly(aryl ether sulfones) display good impact and creep resistance as well as resistance to most aqueous acids and bases.

Bisphenol-A polysulfone may be regarded as an amorphous polymer with a Tg of 190°C at high molecular weight. MacNulty[93] observed crystals of various shapes in very thin films of polysulfone cast from solution, but McGrath[94] has pointed out that crystal formation results from the presence of a cyclic dimer trapped in the solid polymer.

Kambour et al.[95] investigated the effects of organic solvents on the swelling and crazing of polysulfone. They observed that solvents with solubility parameters (9-12) close to that of polysulfone (~10.6) lowered the critical strain for crazing to about 0.2% as opposed to 2.5% for the dry polymer. These same solvents also lowered the Tg of the polymer to room temperature leading the authors to claim that plasticization was the primary route to environmental crazing.

The dynamic mechanical properties of bisphenol-A and bisphenol-S polysulfone have been studied with particular regard to the low temperature loss peaks (-100°C) exhibited by these materials. Baccaredda et al.[96] suggested that the low temperature loss peak, or β relaxation, was due to the motion of water molecules bound to polar groups in the chain. Kurz and coworkers[97] argued that since the peak was still

observed in very dry samples, it was due, in part, to a molecular process somehow enhanced by absorbed water. The bisphenol-S polysulfone exhibited an additional relaxation at approximately 0°C.

A different argument was presented by Chung and Sauer[98] who claimed that the β relaxation was due to the combined motion of the phenylene rings and the sulfone group. Thus, the transition observed in dry samples was attributed to the non-polar groups and was enhanced by the association of water molecules with the sulfone linkage. Robeson et al.[88] have conducted an intensive investigation of the β transition in a series of sulfone containing and sulfone-free poly(aryl ethers). Their findings indicated that even non-sulfone containing polymers display a β relaxation at low temperatures which is not greatly affected by water. The sulfone containing materials displayed significantly higher water absorption which pointed out the sulfone group as the main site for water absorption. The importance of phenyl ring substitution on the mechanical properties was also described. Di and tetrasubstituted polysulfones proved to be brittle materials whereas their non-substituted analogs displayed ductile behavior. The authors explained this finding as a restriction of the main chain transitions thought to influence the brittle-ductile transition of these materials. They concluded that main chain rotations and transitions were responsible for the low temperature relaxation in polysulfone, and that the contribution due to water-sulfonyl interaction merely overlapped the primary relaxation process. As further proof, the effect of small additions of antiplasticizers on eliminating the β relaxation was cited.[99,100] This effect coupled to

the increase in modulus which also resulted was believed to be due to the filling of polymer free volume by the additive.

For the sake of brevity, a list of the important engineering properties of bisphenol-A and bisphenol-S polysulfone are listed in Table I. Note that both materials exhibit excellent thermal and mechanical properties.

The good impact strength of polysulfone remains unchanged down to temperatures as low as -150°C[101] at which 75% of the room temperature properties are retained. The material fails in a brittle mode, since its high yield strength contributes more to impact resistance than does its ductility as demonstrated in low strain rate tensile tests.[102]

The melt flow properties of polysulfone have been studied by Mills et al.[103] and Shaw[104]. Mills investigated the effect of molecular weight on melt flow and concluded that the entanglement molecular weight occurred in the range 2500-5000. The entanglements were thought to persist in the melt, accounting for the high viscosity of the same. An approximation of the activation energy for melt flow in polysulfone as 31 kcal/mole can be made from the data of Cogswell and McGowan.[105]

(c) Polysulfone Block Copolymers. Block copolymers prepared from polysulfone and various glassy, semicrystalline, and rubbery polymers have been extensively studied by McGrath and others.[106] Strictly amorphous block copolymers of polysulfone ($\bar{M}n$=5000) and polycarbonate ($\bar{M}_n$=5000) were prepared by phosgenating a solution of hydroxyl terminated polysulfone oligomer and bisphenol-A in methylene chloride with a pyridine catalyst present. The greater number of hydroxyl groups due to

Table I

Properties of Poly (Aryl Ether Sulfones)*

Property	ASTM Test No.	Bis-A Polysulfone	Bis-S Polysulfone
Tg (oC)	----	190	230
Density	D792	1.24	1.37
Tensile Strength (psi)	D638	10,000 (yield)	12,200 (yield)
Elongation (%)	D638	50-100 (Break)	30-80 (Break)
Impact Strength (ft.lb/in notch)	D256	1.2	1.6
Flexural Modulus (psi)	D790	3.95×10^5	3.7×10^5
Tensile Modulus (psi)	D638	3.7×10^5	3.5×10^5
Thermal expansion (in/in/oC)	D696	5.2×10^{-5}	5.5×10^{-5}
Volume Resistivity (Ω - cm)	D257	3.2×10^{16}	$10^{17} - 10^{18}$
Refractive Index	D542	1.67	1.65

* Modern Plastics Encyclopedia (1976)

the bisphenol-A monomer presumably reacted to form polycarbonate oligomers which then coupled in a statistical fashion with the polysulfone oligomers.

The mechanical properties of the block copolymers were similar to those obtained for the homopolymers themselves as shown in Table II. For example, the notched Izod impact strengths lay within the range encompassed by polycarbonate and polysulfone and were greater than those of the corresponding blends. Moreover, the copolymers exhibited only a single glass transition, indicating a single phase material, as opposed to the blends which displayed two glass transitions since two phases were present. The authors reasoned that two factors, the chemical link between the components and the relatively small difference in solubility parameter ($\delta_{psf}-\delta_{pc} \simeq 0.7$) prevented microphase separation from occuring.

In a similar study, McGrath et al.[106] prepared multiblock copolymers of polysulfone and polystyrene. Since the difference in solubility parameters was greater than in the previous case, ($\delta_{psf}-\delta_{ps} \simeq 1.6$) microphase separation was predicted to occur at low oligomer molecular weights. Hydroxyl terminated polystyrene oligomers were coupled to polysulfone oligomers with phosgene as described above. The molecular weights of the components ranged from 1100 to 10,000 grams per mole. As anticipated, the copolymers exhibited two Tg's characteristic of a phase separated material, but only where the block sizes were above 3,600 grams/mole. A copolymer comprised of polysulfone and polystyrene blocks with molecular weights ($\bar{M}n$) of 1100 and 3600, respectively,

Table II

Mechanical Properties of Polysulfone-Polycarbonate Block Copolymers and Blends*

Material	Wt.% Poly-sulfone	Trans-parency	Glass Transition Temperature(s), °C	Tensile Modulus, psi	Tensile Strength psi	Percent Elongation	Pendulum Impact ft-lb/in^3	Notched Izod Impact, ft-lb/in
Bisphenol A polycarbonate (PC)	---	Yes	150	310,000	10,400	80	135	11
Polysulfone (PSF)	100	Yes	190	360,000	10,200	100	150	1.3
PSF-PC Blend	25	No	150,190	320,000	9,100	60	160	2
PSF-PC Blend	50	No	150,190	330,000	9,500	50	140	1.5
PSF-PC Block copolymer	47	Yes	173	300,000	8,400	80	210	3.6
PSF-PC Block copolymer	50	Yes	176	---	---	---	---	6.0

* McGrath et al.[106]

displayed only a single intermediate glass transition temperature. The copolymers were compression moldable but proved to be very brittle materials.

Block copolymers of semicrystalline polymers and polysulfone have also been investigated by McGrath.[106,107] In these cases, the inclusion of a crystalline phase in an amorphous matrix was expected to improve the solvent resistance of the amorphous component. Block copolymers of Nylon-6 and polysulfone have been prepared via the reaction of chlorine terminated polysulfone and ε-caprolactam. The polysulfone oligomers, in this case, were prepared from bisphenol-A and an excess of dichlorodiphenyl sulfone (DCDPS). Copolymerization was feasible since activated aromatic halides such as DCDPS were excellent initiators for the anionic polymerization of ε-caprolactam. The reactions were carried out by dissolving the polysulfone in molten ε-caprolactam at 160°C in the presence of a basic catalyst. Subsequent extraction procedures pointed out that only about 25% of the polysulfone was actually incorporated into the copolymer. Compositions of higher polysulfone content were prepared by alloying the copolymers with the homopolymer.

As expected, both the copolymers and alloys displayed two phase behavior; a strong extra driving force for phase separation being the crystallinity of the polyamide. The materials were found to be melt processible at temperatures less than those used for polysulfone. The stiffness, % elongation at break, and impact strength of the copolymers were intermediate between those of the components. More importantly, the environmental stress crack resistance of the copolymers became

significantly greater than that of pure polysulfone when the nylon content reached 30 weight percent.

The copolymerization of poly(butylene terephthalate) (PBT) with polysulfone has also been reported.[106] Refluxing of polysulfone in trichlorobenzene in the presence of excess terephthaloyl chloride served to end cap the oligomers which could be further reacted with a stoichiometric amount of 1,4-butanediol. Transparent copolymers with a single glass transition temperature of 139°C were obtained. The latter finding led the authors to believe that the amorphous fraction of PBT might be soluble with polysulfone and that microphase separation was due to crystalline content of the polyester.

Block copolymers of polysulfone and poly(dimethyl siloxane) (PDMS) have been extensively studied by Noshay[108,109] and coworkers. Alternating block copolymers of well defined architecture could be readily prepared by the reaction of hydroxyl terminated polysulfone oligomers with amine terminated PDMS oligomers in chlorobenzene. This procedure has been reviewed in detail by Noshay et al.[108] Dynamic mechanical analysis of these copolymers revealed that their morphology was greatly dependent on the oligomer lengths.[108] Single phase materials were obtained for sulfone block lengths of 4700 and siloxane lengths less than 1700. Increasing the molecular weight of the siloxane segments promoted the formation of microphases. The authors indicated that the high degree of incompatibility exhibited by PDMS and polysulfone resulted from the large difference in solubility parameter ($\delta_{PSF}-\delta_{PDMS} \simeq 3.3$). Recall that the polysulfone-polycarbonate block

copolymers showed one phase behavior at block lengths of 5000 grams/mole where $\delta_{PSF}-\delta_{PC} \simeq 0.7$.

Noshay et al. found that both the tensile modulus and ultimate tensile strengths decreased sharply as the siloxane content increased from 10 to 79%. The elongation at break, however, increased from 5% to 550% over the same composition range. The authors noted that at higher siloxane percentages the copolymers behaved like crosslinked rubbers not unlike many other thermoplastic elastomers. However, a striking difference between the polysulfone-PDMS systems and S-B-S rubbers, for instance, was that they had very poor melt processibility even under conditions of low shear, as in compression molding. The extremely high melt viscosities and resulting inability to be extruded was explained on the basis of a retention of the two phase morphology even in the melt.

The gas permeability of polysulfone-PDMS block copolymers has been investigated by Robeson et al.[110] The impact modification of polysulfone by addition of the siloxane copolymer has also been confirmed. In one example, the notched Izod strength of unmodified polysulfone was increased by a factor of 20 upon introduction of only 5% by weight of the block copolymer.[109] The improvement was achieved with only a minimal sacrifice in polysulfone properties.

Still another approach is the incorporation of polysulfone into high temperature polymers, such as polyimides, to promote solubility and melt processibility. Kawakami et al.[111] have prepared a series of amine terminated polysulfone oligomers from the reaction of chlorine terminated polysulfone with the sodium salt of p-aminophenol. The oligomers

were actually only two or three repeat groups in size yet promoted solubility of the usually intractable polyimides in chlorinated hydrocarbons.[112] In view of the short block lengths of the sulfone oligomers such materials would seem better classed as a type of alternating copolymer.

2. Polycarbonate

(a) Synthesis. In contrast to polysulfone, the synthesis of aromatic polycarbonate is rather simple, but, in spite of this fact, the unique properties of bisphenol-A polycarbonate were not recognized until 1956.[113] Three main routes to polycarbonate have been described in the literature and will be briefly reviewed here.

Aromatic diphenols can be readily coupled with phosgene in methylene chloride solution containing pyridine in stoichiometric quantities as shown below.[114]

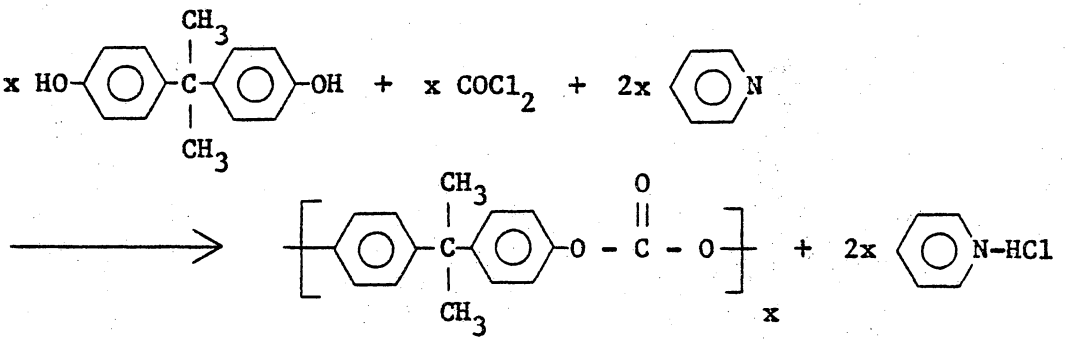

A severe disadvantage of this technique rests with the removal of residual pyridine and the hydrochloride. Schnell[114] has described a procedure for removing these impurities which lead to degradation of the polymer at high temperatures.

A similar but preferred technique is the interfacial method[115] which does not require the use of pyridine. A rapidly stirred methylene

chloride solution of bisphenol-A is phosgenated in the presence of a second aqueous phase containing NaOH and a quarternary ammonium salt as catalyst. The polymer which forms remains in the organic phase and can be easily separated from the aqueous layer containing the dissolved catalyst and NaCl.

The third synthetic route to polycarbonate involves an ester interchange reaction between bisphenol-A and diphenyl carbonate (DPC).[116] The reaction mixture containing a small amount of basic catalyst (ZnO, Sb_2O_3) is first melted and mixed well at 150°C under inert atmosphere. The second step of the reaction is run at 210°C under vacuum to distill off the phenol by-product and followed by a third step at 300°C and 1 mm pressure where conversion to high molecular weight product is formed.

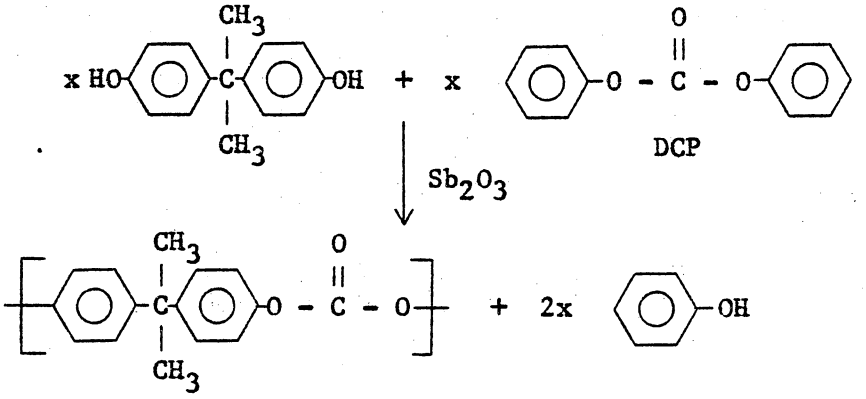

Generally, a small excess of DCP is used to prevent the degradation of bisphenol-A, the products of which lead to discoloration of the polymer. The ester interchange reaction is advantageous since no solvents or other impurities need be removed from the product. However, the apparatus is more complex and the reaction time very much longer.

(b) Properties. The polymer literature abounds with reports dealing with the various properties of polycarbonate and only those of importance to this study can be reviewed here. A number of review articles are available and the reader is referred to these.[117,118,119]

Structure and Morphology. Molded objects of polycarbonate are transparent, a direct result of their amorphous character. However, the fact that the material will crystallize, under certain conditions, has prompted many studied of polycarbonate in both the amorphous and semi-crystalline forms. Frank et al.[120] observed the formation of granular structures on the surface of polycarbonate specimens annealed at 110°C, far below the Tg of 150°C. The grains were believed to be of higher density than the surrounding matrix. Annealing at 160°C (above Tg) followed by quenching reverted the polymer back to the purely amorphous state. Siegmann and Geil[121] found that the ordering phenomena was not completely reversible and that the remaining granules could act as nuclei for crystallization as temperatures above Tg. A more recent study[122] has described the effects of ordering on the properties of polycarbonate. Annealing at 125°C was found to increase the density of polycarbonate while simultaneously changing the fracture mode from ductile to brittle. The brittle films failed by crazing, whereas the unannealed specimens failed by shear yielding preceded by macroscopic cold drawing. The characteristic granules described previously were found to form only at the surface layers where chain mobility was less restricted than in the bulk.

Polycarbonate crystallizes very slowly from the melt. The

crystalline form is thermodynamically favored but the kinetics of crystallization effectively prevent the transition.[123] Carr et al.[124] annealed polycarbonate for 8 days at 140°C before appreciable crystallization occured. The presence of even small amounts of certain non-solvents such as acetone or toluene brought about a rapid increase in the rate of crystallization. The topic of solvent induced crystallization in polycarbonate has been studied by McNulty,[125] Mercier[126] and Gallez,[127] among many others.

Mercier et al.[126] found that the apparent polymer density after crystallization was independent of the crystallizing agent. The rate of crystallization, however, did show a dependence on the nature of the penetrant, acetone being the most powerful. McNulty[125] has described the differences in spherulitic crystals of polycarbonate obtained by thermal and solvent induced methods. The crystallization of polycarbonate by the addition of plasticizers has been studied by Gallez et al.[127] who found that certain plasticizers, trimellitic acid for example, increased the crystallization rate sharply. The addition of nucleating salts did not affect the degree of crystallization of plasticized polycarbonate to the same extent as the pure polymer. Specimens containing 40 to 76% crystallinity by weight with much higher melting points, were obtained in the latter case. The authors gave differences in chain folding morphology as an explanation for this finding.

Like polysulfone, and all amorphous polymers in general, polycarbonate is very susceptible to environmental stress cracking (ESC).

Kambour et al.[128] attributed this solvent induced effect to the reduction in critical strain for crazing, as well as the lowering of Tg, to the plasticization of the polymer. Earlier, Kambour[129] had demonstrated that crazes in polycarbonate were not true cracks, but rather voids transversed by strong fibrils aligned in the principle stress direction. Both polycarbonate and polysulfone behave similarly towards the same ESC agents, apparently due to the similar solubility parameters of the polymers. Miltz et al.[130] have found that the rate of crazing decreased rapidly as the solubility parameter of the liquid approached that of polycarbonate ($\delta_{PC} \simeq 9.6$). A map of penetrant solubility parameter vs. rate of crazing could be divided into inert ($\delta<7$ or $\delta>13$), crazing ($7<\delta<9$ or $11<\delta<13$), and cracking/dissolution ($9<\delta<11$) regions. They concluded that diffusion through the craze tip was the controlling factor of craze growth.

Mechanical Properties. The important mechanical properties of polycarbonate as well as selected other data are listed in Table III. Polycarbonate is characterized by excellent tensile properties providing that the molecular weight ($\bar{M}_w$) is greater than 25,000.[131] At molecular weights below 10,000, molded parts and films become brittle. The material retains its inherent toughness over a wide temperature range (-100 to +150°C) as measured by tensile testing techniques.[132]

Dynamic mechanical analysis of polycarbonate locates two loss peaks located at -100 and +150°C. The latter peak, of course, corresponds to the glass transition whereas the origin of the low temperature or β transition is still not confirmed. Considerable debate

Table III

Properties of Polycarbonate*

Property	ASTM Test No.	Value
Tg (oC)	-----	150
Density (g/cc)	D 792	1.20
Tensile Strength (psi)	D 638	8000-9500
Elongation (%)	D 638	100-130
Impact Strength (ft-lbs/inch of notch)	D 256	12-18
Flexural Modulus (psi)	D 790	$3.2\text{-}3.5 \times 10^5$
Tensile Modulus (psi)	D 638	$3.0\text{-}3.5 \times 10^5$
Volume Resistivity (Ω - cm)	D 257	2.1×10^{16}
Thermal Expansion (in/in/oC)	D 696	6.6×10^{-5}
Refractive index	D 542	1.586

*Modern Plastics Encyclopedia (1976)

over the role of the β transition in determining the unusually high impact strength of polycarbonate has appeared in the literature.

Chung and Sauer[98] reported that a large drop in modulus (G') occured at -98°C along with a broad maximum in G''. The breadth and asymetry of the secondary loss peak led these authors to conclude that the transition was due to overlapping relaxations involving the polar carbonate group as well as the adjacent phenylene groups. An apparent activation energy for the process was estimated at 10.6 kcal/mole.

Using dielectric techniques, Sacher[133] has identified three secondary losses below the glass transition temperature. At a frequency of 100 Hz the β, γ, and δ transitions were located at 133, 34, and -114°C respectively. Annealing decreased the magnitude of the loss peaks as did increasing amounts of crystallinity. Sacher[134] attributed the β transition to motions involving phenyl-oxygen groups and considered it to be a forerunner of the glass transition. The γ transition was thought to have a dual origin in the wagging of carbonate groups coupled to rotations of the adjacent phenyl groups. It was pointed out that the γ peak involved new motions of the same groups responsible for the δ loss. The position of the δ loss marked the onset of both methyl and restricted phenylene motions along with cooperative carbonate motions. Sacher concluded that these transitions were responsible for the excellent impact strength of polycarbonate. The magnitude of the impact strength was found to be directly related to the magnitude of the dissipation factor (tan δ) at similar temperatures and frequencies.[134]

In a contradictory note, Allen et al.[135] determined that two forms

(A and B) of polycarbonate existed. The A form possessed extremely high impact strength whereas the B modification was brittle. These workers found that annealing the polymer above 80°C converted the A form to B, suggesting that a significant relaxation process occured above this temperature. However, it was also pointed out that the magnitude of the secondary loss peaks (-100°C) was not affected by the annealing process.

Watts and Perry[136] located an intermediate dielectric relaxation in polycarbonate at approximately 80°C. The magnitude of the loss peak associated with the transition decreased sharply upon annealing at 120°C for 12 hours. These authors considered the intermediate relaxation to be a remote precursor of the glass transition involving the motion of much shorter chain segments than those associated with the latter. The β or low temperature (-100°C) relaxation was also reduced somewhat in magnitude upon annealing but not to an appreciable degree. Watts and Perry[136] concluded that the main chain motions responsible for the β process contributed to, but did not exclusively determine, the impact strength of polycarbonate.

The high melt viscosity of polycarbonate requires that processing temperatures on the order of 300°C be employed. Between 240 and 300°C the viscosity of a polycarbonate with Mw=33,000 was found to range from 100,000 to 10,000 poise.[137] At 302°C the molecular weight dependence of melt viscosity follows the relation

$$\eta = 1.862 \times 10^{-11} \times Mw\ 3.23$$

where 13,000 < Mw < 80,000. The thermal activation energy for melt

flow was estimated by Baumann and Steingiser[137] to lie in the range 26-30 kcal/mole at zero shear rate. At a shear rate of 3 sec^{-1} an activation energy of 23.5 kcal/mole was obtained.

(b) Polycarbonate Block Copolymers. In 1961 Merrill[138] reported the synthesis of a multiblock copolymer of polystyrene and polycarbonate. A polymeric glycol was first prepared by saponification of a benzoate terminated polystyrene oligomer. Treatment of the polystyrene glycol with a large excess of liquid phosgene resulted in the formation of the corresponding bischloroformate. An interfacial technique was employed to couple the bisphenol-A polycarbonate oligomer ($\bar{M}n$=3300) and polystyrene glycol ($\bar{M}n$=2700) into a high molecular weight copolymer. About 20% of the polystyrene, however, remained unreacted and had to be extracted from the copolymer. The author reported that brittle amorphous films could be cast from solution. The mechanical properties were intermediate between those of the homopolymers, but tended toward the polystyrene side.

Berger et al.[139] synthesized polystyrene diacid chlorides from living polystyrene oligomers via the reaction of excess phosgene with the sodium endgroups of the oligomers. The polymeric diacid chloride which resulted had a viscometry average molecular weight of 18,000. Block copolymers were prepared by phosgenation of a mixture of bisphenol-A and the polystyrene oligomer in toluene at 0°C. Unreacted styrene amounted to only 1% of the original mixture and a yield of >95% was obtained. The melt flow properties of the copolymers were studied as functions of shear stress and composition. It was found that the total

amount of styrene in these systems governed the viscosities to a greater extent than block length. The copolymer melt viscosities were much lower than that of pure polycarbonate.

The search for new types of thermoplastic elastomers has prompted many investigations of block copolymers of polycarbonate and elastomeric materials. Goldberg[140] has completed an extensive study of block copolymers derived from polycarbonate and a large variety of polyether glycols. Solutions of bisphenol-A and polyether glycol in pyridine were phosgenated to high molecular weight. The range of glycol molecular weights ($\bar{M}n$) was 1,000 to 20,000 and the copolymer compositions varied from 5 to 70% polyether in the case of poly(oxyethylene) based copolymers. These materials comprised the bulk of Goldberg's study. At 50:50 weight percent compositions, copolymers derived from poly(oxyethylenes) of 1,000, 4,000 and 6,000 block length displayed elastomeric properties with excellent recovery properties, along with high tensile strengths and ultimate elongations of 700%. A compositional study on copolymers of constant polyether block length ($\bar{M}n$=4000) indicated that a maximum in stiffness occured at ~15% of the polyether. This result was explained on a basis similar to that described for antiplasticization; some of the free volume of the matrix was filled by the additive, resulting in a higher modulus. At ~30% poly(oxyethylene) content the tensile yield stress dropped dramatically from 8000 to 2000 psi and the percent elastic recovery increased from ~20 to 90%. The glass transition temperature of the copolymers decreased from ~130 to 20°C between 0 and 40 wt % of the polyether.

The polycarbonate block copolymers which have received the most attention are those derived from poly(dimethyl siloxane) (PDMS). Vaughn[141] first prepared such materials by capping chlorine terminated PDMS oligomers with bisphenol-A and reacting them with phosgene and more bisphenol in a pyridine-methylene chloride solution. The structure and properties of the copolymers have been studied in great detail by Kambour[142-146] and Le Grand.[147-148] They found that microphase separation occured in cast films due to the large difference in solubility parameters between polycarbonate ($\delta \simeq 9.6$) and PDMS ($\delta \simeq 7.5$). In a copolymer comprised of 35% polycarbonate, for example, polycarbonate domains on the order of 70-190 Å were observed.[143] The phase separation persisted even at polycarbonate block lengths as low as 875 when the siloxane molecular weight was 1500. Like the polysulfone-PDMS block copolymers described earlier, melt processibility of the carbonate containing analogs was poor.

Tensile studies by these investigators showed an increase in ultimate elongation (100-800%) with increasing siloxane content (35-85%) along with a simultaneous decrease in tensile strength (6000-1000 psi). As expected, the mechanical properties changed from elastomeric to rigid over the same composition range.[146]

Kambour[145] has examined the impact strength of some representative copolymers. The introduction of 15 and 25% siloxane lowered the brittle-ductile transition temperature from -15°C to -45 and -110°C respectively while decreasing the tensile modulus and yield stress. The copolymers also displayed better flame retardance than polycarbonate

alone.

Single crystals of polycarbonate-PDMS copolymers were grown by Le Grand[148] from methylene chloride-methyl ethyl ketone solutions. The crystals exhibited higher melting points than those of polycarbonate alone but lower heats of fusion. This was explained on the basis of the closer hexagonal packing in the copolymer crystals than that of orthorhombic polycarbonate single crystals.

3. Polysulfone/Polycarbonate Blends. A few references, mainly patents, dealing with blends of polysulfone and polycarbonate can be found in the literature. The earliest appears to be a patent granted to Union Carbide Corp. in 1966.[149] Blends of bis-A polysulfone and bis-A polycarbonate were prepared at 290°C in a two roll mill and compression molded into sheets. Tensile testing of these blends indicated their ductile nature as evidenced by a yield point and 5 to 30% elongation after yielding.

Myers and Brittain[150] prepared blends of polysulfone and polycarbonate in various weight percentages (5 to 95% PC) by dissolving the polymers in methylene chloride, and evaporating the mixtures to films which were ground and molded. The low temperature loss peaks (-100°C) of each homopolymer and the blends were investigated as functions of composition and thermal history. Single low temperature loss peaks were observed for both polysulfone and polycarbonate homopolymers, whereas a second peak appeared only in the blends containing 75% polysulfone. As this composition coincided with the point of phase inversion in the mixtures, the authors speculated that the second peak

resulted from more intimate mixing of the chains at the phase inversion point.

Films, consisting of a 50:50 mixture of polysulfone and polycarbonate, have been prepared with lower static friction coefficients than either of the two homopolymers.[151] The films were cast from solution (CH_2Cl_2) onto polyester sheets.

A Russian reference[152] described the preparation of blends in a Brabender plastograph at 280°C. The dynamic modulus of the mixtures increased with polysulfone content and the heat resistance was found to be greater than that of polycarbonate alone.

Binsack et al.[153] have obtained a German patent for an extruded film consisting of a mixture of bis-A polysulfone ($\bar{M}w$=20,000) and bis-A polycarbonate ($\bar{M}w$=30-95000). The blends were reported to have similar mechanical properties but better solvent resistance than either of the components.

F. Impact Testing

The impact resistance of polymeric materials often determines their usefulness in many applications. Substitution of plastics for wood, metal, or ceramic parts is determined, to a large extent, by the mechanical durability offered by the replacement materials. Accurate evaluation of a polymer's impact strength is, therefore, essential if optimum part performance is to be obtained.

The impact strength of polymers is one of the most difficult properties to measure. Besides being dependent on the polymer structure itself, the fabrication and environmental conditions, as well as the

type and frequency of the impact, also affect impact resistance. Numerous types of testing machines have been developed for evaluating impact strengths of materials. These include weighted pendulum devices, falling weight testers, tensile impact machines, and numerous specialized techniques. The first two methods are by far the most common, and several variations of each have been chosen as standard testing procedures.

1. Conventional Testing Apparatus

(a) Pendulum Impact Testers. The impact testing technique most popular in the U.S.A. is the Izod pendulum test. In this method, a test specimen is clamped in a vertical cantilever position and then struck by a weighted pendulum. After fracturing the specimen, the pendulum continues on its arc. The height of the excess swing is noted and taken as a measure of the specimen's impact strength. At least ten specimens are necessary to satisfactorally determine a material's impact strength.[154] The standard Izod test is designated D 256-56 by the ASTM.

A similar technique, the Charpy test, is popular in Europe. In the U.S.A., it is designated as ASTM (D 256-56) Method B. In this test the specimen is held horizontally between two supports and struck centrally by the swinging pendulum. Again, the height of the pendulum swing after impact is taken as a measure of the impact strength of the test material.

Test bars for both the Izod and Charpy tests are usually notched in order that the specimen be subjected to the severest impact

conditions. Notching also reduces the effects of random flaws and, thus, limits scatter in the data.[155] However, the shape and method of obtaining the notch require special consideration and are, therefore, carefully specified. Notches must be accurately and reproducibly cut into injection molded specimens or otherwise wide variations in the data will result. Notches cannot be molded into such specimens because the residual stress concentrations near the notch alter the impact strength. The fact that some materials are more notch sensitive than other introduces additional complexities to these techniques.

The total fracture energy, as measured by pendulum type tests, is made up of several components. These factors include the energy to: a) initiate fracture, b) propagate fractures, c) throw the broken test piece, d) deform the specimen plastically, and e) vibrate the apparatus.[156] Large errors may arise if suitable corrections are not applied to the data.

Analysis of pendulum impact data is complicated by the large number of test specimens required and the critical importance of notch size. The results of either the Izod or Charpy test are usually expressed in foot-pounds per inch of notch. Additional disadvantages of the pendulum tests include the dependence of impact strength on clamping pressure[154] and the difficulty encountered in achieving thermal control of the specimen.

(b) Tensile Impact Tests. Tensile impact tests have evolved out of the necessity for more reliable quality control instruments as well as overcoming various problems related to the Izod and Charpy tests.[157]

One method, which involves a simple adaptation of a pendulum impact device, has achieved acceptance in the United States and is designated ASTM D 1822-61. In this test, one end of a standard tensile specimen is clamped into the pendulum head while the other is clamped in a crosshead clamp. The size of the pendulum head is such that it will pass between two anvils which are contacted by the crosshead clamp. After the specimen fractures, the pendulum continues on its arc, the height of which is taken as a measure of the specimen impact strength as before. Five to ten test specimens are recommended and the results are expressed in foot-pounds per unit area of the specimen.

Tensile impact devices have several advantages over Izod and Charpy instruments. First, there is no need for notching, so test specimens may be cut from actual moldings and evaluated in the direction of or at any angle to molecular orientations arising from the molding process. Also, such tests permit the use of small test specimens and, therefore, require less material from the start. Like the other pendulum devices, the tensile impact test is subject to corrections for friction and bouncing of the crosshead. The use of such tests has been discussed by several authors.[158,159]

(c) Falling Weight Tests. Guided falling weight impact testers, while not as popular as the pendulum types, do simulate the types of impact encountered during actual use. Generally, the technique is limited to films or flat plates, but equipment for testing plastic tubing and other shapes has been developed.[160]

The dropped weight may be either a ball striker or a pointed dart

(tup) to which variable weights may be attached. Testing specifications include sample geometry, tup dimensions and weight, and drop height. To minimize wobbling of the dart during flight, teflon guides or air bearings are utilized to reproducibly direct the tup to the target. Additional accuracy may be gained through use of an electromagnetic dart release mechanism.

Clamping of the specimen is an important consideration as in the case of pendulum impact testers. The specimen holder must have a hole cut through it to allow passage of the tup. A vacuum, applied from beneath the specimen, can be employed to hold uniformly flat specimens under reproducible conditions.[154] A clamping ring may also be used to hold the specimen. Pressure on the ring may be applied pneumatically or mechanically, but it must be reproducible if consistent results are to be maintained.

Falling weight tests rarely correlate with either of the pendulum tests. The notched specimens used in Izod and Charpy experiments require only a small amount of energy to initiate a crack and the measured fracture energy is largely that required to propagate the crack. To fracture a sheet of the same material, a major portion of the fracture energy may be required to initiate a crack.[154] Moreover, specimens for pendulum impact tests are usually injection molded and, as mentioned previously, contain residual stresses. Falling weight tests on relatively stress free compression molded sheets should yield somewhat different results. If any anisotropy does exist in the sheet, and leads to failure in a certain direction, for example, visual

observation of such behavior can be readily made.[154]

An additional advantage of the falling weight tester is the relatively easy thermal control of the specimen. The test specimen may be enclosed in a thermostated block equipped with holes for passage of the tup. During the time required for thermal equilibration, the holes can be closed with plugs which are then removed immediately before the tup is dropped.

The chief disadvantages of conventional falling weight impact testing are the difficulty in measuring the fracture energy directly and the large amounts of material needed to establish the failure level. Unlike the Izod or Charpy tests, there is no convenient way to measure the energy absorbed by the specimen so the fracture energy is determined statistically. Currently, two methods of analysis are employed. The Probit method involves testing groups of samples at specific energy levels between the limits of 0 and 100% failure. The results are plotted on probability paper as impact energy vs. failure percentage and the 50% failure level defined as the fracture energy of the material. Although the method provides an insight into the failure distribution, it requires a very large number of test specimens, sometimes as many as 50.[161]

The second method, or Bruceton staircase technique, concentrates testing around the mean fracture level automatically. Initially, a specimen is tested from some energy level. Should the specimen fail, the next specimen is tested at a lower incremental energy, and so on until one specimen passes the test. The height of the next drop is

raised and the procedure continued until a minimum of twenty specimens are tested. The 50% failure level is again reported as the impact strength.

Moritz[161] has developed a third technique for statistically estimating the impact strength of materials measured by the falling weight test. The technique, called a fail-sensitivity method, is basically a combination of the Probit and Bruceton staircase methods.

2. Instrumented Impact Testers

Instrumented impact testers have achieved widespread popularity within the past decade. Unlike conventional impact test equipment, the instrumented devices provide detailed force vs. time plots of the impact process. Such tests can provide data concerning loading patterns and failure mechanisms whereas similar non-instrumented tests yield only the energy required to break the specimen. The instrumented devices are also at an advantage where mixed failure modes are possible. In this section, only previous work dealing with instrumented pendulum and falling weight testers will be considered. High speed tensile testing devices are relatively common.

(a) Pendulum Testers. In 1962, Wolstenholme[162] described the application of an instrumented Izod device which consisted of a transducer activated by the test specimen and wired to an oscilloscope to display the output. A camera was used to record the oscilloscope trace. Three different types of force vs. time curves were obtained for various types of test materials. Brittle polymers provided a linear increase in force with time up to the failure point where upon the

force immediately fell to zero. The second type gave evidence of a yield point followed by ductile drawing while the third type was characteristic of yielding followed by tearing. Representative curves are provided in Figure 4. Force vs. time curves were presented for five commercial thermoplastics and gave good agreement with results from uninstrumented Izod tests.

In a later paper,[163] the same author presented impact data as functions of notch width and temperature for ten thermoplastics. No specific trend for any of the materials was observed as the notch width was varied from 0.125 to 0.5 inches. The peak force exerted on the specimens did, however, increase with notch width.

Wolstenholme pointed out the fact that rate of loading was not constant throughout the duration of the impact and that rate effects could seriously affect the measured impact strengths. However, he found that the measured fracture energies were constant provided that the energy to break comprised no more than 67% of the available kinetic energy of the pendulum. Another important finding was that the measured impulse from the oscilloscope trace did not correspond to the impulse exerted on the pendulum as determined from the excess swing for ductile materials. The measured impulses for materials such as polycarbonate were always lower. Brittle materials displayed a 1:1 correspondence. The reduced specimen cross section upon yielding apparently did not produce the same reaction on the transducer provided by the original cross section.

Arends[164] has also reported impact results obtained from an

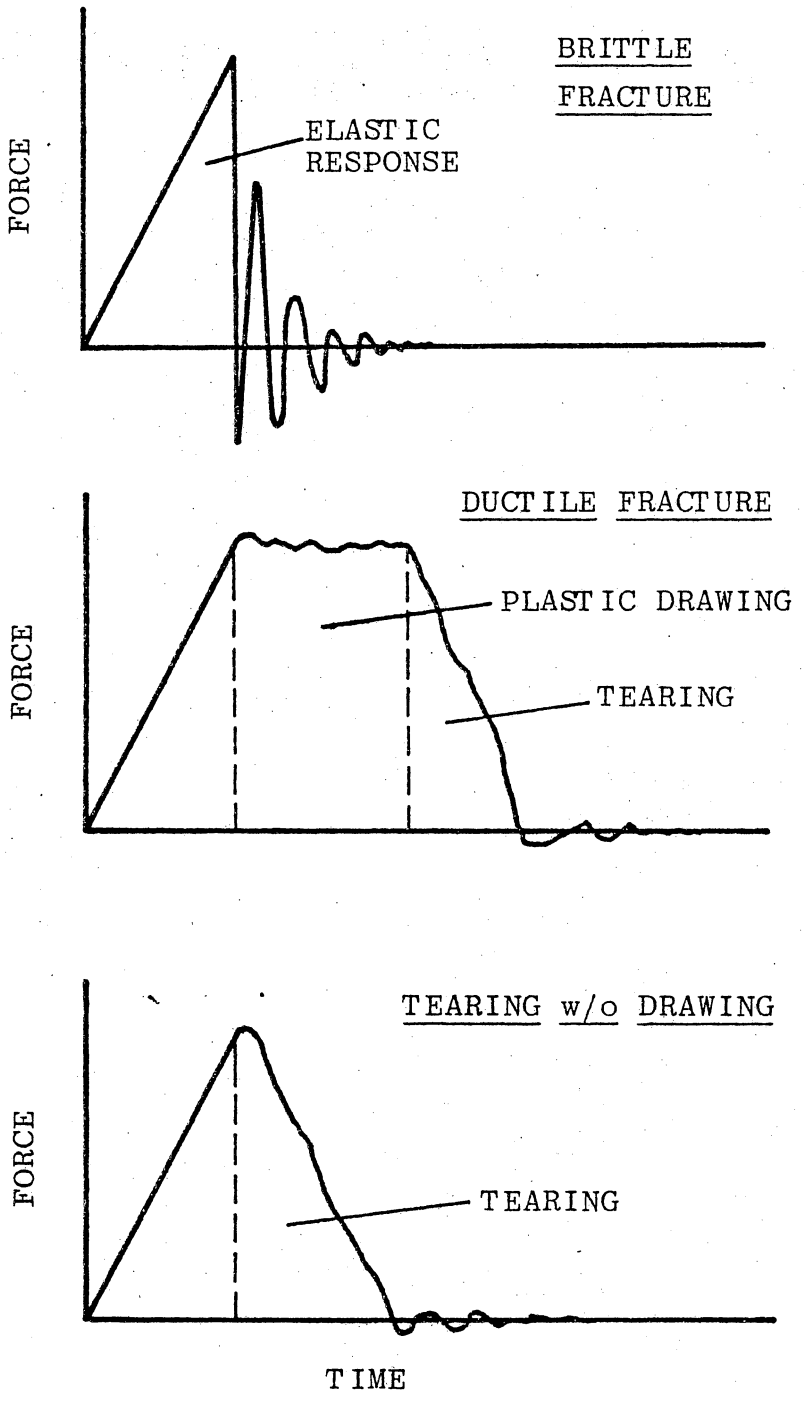

Figure 4. Generalized force-time curves obtained from an instrumented Izod impact device(after Wolstenholme(162)).

instrumented Izod tester. His work was concerned with characterizing the failure of unnotched specimens in which three contributions to the material response were considered: beam bending, shear at the clamp faces, and compression of the material at the strike point. An equation involving corrections for the above terms was derived and a value for the modulus calculated. Surprisingly, the modulus so calculated was nearly equal to that determined via stress-strain testing for polystyrene. A series of force-time curves representing the impact response of impact polystyrene as a function of temperature were also presented. The curves are reproduced in Figure 5. Note the transition from brittle to ductile failure as the test temperature is increased.

A study of ABS plastics containing different amounts of rubber has been carried out by Lubert et al.[165] using an instrumented Izod device. At a temperature of 25°C, the fracture mode was shown to progress from brittle to intermediate to ductile as the rubber content varied from 0-40%.[166] The authors gave reasons for taking the maximum force sustained by the specimen as a better index of impact strength than the energy to fracture since it represented a threshold beyond which yielding or brittle failure occured.

An instrumented Charpy device capable of measuring deflection as well as load vs. time has been described by Radon.[167,168,169] Notched specimens of rigid PVC were precracked in order that the measured fracture energies would represent only that necessary to propagate the crack. The fracture toughness or stress intensity factor (K_{1c}) was evaluated through the application of linear elastic fracture mechanics.

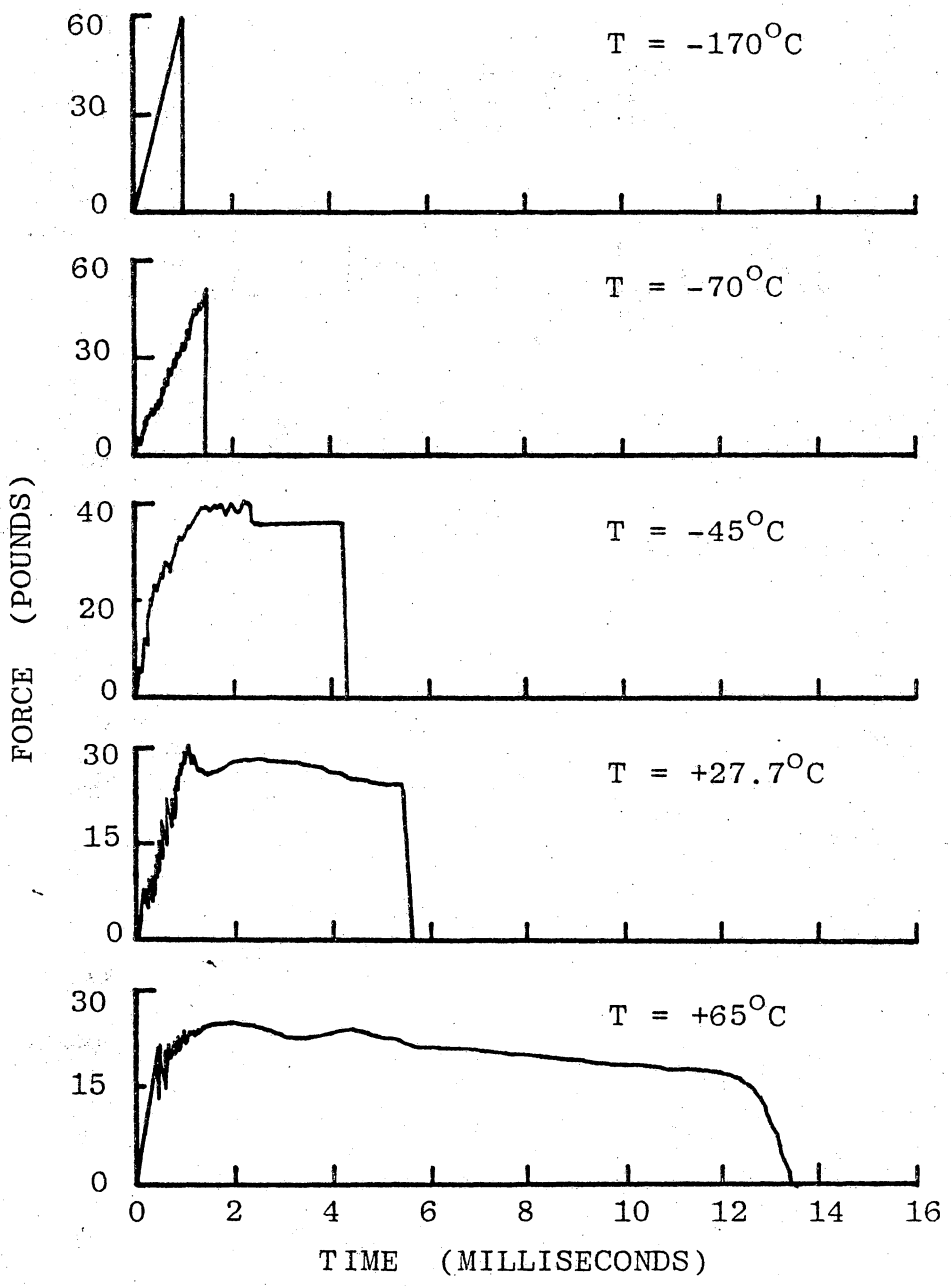

Figure 5. Force-time curves obtained for impact-modified polystyrene at several temperatures (after Arends[164]).

The stress intensity factor relates the applied stress necessary for fracture to the size of a crack or other defect and the elastic field surrounding the crack tip. A means of calculating K_{1c} from the impact data was derived on the basis of a technique for evaluating the same under conditions of static three-point bending. Radon found that the static toughness of rigid PVC was greater than the dynamic toughness from -197°C to room temperature.[167] The strain rate dependence of PVC toughness was found to decrease over the same temperature range. At room temperature, the impact and static toughness were nearly identical.

At low strain rates (20 mm/sec), nearly linear load-displacement curves were obtained whereas at much higher strain rates (5000 mm/sec), the curves became oscillatory. In such tests the fracture toughness would not be evaluated directly. A special type of "low blow" or low speed impact test was developed to provide a model for calculating K_{1c} at higher strain rates.[169]

(b) Falling Weight Tests. Perhaps the earliest description of an instrumented falling weight impact test is that due to Fujioka.[170] The device dropped a heavy dart on a clamped specimen from a fixed height of 45 cm. The dart contained an accelerometer which permitted the deceleration of the weight, as it struck and pierced the specimen, to be followed with time on an oscilloscope. Load vs. time curves were also obtained via a stress gauge in the specimen clamp. An environmental chamber was constructed around the sample clamping assembly such that the temperature could be varied from -50 to +50°C. The integral of the acceleration time trace between the time of first contact (t_1) and

$$\int_{t_1}^{t_2} a(t)\, dt = \Delta v = v_2 - v_1$$

specimen failure (t_2) gave the change in velocity of the falling dart. The puncture energy (E) was expressed by the relation

$$E = 1/2\ M\ (\Delta v)^2$$

where M is the mass of the dart. This reported equation does not appear correct since the difference in kinetic energies before and after impact should be used as follows:

$$E = 1/2\ M\ (v_1^2 - v_2^2) = E_1 - E_2$$

Fujioka examined the impact properties of polypropylene homopolymers and a series of ethylene/propylene copolymers. A direct correlation between puncture energy and yield strength obtained in a tensile impact test was found for both brittle and ductile compositions. The author concluded that the energy to fail in ductile systems depended mainly upon deformation after the yield point. In brittle systems, the ultimate strength governed the measured puncture energy.

Cessna et al.[171] have also constructed an accelerometer equipped falling weight impact tester. The acceleration-time curves were integrated once to provide a velocity-time curve of the impact and a second time to provide a displacement-time curve. Force-deflection plots were obtained by crossplotting acceleration and displacement data. The authors calculated fracture energies for unfilled, impact modified,

and fiber reinforced polypropylene by integrating the force-displacement curves up to the failure point. An important point was made concerning the effects of different weights or drop heights. It was found that the energy to fail measured for brittle specimens was independent of the weight or drop height providing that enough energy was available to fracture the specimen. In the case of ductile materials, however, significant reductions in impact strength were observed when increased drop heights were employed. The authors indicated that the projectile velocity, and hence the local deformation rate, at failure initiation was the controlling variable, not drop height or weight. A study of the impact response of polypropylene between -90 and 0°C was carried out using an environmental chamber. The brittle ductile transition of unmodified polypropylene was located at approximately -30°C whereas that of an impact modified material occured at roughly -70°C.

By mounting a strain gauge transducer behind the impacting tup, Gonzalez and Stowell[172] obtained force-time traces directly from a falling weight device. The transducer was calibrated on a tensile tester prior to any experimentation. Polypropylene, cellulose acetate butyrate, and a series of polyesters were investigated. Excellent agreement between the autographic technique and normal falling weight data was obtained. In contrast to Fujioka[170] and Cessna[171], these workers found that the energy absorbed by the specimen was essentially independent of drop height or weight. However, it should be pointed out that the materials in question were in fact rather brittle. Highly ductile polymers such as polycarbonate or polyethylene were not examined.

III. Experimental Procedure

A. Polymer Synthesis

1. Poly (aryl ether sulfones). As mentioned earlier, three different types of poly (aryl ether sulfones) were investigated during the course of this study. Since this author participated very little in the synthesis of the various materials employed here, only brief descriptions of their synthesis will be given.

Bisphenol-A polysulfone oligomers were prepared from high purity bisphenol-A and 4,4' dichlorodiphenylsulfone (DCDPS), both obtained from Union Carbide Corp.* The oligomers were prepared according to the reaction scheme below which has been described elsewhere.[85]

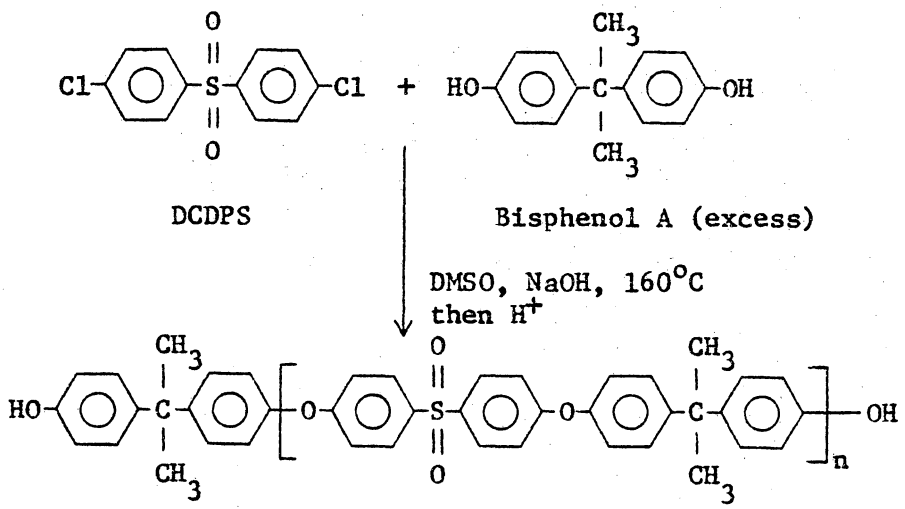

Hydroxyl termination of the oligomers was insured by using a calculated excess of bisphenol-A which also permitted the molecular weights to be

*Union Carbide Corp., Bound Brook, NJ

controlled. Bisphenol-T polysulfone oligomers were prepared using the same procedure except that 4,4'-thiodiphenol* was substituted for bisphenol A.

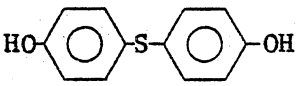

4,4'-Thiodiphenol(Bisphenol-T)

Bisphenol-S polysulfone oligomers were prepared from 4,4'-difluorodiphenyl sulfone and 4,4'-sulfonyldiphenol* as shown below.

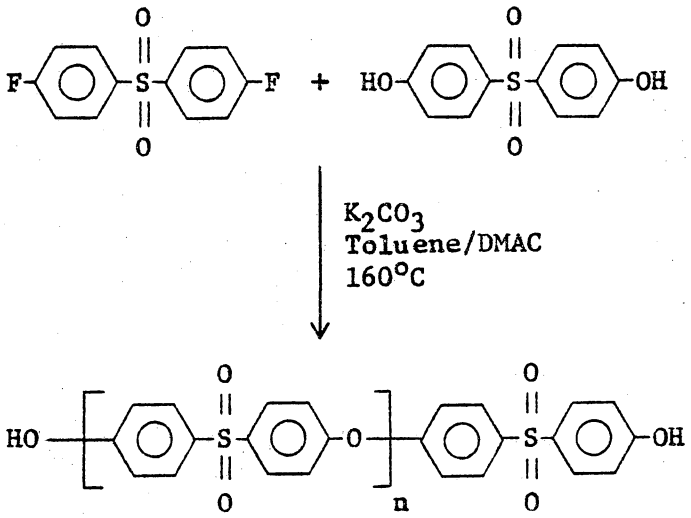

Again, an excess of the bisphenol was employed to insure hydroxyl termination of the oligomers.

2. Polycarbonate Oligomers. Bisphenol-A and phosgene were utilized to prepare hydroxyl terminated polycarbonate oligomers. An interfacial technique,[115] involving the phosgenation of bisphenol-A in

*Crown Zellerbach Corp., Camas, Washington

methylene chloride in the presence of an aqueous phase containing a phase transfer catalyst (tetraethyl ammonium chloride) and sodium hydroxide, was used. The reaction mixture was rapidly agitated in a Waring Blender while phosgene was bubbled through it at a controlled rate.

3. Polysulfone - Polycarbonate Block Copolymers. For the most part, the polysulfone-polycarbonate block copolymers were synthesized interfacially using the same procedure described above for the polycarbonate oligomers. Bisphenol-A or bisphenol-T oligomers and polycarbonate oligomers were dissolved in methylene chloride and phosgenated to form block copolymers. However, the bisphenol-S polysulfone oligomers were not soluble in methylene chloride which necessitated the use of tetrachloroethane for the coupling reaction. A typical synthesis of a bisphenol-S polysulfone-bisphenol-A polycarbonate copolymer is outlined below.[173]

Bis-S-polysulfone oligomer (5.0 g, $\bar{M}_n$ ~ 5300 by titration) and Bis-A-polycarbonate oligomer (5.0 g, $\bar{M}_n$ ~ 5000 by UV) were dissolved in 300 mL of tetrachloroethane in a hood. The solution was somewhat hazy even at these concentrations. (By contrast, Bis-A-polysulfone oligomers and Bis-A-polycarbonate oligomer yield clear solutions at comparable molecular weights and concentrations.) Separately, 0.2 g of sodium hydroxide and 2.0 g of tetraethyl ammonium chloride were dissolved in 120 mL of distilled water. The oligomer solutions and the aqueous solution were combined in a Waring blender. The blender was fitted with a phosgene inlet. A combination pH electrode connected to a digital pH

meter (Orion 601) was used to monitor pH during the polymerization. The two layers were rapidly mixed and phosgene addition was started. A reaction time of 30 min. was used, although high molecular weight could be achieved at considerably shorter times. The pH was maintained at about 8.8 via addition of 20% sodium hydroxide solution from a buret. After the phosgene flow was stopped, the reaction product was placed in a separation funnel for 30 min. An organic phase and a "foamy" aqueous layer separated. The organic phase was precipitated in excess isopropyl alcohol separately from the foam layer. Each precipitate was collected by vacuum filtration, washed with three 200-mL volumes of isopropyl alcohol, three 200-mL volumes of distilled H_2O, and then one 200-mL volume of isopropyl alcohol. The two precipitates were dried 24 hr. at 120°C under an aspirator vacuum (~30 Torr).

7.59 g were collected from the organic phase and 2.33 g from the "foamy" layer. DSC studies of each precipitate were identical. Two T_gs were observed at 166° and 229°C. Total weight was 9.92 g of copolymer (99% yield). Cast films from tetrachloroethane solutions were transparent and ductile. A compression-molded (280°C) film was transparent but brown.

B. Characterization

1. Molecular Weights.

(a) End Group Analysis. As mentioned previously, both the polysulfone and polycarbonate oligomers were prepared with phenolic end groups which permitted simple and rapid analyses to be developed. A technique developed by the author and others[174] to potentiometrically

titrate the end groups of polysulfone oligomers will be described in detail here.

Titrations in nonaqueous media are particularly useful in the analysis of organic acids and bases. In addition to dissolving water insoluble substances, the use of nonaqueous solvents greatly extends the range of acid and base strengths which can be determined by direct neutralization. Moreover, the proper solvent choice permits acids or bases of different strengths to be distinguished simultaneously. Substances sensitive to the presence of water can also be analyzed in nonaqueous media. The scope of nonaqueous titrimetry is extensive and the topic has been reviewed in depth by several authors.[175-178]

Phenolic compounds are usually so weakly acidic that they cannot be titrated in water. In basic nonaqueous solvents such as ethylenediamine,[179] dimethylformamide,[180] pyridine,[181] and dimethylsulfoxide,[182] phenols can be titrated as very weak acids. In actual fact, weak acids can be analyzed in solvents less acidic than they are providing the titrant is a strong base.[182] Neutral aprotic solvents such as acetone,[183] methylethylketone,[184] or methylisobutylketone[185] have been utilized for potentiometric titrations of phenols with satisfactory results.

Deal and Wyld[180] have described a potentiometric method of titrating phenols, dihydroxy phenols, and polyphenolic compounds in DMF and ethylenediamine solvents utilizing a glass-calomel electrode system. Alcoholic solutions of potassium hydroxide and tetrabutylammonium hydroxide were investigated as titrants.

The titrations carried out in DMF using tetrabutylammonium hydroxide as titrant were found to be superior to those employing other solvent-base combinations for several reasons. First, because DMF was less basic than ethylenediamine, the titration took place over a much wider millivolt range, enabling the endpoint potentials to be more readily determined. Secondly, most tetraalkylammonium salts of weak acids remain soluble and such bases can be used with ordinary glass electrodes without affecting electrode performance.[175]

End group analysis of functionally terminated polymers may also be accomplished by nonaqueous titration. Molecular weight determinations of condensation polymers with poor solubility characteristics, such as polyamides and polyesters, can be carried out using relatively low cost equipment. A recent review by Garmon[186] evaluates these procedures as well as other types of end group analysis.

(i) Apparatus. An Orion 601A* digital pH meter was used in conjunction with a glass electrode** (Thomas, No. 4092-F15) and a calomel reference electrode** (Thomas, No. 4090-B 15). Several 40 mm diam. x 65 mm high glass vials equipped with tight fitting polyethylene caps served as titration vessels. Holes in the cap to permit passage of the electrodes, syringe, and nitrogen inlet were carefully sized so as to retain a tight seal.

The titrant was dispensed by means of a 2 ml Gilmont microburet** (Thomas, No. 1996-B55), graduated in 0.002 ml increments, and equipped

---

* Orion Research, Inc., Cambridge, Mass.
** A. H. Thomas Co., Philadelphia, PA

with a Luer syringe tip. The solution was mixed via a small (4 mm x 10 mm) teflon coated stirring bar - magnetic stirrer system. A schematic diagram of the apparatus is given in Figure 6.

(ii) Reagents. Practical grade DMAC (Eastman Kodak Co.) was vacuum distilled over calcium hydride and stored under argon in a sealed flask. An alternative procedure involved the passage of DMAC through a basic alumina* column (Fisher Certified Basic Alumina, Brockman Activity 1) immediately before beginning a titration. The column measured 45 cm long by 2.5 cm in diameter and contained approximately 500 grams of alumina. One liter of DMAC could be safely purified of acidic contaminants in this manner before the alumina was saturated.

Tetraethylammonium hydroxide (10% in water, Eastman Kodak Co.) was diluted to approximately 1.0% with distilled water. The concentration of the base was then accurately determined by titration with standardized 0.1 N HCl. Water was employed as the diluent, rather than isopropanol, because quaternary ammonium bases are known to be less stable in weakly acidic solvents such as alcohols.[180] Moreover, the presence of isopropanol, an effective nonsolvent for polysulfone, might be likely to cause precipitation of the polymer during the titration.

(iii) Procedure. Preconditioning electrodes in nonaqueous media allows for fast and relatively reproducible potential measurements to be made.[175] In this study, new glass and calomel electrodes were immersed in DMAC for three days before they were used in any titrations.

---

*Fisher Scientific Co., Pittsburg, PA

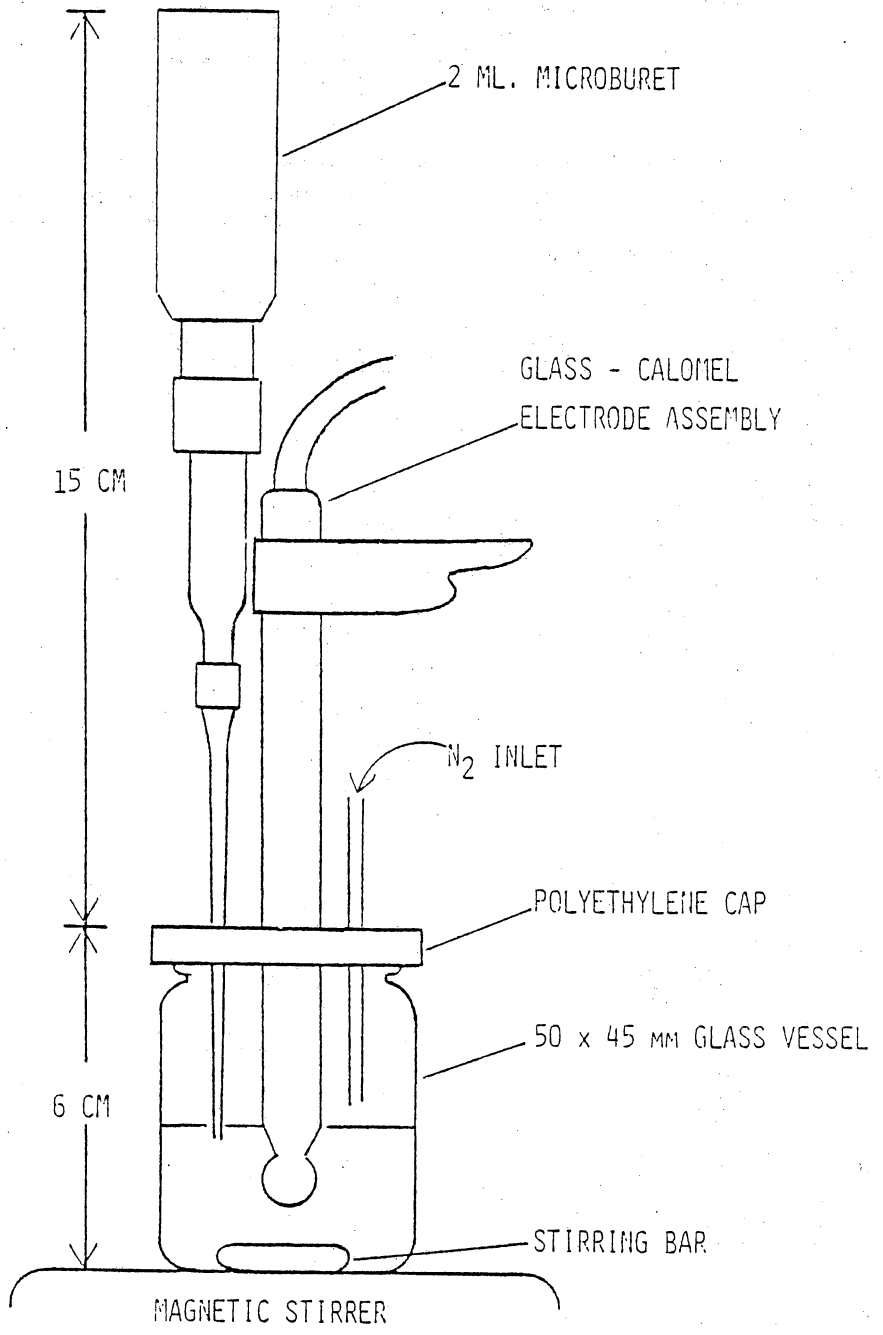

Figure 6. Apparatus for potentiometric titrations.

Immediately before starting a series of molecular weight determinations, a blank titration of the solvent was made employing the same procedures to be followed in the actual experiment. The electrodes were then rinsed with clean DMAC and allowed to dry.

A sample of hydroxyl terminated polysulfone was accurately weighed into a titration flask and dissolved in 20 ml DMAC with stirring, while dry, CO_2 free, nitrogen was passed over the solution.

Thirty minutes was allowed to complete dissolution of the polymer, after which, the electrodes were immersed in the solution and the buret lowered such that the tip just pierced the surface. After recording the initial volume and cell potential, 0.05 ml portions of titrant were added, followed by a 30 second period to allow for stabilization of the cell potential. In the vicinity of the equivalence point the volume increments were decreased to 0.01 ml. If the cell potential reached a maximum and then decreased slowly with time, the maximum reading was recorded.[180] The titration was continued until the cell potential dropped steadily with each addition of titrant. Throughout the analysis the nitrogen flow was maintained at a slow steady rate.

After plotting both the blank and experimental titrations as volume of titrant vs. the corresponding millivolt reading, the endpoints were determined using the second derivative technique. The molecular weight of the polymer was calculated from the equation

$$M = \frac{2\ (W)}{(v)\ (c)}$$

where

W = weight of sample in grams

V = volume of titrant in liters (corrected for the blank)

C = concentration of titrant in moles per liter.

A series of model bisphenol compounds was employed to monitor the accuracy of the titration. Their structures are provided in Table V. Titrations involving these compounds were carried out using 10% TEAOH due to their low molecular weights (218-366 g/mole).

Polycarbonate oligomers were rapidly degraded by strong base and could not be titrated. However, a uv spectroscopic analysis was employed to assess their hydroxyl content. The details of this procedure have been described elsewhere.[187]

(b) Gel Permeation Chromatography. The molecular weight distributions of the oligomers and copolymers were determined on a Waters* high pressure liquid chromatograph. Tetrahydrofuran (THF) solutions, approximately 0.2 weight percent concentration, were carefully filtered and injected into the chromatograph at a flow rate of 1.0 ml/min at 25°C.

Dual U.V. and differential refractometer detectors were used.

(c) Membrane Osmometry. The number average molecular weights ($\bar{M}_n$) of high molecular weight oligomers (Mn > 20,000) and block copolymers were determined with a Wescan** Model 231 recording membrane osmometer. Unlike classical osmometry in which changes in the height of a column of solution are measured, the Wescan device measures the osmotic

---

* Waters Associates, Milford, Mass.
**Wescan Instruments, Inc., Santa Clara, CA

pressure in a feed-back mode. A stainless steel cell is divided into two chambers, one for solvent, the other for solution, separated by a thin cellulose membrane.* One wall of the solvent chamber is a flexible diaphragm connected to a strain gage detection system. As solvent molecules diffuse through the membrane, the flexible diaphragm compensates for the change in volume which is coincident with the change in osmotic pressure. The osmometer is calibrated with pure solvent in each chamber. The solution inlet is filled with solvent to an arbitrary level to provide a zero point. The meniscus is lowered 5 cm and the recorder set to full scale.

A series of four or more concentrations of the polymer under investigation (2-10 g/l) were prepared in chlorobenzene and carefully filtered to remove dust and other debris. An aliquot of solution was injected into the inlet tube of the osmometer and the level set to that established during the calibration steps. The change in pressure with time was followed directly on a strip chart recorder until a constant pressure level was achieved. At least two points were obtained for each concentration. The results were plotted as π/c vs C and extrapolated to zero concentration. From the theory of membrane osmometry,[188]

$$\lim_{c \to o} (\pi/c) = \frac{RT}{\langle M_n \rangle}$$

where R is the gas constant and T is absolute temperature in degrees Kelvin. The operating temperature was kept constant at 40°C throughout

*Type RC-52, Arro Laboratories, Joliet, Ill.

the study.

(d) Dilute Solution Viscometry. The intrinsic viscosity [n] of each oligomer and copolymer prepared during this study was determined in THF at either 25° or 30°C. The theory of dilute solution viscometry has been presented elsewhere[189] and will not be considered here.

Two ml of filtered THF were added to a semi-micro dilution viscometer* and placed in a thermostatted water bath to equilibrate for least ten minutes. Using nitrogen pressure, the solvent was forced up the viscometer tube until the meniscus rose above the upper fiduicial mark. The solvent was then allowed to drain through the tube and the time for the meniscus to pass the two marks measured with a stopwatch to the nearest 0.1 sec. At least three readings within 0.2% were taken and the average value noted as the solvent flow time t_o. Next, an aliquot of a previously prepared polymer solution (~20 g/l) was added to the viscometer such that the new concentration was approximately 10 g/l. After a ten to fifteen minute equilibration time, the solution was forced through the viscometer and its flow time determined. The same procedure was employed for at least three other concentrations prepared by continuously diluting the initial solution. The relative viscosity (η_r) was taken as the ratio of solution flow time to solvent flow time ($\eta_r = t/t_o$). Two terms, the reduced viscosity ($\eta_{red} = \frac{\eta_r - 1}{c}$) and the inherent viscosity ($\eta_{inh} = \ln \eta r/c$), were calculated for each

*Cannon Instrument Co., State College, Pa.

solution and plotted versus concentration. Extrapolation of both curves to zero concentration provided the intrinsic viscosity [η]. Comparison of [η] values for a series of similar oligomers provided an idea of their molecular weights relative to one another. Exact values of the Mark-Houwink constants, and their molecular weight dependence, would be needed for obtaining absolute values.[190]

2. Thermal Analysis. The transitional properties of polysulfone and polycarbonate oligomers, copolymers, and several commercial materials were studied by means of differential scanning calorimetry (DSC). DSC scans were obtained at 40°C/minute on a Perkin-Elmer* DSC-2 for dried polymer powders as well as solution-cast and molded polymer films. In cases where microphase separation was thought to be possible in the block copolymers, specimens of the dried polymer powders were annealed in sealed pans at temperatures as high as 300°C for periods extending up to three hours.

Heats of fusion were determined for several polypropylene impact specimens since their amounts of crystallinity affected their impact strength. Small pieces were cut from the specimens, accurately weighed on an analytical balance, and sealed in aluminum pans. A DSC trace was obtained for each specimen at 40°C/minute and a sensitivity of 20 millicalories/sec. A similar trace was also obtained for an indium reference (T_m = 156.6°C, ΔH_f = 6.8 calories/gram). At the melting points of these materials, an endothermic peak was observed, the area

---

*Perkin-Elmer Corp., Norwalk, Conn.

of which was proportional to the heat of fusion. The heats of fusion for the polypropylene specimens were calculated by cutting out the peaks and weighing them on an analytical balance and substituting these values in the relation below.[191]

$$\Delta H_{Sam} = \Delta H_{In} \times \frac{W_{In}}{W_{Sam}} \times \frac{P_{Sam}}{P_{In}} \times \frac{S_{In}}{S_{Sam}}$$

where W = weights of the samples, P = weight of the peak cut from the DSC curve and S = chart speed.

3. Mechanical Properties

(a) Dynamic Mechanical Response. A Rheovibron DDV-II* was employed to examine the dynamic mechanical response of the polysulfone-polycarbonate block copolymers between -160 and +250°C. Small samples (5 cm x 0.5 cm x 0.05 cm) of either cast or compression molded films were placed in the specimen clamps and subjected to a small sinusoidal tensile stress at a constant frequency of 3.5, 11, 35, or 110 Hz. By means of independent stress and strain gages both the applied stress and resulting strain were measured simultaneously. Owing to the viscoelastic nature of polymeric materials, the stress and strain were out of phase giving rise to a phase angle difference (δ) which was indicated directly on the Rheovibron as the tangent of the angle, or tan δ. The complex modulus (E^*) was also calculated from the Rheovibron data and plotted as a function of temperature. The specimens were enclosed in

*Imass, Inc., Accord (Hingham), Mass.

an environmental chamber and heated at a rate of 2°C/minute.

In order that the reader fully understands the meanings of tan δ and E^* a brief analysis of dynamic mechanical testing will be presented.[192] The diagram in Figure 7 will be called upon to provide a simplistic picture of stress and strain under conditions of forced vibration.

The sinusoidal stress applied to the specimen can be imagined as a vector in stress-time space rotating with frequency ω or $\sigma(t) = \sigma_o$ Sin ωt where σ_o is the maximum stress. As mentioned previously, the strain (ε) lags behind or is out of phase with the stress by the phase angle δ as shown in the figure. In the limit of small strains, polymers may be considered linearly viscoelastic materials implying that δ is a constant at a given frequency and temperature. Thus, one may write

$$\varepsilon(t) = \varepsilon_o \text{Sin } (\omega t - \delta).$$

It can also be seen that the stress vector can be represented by the sum of two components, one lying along ε_o and the other at right angles to ε_o. The two component stresses may be expressed as

$$\sigma' = \sigma_o \cos\delta \text{ and } \sigma'' = \sigma_o \sin\delta$$

Note that σ' is in phase with ε_o while σ'' is 90° out of phase. It follows that two different moduli (stress/strain) can now be defined, an in-phase modulus (E') and an out-of-phase modulus (E'') given by

---

*Imass, Inc., Accord (Hingham), Mass.

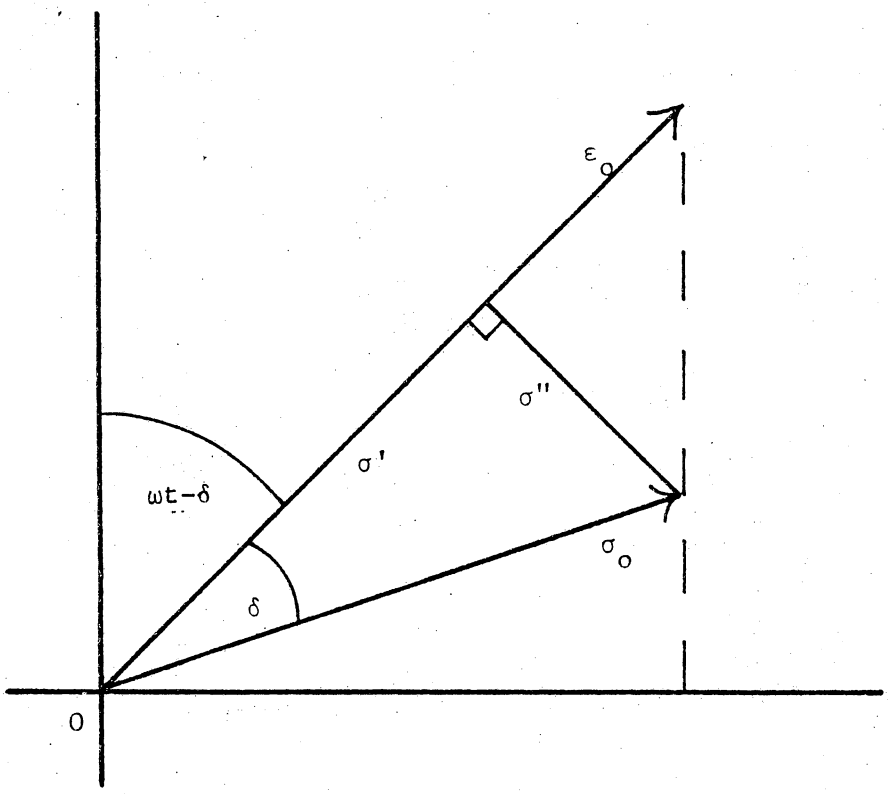

Figure 7. Schematic representation of stress (σ), strain (ε), and phase angle (δ) in sinusoidal oscillation (after Koo (192)).

$$E' = \sigma'/\varepsilon_o = (\sigma_o/\varepsilon_o) \cos \delta$$

$$E'' = \sigma''/\varepsilon_o = (\sigma_o/\varepsilon_o) \sin \delta$$

The ratio σ_o/ε_o yields the complex modulus (E^*) whereas the ratio E''/E' defines tan δ. The significance of E' and E'' rests with their proportionality, respectively, to the energy stored and the energy dissipated during each cyclic oscillation.

The low temperature loss peaks of polysulfone and polycarbonate have been thought to play a role in determining the impact strengths of these materials. Since the single or multiphase character of the copolymers was being compared, the effect of microphase separation on the low temperature (-100°C) loss peaks was also investigated.

(b) Tensile Testing. The stress-strain properties of some representative block copolymers and commercial homopolymers were examined on a Scott* tester. Thin polymer sheets (18 cm x 18 cm x 0.03 cm) were compression molded at 260°C and 15,000 lbs. pressure on a Dake** 44225 hydraulic press. Dogbone shaped test specimens were stamped from the sheets using an ASTM D412-E die.*** The specimens were held between the jaws of the pneumatic clamps at a pressure of 90 psi at 25°C and strained at two inches per minute until they fractured. At least five specimens of each polymer type were tested and average values for the yield stress and elongation as well as the ultimate stress and elongation were calculated. The yield values were

---

* CRE 500: GCA/Precision Scientific, Chicago, Ill.
** Dake Corp., Grand Haven, Mich.
*** Testing Machines, Inc., Mineola, N.Y.

taken at the point where the stress-strain curve achieved zero slope.

(c) Melt Rheology. The melt flow properties of polycarbonate, polysulfone, and several block copolymers were studied on an R-18 Weissenberg Rheogoniometer[‡] set up for cone and plate viscometry. This work was undertaken to see if the two phase block copolymers exhibited melt viscosities greater than their single phase counterparts. Such observations have been made for styrene-butadiene block copolymers.[35]

The theory of cone and plate viscometry has been discussed elsewhere.[193] The device consists of a flat plate and a truncated cone, between which a molten polymer sample is sheared. The gap between the cone and plate is set such that the imaginary tip of the cone just touches the plate. The angle between the cone and plate is kept very small, usually less than 1^{o}, such that the shear rate and shear stress are essentially constant throughout the gap.

In this study, a 1.0 inch (2.5 cm) diameter cone and plate was used. The cone angle was 2^{o} 1'25" and the gap set to 89μ. On the Rheogoniometer, the cone and plate were held vertically with the cone on the bottom or driven rotor. The plate was mounted on a universal air bearing rotor supported by a torsion bar, the purpose of which was to transfer the torque exerted on the plate to a transducer. The torsion bar constant (k_t) for these particular experiments was 10.06×10^3 dyne cm/μ.

Since the melt rheology experiments were run at elevated

[‡]Sangamo Controls, Ltd., Bognor Regis, England.

temperatures between 250 and 315°C the gap setting was adjusted at these temperatures. A thin sheet of the polymer under investigation was loaded between the cone and plate such that the gap just overflowed. The excess sample was removed with a spatula and the sample allowed to equilibrate inside the environmental chamber. All viscosity measurements were made under conditions of steady shear, at a shear rate ($\dot{\gamma}$) of 21.2 sec^{-1}. The motion of the top plate was followed on an SEL-3006 ultraviolet recorder* and the torque (T) on the top platen calculated as

$$T = \Delta_t k_t$$

where Δ_t is the movement of the torsion head transducer in microns and k_t is the torsion bar constant.

The viscosity of the sample was calculated from

$$\eta = \frac{\alpha T}{15 d^3 \beta} = \frac{\alpha \Delta_t k_t}{15 d^3 \beta}$$

where d is the diameter of the cone and plate assembly, and β is the angular velocity of the rotating cone which is set by the operator. The rate of shear ($\dot{\gamma}$) was calculated as $\dot{\gamma} = \beta/\tan \alpha$ or for very small values of α where $\alpha \cong \tan \alpha$

$$\dot{\gamma} = \frac{180}{\pi} \frac{\beta}{\alpha} \ (sec^{-1})$$

The melt flow of a polymer is an energy activated process, and,

---

*S. E. Laboratories, Feltham, England.

under condition of constant $\dot{\gamma}$ and volume, one may write

$$\eta = A \exp(E_A/RT)$$

where A is a constant, E_A is the thermal activation energy for melt flow, R is the gas constant and T is absolute temperature (^oK). Activation energies were calculated for each of the materials studied from the slope of a log η vs 1/T plot.

(d) Impact Testing. Since polycarbonate and polysulfone are tough, impact resistant materials in their own right, it was important that the impact properties of the copolymers be investigated. In order to carry out such a study, a fully instrumented falling weight impact tester was designed and constructed. The device was equipped with an accelerometer which permitted direct observation of the weight's deceleration as it struck and pierced the test specimen. The following is a description of the principles and procedures involved with the impact tester.

(i) Principle of Operation. The heart of the VPI and SU falling weight impact tester is the piezoelectric accelerometer. Piezoelectric materials can be defined as crystals which do not have identical centers of positive and negative charge. Under an alternating electric field, such a material will vibrate since the various dipole lengths within the crystal change with the voltage gradient. On the other hand, an applied force or vibration can be converted to electrical energy by the reverse process. Electrical dipoles within a crystal are displaced from their equilibrium positions by the force and give rise to a charge

imbalance across the crystal. Since the charge which develops depends upon the extent of crystal distortion and, hence, the applied force, devices capable of accurately sensing the voltage output of the crystal can be prepared. Examples of piezoelectric materials include intrinsic monocrystals such as quartz or Rochelle Salt or artifically polarized ceramics such as barium titanate ($BaTiO_3$), lead zirconate ($PbZrO_3$) and lead metaniobate.

The basic construction of a piezoelectric accelerometer is shown in Figure 8. The device consists of several piezoelectric discs upon which rests a heavy mass preloaded by a stiff spring. The entire assembly is hermetically sealed by a metal housing with a thick base threaded to accept a mounting stud. When subjected to vibrations or an applied force (acceleration), the mass exerts a force on the discs proportional to the applied force or acceleration of the mass. At frequencies much less than the resonant frequency of the accelerometer assembly, the acceleration of the mass is proportional to that of the entire transducer and, in the case here, proportional to that of the falling weight.

In designing the impact tester, several important criteria were adhered to in order to achieve maximum instrument flexibility and reproducibility. First, both the weight and drop height are variable, thus providing a wide range of impact energies. Second, the release mechanism operates smoothly in order to reduce possible wobble of the falling weight. Third, the specimen clamp pressure can be reproducibly applied, an important detail since it is known that impact strength varies inversely with clamp pressure.[154] Last, and above all, the

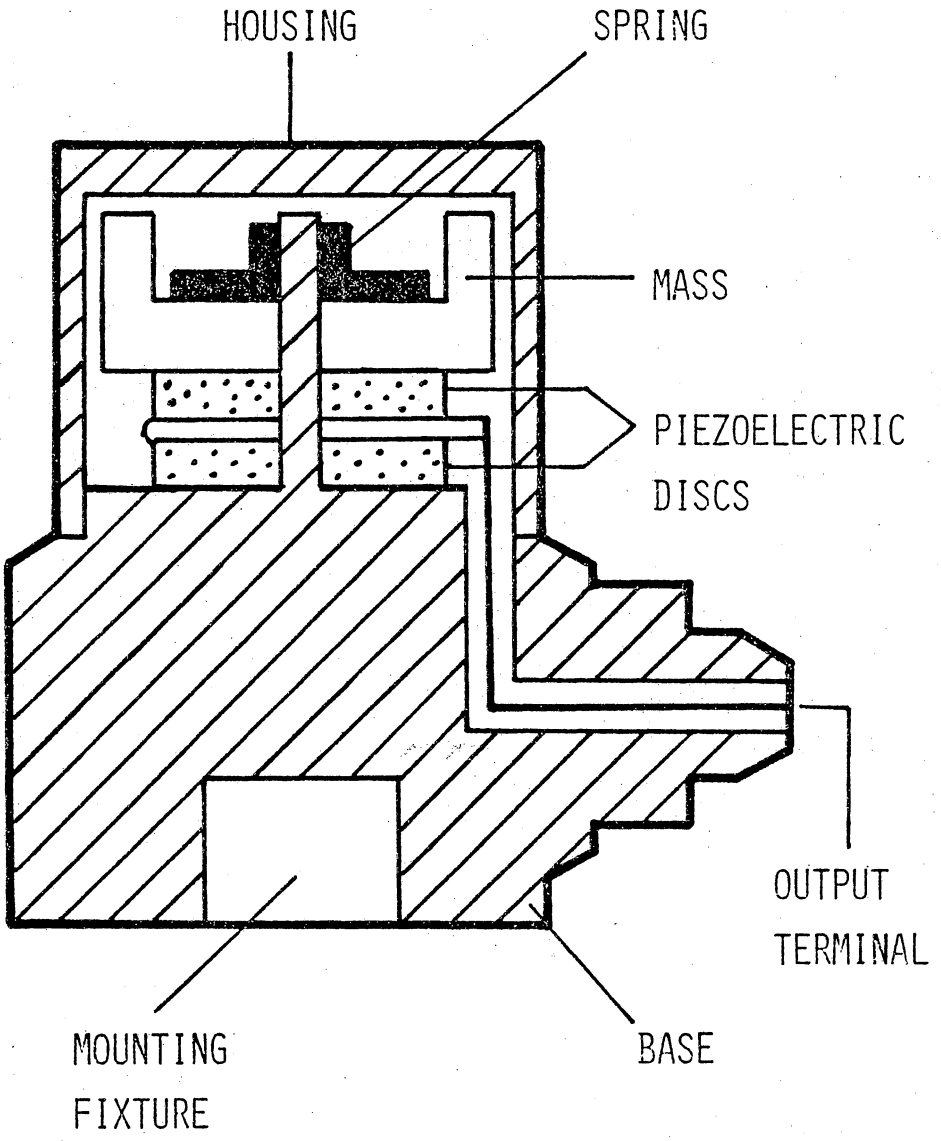

Figure 8. Schematic diagram of an accelerometer[194].

device is capable of accepting a variety of test specimen shapes and sizes and is especially useful where small amounts of material are at hand. These features will be discussed in detail in the next section.

(ii) Instrument Design.

Mechanical Aspects. A picture of the VPI impact tester is shown in Figure 9. Basically, the device consists of a heavy frame constructed from 3" x 3" x 0.25" steel angles, a 2.75" inside diameter guide tube for the falling weight, a release mechanism, a specimen clamping assembly, and the necessary electronic equipment. The steel frame is mounted on leveling feet to insure the stability of the instrument. A heavy steel channel is vertically bolted to the frame and serves to support the guide tube. The bottom of the tube is supported by an aluminum collar and five set screws which permit rapid allignment of the tube when necessary. Two slits, 0.5" wide, on opposite sides of the tube, allow access to the weight and release mechanism. The slits also prevent air pressure buildup as the weight drops. The overall length of the tube is 5.0 feet.

The current falling weight is shown in Figure 10. It is 7 inches long, 2.5 inches in diameter and machined from aluminum. Six teflon spacers are mounted on the weight to reduce friction in case it should contact the wall of the guide tube. Two threaded holes on opposite sides of the weight aid in lifting the weight when engaged by two removable handles. The striker, which is located at the base of the weight and the only part to actually touch the specimen, is machined from stainless steel (2 inches long and 0.25 inches in diameter) and

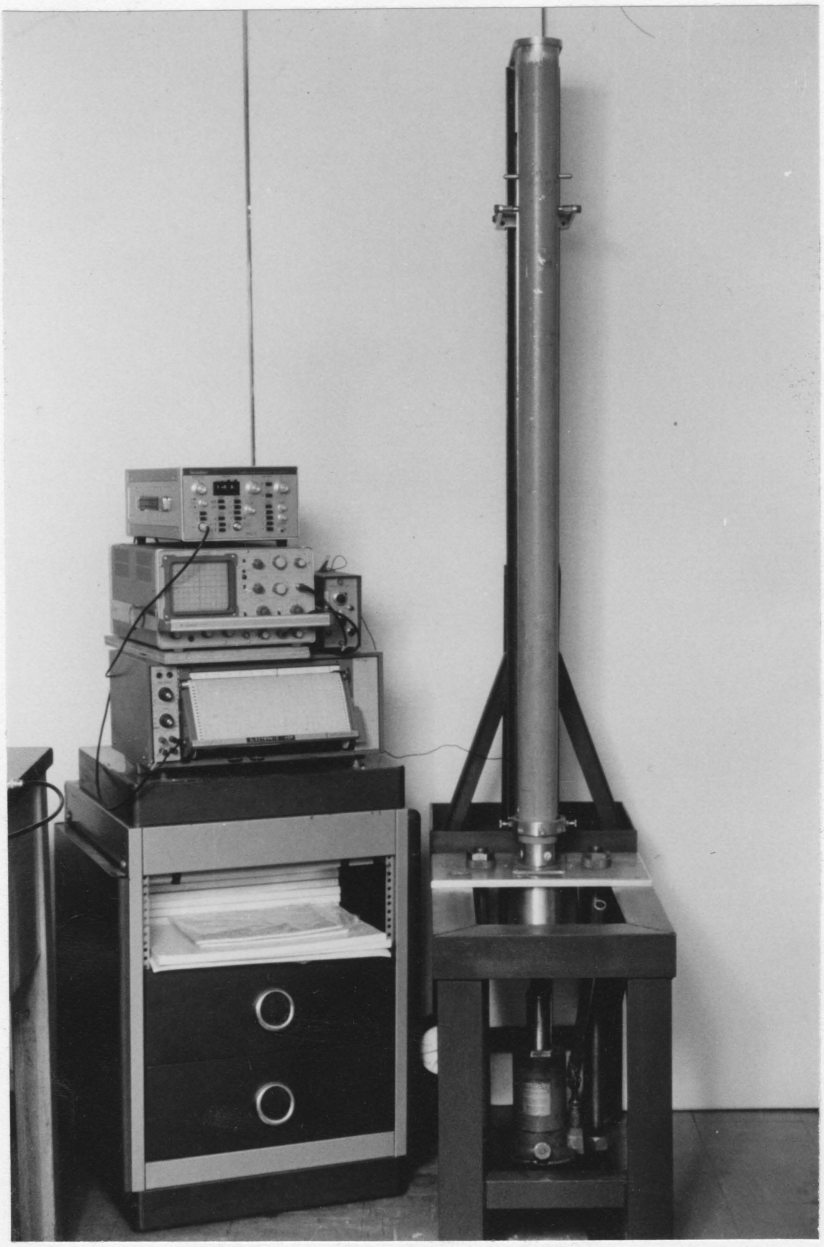

Figure 9. The VPI & SU falling weight impact tester.

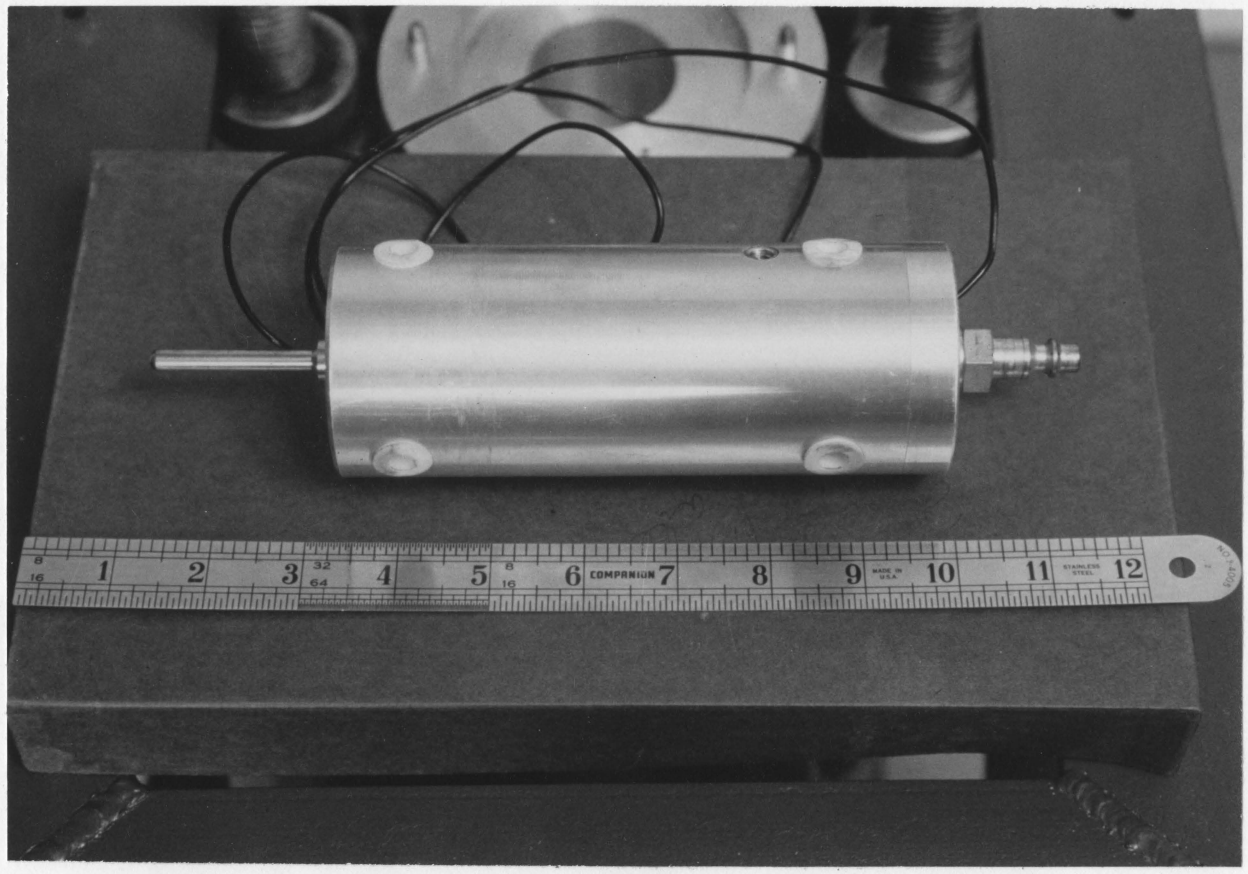

Figure 10. A photograph of the weight assembly showing the striker (left) and the release fitting (right).

hemispherically tipped. It can be replaced by strikers of varying geometry, thus enhancing the instrument's general flexibility.

The accelerometer is housed in a 2 inch deep well at the opposite end of the weight. As shown in Figure 11, the accelerometer is centrally located along the axis of the cylindrical weight. A torque wrench is used to mount the accelerometer at the required 15 inch pounds. Four screws firmly fasten the weight cap to the weight. The cap not only protects the accelerometer, but also carries a fitting designed to engage the release mechanism. The entire weight assembly weighs 2.903 pounds (1317 g).

In order to allow the weight to hang perfectly plumb before release, a novel release mechanism was designed based on a quick-connect pressure hose coupling*. Three spring loaded ball bearings firmly hold the nipple screwed into the weight cap. A light downward force is enough to release the weight. The heavy spring inside the body of the coupling was removed in order that the weight not be given any additional force when released.

Specimen clamping is of extreme importance if reproducible impact data is to be obtained. The clamping system on the VPI device is of simple design, yet readily accepts specimens of varying shape or thickness. Currently, circular specimens 3 inches in diameter and up to 0.125 inches in thickness are usually employed, but 2 inch by 2 inch squares can also be accomodated. The clamping assembly is shown dismantled in Figure 12. The specimen is contained between two aluminum

---

*Sears, Roebuck and Co., Chicago, Ill.

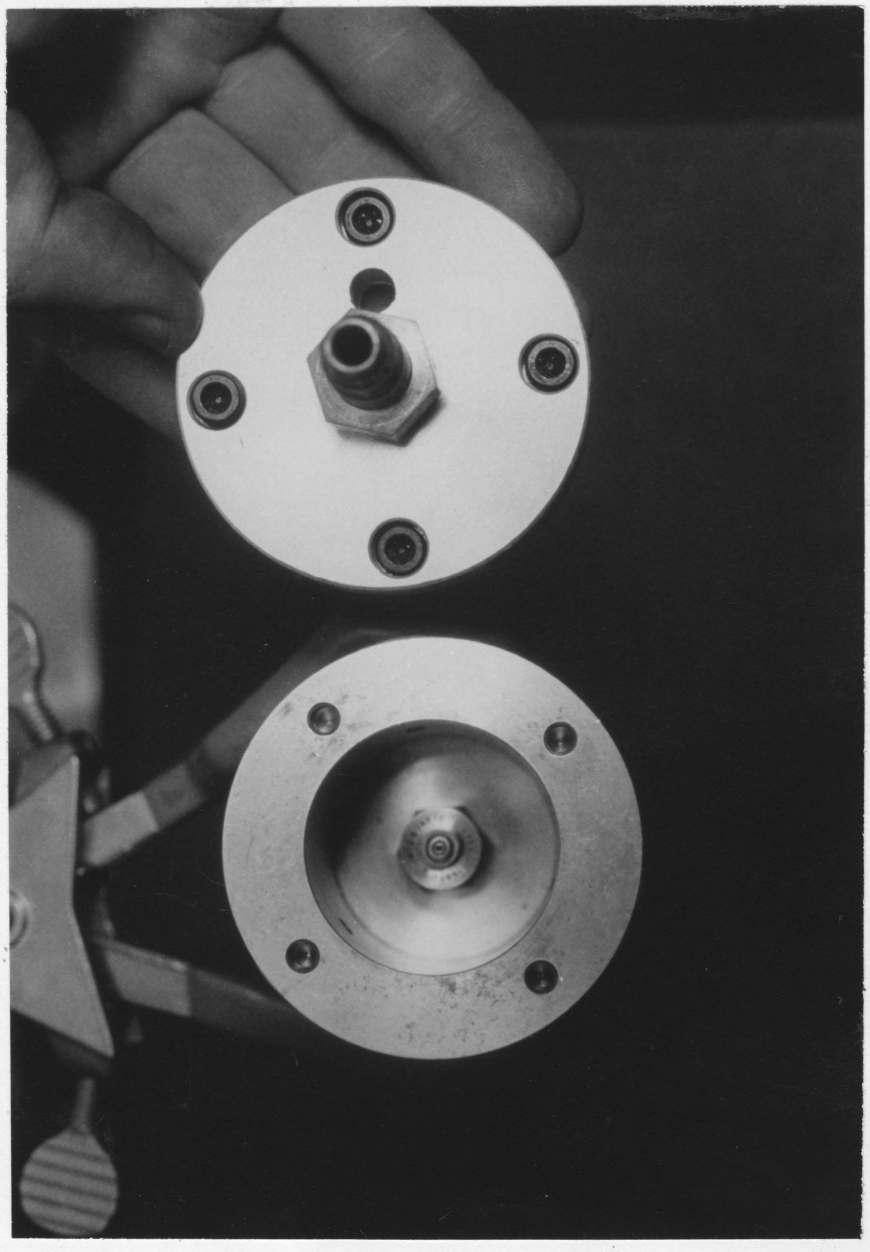

Figure 11. A top view of the weight with the cap removed to show the accelerometer. The diameter of the weight is 2.5 inches (6.35cm).

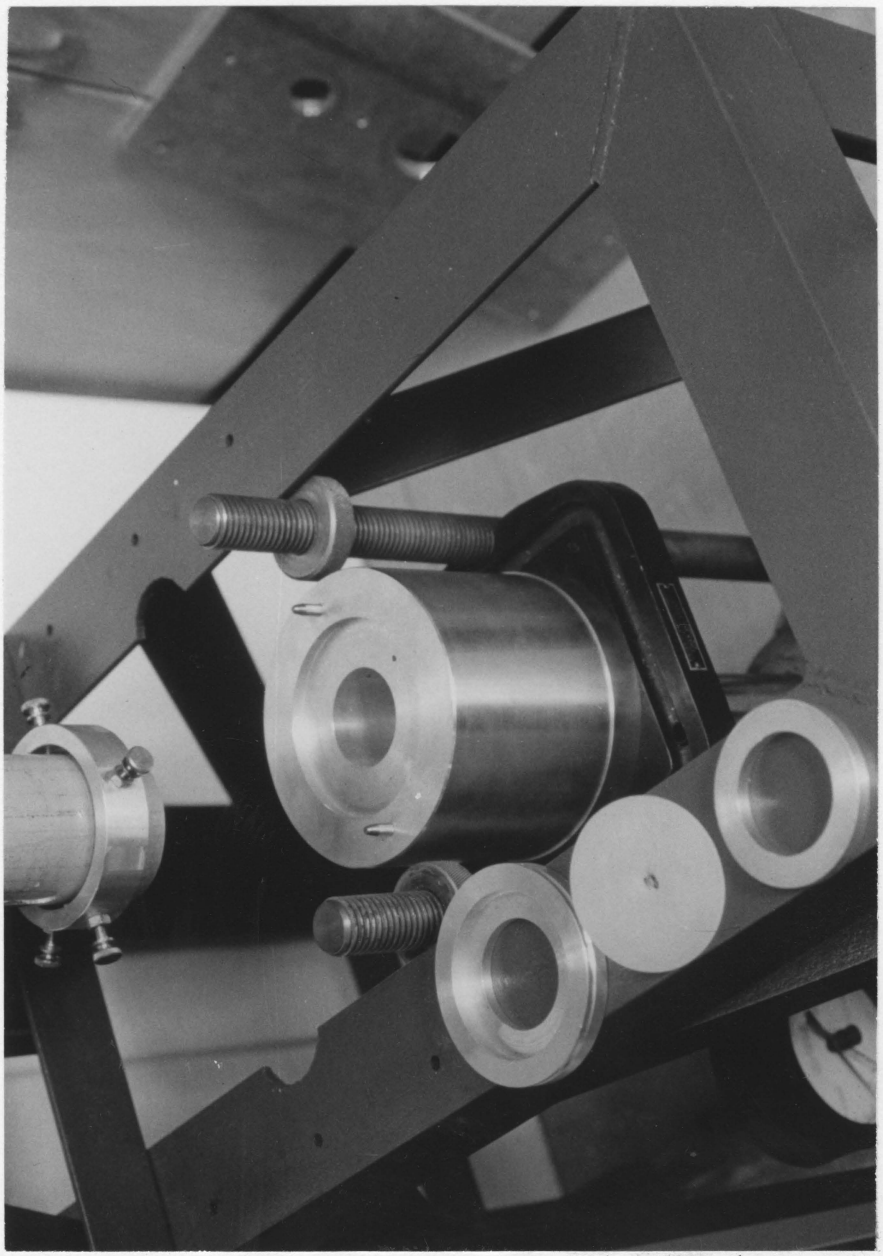

Figure 12. The specimen clamping assembly dismantled.

rings and placed in a shallow well on the top surface of a large aluminum cylinder bolted to the ram of a hydraulic Carver* press. The entire assembly is jacked against a 0.75 inch thick aluminum plate firmly bolted to the heavy instrument frame. Clamping rings offering unsupported specimen diameters of 2 inches and 1.5 inches are currently available. Note also in Figure 12 the bottom of the drop tube with the previously mentioned allignment ring and set screws.

Electronic Aspects. The critical component of the impact tester is the accelerometer. It must be chosen so that the frequency response is linear across the range of frequencies encountered during impact tests. The weight of the accelerometer should be at least ten times less than the weight of the test device in order to overcome any loading effect. In other words, the weight of the accelerometer must not influence the measured vibrations. It must be insensitive to environmental transients such as temperature and humidity. Lastly, the maximum vibration level expected during the impact should not exceed one third of the accelerometer's maximum shock rating.[194]

A Bruel and Kjaer** Model 4369 accelerometer was chosen for the VPI impact tester. This particular accelerometer has a maximum shock level of 10,000 g's or 100,000 m/sec^2. Its output of 2.18 picocoulombs per m/sec^2 (1.85 $mv/m\ sec^{-2}$) is linear up to vibration frequencies of 10,000 Hz. It weighs only 14 grams and can operate at temperatures as high as 180°C.

---

* Fred S. Carver, Inc., Summit, N.J.
** Farrell Associates, Inc., Rockville, Md.

As indicated above, the output of the accelerometer is, indeed, small and, therefore, a charge amplifier is necessary. The amplifier also serves to protect the accelerometer output from high impedance loads which may reduce sensitivity as well as limit the low frequency response.[194] A Bruel and Kjaer* Type 2635 charge amplifier is an acceptable choice for a falling weight impact tester. The device is equipped with a built-in integrator which provides either acceleration, velocity, or displacement data. The output can be varied from 0.1 to 1000 millivolts per unit of measurement (m/sec^2, m/sec, mm). The charge amplifier is also equipped with high and low pass filter networks which allow the operator to select an upper and lower frequency limit. In this way, undesirable signals such as high frequency resonance (ringing) can be eliminated.

From the charge amplifier, the signal is passed to a Biomation** Waveform Recorder Model 805. The waveform recorder is basically an analog/digital converter integrated with a digital memory which will store a preselected portion of a digital signal as it varies with time. The signal is recorded in the form of 2048 data points at a sample rate which can be varied from 0.2 sec to 100 m sec per point. The voltage sensitivity can be varied from 0.1 to 50 volts full scale. A unique feature of the waveform recorder is the pretrigger which allows the input signal to trigger the recorder without losing any of the signal itself. The operator can set the pretrigger in such a way that a

---

* Farrell Associates, Inc., Rockville, MD
** Biomation Corp., Cupertino, CA

fraction of 1000 data points are recorded before the trigger point is reached. Thus, there is no need for separate trigger circuitry such as a photocell and lamp.

As the recorder stores information in its memory, it also provides for real-time data output in the form of an oscilloscope display, strip chart recorder hard copy, or digital output for subsequent computer processing. For impact testing, acceleration vs. time or velocity vs. time curves are most useful and are easily obtained with the current equipment.

(iii) Experimental Procedure

Commercial Polymers. In order to assess the performance of the falling weight impact tester, a series of commercial polymers were investigated. The polymers were chosen so as to provide a wide range of impact strengths and failure modes. Each of the polymers listed in Table IV was thoroughly dried in a vacuum oven for 24 hours before molding. Thin sheets, 18 cm square and less than 0.05 cm thick, were compression molded using a Dake Model 44225 hydraulic press. A circular die was employed to cut 3 inch (7.62 cm) diameter test specimens from the sheets. All specimens were tested within several hours of molding. No storage or preconditioning of the materials was carried out after they had been molded. At least three specimens from each sheet were tested after being inspected for flaws and measured for thickness. The specimens were mounted between the clamping rings at a pressure of 600 psi. Initially, a 1.317 kg mass and a drop height of 1.0 meter were employed to characterize the commercial polymers.

Table IV

Commercial Polymers for Impact Testing

Polymer	Source
Polycarbonate	General Electric Lexan 114-112
Polysulfone	Union Carbide Corp. P-3703
Polypropylene	Shell
High Density Polyethylene	Synthetic Materials Corp.
Impact Polystyrene	Union Carbide Bakelite
Polystyrene	"Crystal Grade"
Poly (methyl methacrylate)	Matheson, Coleman and Bell

The rate of deformation during impact loading has been found to influence the measured impact strength of polymeric materials. Using an accelerometer-equipped falling weight device, Cessna[171] has found that the impact strength of ductile polymers varies inversely with drop height or projectile velocity. Brittle polymers displayed very little dependence on either drop height or mass as long as enough energy was available to initiate fracture.

A similar study was carried out using the VPI impact tester and samples of polycarbonate, polypropylene, and poly(methyl methacrylate). The strength of these materials ranges from tough and ductile (polycarbonate) to very brittle (PMMA). Polypropylene exhibits intermediate properties. Test specimens were fabricated in the same manner discussed earlier and tested using drop heights of 0.75, 0.50, and 0.35 meter. Again, the mass employed was 1.317 kg.

Composite Materials. Two series of graphite fiber reinforced composites were obtained from the NASA-Langley Research Center. One group of composites was designated LaRC-160 and contained 0, 5, and 15 weight percent elastomer incorporated with the matrix material. Five specimens of each type were examined using the 1.317 kg mass and a drop height of 1.0 meter.

The second group of composites was designated LARC-13 and consisted of five types containing either 0% elastomer, 15% Sylgard elastomer, or 15% AATR. The Sylgard-containing composites consisted of a silastic rubber blended with the matrix material whereas an aromatic amine terminated rubber (AATR) was chemically linked with the matrix

molecules in the latter case. The composite samples were nominally 5 cm square and approximately 0.070 cm thick. The materials were tested using the same procedure described above.

Instrument Settings and Calculations

Acceleration Mode. As mentioned earlier, the B + K type 2365 charge amplifier used on the VPI impact tester allows acceleration, velocity, or displacement data to be collected. With the current equipment, either acceleration or velocity output can be used to calculate the energy absorbed by the test specimen. For testing commercial polymers, the acceleration mode proved more useful since it provided a unique acceleration-time curve for each type of polymer examined.

The optimum charge amplifier and wave form recorder settings were found through trial and error using a variety of target materials. The charge amplifier output was set at 10 mv/m sec^{-2} for all tests. Initially, it was observed that transducer ringing sometimes obscured parts of or all of the acceleration-time curve especially in the case of brittle polymers. Setting the upper frequency limit of the charge amplifier to 3000 Hz and the lower frequency to 2 Hz eliminated most of the ringing without affecting the acceleration curve. These settings were maintained throughout all tests.

The voltage sensitivity of the waveform recorder was set at 2 volts for thin polymer films (5 volts for polycarbonate), providing an overall shock sensitivity of 200 or 500 m/sec^2 full scale. The time base (time per data point) was set at 5 μ sec which conveniently provided a total time of 10.2 milliseconds in which to observe the impact.

Both the oscilloscope and strip chart recorder were calibrated as outlined in the Biomation manual. The recorder chart speed was set to provide one inch of recorder travel to one millisecond portion of the stored curve.

In the acceleration mode, the deceleration of the falling projectile is followed with time as it strikes and breaks the specimen. The projectile, traveling at a velocity v_o contacts the target at time t_o, and begins decelerating. At time t_f the specimen fails and the striker continues on through it. The integral of the acceleration-time curve between the limits t_o and t_f is given by

$$\int_{t_o}^{t_f} a(t)\, dt = v_f - v_o = \Delta v$$

and provides the change in velocity of the projectile upon impact. All integration was carried out graphically. The initial velocity must be calculated from the physics of a falling body assuming negligible air resistance and no contact with the walls of the drop tube. Since the initial velocity and change in velocity are known, the velocity at fracture (v_f) can be found. The energy required to break the specimen (E_B) becomes simply the difference in kinetic energies before and after impact or

$$E_B = 1/2\ Mv_o^2 - 1/2\ Mv_f^2$$

Velocity Mode. In some cases, the acceleration curve itself is not useful in calculating fracture energies. Certain materials, particularly composites, display mixed failure modes and acceleration-

time curves which are difficult to integrate graphically. Thus, it becomes necessary to use the velocity output mode of the charge amplifier to obtain the change in velocity upon impact directly.

In testing the NASA composites, the charge amplifier output was set to 1000 $mv/msec^{-1}$ and the waveform recorder sensitivity set to 2 volts or 2 m/sec full scale. Once again, the calibration of both the oscilloscope and the strip chart recorder was checked to insure that the full scale output of the waveform recorder corresponded to full scale on these instruments. As will be shown later, the velocity changes measured in this way ranged from 0.1 to 0.25 m/sec.

4. Surface Properties.

(a) Scanning Electron Microscopy. Polycarbonate is readily crystallized by certain solvents such as acetone. Several copolymers were exposed to the same along with commercial polycarbonate and polysulfone films. The molded films were immersed in acetone for one hour, air dried overnight, and vacuum dried at 100°C for 12 hours. The surface morphology of the films before and after treatment was observed with the aid of a scanning electron microscope.* The specimen was irradiated with a focused electron beam which released secondary electrons, back-scattered electrons, and characteristic x-rays. Photographs of the specimen surface were obtained from secondary electron images.

---

*AR 900, Burlington, Mass.

IV. Results

A. Polymer Characterization. During the course of this investigation two series of polysulfone/polycarbonate oligomers were studied. The first series was limited to 50/50 weight percent compositions whereas the second spanned a composition range of 20 to 80 percent polycarbonate. Two separate sets of polycarbonate and polysulfone oligomers were employed to prepare these block copolymers and were separately characterized. The second series of block copolymers was specifically used to study the effects of composition on impact strength.

In order to adequately describe the nature of each copolymer, a code was devised to provide the block lengths and approximate weight percent composition. Thus, a bisphenol-A polysulfone oligomer of 10,000 g/mole molecular weight will be designated AS-10K. A bisphenol-T polysulfone will be represented by TS and a bisphenol-S polysulfone as SS. Since only bisphenol-A polycarbonate was utilized in preparing copolymers it will be designated as AC. A block copolymer made up of 10,000 g/mole oligomers of bis-A polysulfone and polycarbonate in 50/50 composition is, thus, represented by AS/AC - 10/10 (50/50). Such nomenclature facilitates discussion of the results presented in this section.

1. Oligomer Characterization.

The molecular weights of polysulfone oligomers were determined by potentiometric titration. Prior to analyzing the oligomers, a series of bisphenol model compounds was examined in order to assess the accuracy

of the titration method. The data for the model compounds is shown in Table V. It will be noted that both the precision and accuracy are very good. The maximum deviation from the average molecular weight calculated is generally less than ±1.5% and the percent error from the actual value ranges from 0.4 to 3.0%.

Titration data for the polysulfone oligomers is given in Table VI along with their intrinsic viscosities. The level of precision is not as good as that calculated for the model compounds (which were less than ±5.2%) but is in good agreement with other techniques for determining $<\bar{M}_n>$ of polymers.[195]

Representative titration curves for each type of polysulfone studied are presented in Figures 13, 14 and 15. Here it is interesting to note that the height of the break at the equivalence point is strongly dependent upon the acidity of the bisphenol. The acidity increases in going from bisphenol-A to bisphenol-T to bisphenol-S.

Number average molecular weights of polycarbonate oligomers were determined by a UV spectroscopic technique.[187] The results for the initial series of polycarbonate oligomers are listed in Table VII. The accuracy of this technique was comparable to that of the potentiometric titration.

2. Polysulfone/Polycarbonate Block Copolymers (Series 1).

The number average molecular weight $<\bar{M}_n>$ and intrinsic viscosity for the first series of block copolymers is given in Table VIII. Since a calibration curve was not available, absolute values of $\bar{M}_n$ and $\bar{M}_w$ could not be determined by high pressure liquid chromatography (HPLC).

Table V

Analysis of Bisphenol Compounds

Compound	Molecular Weight (g/mole) I	II	III	Average MW $\bar{M} + S_N$	Actual MW (M_A)	% Error $\frac{\lvert \bar{M} - M_A \rvert}{M_A} \times 100$
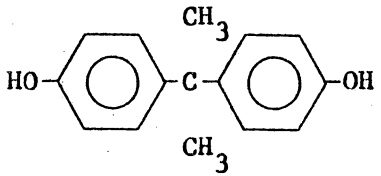 Bisphenol A	225	227	229	227 ± 2.0(±0.9%)	228	0.4
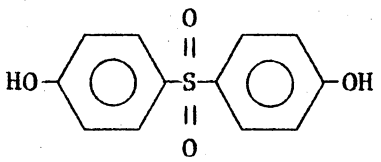 Bisphenol S	249	225	248	251 ± 3.8(±1.5%)	250	0.04
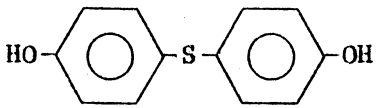 Bisphenol T	215	216	212	214 ± 2.1(±1%)	218	1.8
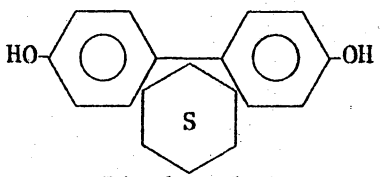 Bisphenol C	267	263	260	263 ± 3.5(±1.3%)	268	1.9

Table V (continued)

Compound	Molecular Weight (g/mole) I	II	III	Average MW $\bar{M} + S_N$	Actual MW (M_A)	% Error $\frac{\lvert\bar{M}-M_A\rvert}{M_A} \times 100$
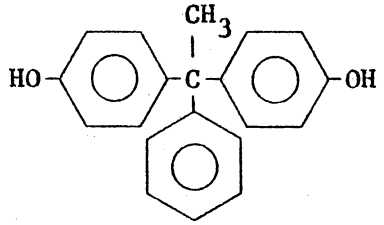 Bisphenol ACP	293	294	289	292 ± 2.6(±0.9%)	290	0.7
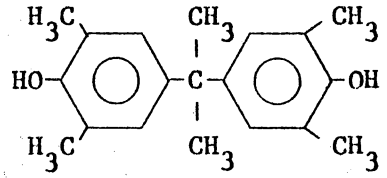 TETRAMETHYL Bisphenol A	282	277	274	278 ± 4.1(±1.5%)	284	2.1
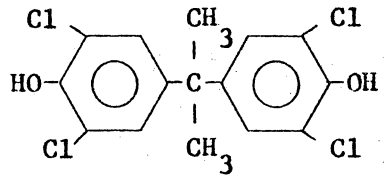 TETRACHLORO Bisphenol A	360	352	351	355 ± 5.0(±1.4%)	366	3.0

Table VI

Analysis of Polysulfone Oligomers

	Molecular Weight (g/mole) I	II	III	Average ($\bar{M} \pm S_N$)	M_n(UV)*
A. Bisphenol A Polysulfone					
PSf-A_1	2,500	2,400	2,250	2,380 ± 125 (±5.2%)	--
PSf-A_2	4,050	4,360	4,350	4,250 ± 176 (±4.1%)	4,250
PSf-A_3	8,200	7,860	8,450	8,170 ± 296 (±3.6%)	8,900
PSf-A_4	24,800	25,700	26,800	25,760 ± 1001(±3.9%)	26,600
B. Bisphenol-T Polysulfone					
PSf-T_1	10,270	10,270	10,050	10,250 ± 40 (±0.4%)	--
C. Bisphenol-S Polysulfone					
PSf-S_1	8,740	9,500	9,250	9,160 ± 387 (±4.2%)	--

*Determined by UV spectrophotometric technique (187)

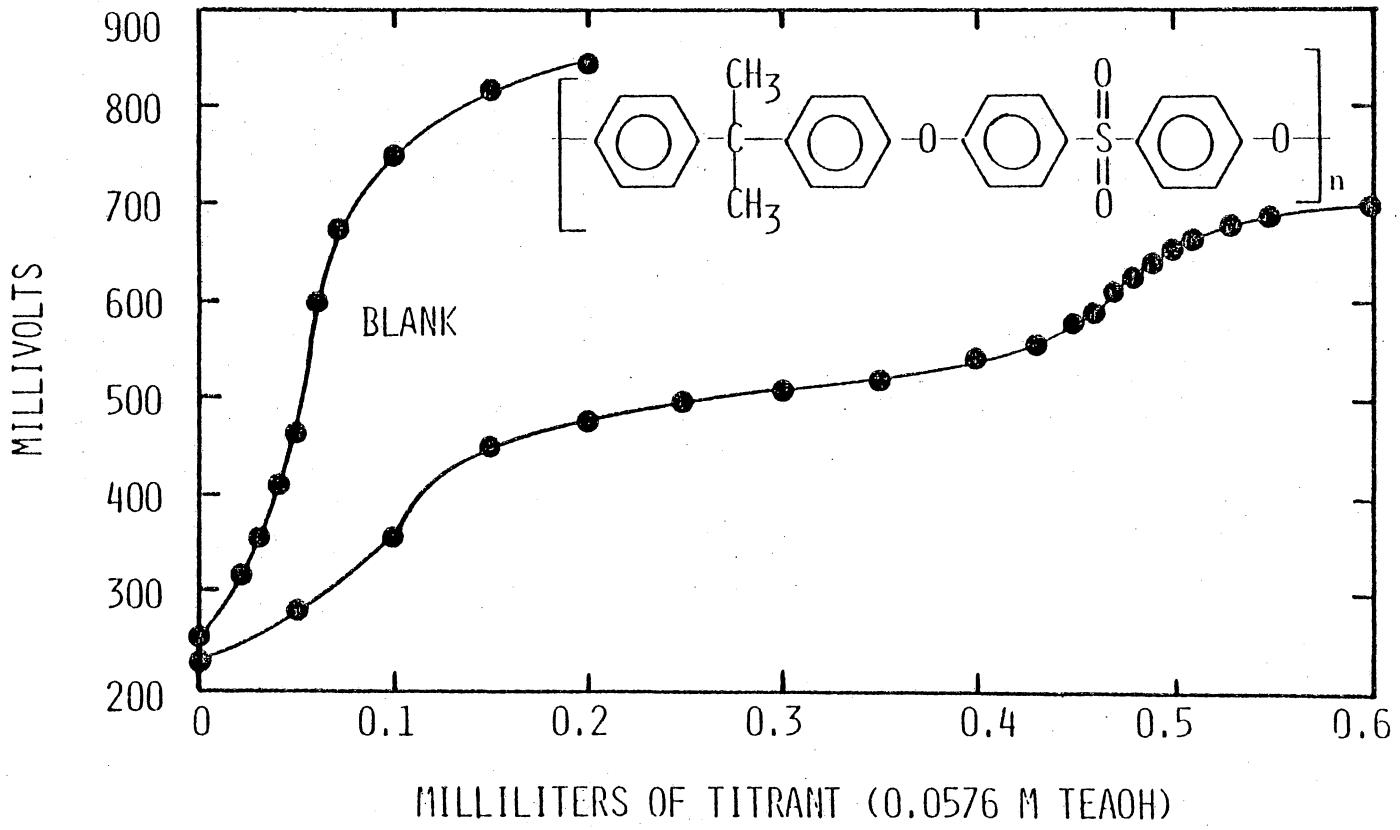

Figure 13. Titration curve obtained for bisphenol-A polysulfone.

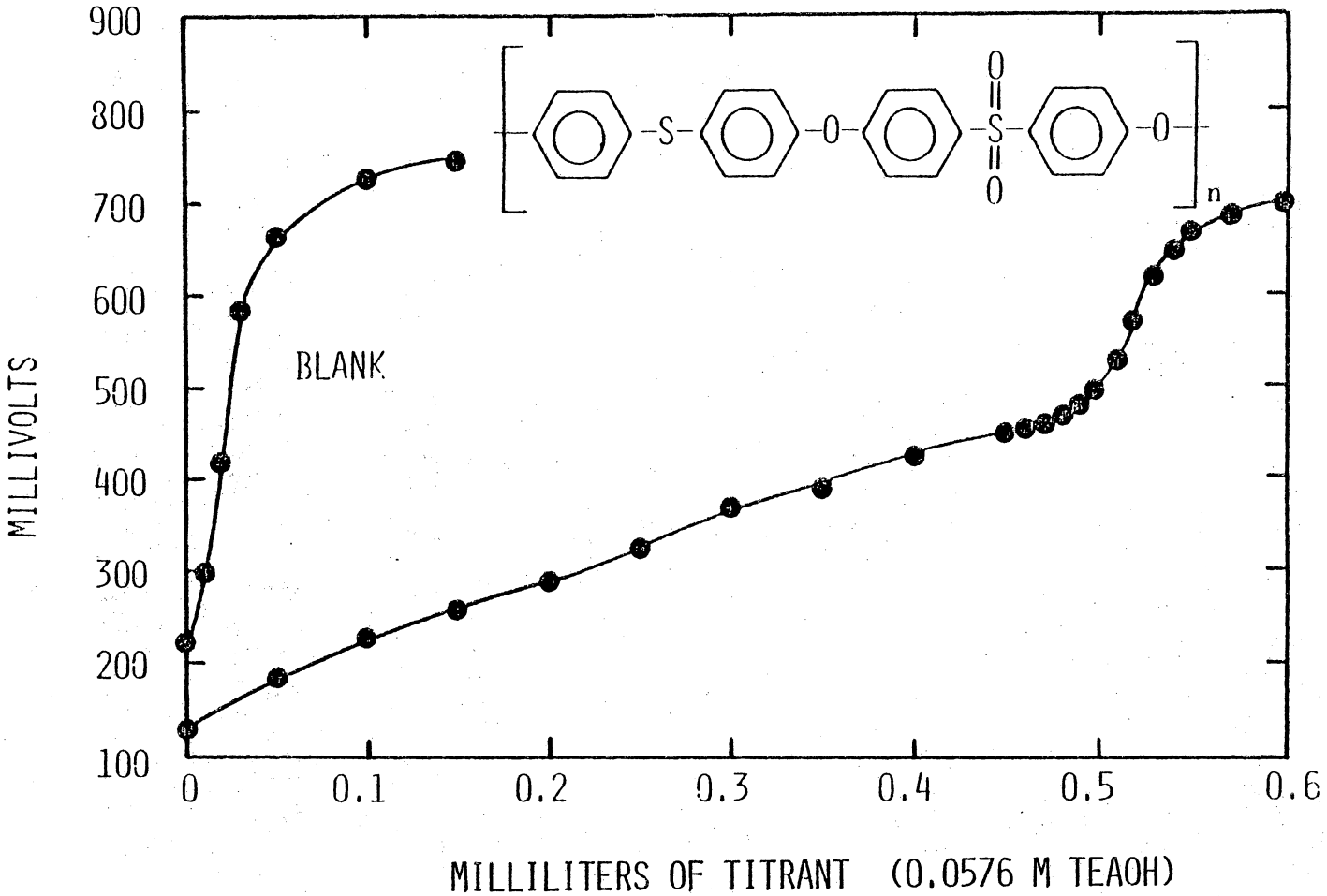

Figure 14. Titration curve obtained for bisphenol-S polysulfone.

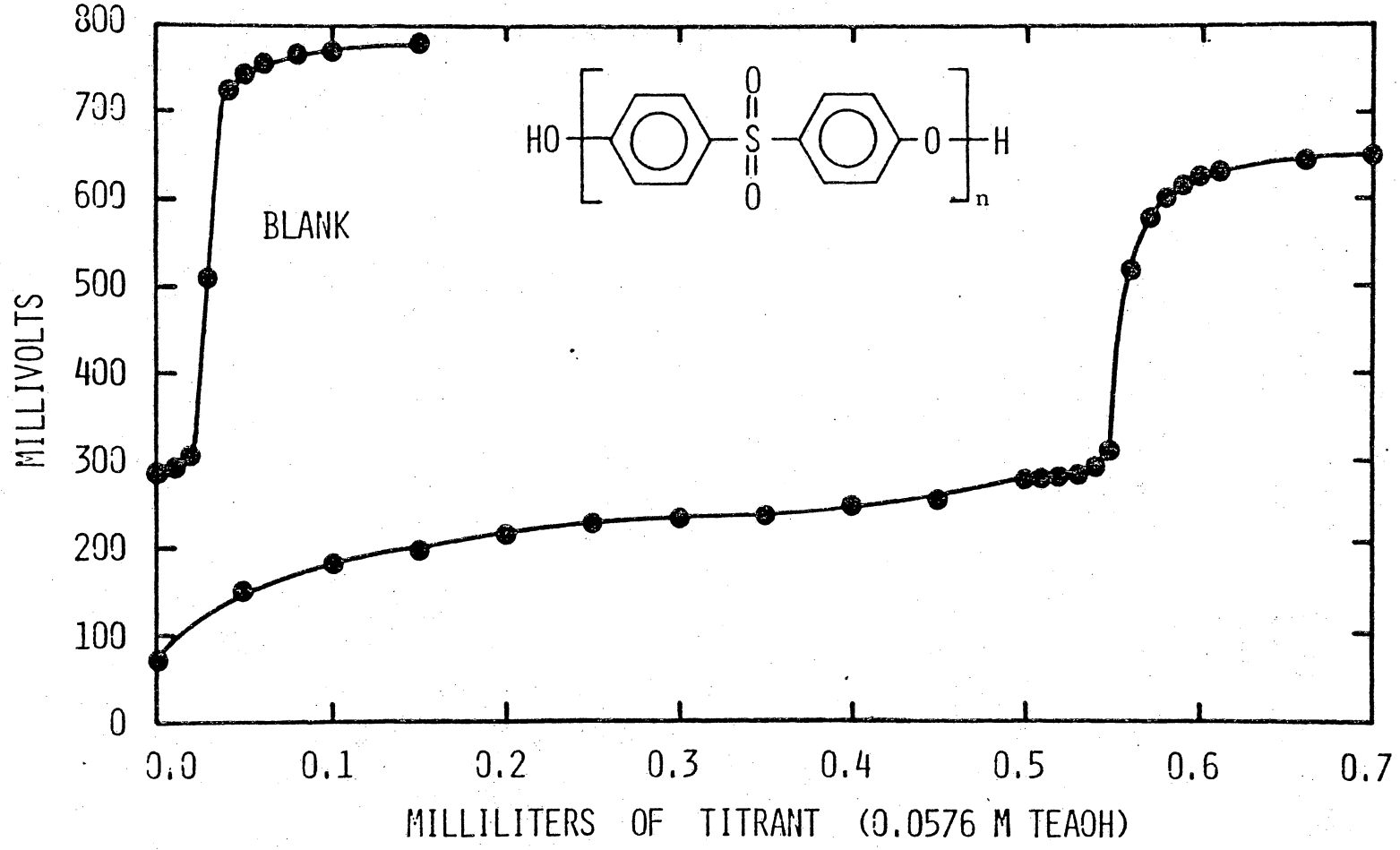

Figure 15. Titration curve obtained for bisphenol-S polysulfone.

Table VII

Characterization of PC Oligomers

No.	$[\eta]^{30^{\circ}C}_{THF}$	$\overline{Mn}$ g/mole
1	0.23	5,000[a]
2	0.31	8,000[a]
3	0.32	10,000[a]
4	0.55	17,000[b]
5	0.53[c]	22,000[a]

a) U.V. Analysis
b) Membrane Osmometry
c) $[\eta]^{30^{\circ}C}_{CHCl_3}$

Table VIII

Characterization of Polysulfone/Polycarbonate Block Copolymers[a]

ID	Oligomer PSf $\overline{<Mn>}$	PC $\overline{<Mn>}$	$[\eta]^{30}_{THF}$	$\overline{<Mn>}$[b]	Tg (°C)
AS/AC - 5/5	4,200	5,000	0.57	--	173
AS/AC - 10/10	8,200	10,000	0.59	36,000	185
AS/AC - 16/17	15,900	17,000	0.63	71,000	175[c]
AS/AC - 26/22	25,800	22,000	0.74	40,000	163,184
SS/AC - 5/5	5,000	5,000		--	167,229
SS/AC - 10/10	10,000	10,000		--	161,231
TS/AC - 10/10	10,000	10,000		--	162

a) Nominally 50/50 by weight
b) Membrane Osmometry
c) Displays two phase behavior also. Tg = 163,184°C

However, the HPLC curves shown in Figure 16 for AS/AC-10/10 indicate that both oligomers and the resulting copolymer have relatively sharp molecular weight distributions. A comparison of the molecular weights ($\bar{M}_n$) of the oligomers and the block copolymer reveals that four number average blocks are coupled to form the latter. Very little homopolymer contamination is apparent in the HPLC curve of AS/AC-10/10 shown in Figure 16. It is interesting to note, however, that a small amount of low molecular weight material is present in the HPLC curves of the polysulfone oligomer and the block copolymer. This is suspected to be the cyclic dimer mentioned earlier.[94]

B. Transitional Behavior

1. Dynamic Mechanical Analysis. The dynamic mechanical response of polysulfone (PSf) and polycarbonate (PC) homopolymers as well as the block copolymers was investigated on a Rheovibron DDV-II at 3.5 Hz. Plots of complex modulus (E^*) and tan δ for commercial polysulfone and polycarbonate are shown in Figures 17 and 18, respectively. The Tg of PSF occurs at 190°C whereas that of PC is located at 150°C.

The dynamic mechanical spectrum of AS/AC-10/10 shown in Figure 19 indicates only a single glass transition at about 175°C, about midpoint between those of the homopolymers. The curves for AS/AC-16/17 (50/50) shown in Figures 20 and 21 were obtained for a cast film (THF) and a compression molded film (260°C), respectively. Note that the cast film is characterized by a single Tg at -178°C and that the molded film exhibits two Tg's at 162 and 182°C. From the large difference in the size of the loss peaks in the two-phase material it would appear that

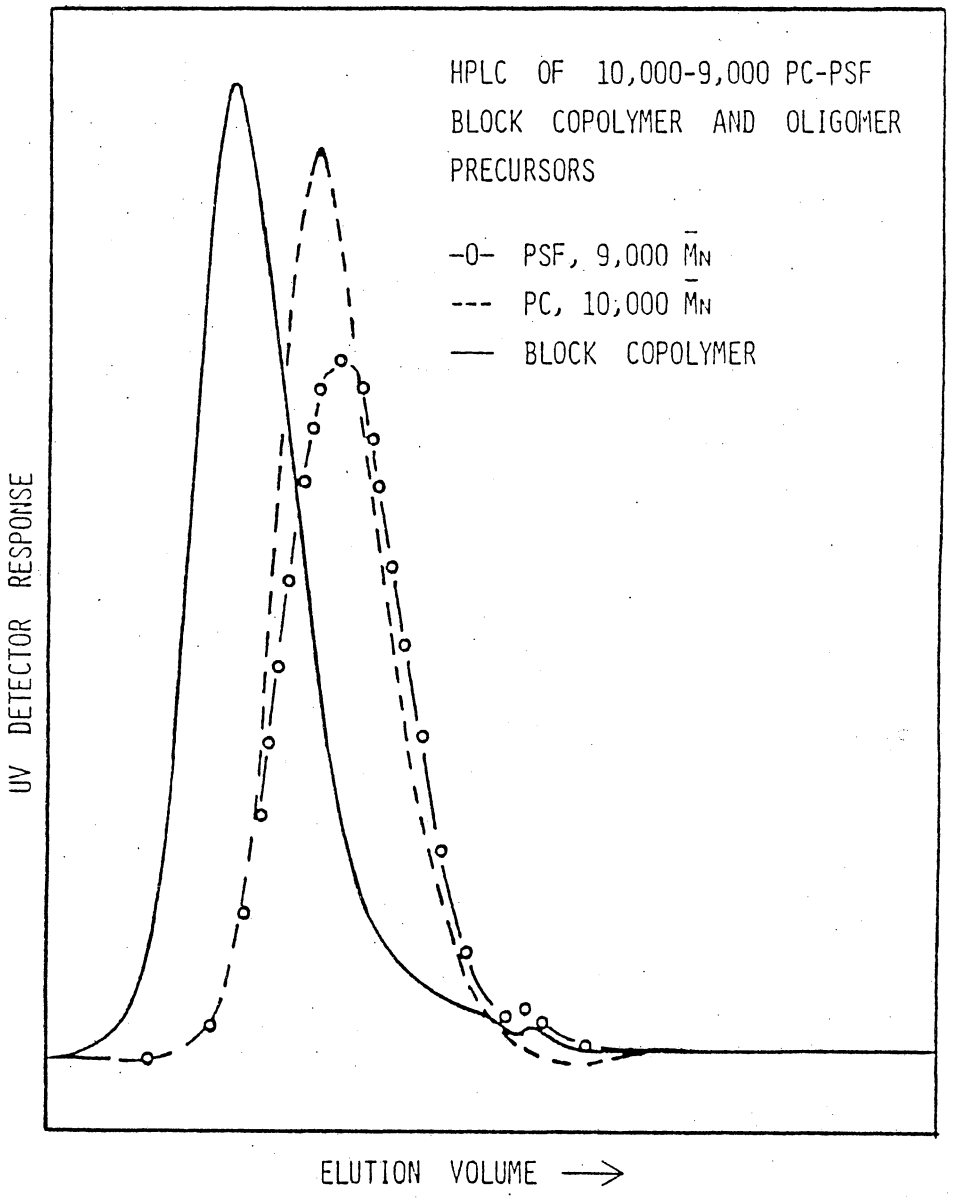

Figure 16. High pressure liquid chromatograms of a polysulfone/polycarbonate block copolymer (AS/AC-10/10) and its oligomer precursors.

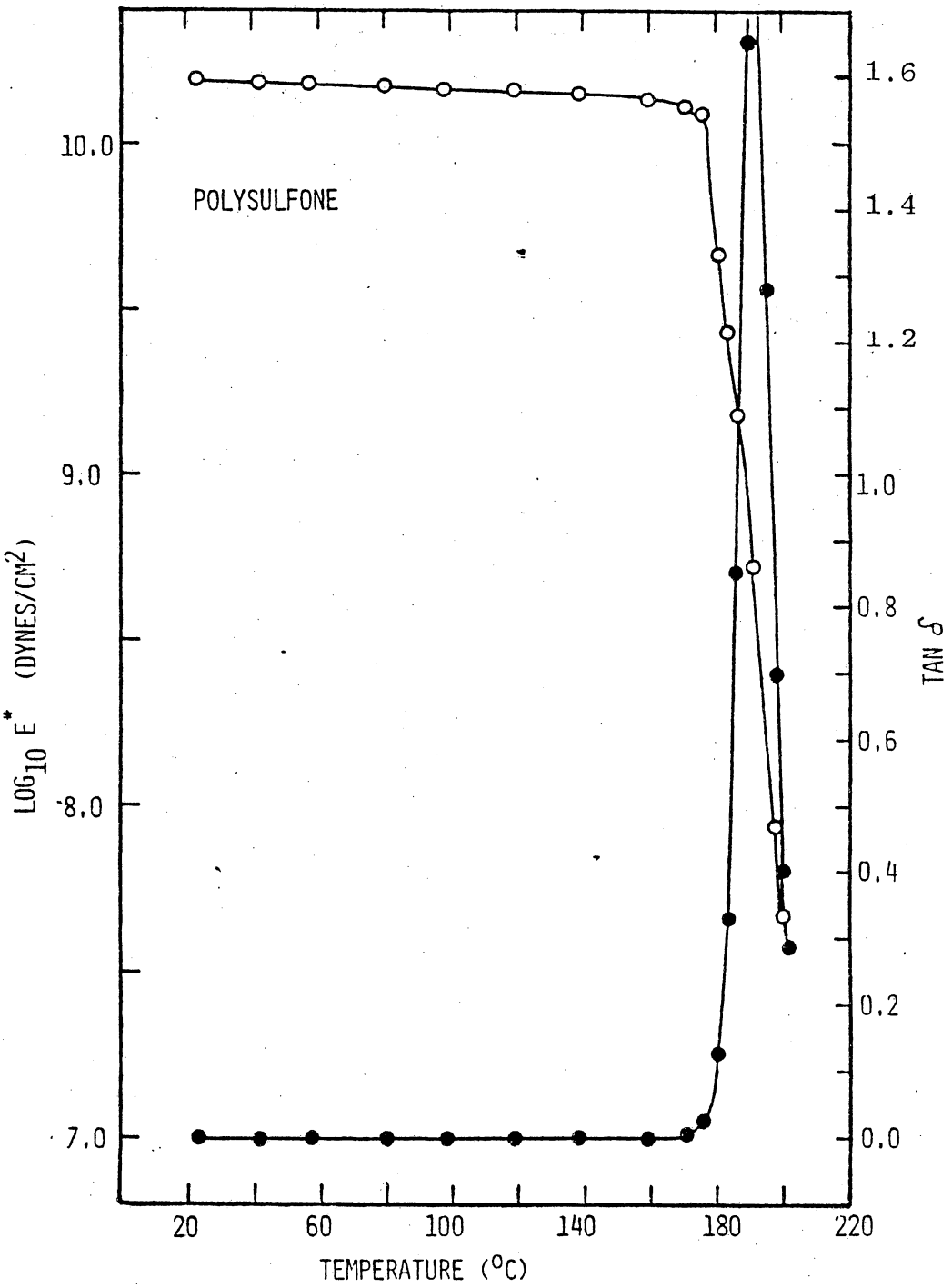

Figure 17. High temperature dynamic mechanical properties of bisphenol-A polysulfone.

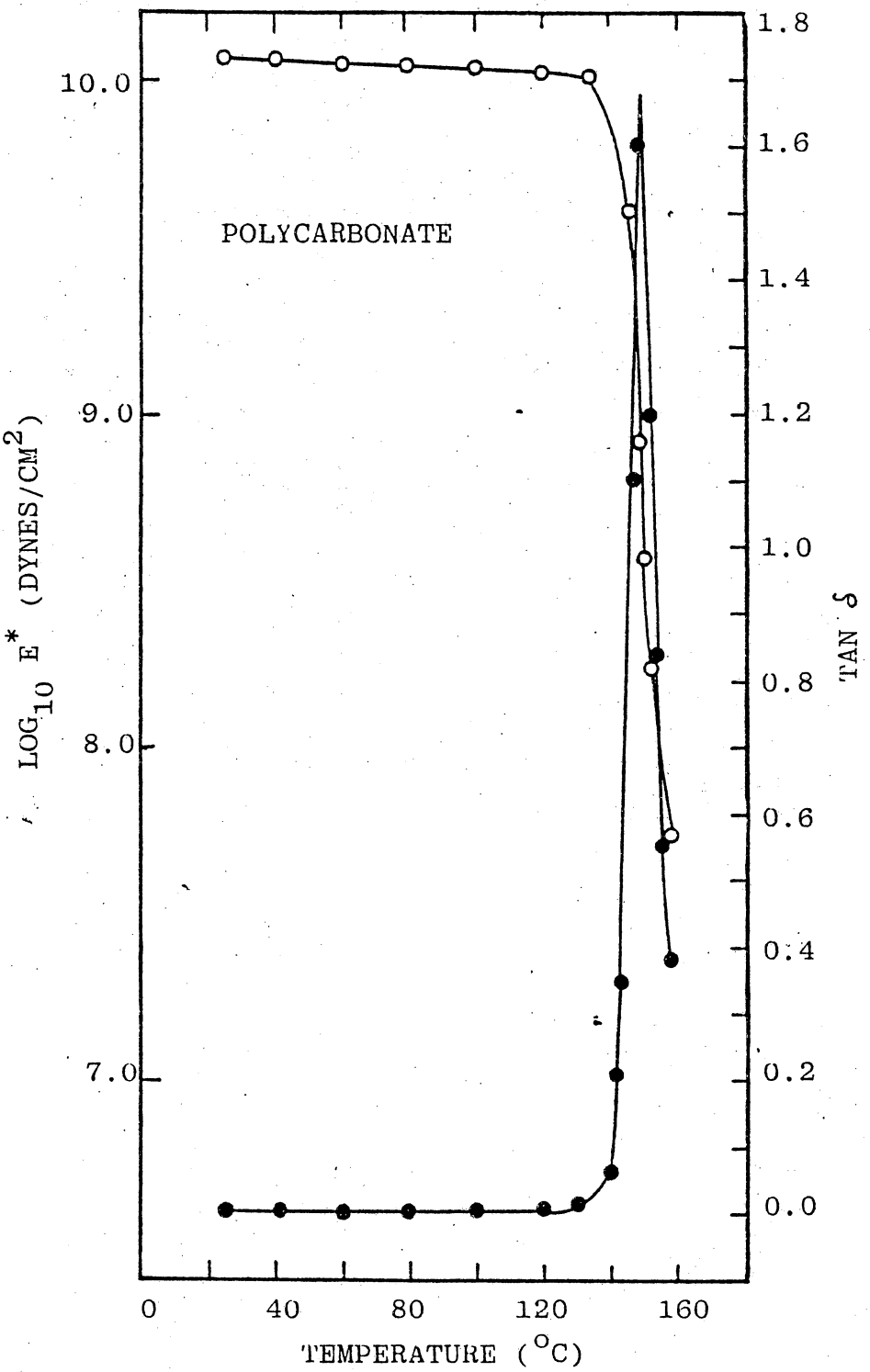

Figure 18. High temperature dynamic mechanical behavior of bisphenol-A polycarbonate.

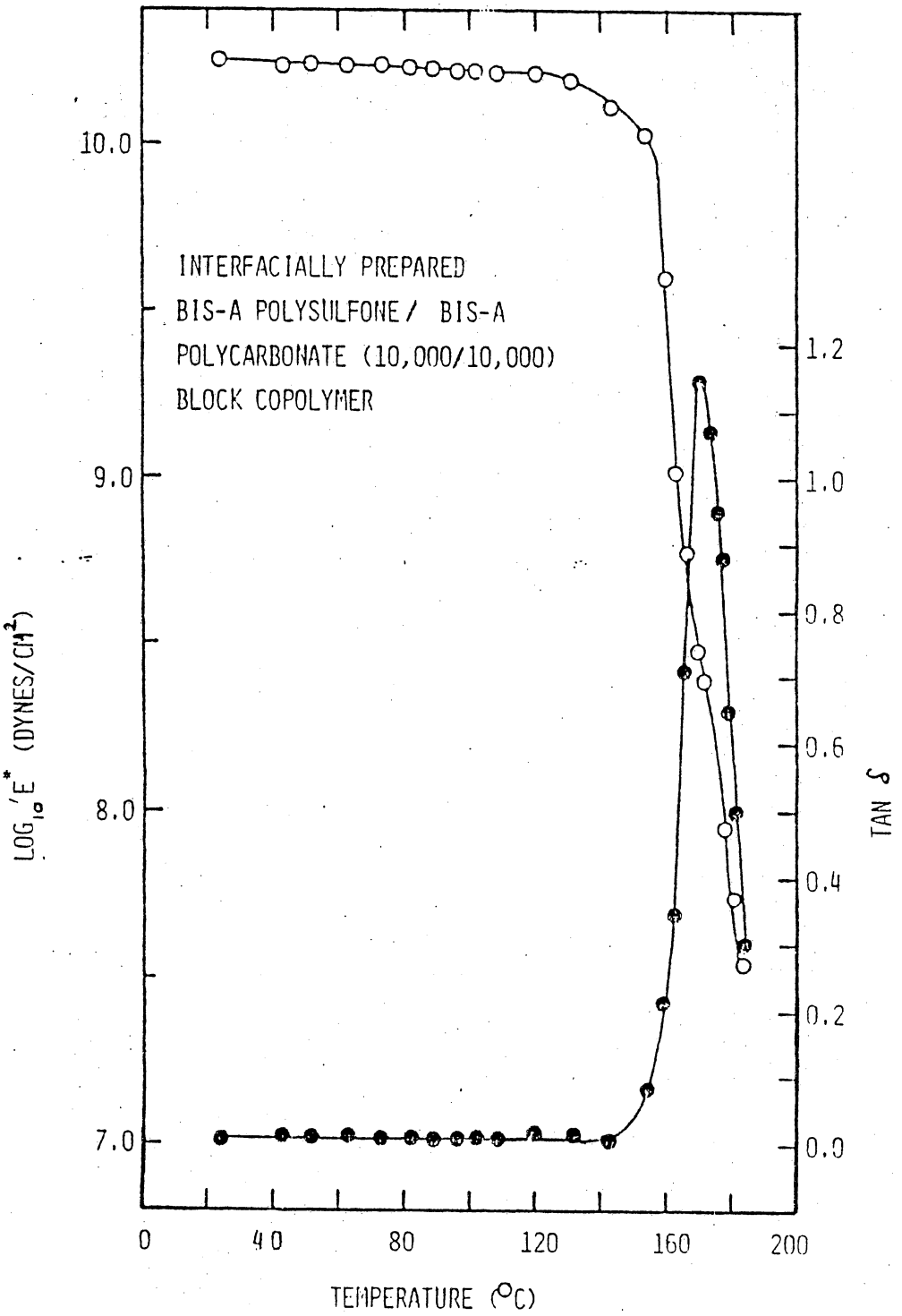

Figure 19. High temperature dynamic mechanical behavior of AS/AC - 10/10.

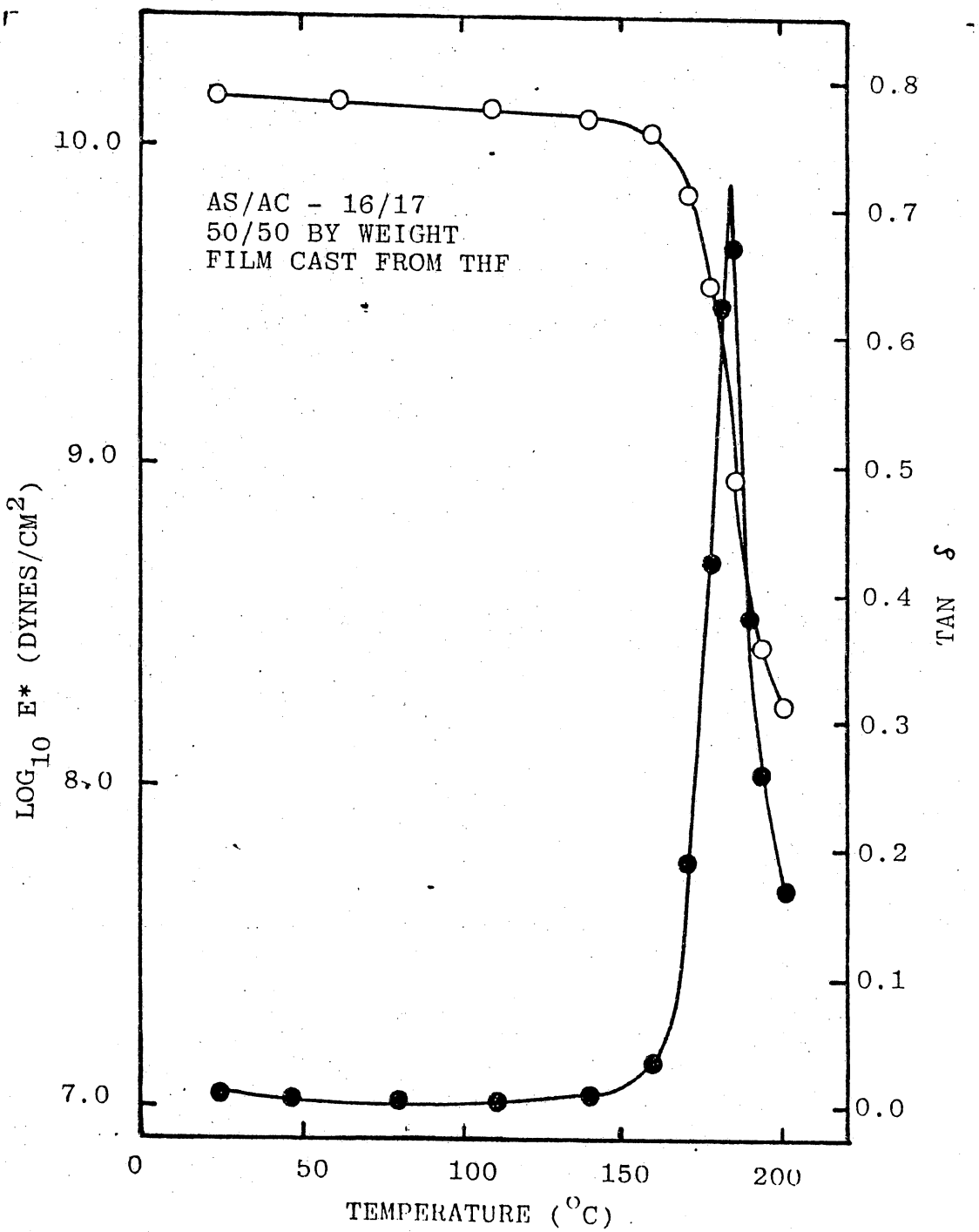

Figure 20. High temperature dynamic mechanical behavior of AS/AC - 16/17 film cast from THF solution.

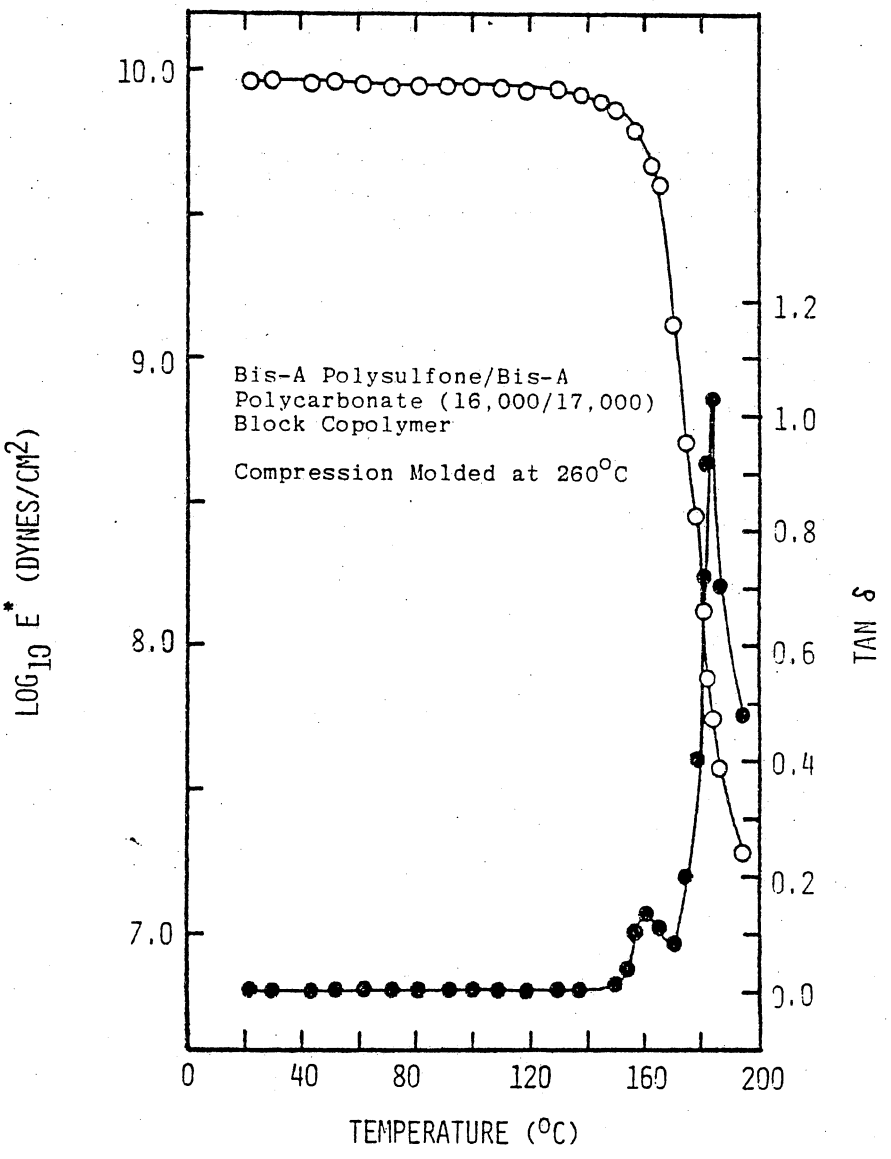

Figure 21. High temperature dynamic mechanical behavior of compression molded AS/AC - 16/17 film.

the copolymer contains substantially more PSF than PC. However, a plot of E' and E" vs. temperature reverses the size of the loss peaks as illustrated in Figure 22. More will be said of this phenomena later. A molded specimen of AS/AC-26/22 (50/50) gave the curves pictured in Figure 23 showing two glass transitions at 162 and 190°C. Cast films (CH_2Cl_2) of the same polymer also showed two phase behavior.

Dynamic mechanical spectra obtained for TS/AC - 10/10 (50/50) and SS/AC - 10/10 (50/50) are provided in Figures 24 and 25, respectively. The TS/AC copolymer has a Tg of 162°C whereas the SS/AC material displays two well defined transitions at 160 and 240°C. Once again, the apparent discrepancy between the height of the tan peaks and composition is reversed when E" is plotted as shown in Figure 26.

The low temperature loss peaks of the homopolymers and copolymers were also studied on the Rheovibron at 3.5 Hz. Plots of tan δ, E^*, and E" are shown in Figures 27 and 28 for polysulfone and polycarbonate. The low temperature or β relaxation is centered around -110°C in both cases. The breadth of the transition is much wider than that of the α or glass transitions which occur at higher temperatures. Note that the E" peak heights are similar also. Low temperature dynamic mechanical data for AS/AC-10/10 (50/50) and AS/AC-26/22 (50/50) are provided in Figures 29 and 30. No significant differences in their shapes are apparent although the temperatures corresponding to the peak maximums are slightly lower (~ -90°C) than those of the homopolymers. Similar behavior is displayed by SS/AC-10/10 (50/50) in Figure 31.

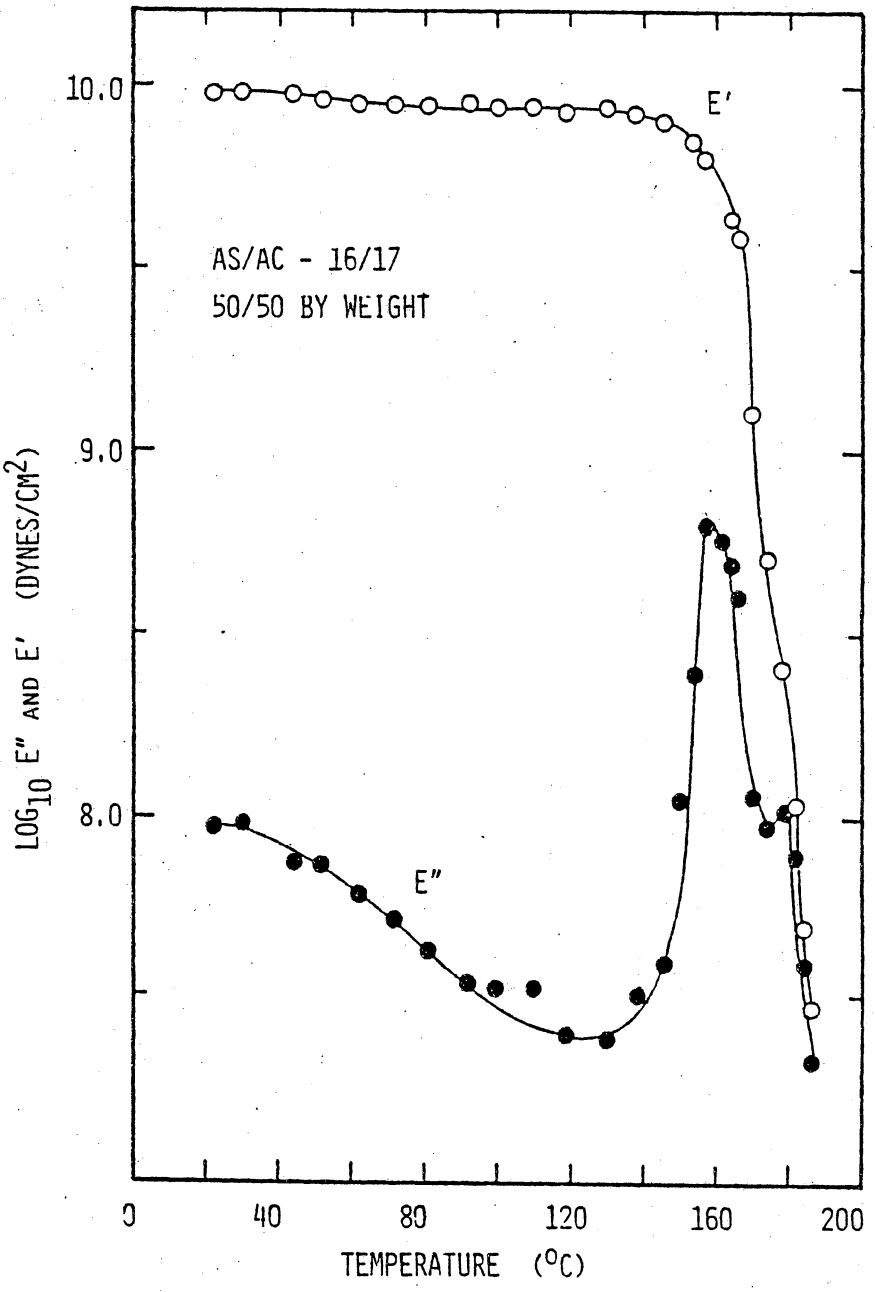

Figure 22. High temperature dynamic mechanical behavior of AS/AC-16/17 in terms of the storage (E') and loss (E") moduli.

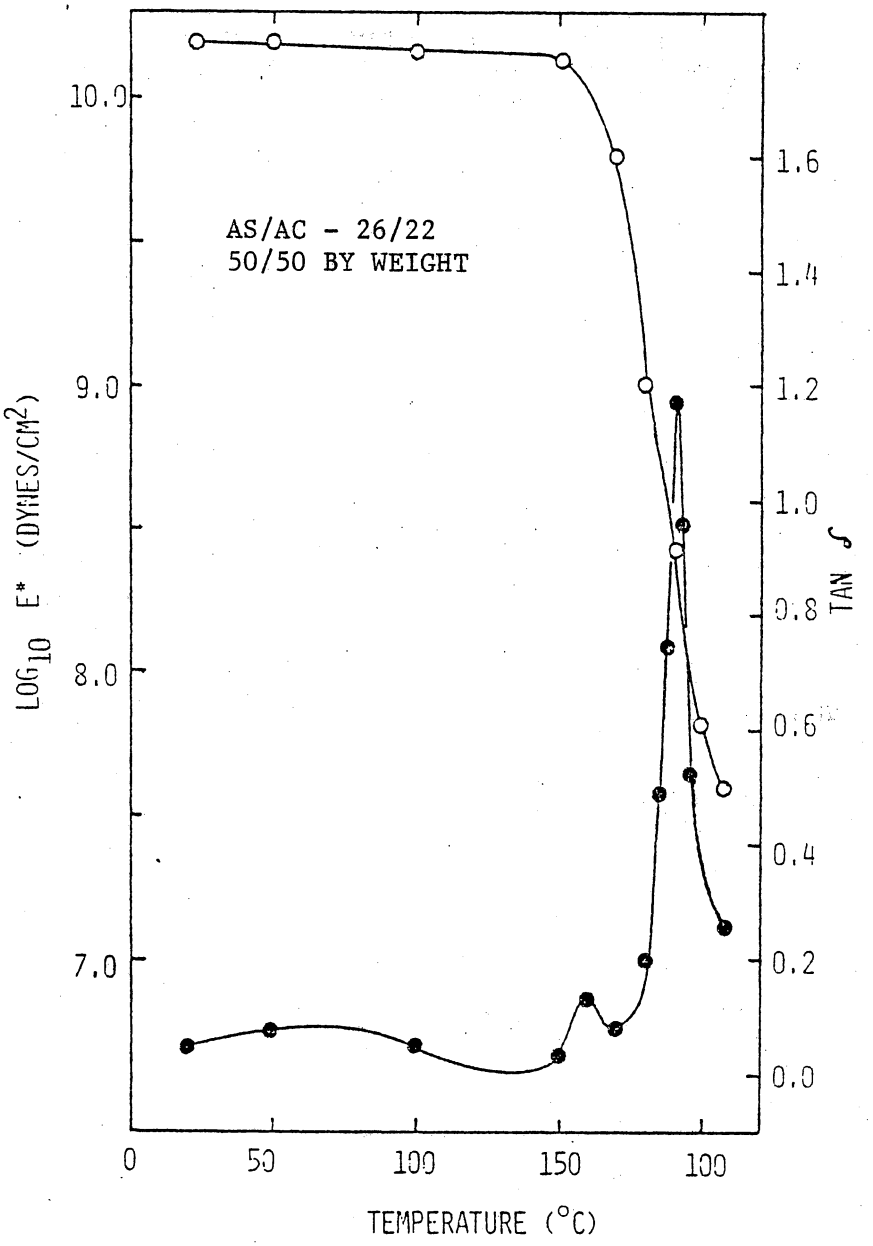

Figure 23. High temperature dynamic mechanical behavior of AS/AC - 26/22.

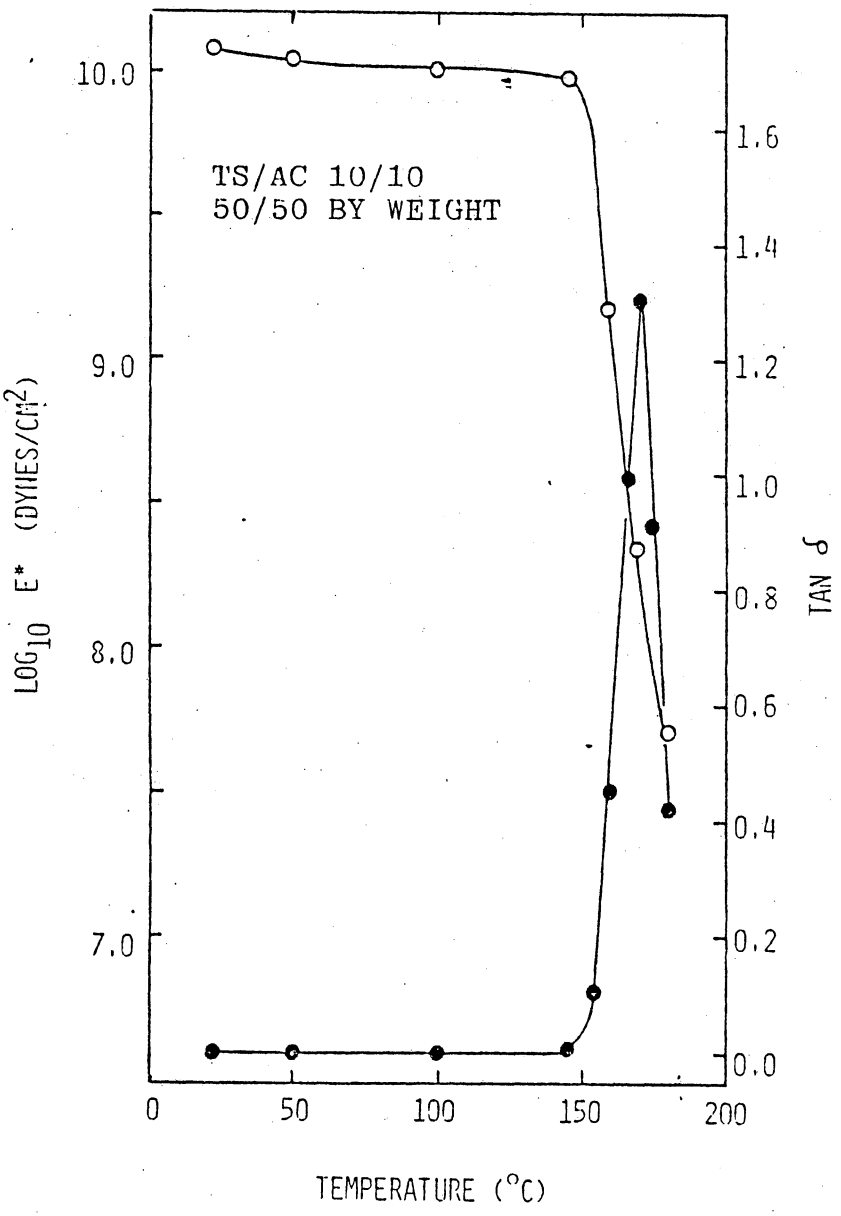

Figure 24. High temperature dynamic mechanical behavior of TS/AC - 10/10.

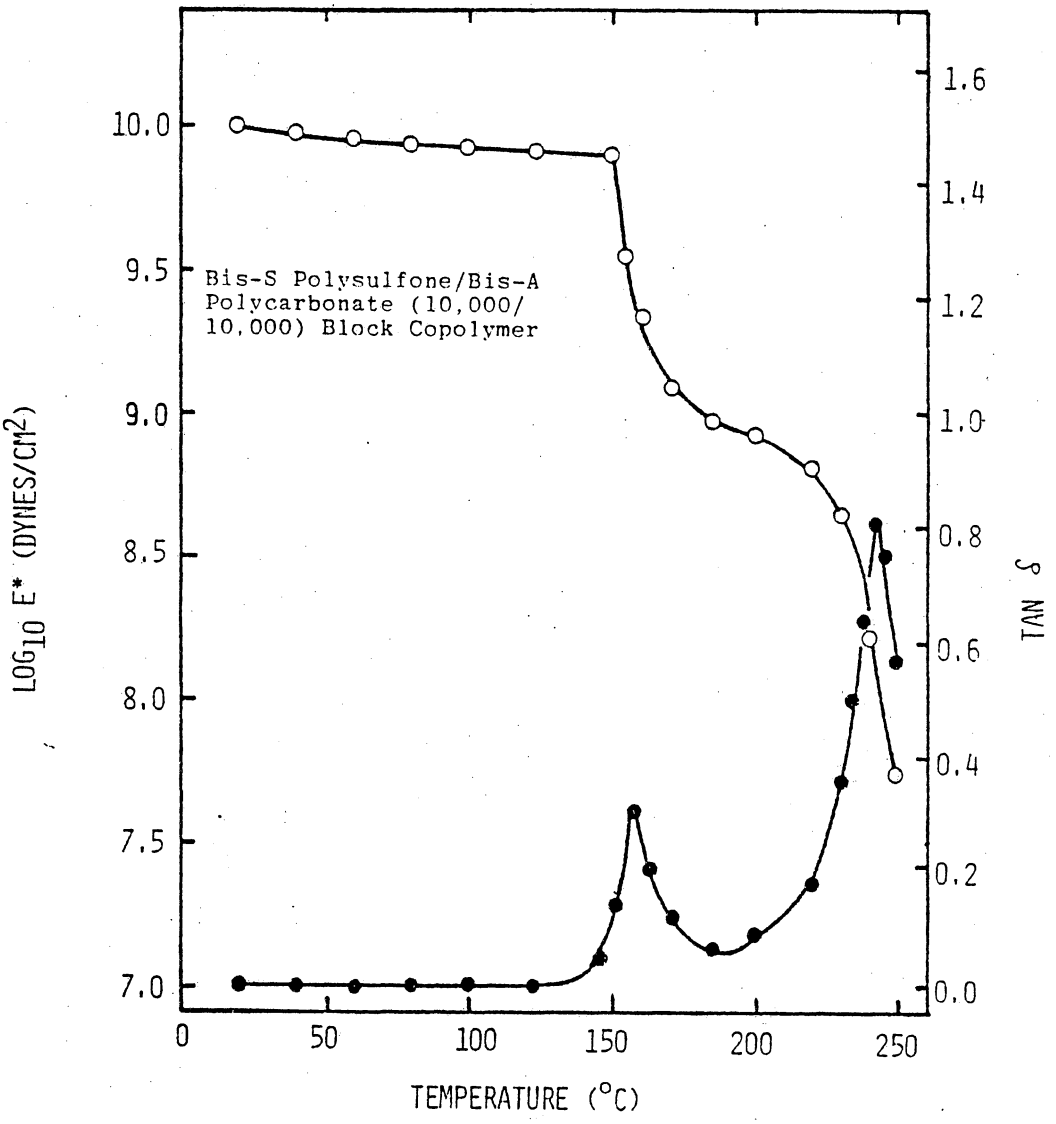

Figure 25. High temperature dynamic mechanical behavior of SS/AC -10/10.

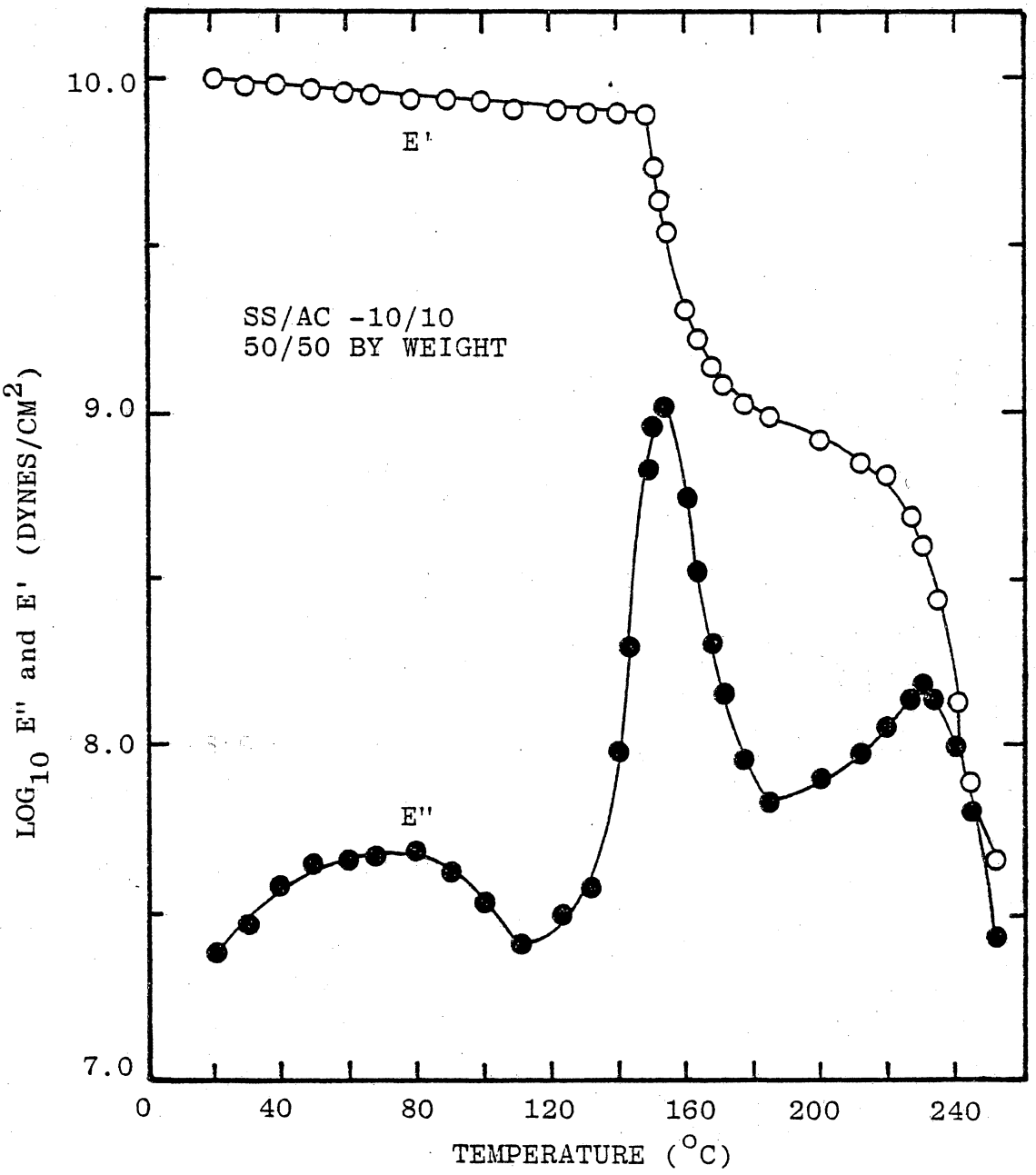

Figure 26. High temperature dynamic mechanical behavior of SS/AC-10/10 in terms of the storage (E') and loss (E") moduli.

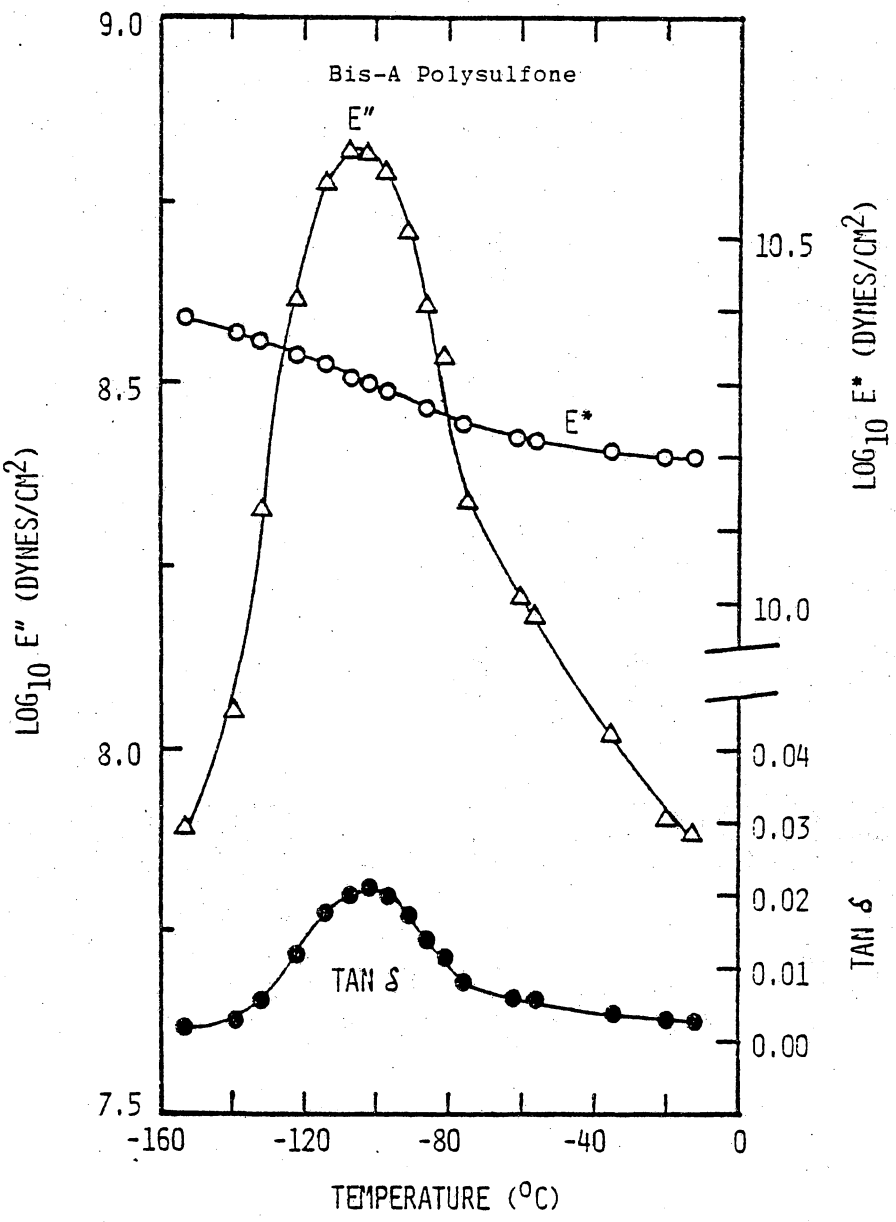

Figure 27. Low temperature dynamic mechanical behavior of polysulfone.

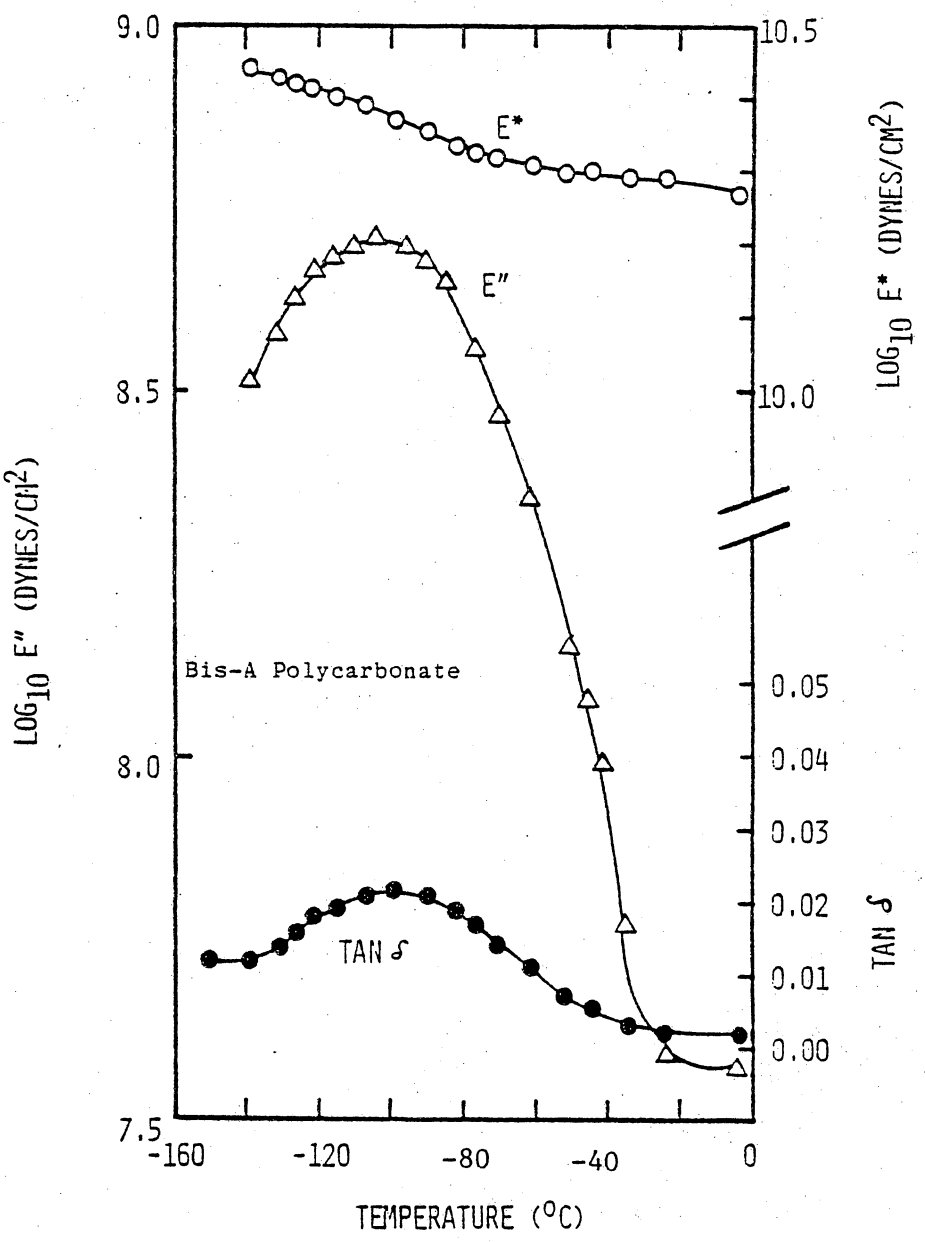

Figure 28. Low temperature dynamic mechanical behavior of polycarbonate.

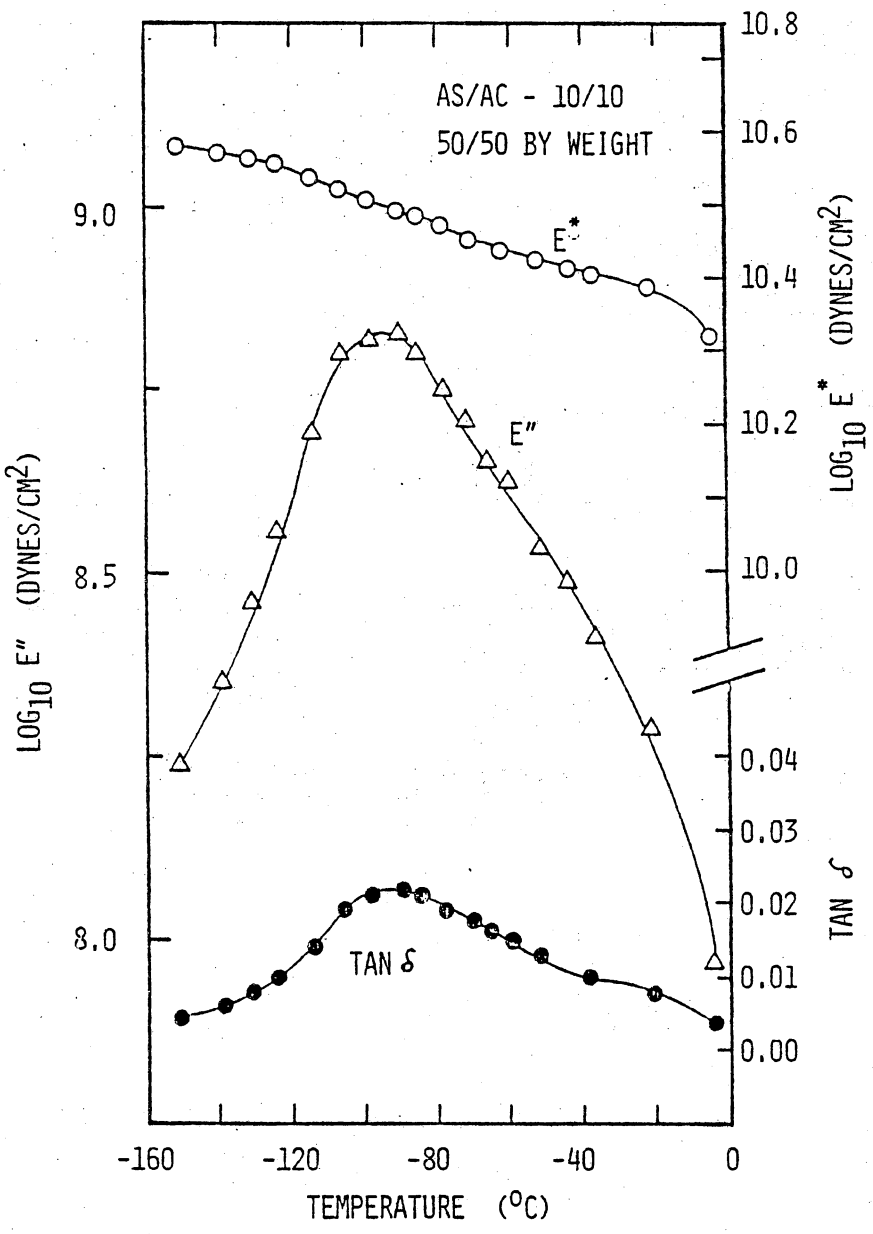

Figure 29. Low temperature dynamic mechanical behavior of a homogeneous polysulfone/polycarbonate block copolymer (AS/AC-10/10).

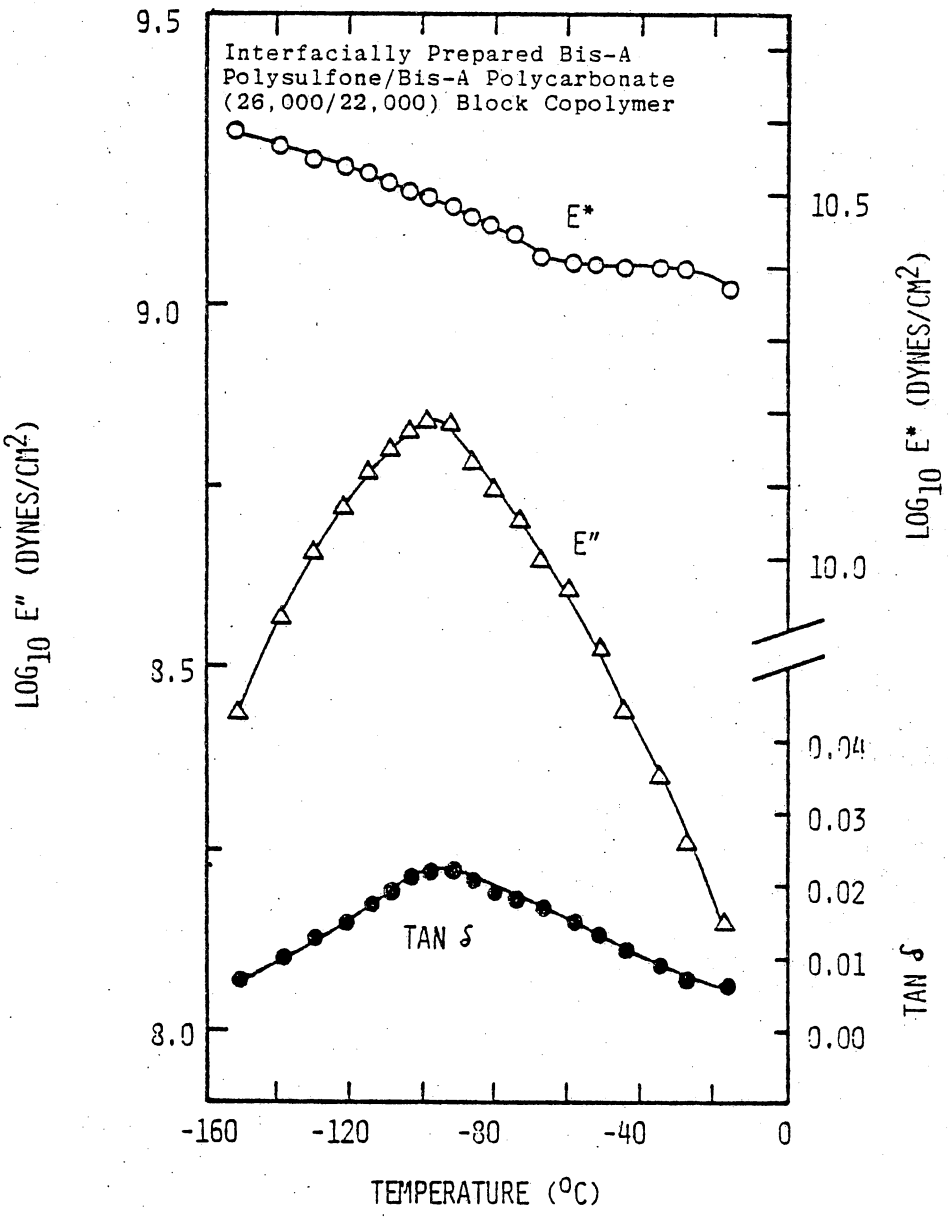

Figure 30. Low temperature dynamic mechanical behavior of a microheterogeneous polysulfone/polycarbonate block copolymer (AS/AC-26/22).

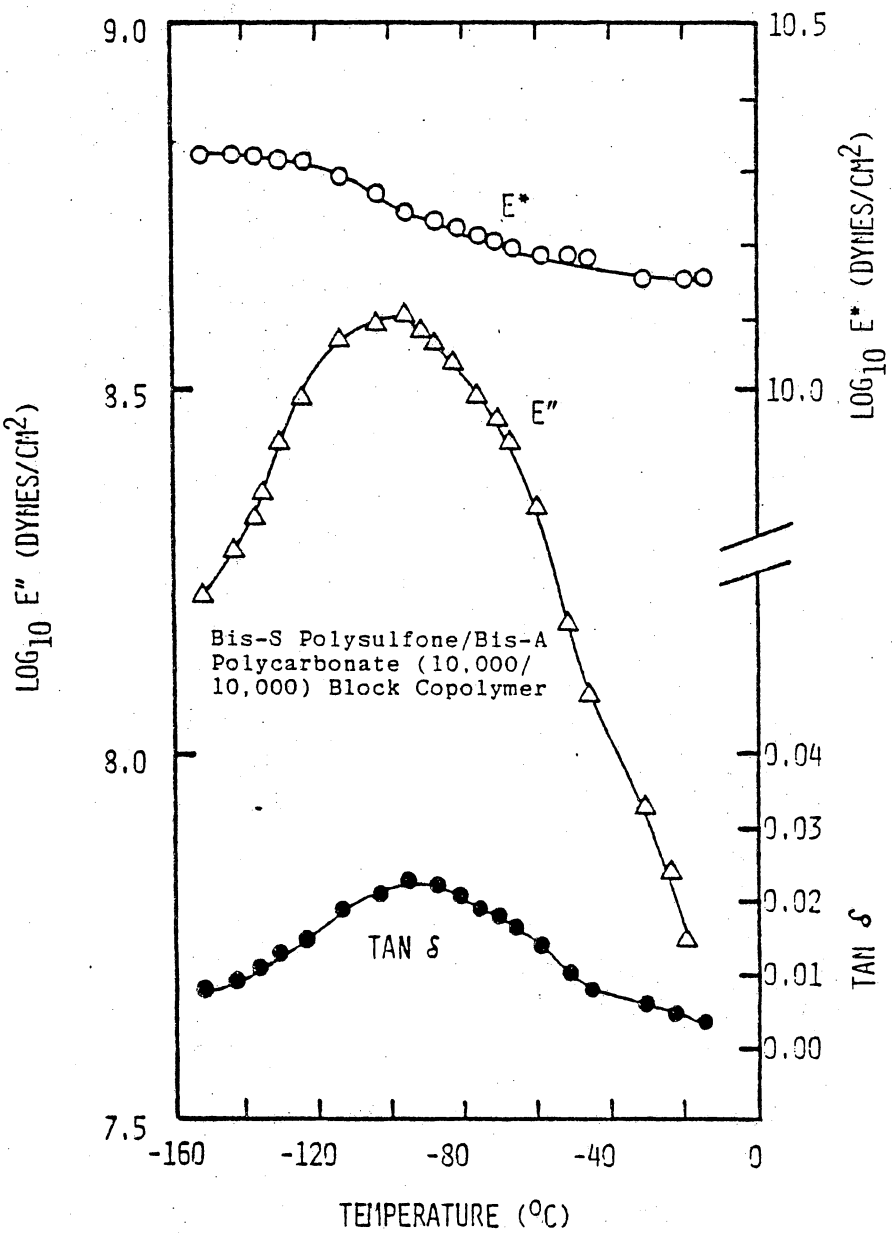

Figure 31. Low temperature dynamic mechanical behavior of a microheterogeneous bisphenol-S polysulfone/polycarbonate block copolymer (AS/AC-10/10).

The activation energies (E_A) for the low temperature transitions were calculated from additional experiments run at 35 and 110 Hz. The values of E_A ranged between 8-11 kcal/mole for both homopolymers as well as the copolymers.

2. Thermal Analysis

a) AS/AC Systems. The one and two-phase character of the AS/AC copolymers was further studied by differential scanning calorimetry (DSC). Powders, cast films and molded sheets were analyzed at a scan rate of 40°C per minute. The glass transition temperatures for the block copolymers analyzed by this method were presented in Table IV with the molecular weight data.

Earlier, it was noted that the AS/AC-16/16 copolymer could be obtained as either a one or two phase material depending upon whether the film was cast or molded. A series of annealing experiments was undertaken to investigate the effects of thermal treatment on the copolymers. In Figure 32, the effects of annealing the as-precipitated AS/AC-16/16 powder at various temperatures for 15 minutes are represented. The single Tg at 175°C disappears and is replaced by two Tg's at roughly 163 and 184°C which become more resolved as the annealing temperature is increased. A similar trend is noted in Figure 33 where the annealing temperature was held constant and the annealing time or cooling rate varied.

Annealing the AS/AC-10/10 copolymer at temperatures as high as 300°C for 15 minutes did not induce microphase separation. The curves in Figure 34 illustrate this point clearly. The AS/AC-26/22 copolymers

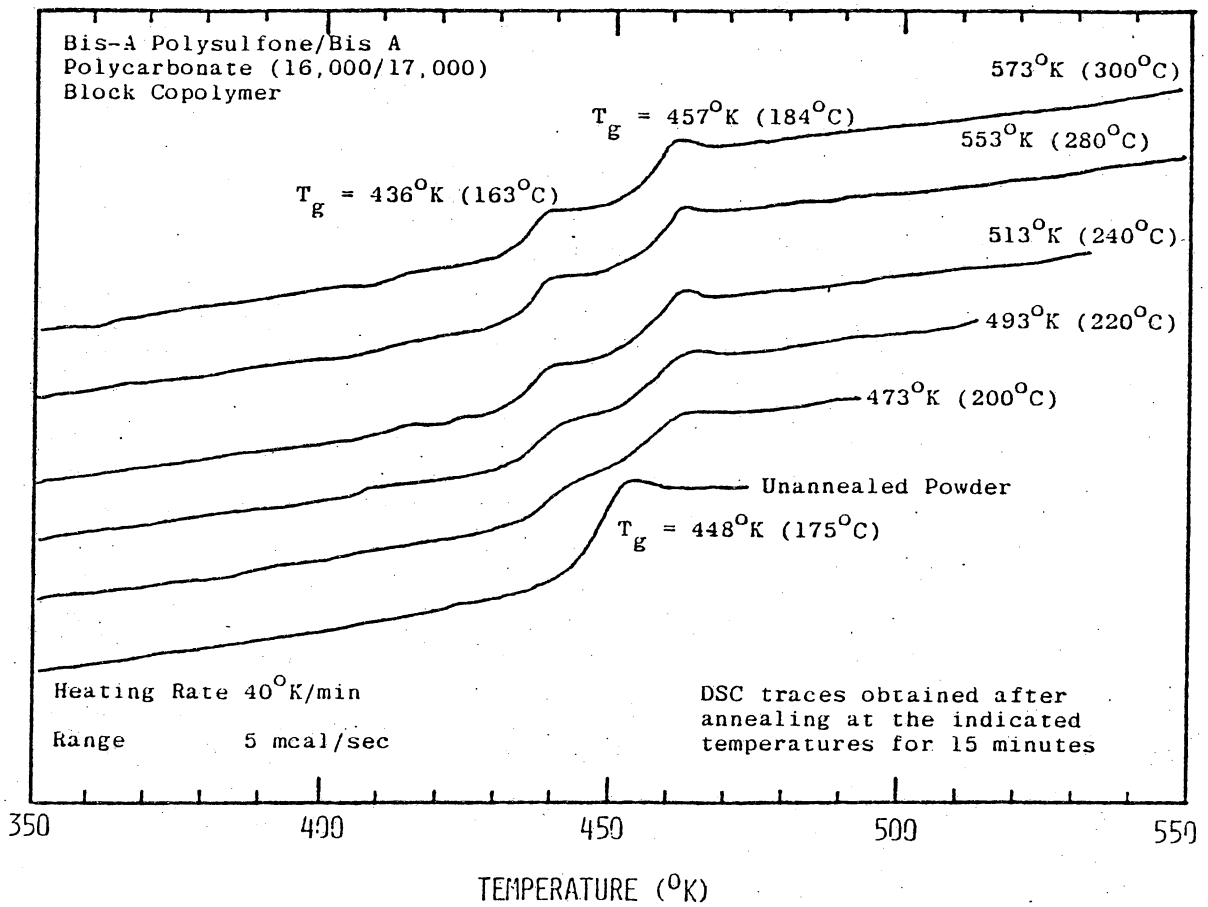

Figure 32. Effect of annealing on the phase behavior of AS/AC-16/17. The specimens were cooled at 320°K/min. after the annealing step.

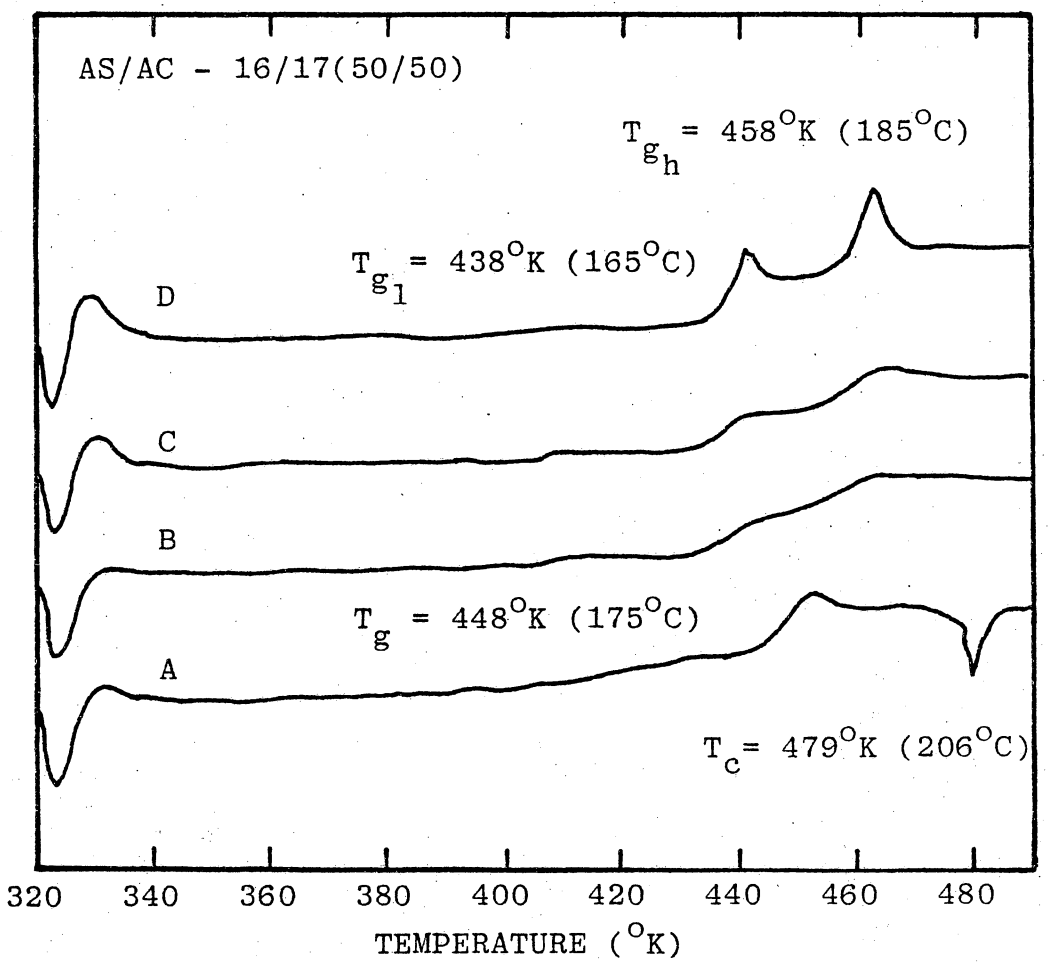

Figure 33. Effect of annealing time (220°C) on the phase behavior of AS/AC-16/17. The DSC traces correspond to (A) dried polymer powder - no pretreatment, (B) annealing 1 minute followed by quenching to 50°C, (C) annealing 30 minutes followed by quenching to 50°C, and (D) annealing 30 minutes followed by slow cooling at 1.25°C/min. to 50°C.

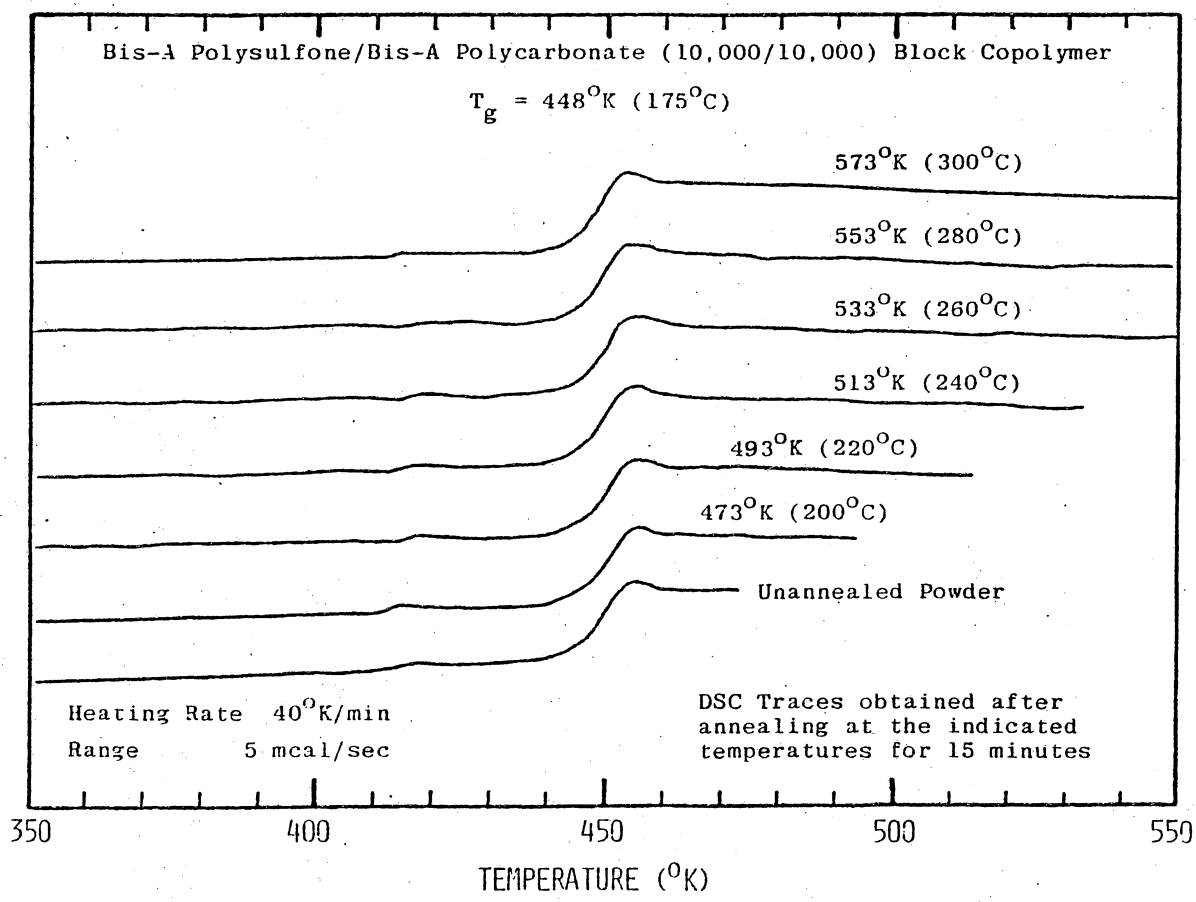

Figure 34. Effect of annealing on the phase behavior of AS/AC - 10/10.

showed two phase behavior even in the virgin powder form.

The effects of acetone immersion on a piece of AS/AC-16/17 film cast from THF, as revealed by thermal analysis, are demonstrated in Figure 35. The as-cast film exhibits a single Tg at 175°C and a very small broad endothermic peak indicating the presence of some crystallinity. Immersion in acetone for one hour at 25°C significantly increased the magnitude of the melting transition but did not affect the glass transition temperature. Subsequent annealing at 260°C for one hour induced microphase separation to take place and eliminated the melting endotherm completely.

(b) TS/AC System. The DSC traces obtained for TS/AC-10/10 are shown in Figure 36. The material remains a one phase system with a Tg at 162°C even after annealing at 300°C for 30 minutes. The behavior is similar to that observed for AS/AC-10/10.

(c) SS/AC System. The DSC scan for SS/AC-10/10 is shown in Figure 37 and indicates that the as-precipitated material is a two phase system with Tg's at 161 and 231°C. A similar material, SS/AC-5/5 (50/50) also displayed two phase behavior. The Tg's were slightly different, however, occuring at 167 and 229°C.

C. Mechanical Properties

1. Stress-Strain Properties. The tensile behavior of several representative block copolymers was investigated at a strain rate of 2.0 inches (5 cm) per minute at room temperature. Results obtained for polycarbonate, polysulfone and a few one and two-phase block copolymers are summarized in Table IX. No significant differences in the tensile

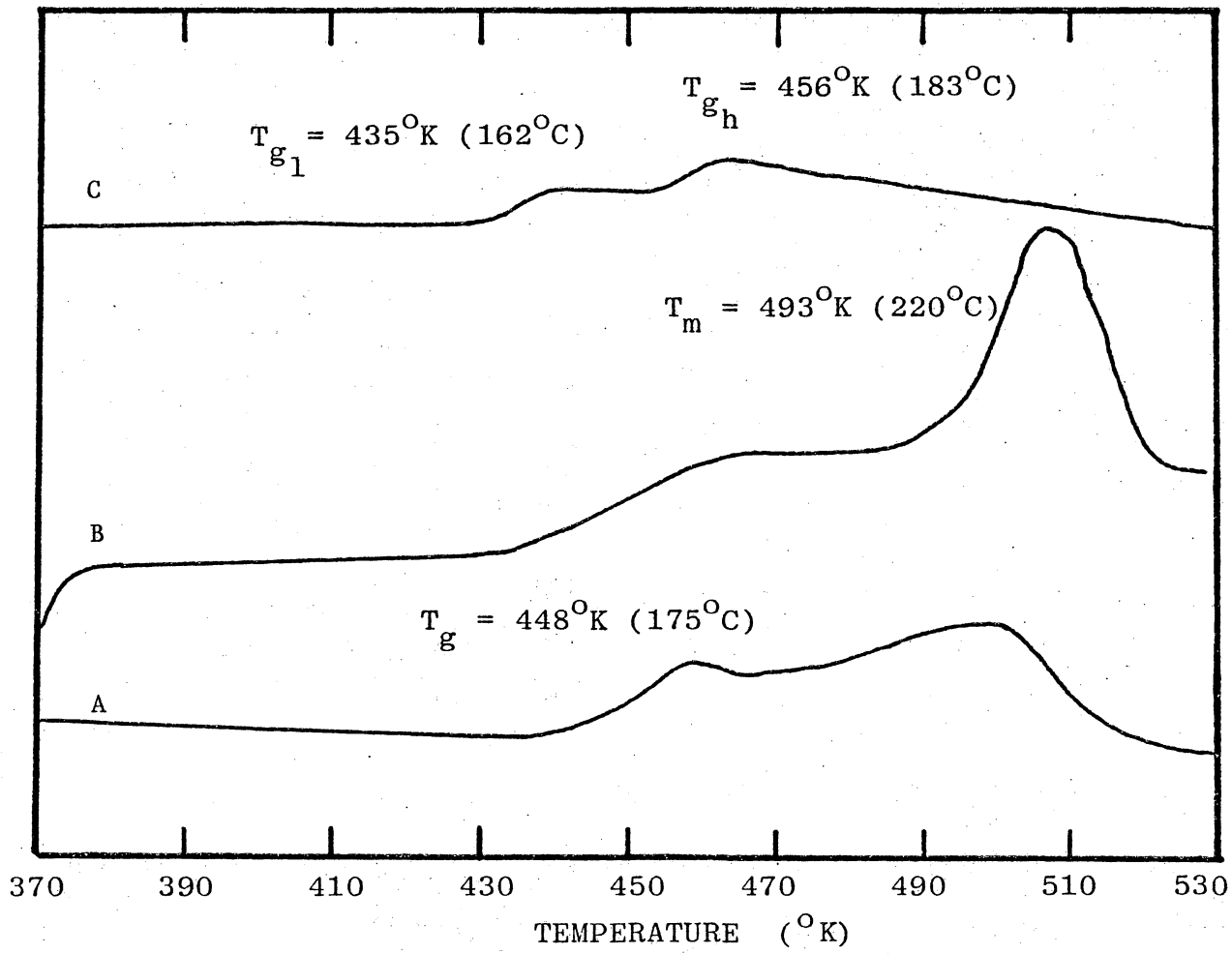

Figure 35. DSC traces obtained for AS/AC-16/17 film cast from THF (A), after 1 hour acetone immersion (B), and after annealing for 1 hour at 260 °C(C). Each trace was obtained at 40°C/min.

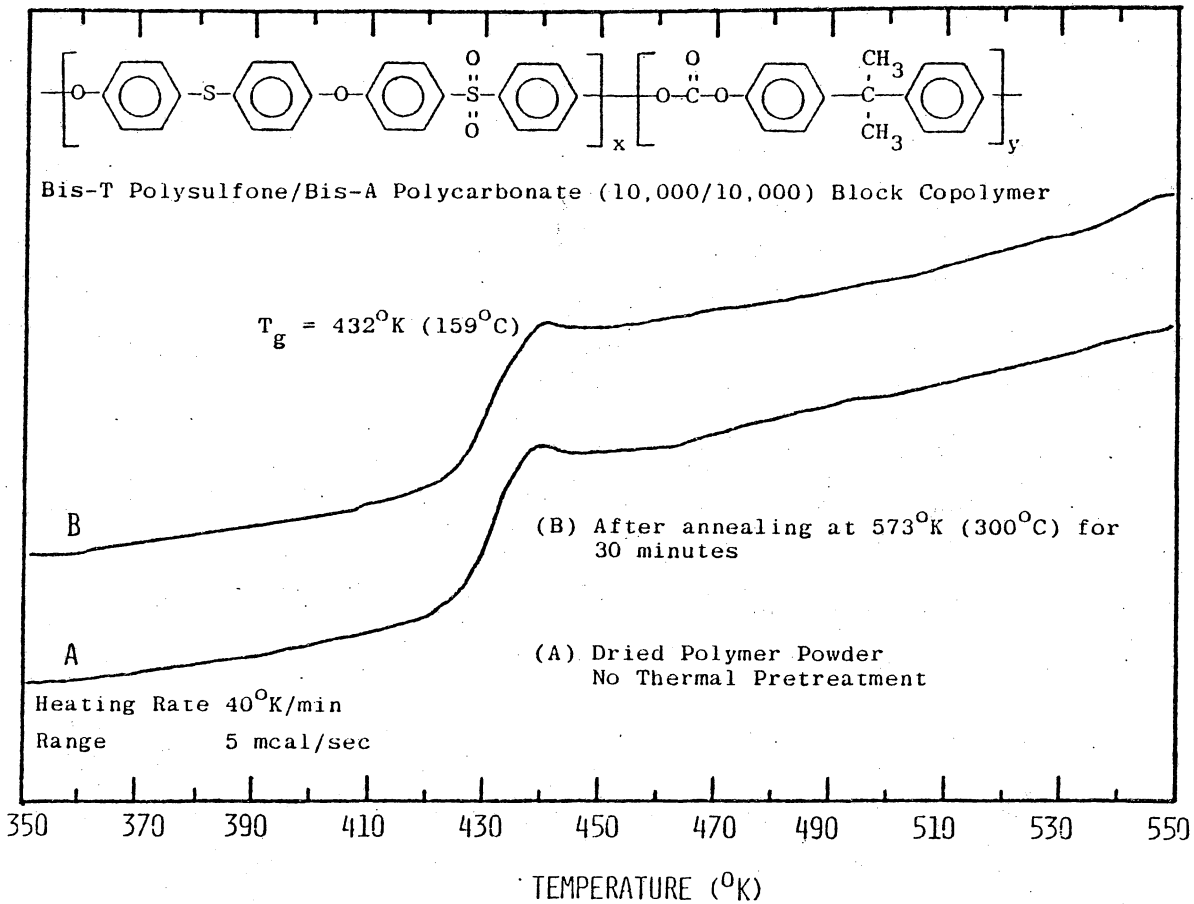

Figure 36. Effect of annealing on the phase behavior of TS/AC - 10/10.

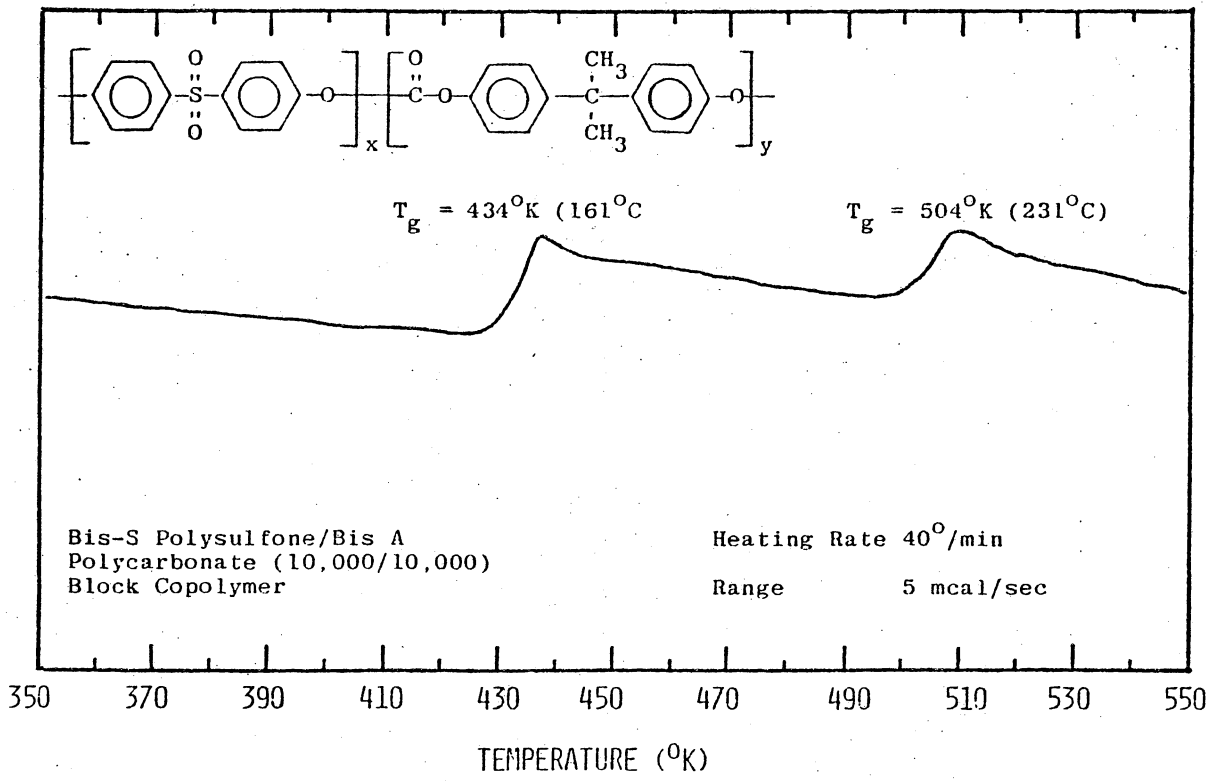

Figure 37. DSC trace obtained for SS/AC - 10/10 powder as precipitated.

Table IX

Stress-Strain Data*

Sample	Yield Stress (kg/cm^2)	Yield Elongation (%)	Fracture Stress (kg/cm^2)	Elongation at break (%)
Polycarbonate	3,220 - 3,580	8.0 - 8.8	3,270 - 3,650	120 - 140
Polysulfone	3,170 - 3,650	5.5 - 6.5	2,010 - 2,970	75 - 100
AS/AC-5/5	2,800 - 3,240	6.5 - 7.5	2,350 - 2,660	15 - 35
AS/AC-26/22	2,830 - 3,100	6.0 - 7.5	2,220 - 2,490	10 - 66
TS/AC - 10/10	2,560 - 3,340	5.5 - 7.0	2,560 - 3,340	6 - 10

*All at 2.0 inches (5 cm) per minute crosshead speed at 25°C.

properties of the copolymers can be observed. Both the one and two phase materials exhibit properties intermediate to those of polycarbonate and polysulfone. Further studies with a much wider range of samples are obviously needed.

2. Melt Rheology. The melt rheology data shown in Figures 38-41 were obtained on a Weissenberg Rheogomeometer at a steady shear rate of 21.2 sec^{-1}. The results are plotted as the logarithm of viscosity vs. inverse temperature to facilitate calculation of the thermal activation energy for melt flow (E_A). It should be pointed out that these measurements were very difficult to obtain since the homopolymers and copolymers exhibited highly elastic melts which tended to exude from the cone and plate. Each of the data points was taken on a separate polymer specimen at each indicated temperature.

As shown in Figures 38 and 39, the melt viscosity of the commercial polysulfone sample was greater than that of the polycarbonate sample although their activation energies are quite similar. These values correspond well with literature values for polysulfone (31 Kcal/mole)[105] and polycarbonate (26-30 Kcal/mole).[137]

The melt viscosity temperature dependence of AC/AS-5/20 (33/67) is presented in Figure 40. This particular sample was one of the earlier 33/67 compositions that was investigated. It is a single phase copolymer with a Tg of 166°C and a number average molecular weight of 30,000. The thermal activation energy calculated for this polymer (27.1 Kcal/mole) is only slightly greater than that measured for the two homopolymers. On the other hand, the value of E_A calculated for

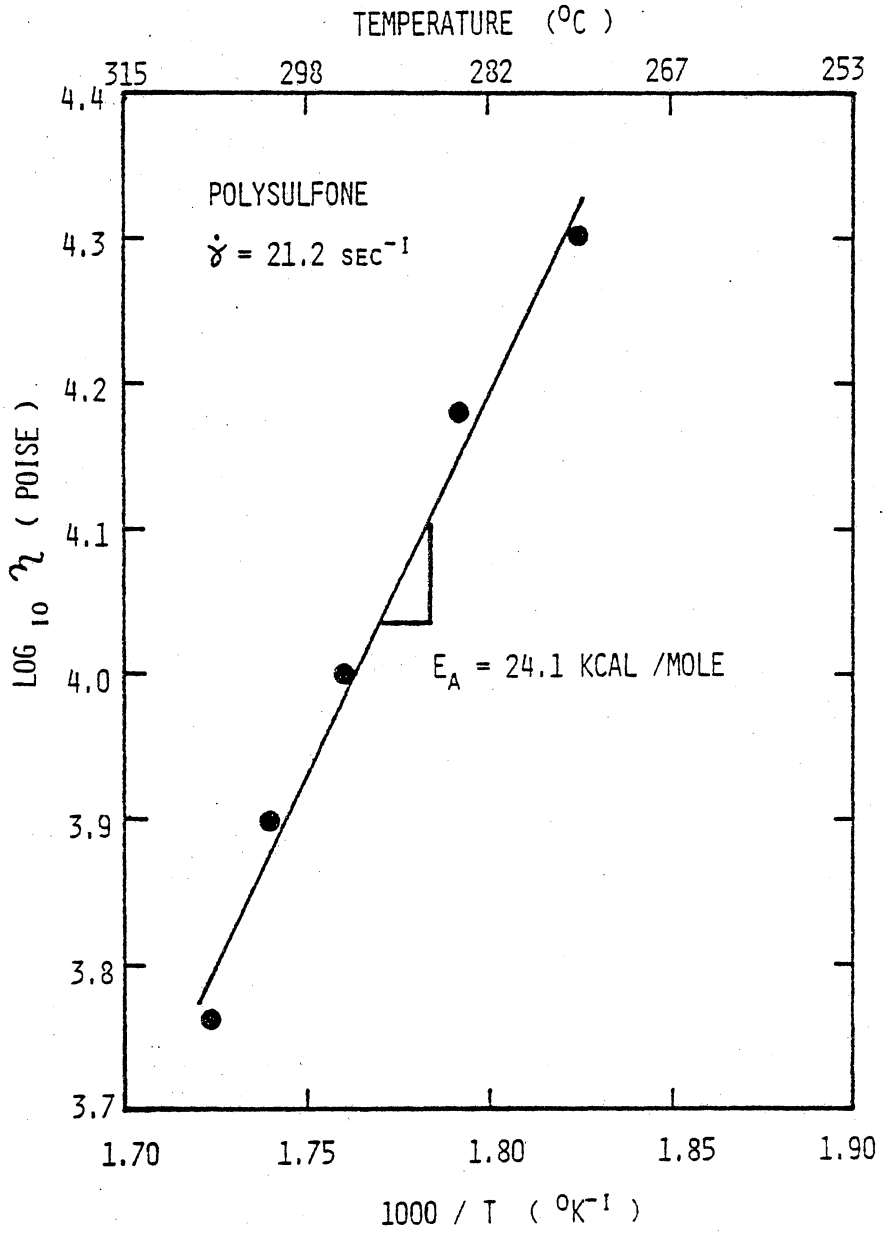

Figure 38. Temperature dependence of melt viscosity for polysulfone.

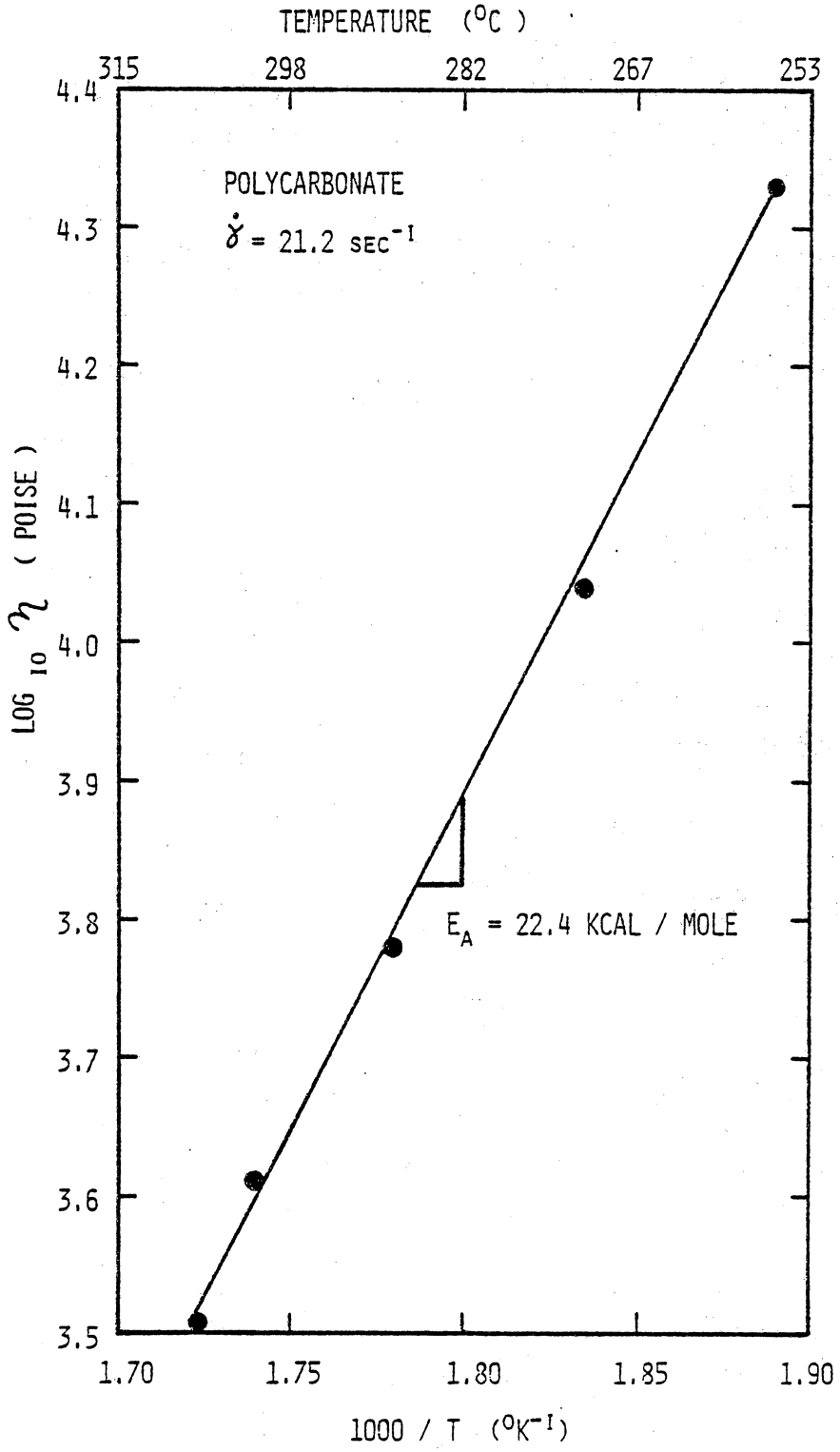

Figure 39. Temperature dependence of melt viscosity for polycarbonate.

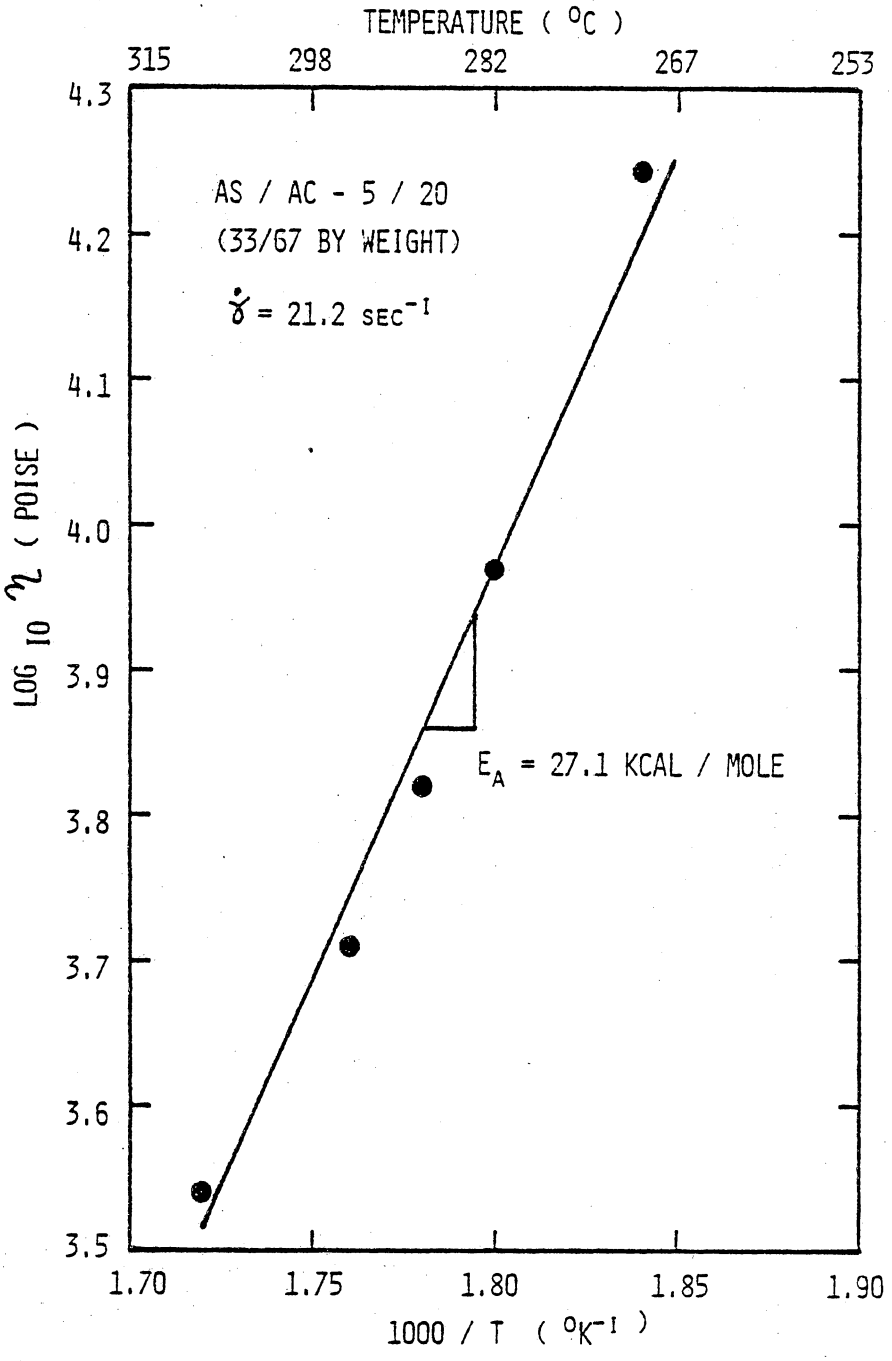

Figure 40. Temperature dependence of melt viscosity for a homogeneous polysulfone/polycarbonate block copolymer (AS/AC-5/20).

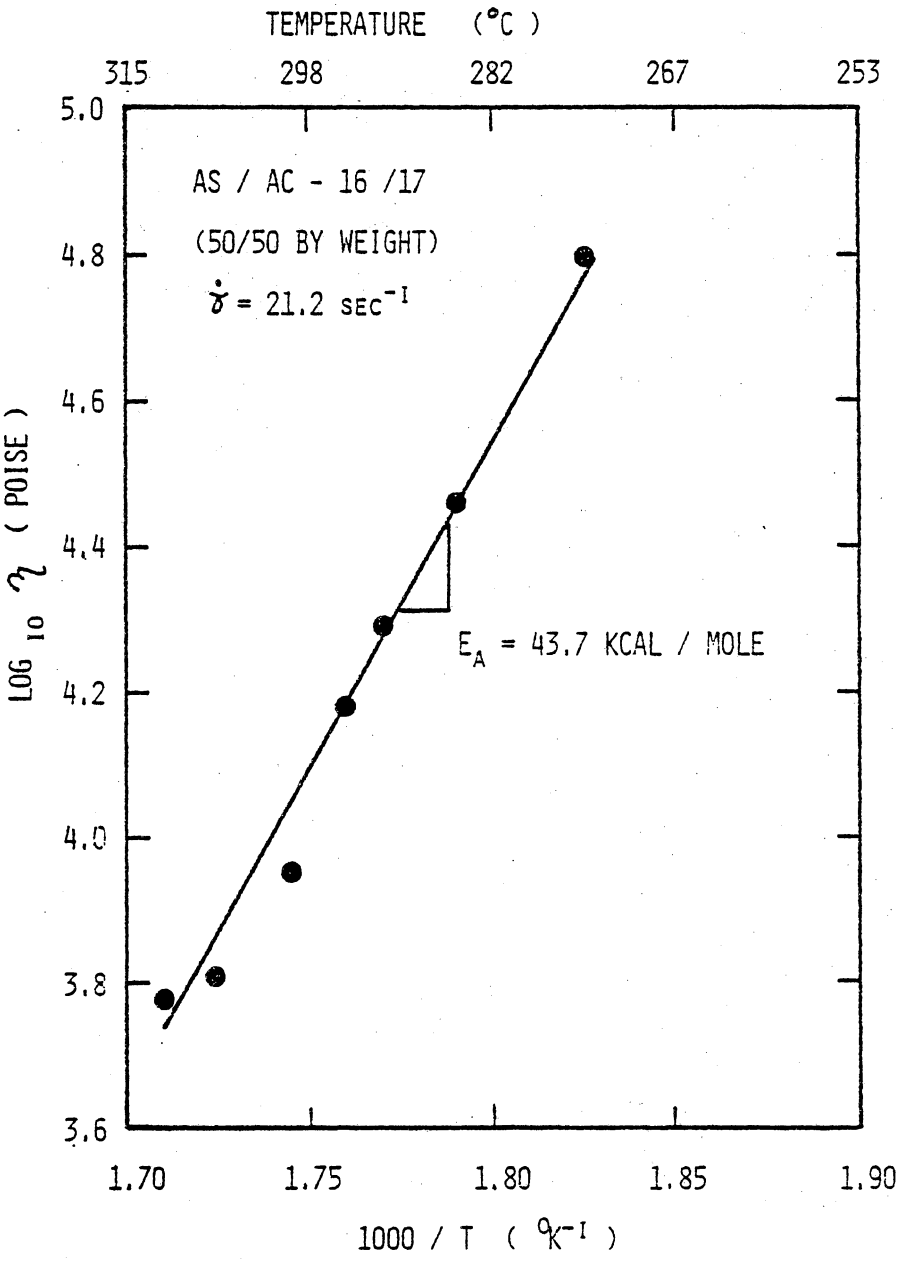

Figure 41. Temperature dependence of melt viscosity for a microheterogeneous polysulfone/polycarbonate block copolymer (AS/AC-16/17).

AS/AC-16/17, a two phase system, was 43.7 Kcal/mole as shown in Figure 41, much greater than those of either the homopolymers or the single phase copolymer.

It is also interesting to note that the melt viscosity of the single phase copolymer lies between those of the commercial materials. Since the molecular weight of AS/AC-5/20 is close to those of the polysulfone ($\bar{M}_n$ = 28,000) and the polycarbonate ($\bar{M}_n$ = 20,000) such intermediate behavior is not surprising. The melt viscosity of AS/AC-16/17, on the other hand, is nearly an order of magnitude greater than that of the polysulfone due partly to its high molecular weight ($\bar{M}_n$ = 71,000) as well as the two-phase nature of this particular copolymer.

3. Impact Testing

(a) Commercial Polymers. Representative acceleration-time curves obtained for each of the commercial polymers are shown in Figures 42-47. These curves correspond to the fractured specimens pictured in Figures 48-50. Three main types of failure can be readily observed: ductile, crack, and very brittle. Ductile failure shows up as a neat hole punched in the specimen coupled with deep drawing on the side opposite the strike. Polycarbonate, polysulfone and high density polyethylene fail in this manner with most of the damage localized about the strike point. A small amoung of cracking or tearing occurs with high density polyethylene. Note that on the impact curves in Figures 42-47 the data for polycarbonate is plotted on a different scale in view of this material's superior impact strength.

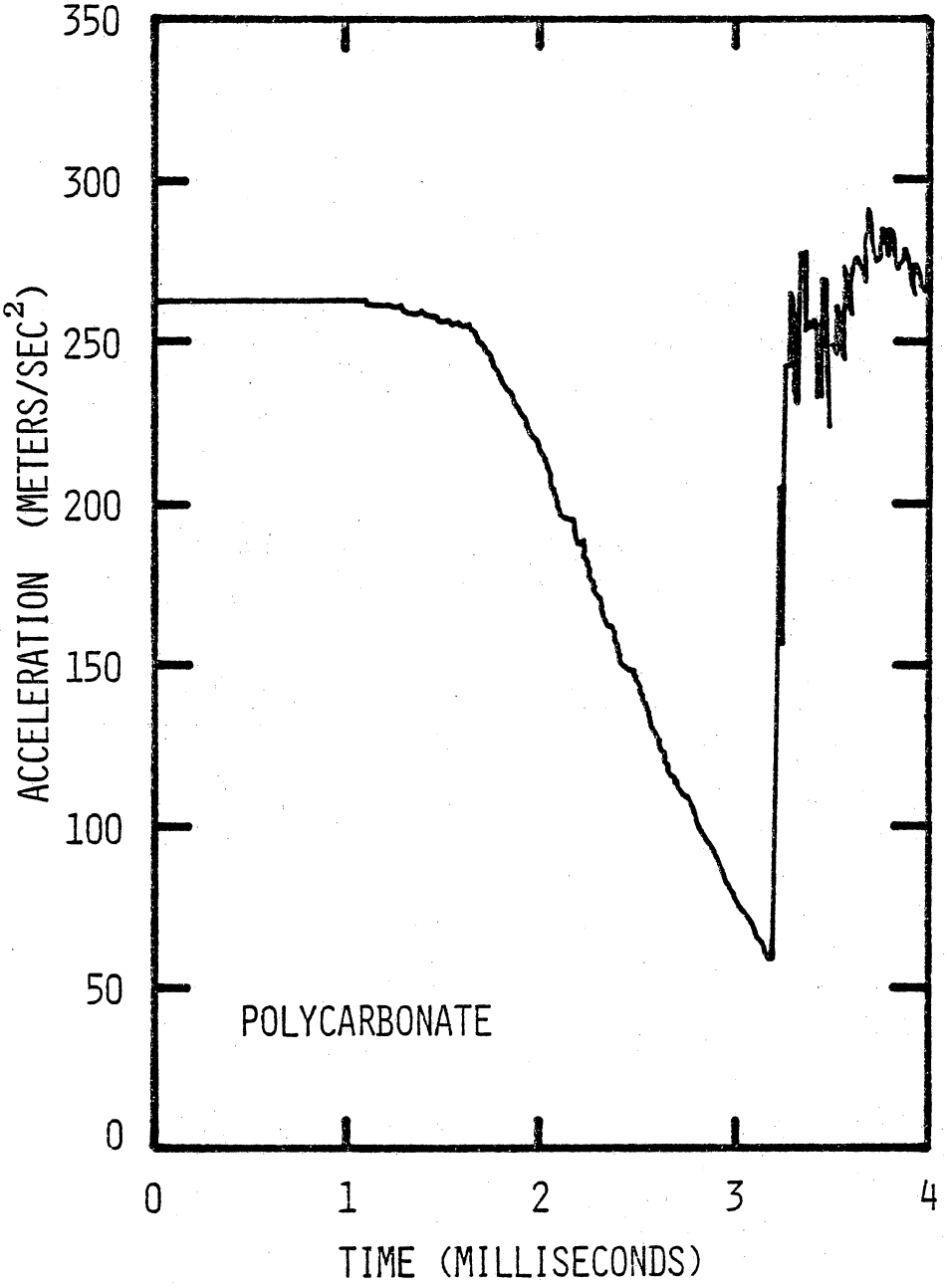

Figure 42. Acceleration-time curve obtained for a polycarbonate specimen 0.33 mm thick.

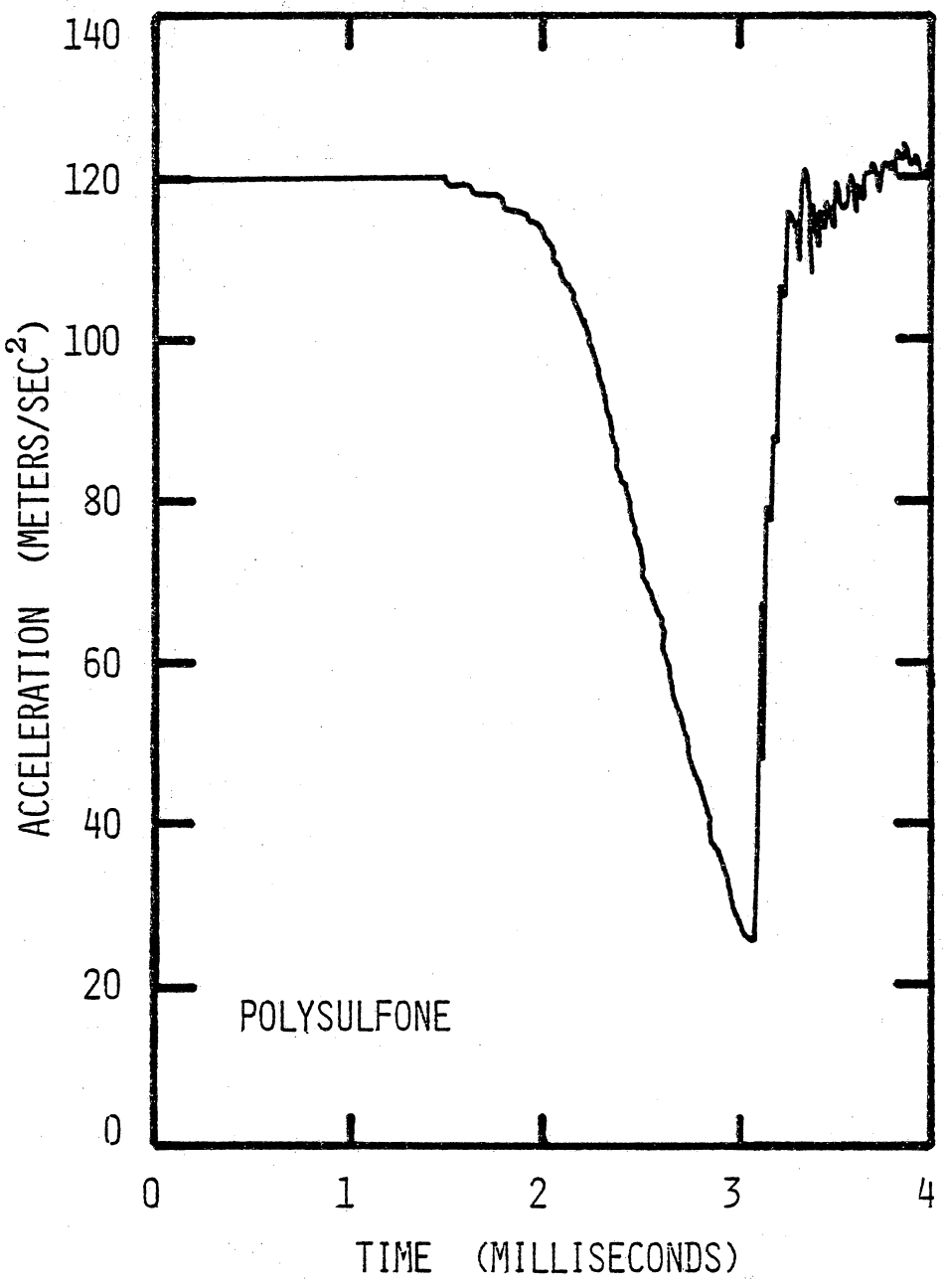

Figure 43. Acceleration-time curve obtained for a polysulfone specimen 0.20 mm thick.

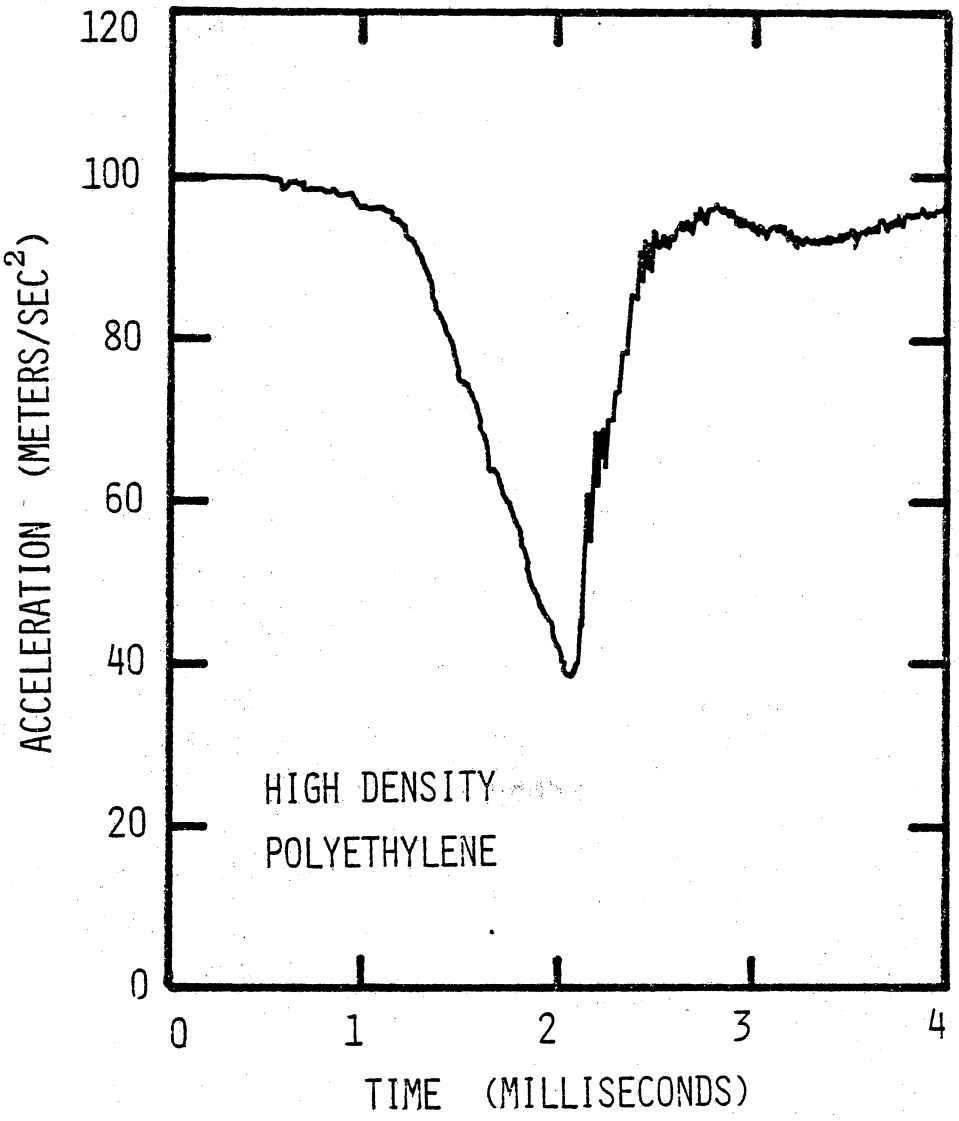

Figure 44. Acceleration-time curve obtained for a high density polyethylene specimen 0.31 mm thick.

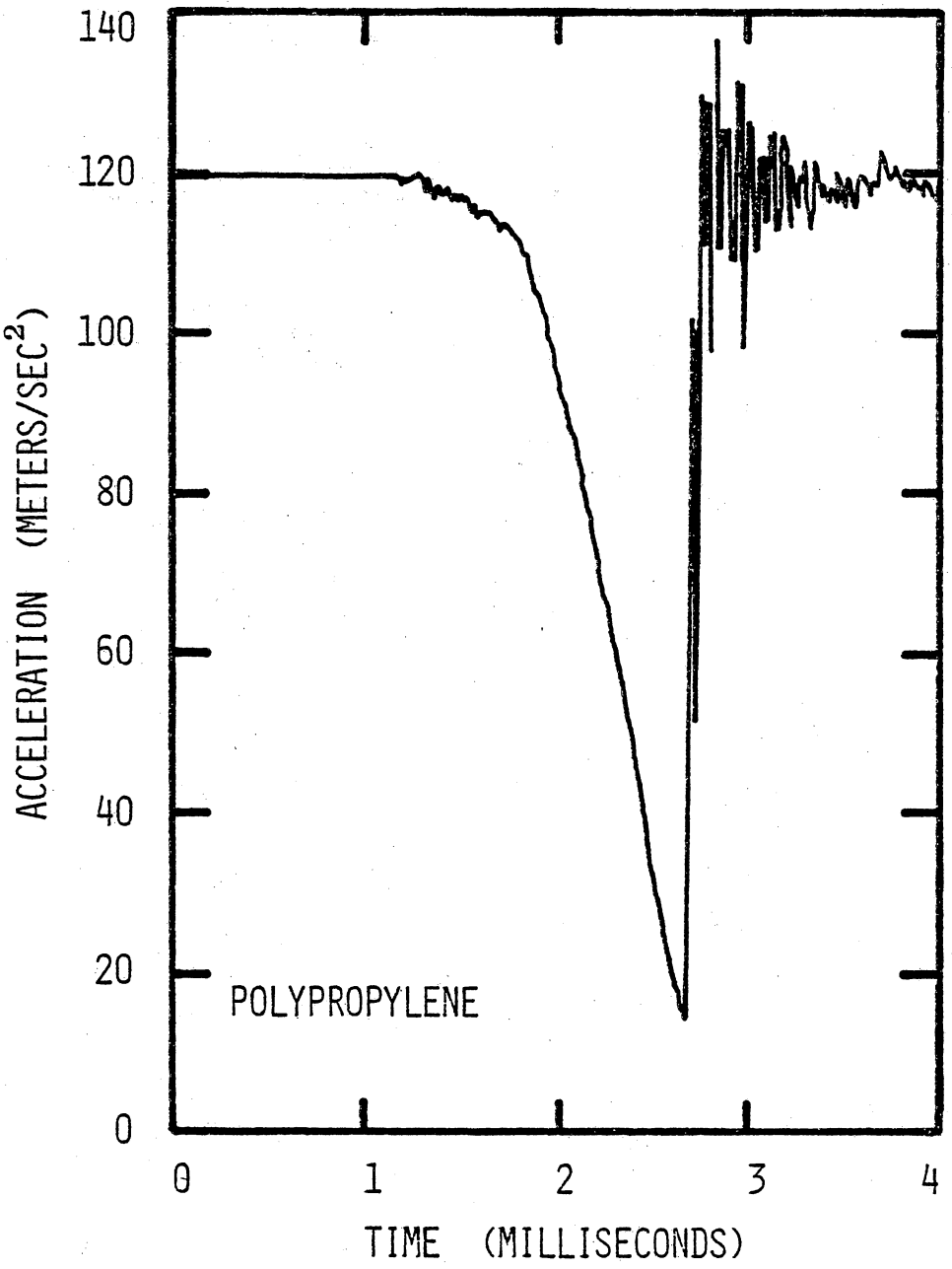

Figure 45. Acceleration-time curve obtained for a polypropylene specimen 0.43 mm thick.

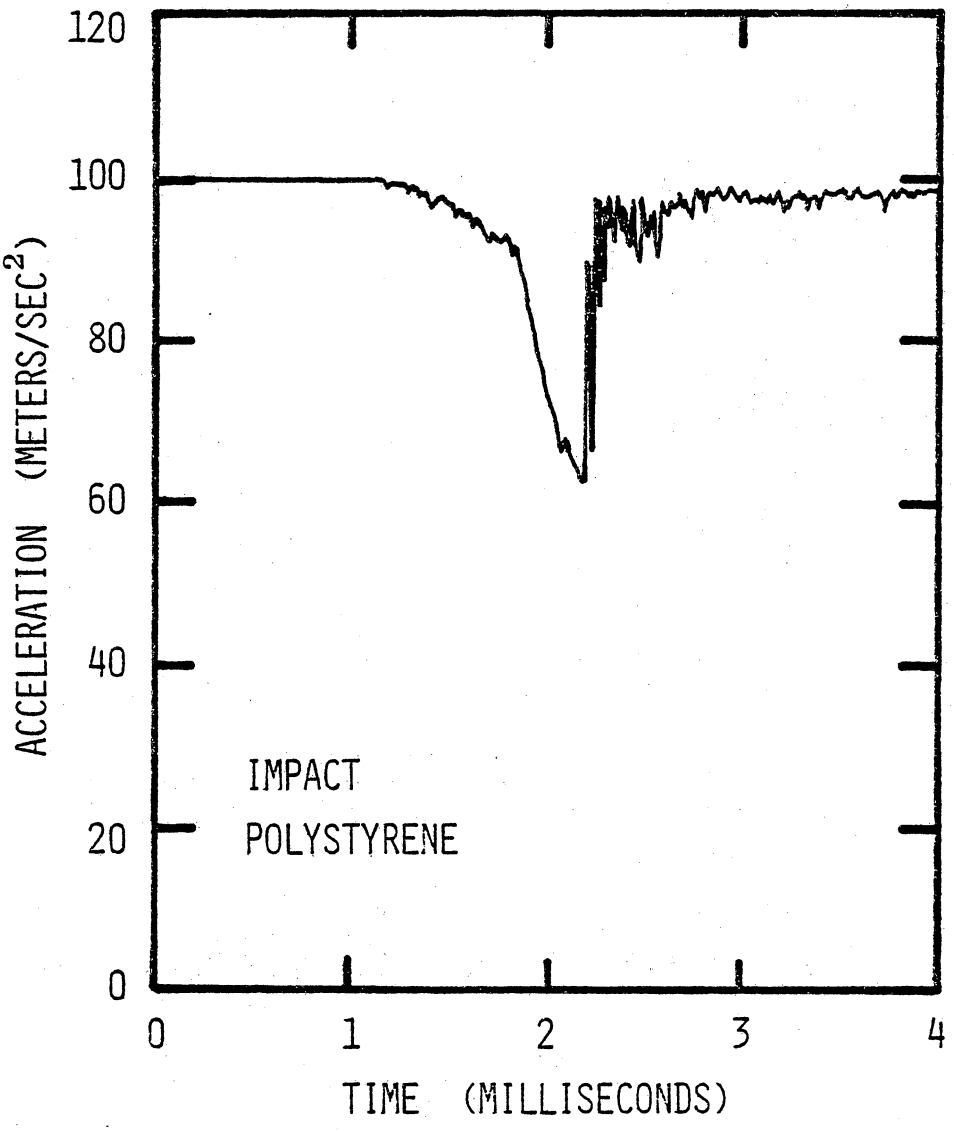

Figure 46. Acceleration-time curve obtained for an impact modified polystyrene specimen 0.33 mm thick.

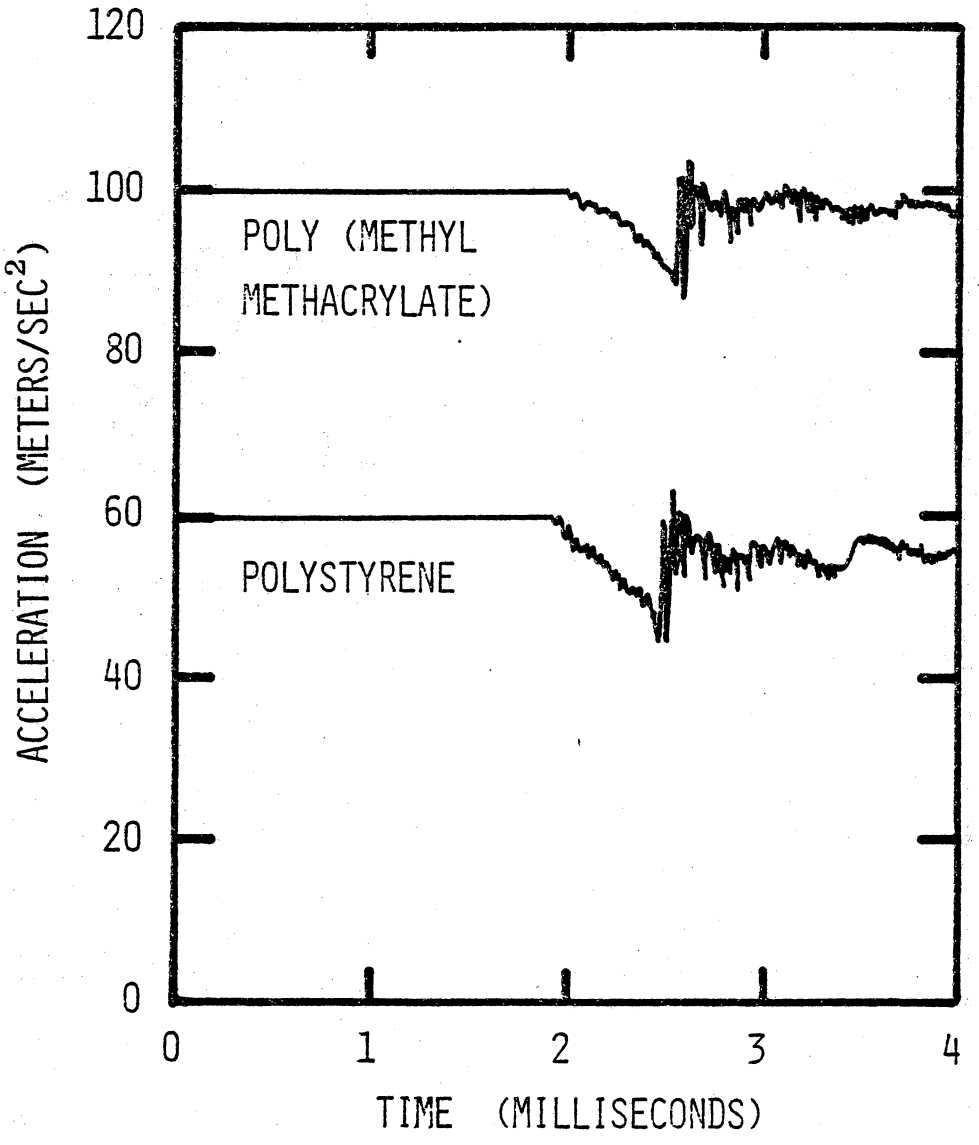

Figure 47. Acceleration-time curves obtained for poly(methyl methacrylate) (0.20 mm thick) and polystyrene (0.23 mm thick).

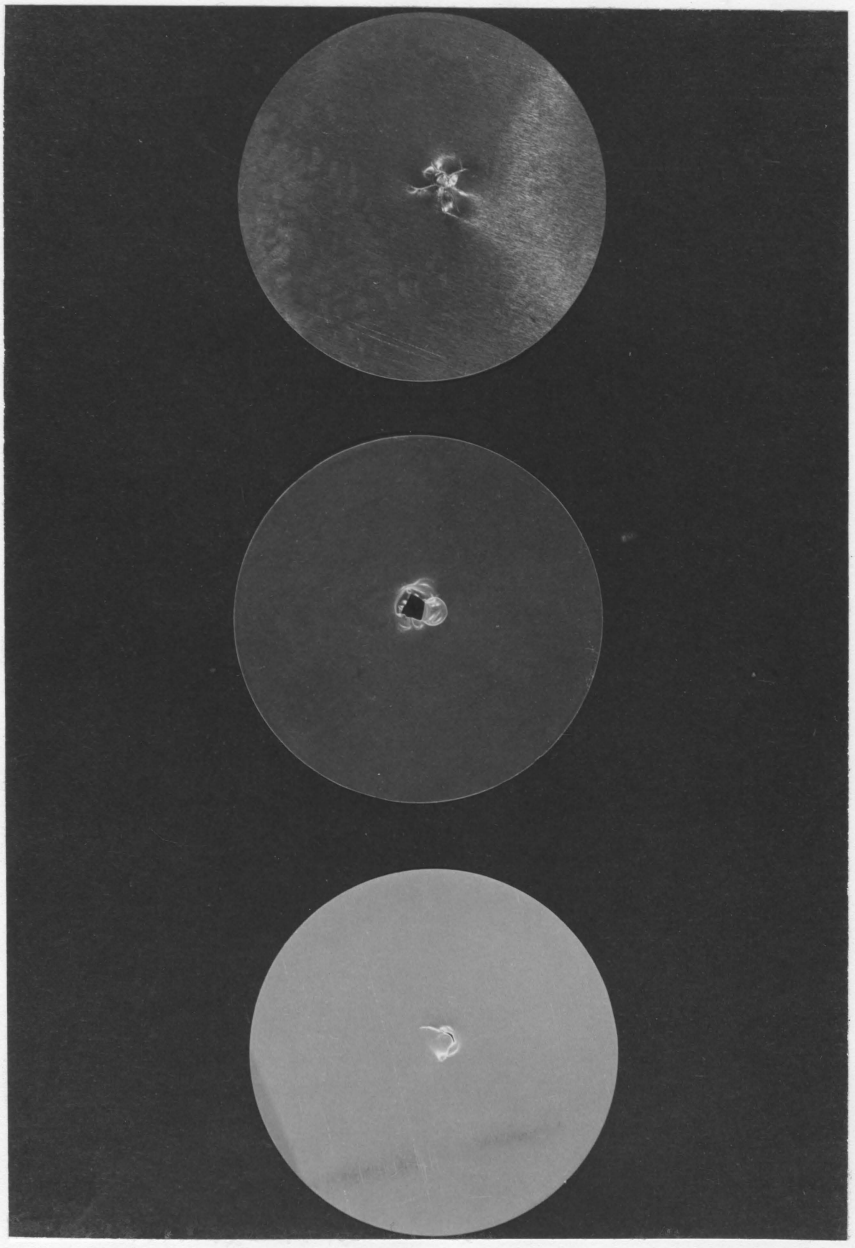

Figure 48. Three polymers which fail in a ductile mode: polysulfone (top), polycarbonate (center), and high density polyethylene (bottom).

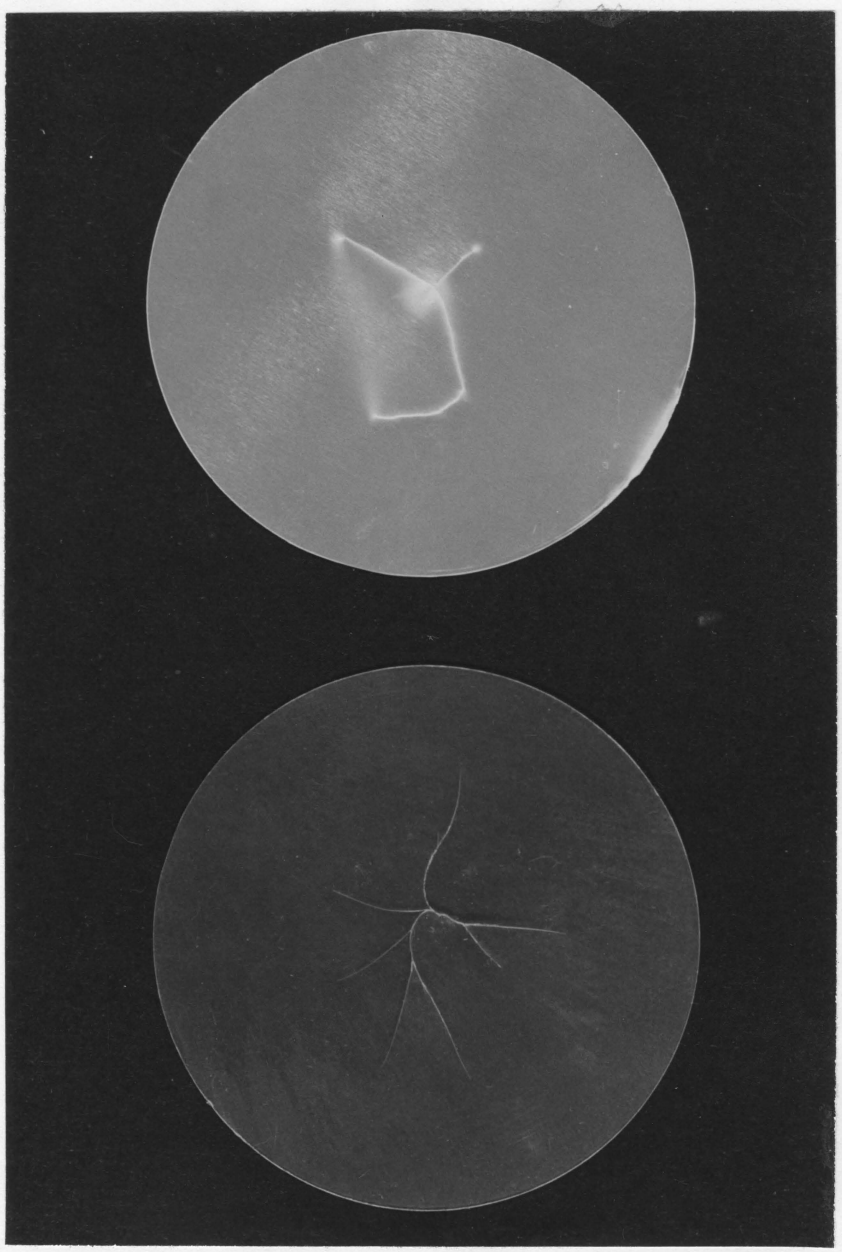

Figure 49. Two polymers which fail by cracking: impact-modified polystyrene (top) and polypropylene (bottom).

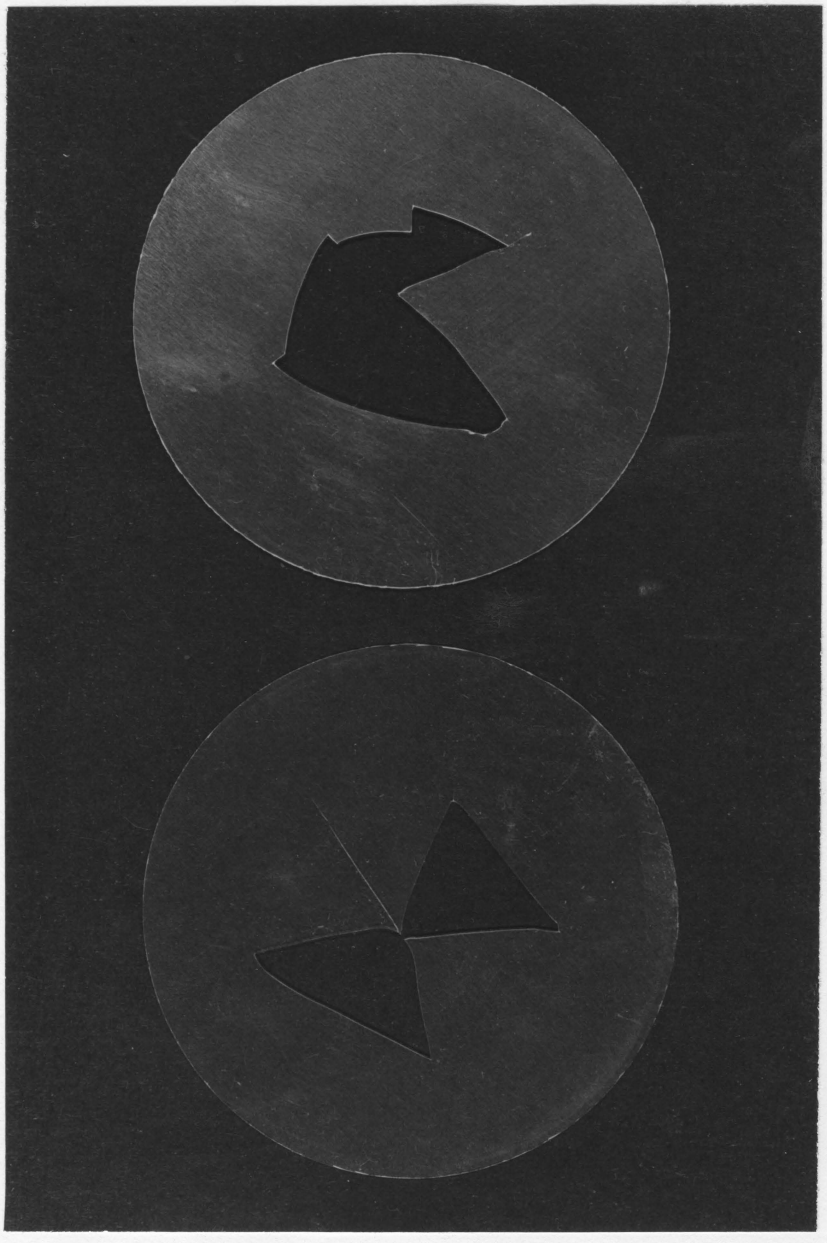

Figure 50. Two polymers which display very brittle failure modes: poly(methyl methacrylate) (top) and polystyrene (bottom).

Polypropylene and impact-modified polystyrene fail by cracking. The crack patterns displayed by the two specimens in Figure 49 are quite reproducible as long as the specimens are prepared in the same manner. One can observe a higher degree of crack formation in polypropylene than in impact polystyrene and, correspondingly, a higher impact strength in the former. In such materials, impact strength appears to depend upon the ability of the substance to dissipate energy by cracking. Very little deformation takes place before catastrophic failure occurs. The impact curve shown in Figure 46 for impact polystyrene indicates that the failure process may involve two separate mechanisms. As this material is a multiphase rubber modified compound, such a mixed mode failure is not surprising. One might imagine the first stage, which is nearly linear with time, to involve the formation and propagation of cracks. The second stage probably results from the increased energy required to propagate cracks through or around the rubber microphase dispersed through the brittle matrix. It is interesting to note that the impact curve for impact polystyrene is superimposable with the initial section of that shown for polypropylene in Figure 45, an indication that the mechanisms for energy dissipation in these materials are similar.

Impact curves for both polystyrene and poly(methyl methacrylate) are shown in Figure 47. Note that the curves are very similar and that the deceleration is linear with time up to the fracture point. Such a curve is reminiscent of a stress-strain curve characteristic of a brittle material; a linear increase in load with strain or time up to

fracture. The fractured specimens pictured in Figure 50 have large jagged holes covering most of their original area. The pieces removed from the centers showed no signs of stress whitening as did impact polystyrene specimens. Virtually no local deformation occurs in polystyrene or PMMA before complete and rapid fracture takes place.

The impact data compiled for the commercial polymers is listed in Table X. Included are the specimen thickness, velocity change on impact, and the energy to fracture each specimen (E_B). Since this particular device is quite sensitive to small specimen variations, a value for the fracture energy corrected for thickness is reported in joules per millimeter of thickness. As can be seen, the reproducibility of the data obtained under the listed conditions is very good. The standard deviation (S_n) was calculated for each polymer type as

$$S_n = [\Sigma (E_B/t - \overline{E_B/t})^2/(N-1)]^{1/2}$$

where $\overline{E_B/t}$ is the average fracture energy and N is the number of measurements. Under the designated test conditions, these impact values can be taken plus or minus 10% or less.

It is, of course, important to compare the impact strengths obtained on the falling weight tester with those obtained by some other method such as the notched Izod test. Such a comparison is provided in Table XI and indicates that the agreement between both methods is very good. An exact correlation cannot be expected due to the various degrees of notch sensitivity exhibited by these polymers. The dependence of impact strength on molecular weight also differs between polymer

Table X

Impact Strengths of Commercial Polymers

Polymer	Sample No.	t (mm)	Δv (m/sec)	E_B (joules)	E_B/t (joules/mm)	$(E_B/t) \pm \bar{S}_n$ Avg.
Polycarbonate	1	0.28	0.157	0.900	3.22	
	2	0.31	0.164	0.940	3.08	3.07 ± 0.16
	3	0.33	0.168	0.962	2.91	(±5.2%)
Polysulfone	1	0.25	0.0814	0.467	1.84	
	2	0.23	0.0693	0.400	1.75	1.75 ± 0.09
	3	0.20	0.0579	0.336	1.65	(±5.1%)
Polypropylene	1	0.43	0.0514	0.298	0.690	
	2	0.46	0.0518	0.301	0.658	0.679 ± 0.018
	3	0.43	0.0512	0.297	0.688	(±2.7%)
High Density Polyethylene	1	0.25	0.0269	0.157	0.618	
	2	0.31	0.0320	0.186	0.610	0.606 ± 0.014
	3	0.31	0.0307	0.180	0.590	(±2.3%)
Impact Polystyrene	1	0.33	0.0138	0.080	0.242	
	2	0.33	0.0121	0.070	0.212	0.221 ± 0.016
	3	0.31	0.0114	0.064	0.210	(±7.2%)
Poly(methyl Methacrylate)	1	0.20	0.0021	0.012	0.060	
	2	0.28	0.0026	0.015	0.054	0.057 ± 0.003
	3	0.28	0.0028	0.016	0.057	(±5.3%)
Polystyrene	1	0.23	0.0037	0.022	0.096	
	2	0.20	0.0030	0.018	0.089	0.092 ± 0.004
	3	0.21	0.0033	0.019	0.092	(±4.3%)

Table XI

Comparison of Data Obtained from Notched Izod and Falling Weight Impact Tests

Polymer	Izod* ft-lbs inch	Falling weight test (joules/mm)
Polycarbonate	12-18	3.07
Polysulfone	1.2	1.75
Polypropylene	0.5-2.2	0.68
High Density Polyethylene	0.5-20**	0.61
Impact Polystyrene	0.5-8.0	0.22
Poly(methyl methacrylate)	0.3-0.4	0.057
Polystyrene	0.25-0.4	0.092

* Modern Plastics Encyclopedia, 1976
**Value depends strongly on molecular weight

types and is especially important in the case of high density polyethylene.[154]

Variation of E_B with Drop Height. The dependence of impact strength on drop height is illustrated for each of the polymers tested in Figures 51, 52 and 54. Neither polypropylene nor poly(methyl methacrylate) show any particular trend. However, polypropylene is a semicrystalline polymer whose crystallinity and impact strength depend greatly on the means on preparation. Differential scanning calorimetry (DSC) was employed to explore this possibility and proved quite significant. Samples for DSC were punched from each test specimen and the heat of fusion (ΔH_f) measured for each. Indium, with a melting point of 430°k (157°C) and a heat of fusion equal to 6.80 cal/g, was employed as the reference. A plot of ΔH_f vs. impact strength is shown in Figure 53. A reasonable trend does, in fact, appear. The seemingly anomalous value of impact strength obtained at a drop height of one meter is most likely due to the lesser degree of crystallinity in these specimens.

The PMMA specimens tested from one meter also showed a higher impact strength than those examined from lesser heights as shown in Figure 51. Since PMMA is an amorphous polymer, differences in crystallinity cannot be the cause. It is possible that slight differences in the molding procedures might have gone undetected. The press used to mold the films was cooled with water flowing at an unknown rate. It is likely that differences in cooling rates, which would affect the crystallinity of polypropylene, might also affect the structure of PMMA. A sensitive density gradient column would have been useful in

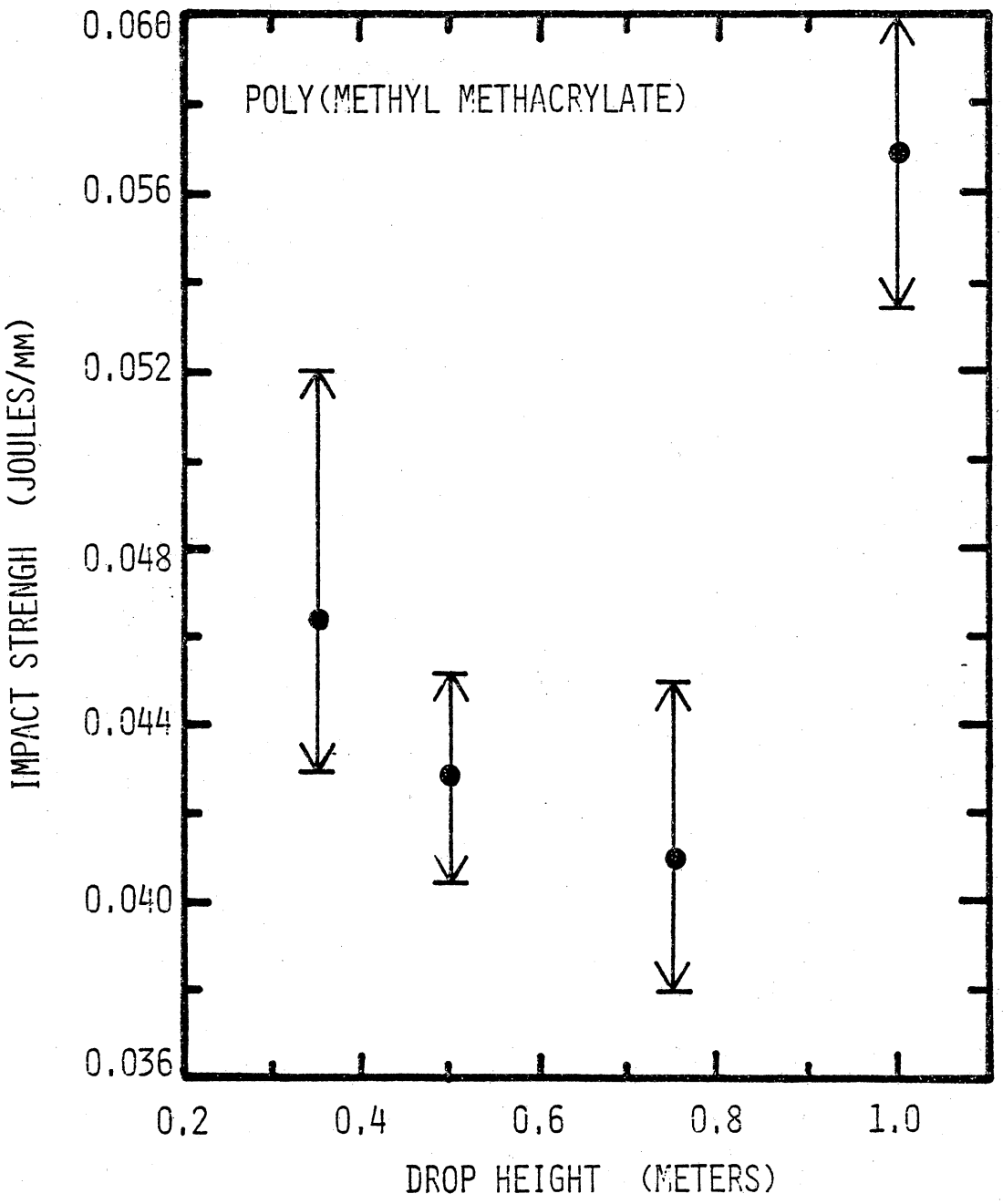

Figure 51. Variation in measured impact strength with drop height for poly(methyl methacrylate).

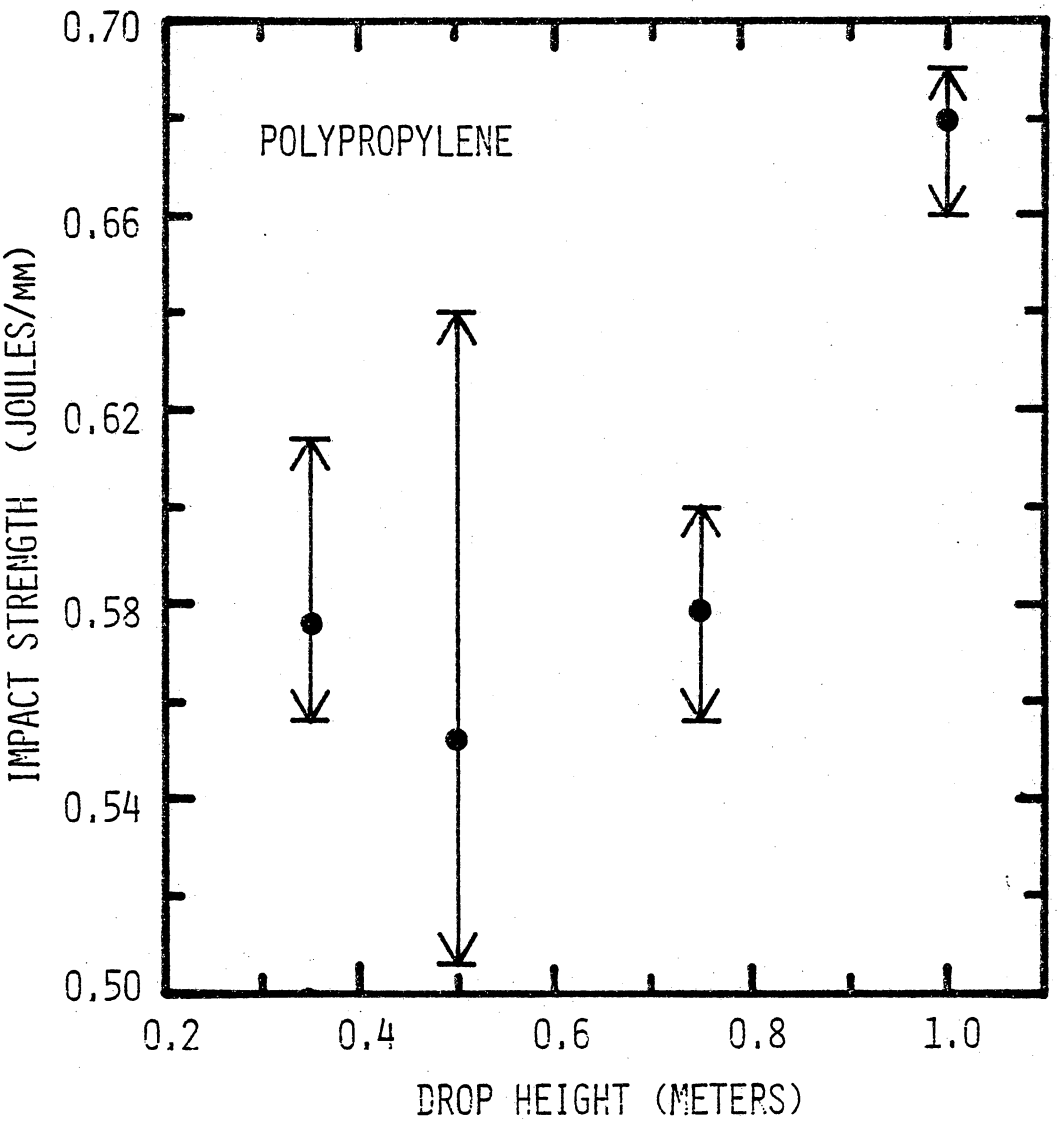

Figure 52. Variation in measured impact strength with drop height for polypropylene.

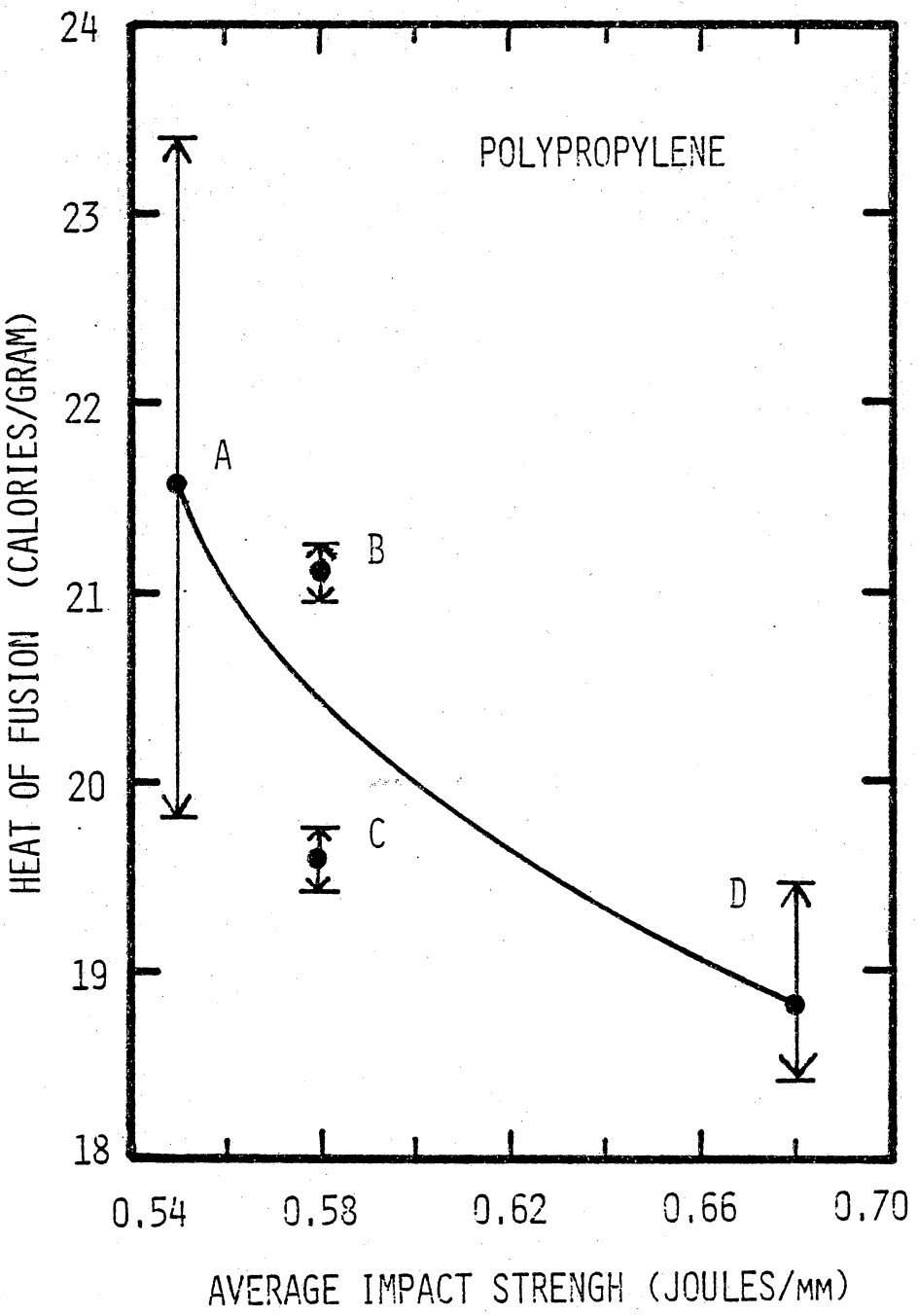

Figure 53. Effect of crystallinity (ΔH_f) on the impact strength of polypropylene.

exploring this concept.

The data shown for polycarbonate in Figure 54 appear to confirm Cessna's findings concerning impact strength and rate of loading.[171] The impact strengths determined at the four drop heights do decrease with increasing drop height, but the scatter in the data precludes a straightforward conclusion. However, in Figure 55 it can be seen that the duration of the impact up to the failure point increases dramatically with decreasing drop height while the maximum force (deceleration) remains nearly constant. Similar trends also exist in the case of polypropylene and PMMA, but the rate of increase for polycarbonate is 50% greater as the drop height is varied from 1 meter to 0.35 meter. This effect is illustrated in Figure 56. It does appear then that the impact strength of ductile polymers varies with test conditions and cannot be taken as a material constant.

(b) Composite Materials. It was mentioned earlier that the complex acceleration vs. time trace obtained for graphite reinforced composites required the use of direct velocity data. An acceleration trace and a velocity trace for LaRC-160 (0% Elastomer) are shown in Figure 57. Note that the acceleration curve appears to be a two step mechanism. The first is a sharp decrease in acceleration characteristic of a brittle polymer (i.e. the composite matrix). The second step appears as a jagged succession of vibrations and might be due to the fracture of subsequent plies in the laminate or due to breakage of the fibers themselves. In most cases, the striker did puncture and pass through the specimen.

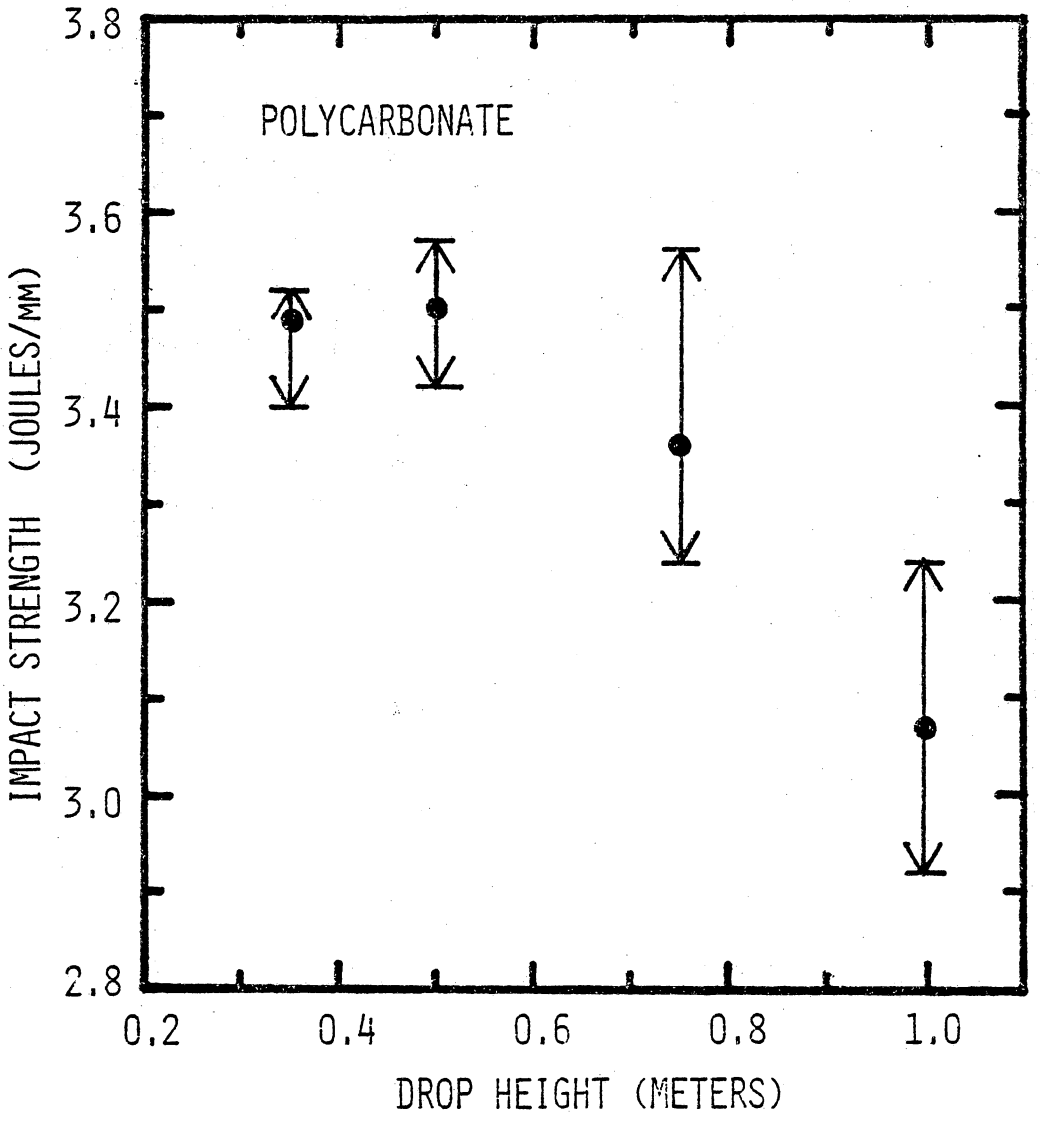

Figure 54. Variation in measured impact strength with drop height for polycarbonate.

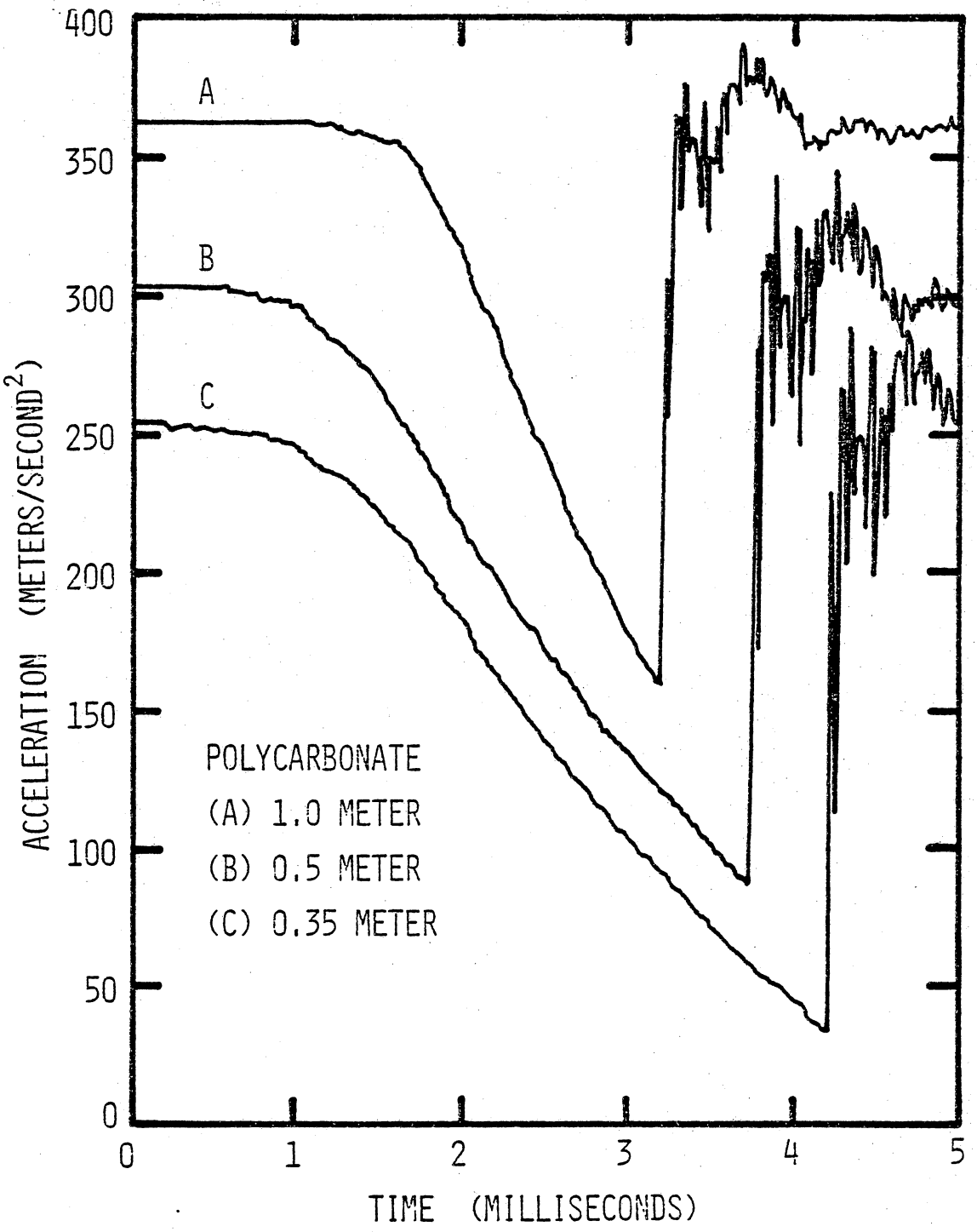

Figure 55. Three acceleration-time curves obtained for polycarbonate specimens at various drop heights. Specimen thicknesses are A (0.33 mm), B (0.34 mm), and C (0.34 mm).

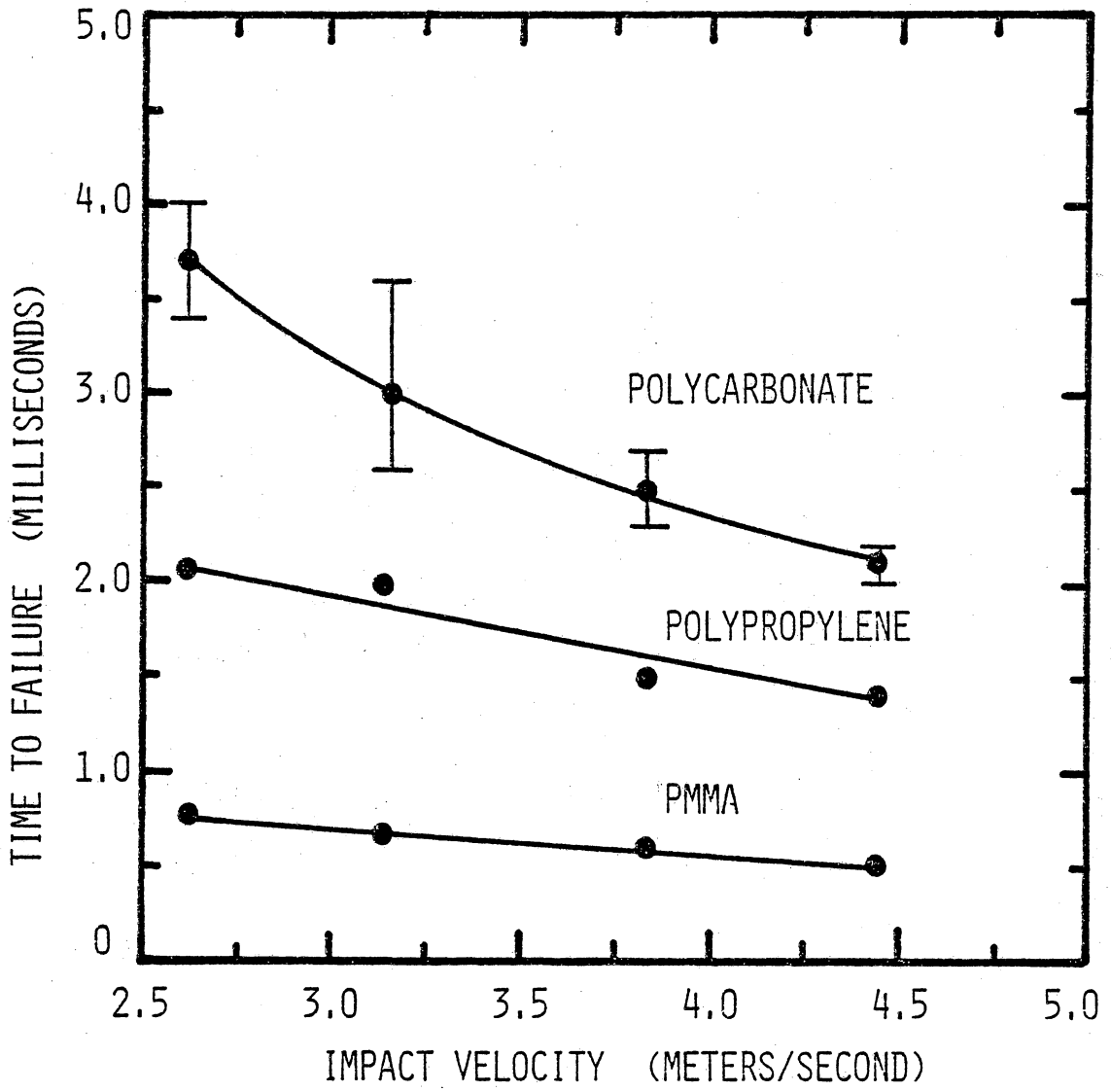

Figure 56. Dependence of impact duration ($t_f - t_o$) on impact velocity (v_o). The error bars in the polycarbonate data are due to variations in specimen thickness.

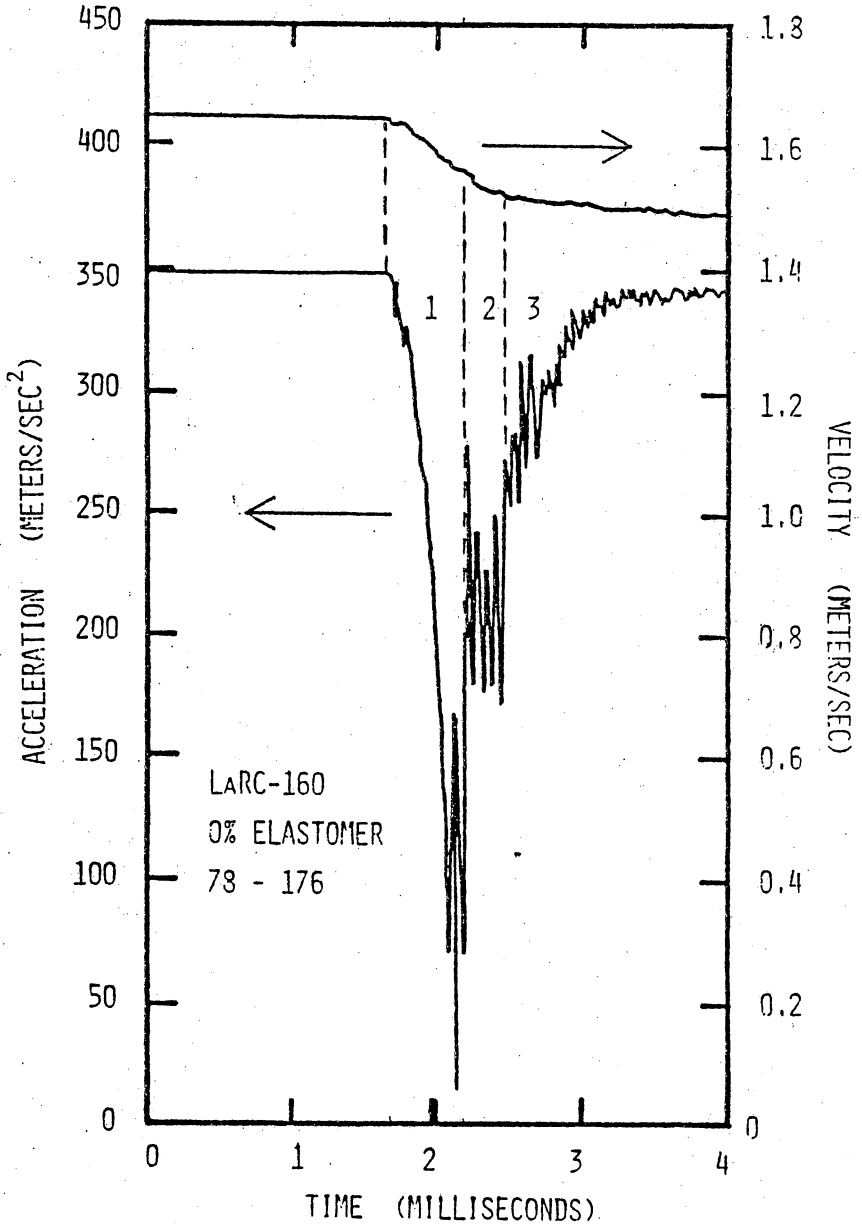

Figure 57. Typical acceleration-time and velocity-time curves obtained for graphite fiber reinforced composites.

The velocity trace provides the overall change in velocity after fracture has occured. Note that the end of step two in the acceleration curve corresponds to the change in slope of the velocity curve. The "excess" area of the acceleration trace (zone 3) is most likely due to the drag on the striker as it passes through the composite.

The impact strengths measured for the rubber modified LARC-160 composites is listed in Table XII. Since some of the specimens provided by NASA were used for acceleration traces, data are available for only three specimens of each type. The data indicate that the impact strength of the material is enhanced somewhat by the addition of rubber to the matrix. It is clear, however, that more specimens of each type are needed to properly assess their impact strengths. Also, a series of specimens containing 10% elastomer would help point out any trend more adequately.

The impact strengths compiled for the LaRC-13 series is listed in Table XIII. Each of the rubber modified samples exhibits a very small increase in impact strength over the unmodified sample. The sample containing 15% AATR looks most promising with an impact strength approximately 20% greater than the unmodified material. Difficulties encountered with early triggering of the waveform recorder prevented results from being obtained for all five specimens of each type.

Table XII

Impact Strengths of LaRC-160 Composites

Sample	No.	t (mm)	Δv (m/sec)	E_B (joule)	$(E_B)_{Avg} \pm \bar{S}n$
LaRC-160	1	0.60	0.13	0.75	
0% Elastomer	2	0.66	0.09	0.52	0.63 ± 0.12
78-176	3	0.62	0.11	0.63	(±19.0%)
LaRC-160	1	0.58	0.20	1.14	
5% Elastomer	2	0.60	0.13	0.75	0.92 ± 0.20
78-179	3	0.56	0.15	0.86	(±21.8%)
LaRC-160	1	0.58	0.15	0.86	
15% Elastomer	2	0.60	0.14	0.80	0.80 ± 0.06
78-178	3	0.62	0.13	0.75	(±7.5%)

Table XIII

Impact Strengths of NaRC-13 Composites

Sample	No.	t (mm)	Δv (m/sec)	E_B (joules)	$(E_B)_{Avg} \pm \bar{S}_n$
LaRC-13	1	0.72	0.16	0.92	
78-189	2	0.72	0.18	1.03	1.03 ± 0.08
	3	0.70	0.18	1.03	
	4	0.70	--	--	(±8.0%)
	5	0.70	0.20	1.14	
LaRC-13	1	0.74	0.20	1.14	
15% Sylgard	2	0.72	--	--	1.10 ± 0.06
78-191	3	0.74	0.20	1.14	
	4	0.74	--	--	(±5.7%)
	5	0.74	0.18	1.03	
LaRC-13	1	0.72	0.19	1.09	
15% Sylgard	2	0.78	0.20	1.14	
78-192	3	0.74	0.19	1.09	1.14 ± 0.06
	4	0.74	0.21	1.20	(±4.8%)
	5	0.74	0.21	1.20	
LaRC-13	1	0.72	0.21	1.20	
15% AATR	2	0.70	--	--	
78-186	3	0.72	0.21	1.20	1.21 ± 0.02
	4	0.72	--	--	(±1.9%)
	5	0.74	0.23	1.23	

Table XIII

(continued)

Sample	No.	t (mm)	Δv (m/sec)	E_B (joules)	$(E_B)_{Avg} \pm \bar{S}_n$
LaRC-13	1	0.72	0.20	1.14	
15% AATR	2	0.70	--	--	
78-187	3	0.76	0.19	1.09	
	4	0.75	0.20	1.14	1.14 ± 0.04
	5	0.72	0.21	1.20	(±3.4%)

(c) AS/AC Copolymers. As mentioned earlier, a separate series of AS/AC copolymers was prepared especially for impact testing. The copolymers and oligomers were characterized in the usual manner. The results are listed in Table XIV.

The impact strength of the AS/AC copolymers is represented as a function of composition in Figure 58. Each data point represents the average of three determinations on the indicated sample. The points fall very close to a line corresponding to the weighted average of the impact strengths for commercial Lexan polycarbonate and polysulfone P-3703. All failures were recorded as ductile except two, AS/AC-20/6 and AS/AC-16/16 which failed in a brittle mode. Further investigation by DSC and GPC indicated that these two materials had degraded during the molding process, perhaps due to residual impurities remaining in the polycarbonates.

D. Electron Microscopy. Small pieces of compression molded copolymers and commercial homopolymers were immersed in acetone for one hour, dried, and examined for crystallinity on a scanning electron microscope. Typical surface morphologies for treated polysulfone and polycarbonate homopolymers are provided in Figure 59. The polysulfone surface displays many small bubbles probably caused by escaping acetone during the drying process. The surface of polycarbonate, on the other hand, is covered by spheruletic crystals about 20 μ in diameter.

The surface of AS/AC-10/10 before and after acetone treatment is

Table XIV

Characterization of Polysulfone/Polycarbonate Block Copolymers
(Series II)

Copolymer	Composition[A] Wt. % PSf	PSf $\bar{M}_n$ Titration	PC $\bar{M}_n$ U.V.	Tg (^oC) Molded Film	$\langle\bar{M}_n\rangle$[C] g/mole
AS/AC-20/6	83.1	20,500	5,700	155[B]	78,000
AS/AC-20/12	68.2	20,500	12,200	177	60,000
AS/AC-12/6	63.8	11,600	5,700	178	52,000
AS/AC-8/6	49.1	7,600	5,700	168	39,000
AS/AC-16/16	50.1	15,900	16,200	160,178	69,000
AS/AC-20/27	47.3	20,500	26,600	165,184	85,000
AS/AC-8/17	33.0	7,600	16,900	165	28,000
AS/AC-12/23	31.0	11,600	22,800	167	52,000
AS/AC-8/29	19.2	7,600	28,800	163	42,000

(A) Gailbraith Labs
(B) Tg of powder was 178^{o}C. Polymer degraded during molding.
(C) Membrane Osmometry

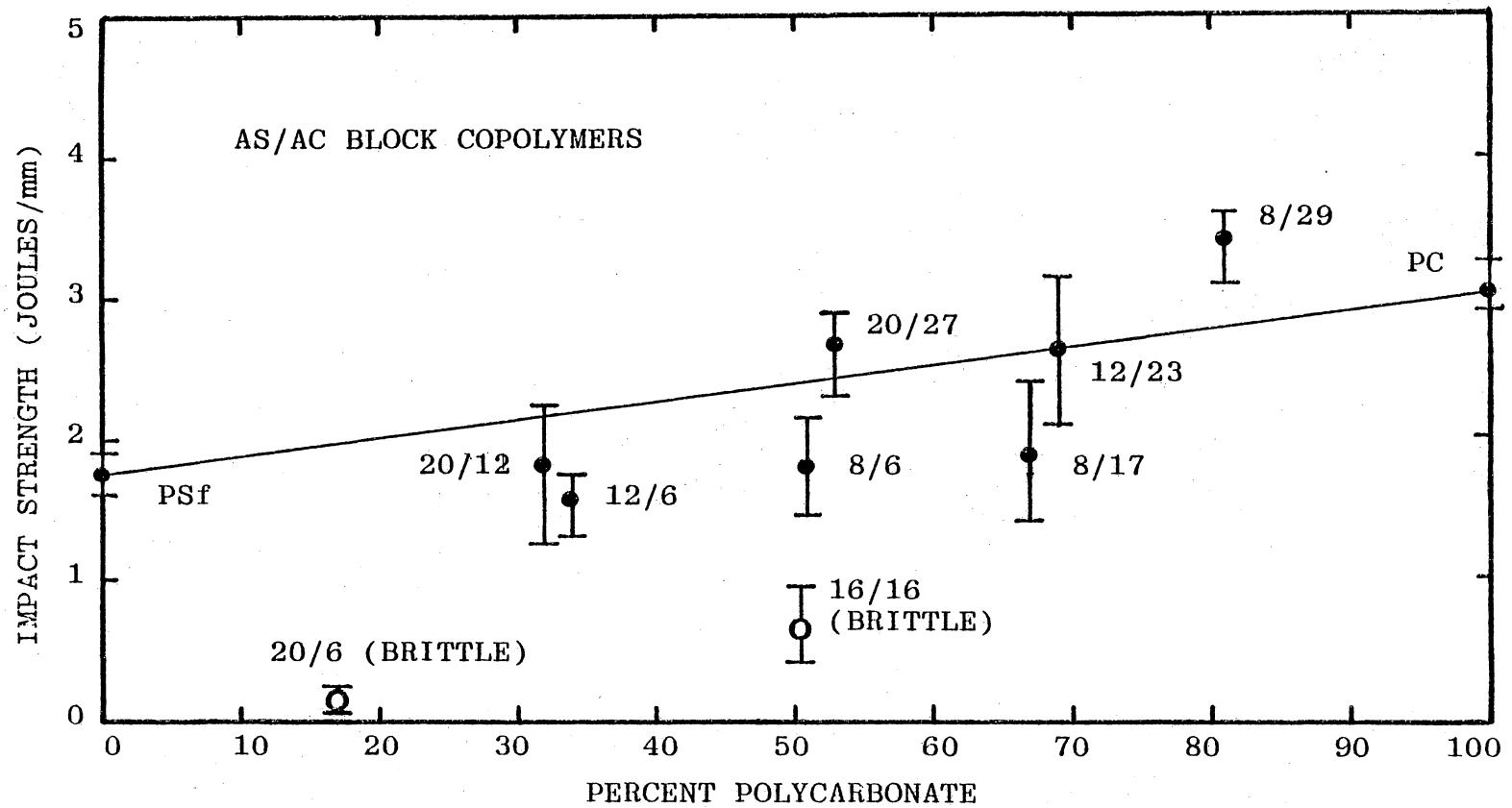

Figure 58. Impact strength of polysulfone/polycarbonate block copolymers as a function of composition.

shown in Figure 60. No signs of crystallinity are apparent in the SEM photograph even though a very small endothermic peak was observed by DSC at approximately 210°C, indicating that a slight amount of crystalline polycarbonate was present.

Before and after surfaces of AS/AC-26/22 are shown in Figure 61. Note that the treated material shows some small scattered spherulites on the surface. The crystallites are much smaller than those obtained for pure polycarbonate and are on the order of 2 μ in diameter.

A similar surface morphology is shown for acetone treated SS/AC-10/10 in Figure 62. Here the crystallites are even smaller than that observed for AS/AC-26/22. Like the AS/AC material, SS/AC-10/10 is a two phase system. It is apparent that only the two phase block copolymers are capable of crystallizing to a large extent.

E. Environmental Stress Crack Resistance (ESCR). In conjunction with the acetone-induced crystallization studies, the ESCR of the homopolymers and several AS/AC block copolymers was also examined. Tensile specimens were loaded in tension to 1000 psi (341 Kg/cm^2) on the Scott tester described earlier. A jet of acetone was directed at a cotton wick clipped to the center of the specimen and the time to fail measured with a stopwatch. All the materials tested, including single and multiphase copolymers, failed immediately. Further experiments conducted at 500 psi (170 Kg/cm^2) gave similar results.

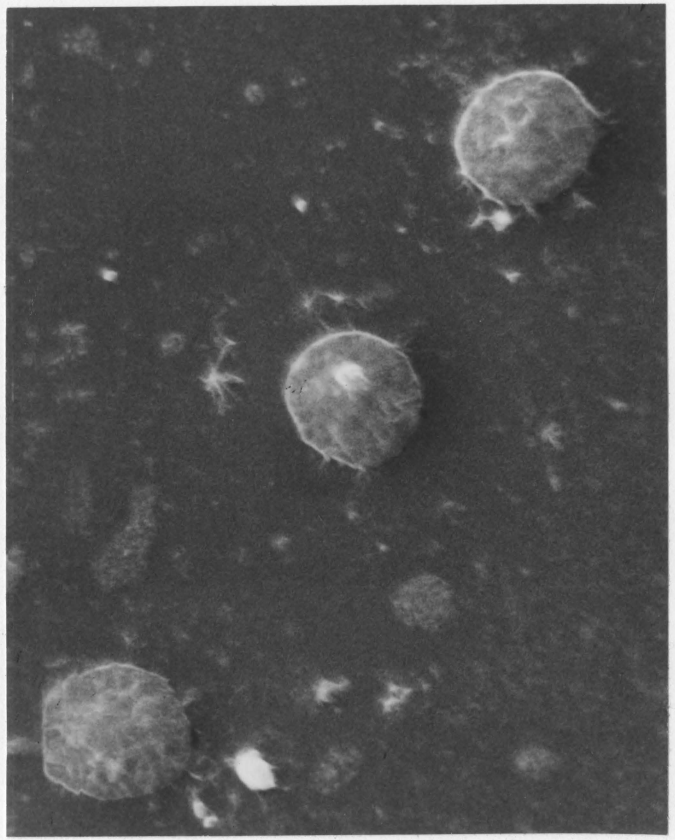

POLYSULFONE

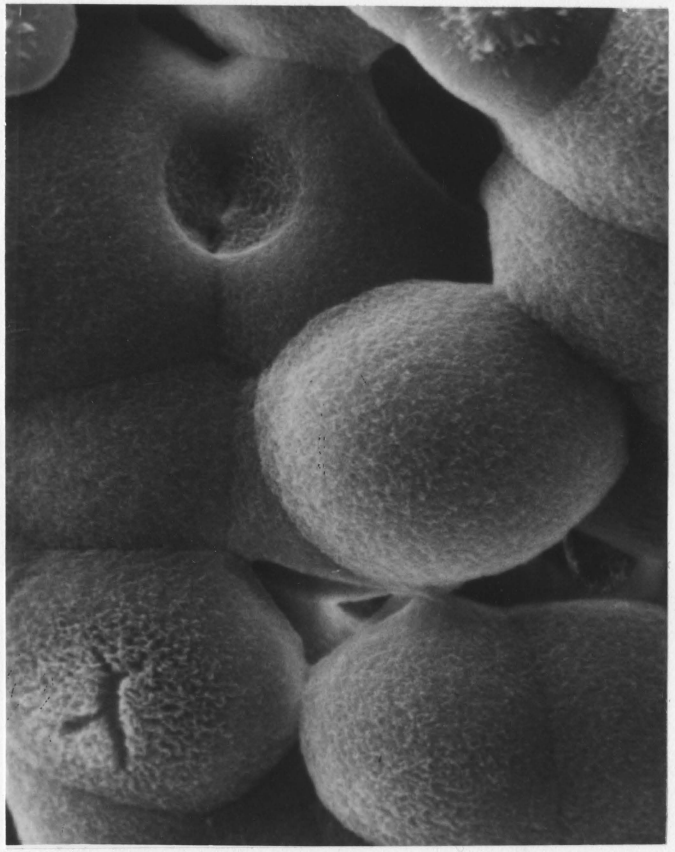

POLYCARBONATE

Figure 59. Scanning electron micrographs comparing the surface morphologies of acetone treated polysulfone and polycarbonate (2000X, 1 cm = 5 μ)

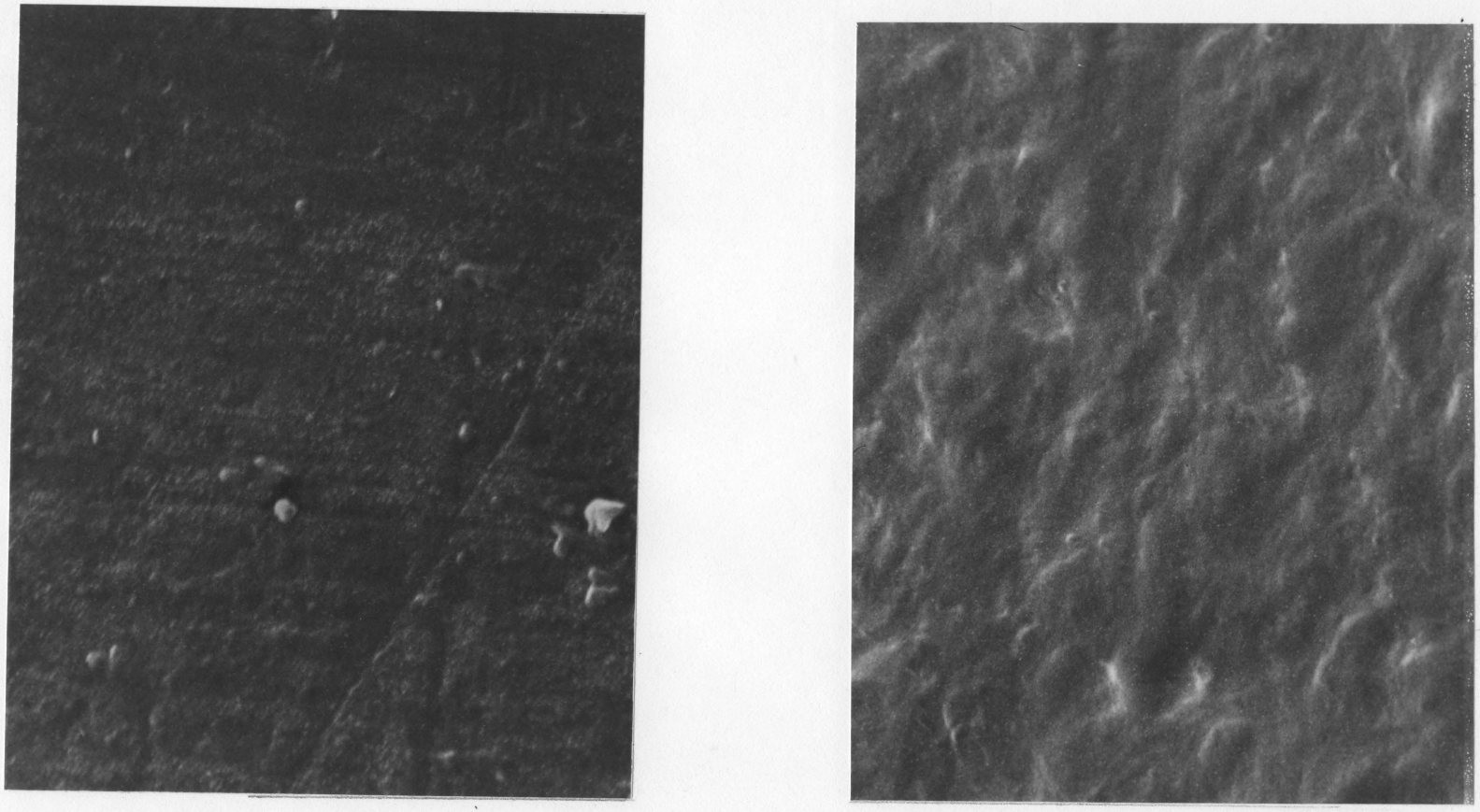

BEFORE AFTER

Figure 60. Scanning electron micrographs comparing the surface morphology of AS/AC -10/10 before and after acetone immersion (5000X, 1 cm = 2 μ).

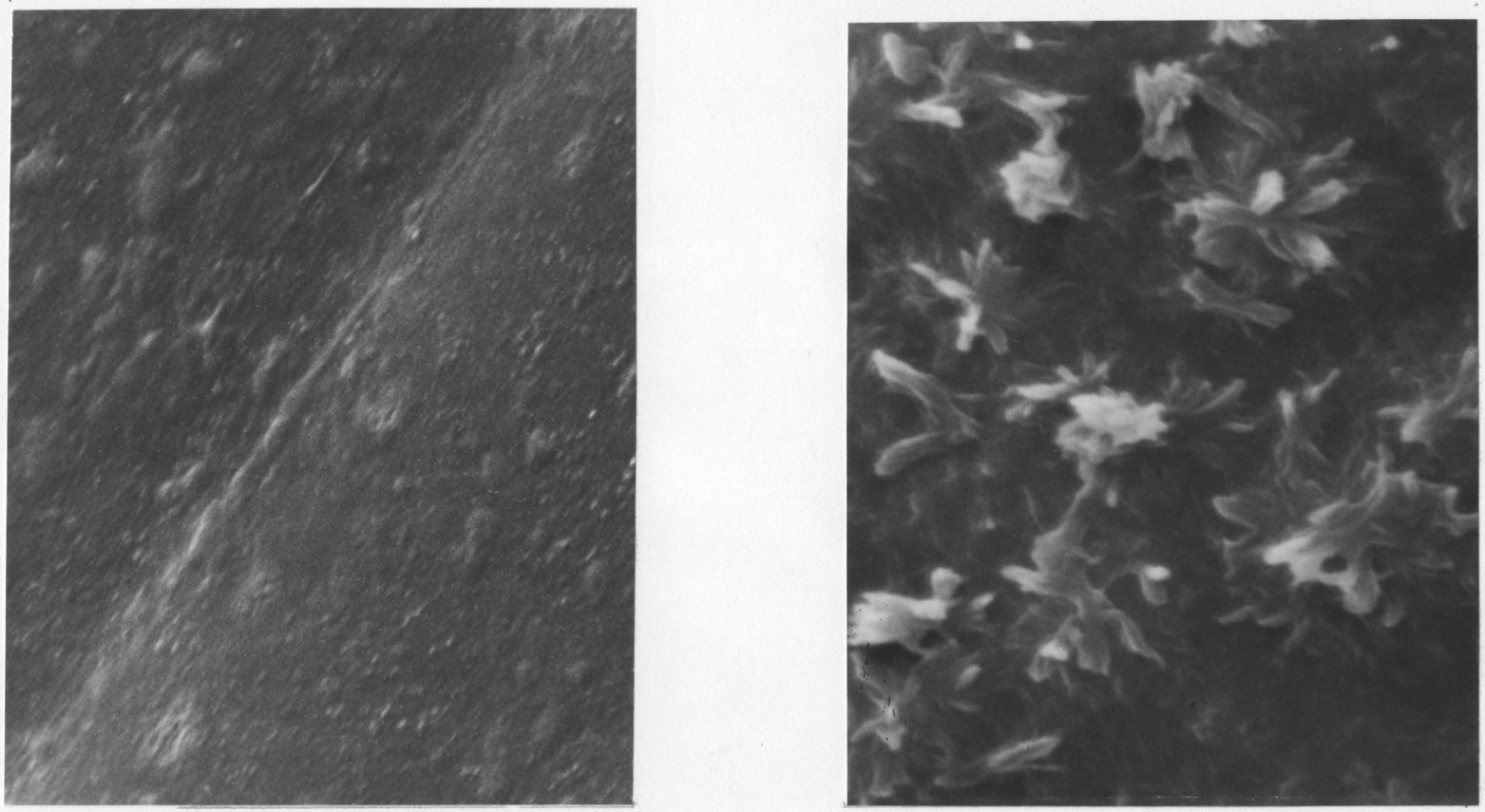

BEFORE AFTER

Figure 61. Scanning electron micrographs comparing the surface morphology of AS/AC - 26/22 before and after acetone immersion (5000X, 1 cm = 2 μ).

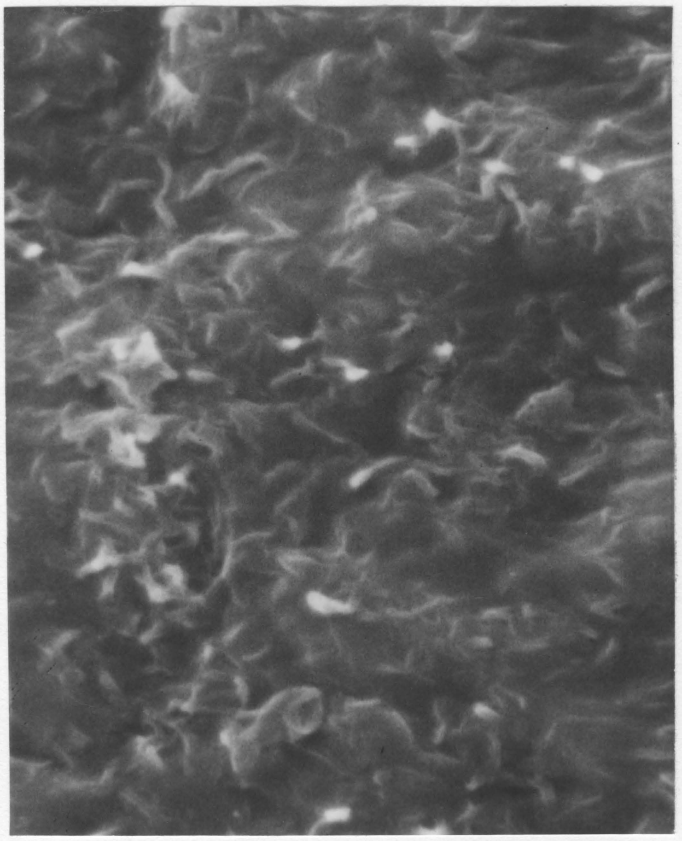

Figure 62. Scanning electron micrograph of the surface of SS/AC - 10/10 after acetone immersion (5000X, 1 cm = 2 μ).

V. Discussion

A. Synthesis of Polysulfone-Polycarbonate Block Copolymers.

Block copolymers of polysulfone and polycarbonate, prepared via the interfacial coupling of hydroxyl terminated oligomers, are composed of three to five number average blocks as judged from membrane osmometry data. The efficiency of the coupling reaction is good as indicated by the very low levels of residual homopolymer found in GPC analyses. The interfacial synthesis technique also provides for rapid reaction times (less than 30 min.) and simple separation of the copolymer from the reaction mixture.

The glass transition temperatures of single phase AS/AC block copolymers (Series II) increase with increasing polysulfone content as expected. The Tg's of the starting oligomers increase dramatically with molecular weight as shown in Figure 63. If these values of Tg are substituted into the empirical Fox[196] relation below for random

$$\frac{1}{Tg} = \frac{W_A}{Tg_A} + \frac{W_B}{Tg_B}$$

copolymers, where W_A and W_B are the weight fractions of the components, it is found that the calculated values fall below those actually measured as indicated in Table XV. This result might be interpreted as evidence for preferential coupling of like oligomers but even random coupling should lead to increased Tg values. The increase in Tg of a homopolymer with increasing molecular weight is usually attributed to the decrease in free volume associated with chain ends.[197] Coupling

Table XV

Tg of Single Phase AS/AC Block Copolymers*

AS/AC	W_{PSf}	Tg(°C) Measured**	Tg(°C) Calculated
20/6	83.1	178	180
12/6	63.8	178	161
20/12	68.2	177	175
8/6	49.1	168	154
8/17	33.0	165	157
12/23	31.0	167	163
8/29	19.2	163	163

* Series II
**DSC Measurements at 40°C/min.

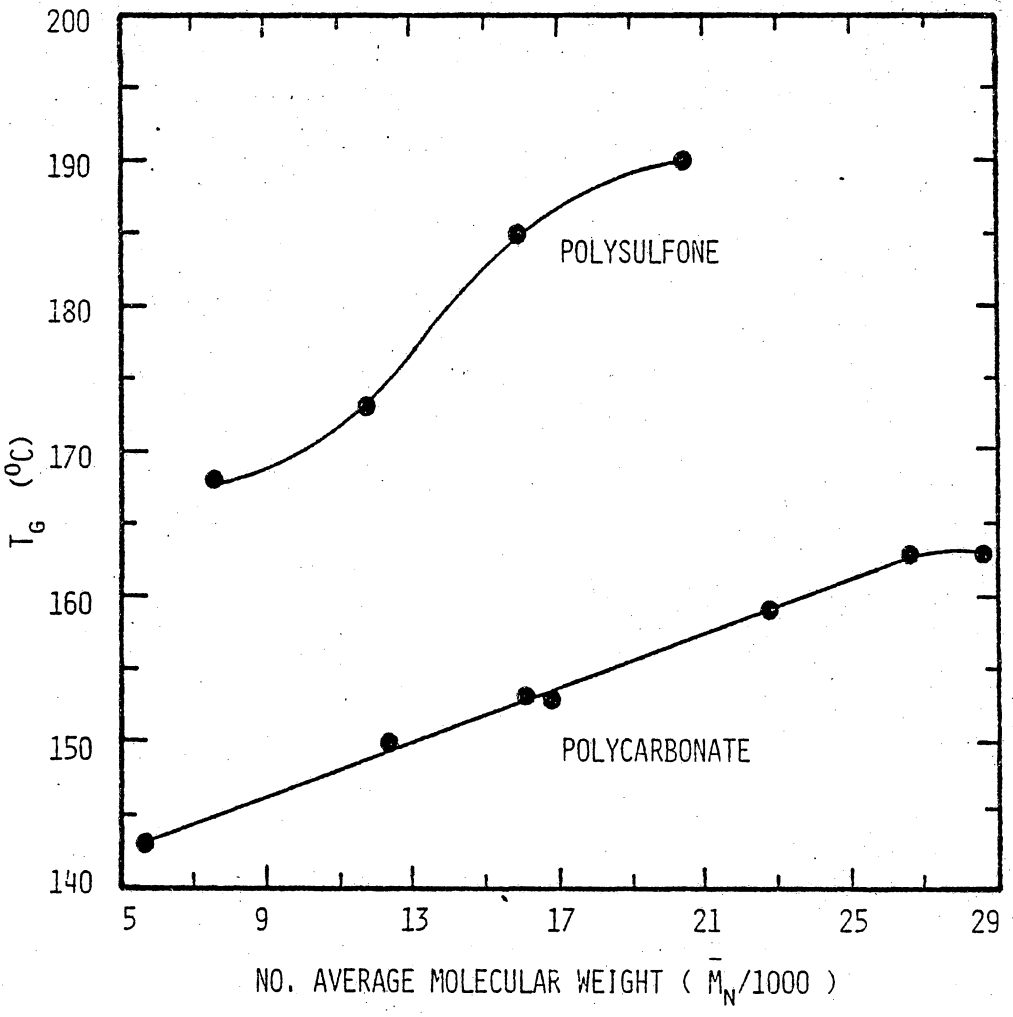

Figure 63. Molecular weight dependence of the glass transition temperatures (T_g) of polysulfone and polycarbonate oligomers based on DSC measurements at 40°C/min.

low molecular weight oligomers into a block copolymer should raise the Tg of the single phase copolymer over the expected value as the number of chain ends decrease, assuming no other interactions are initiated. The modest differences between the measured and calculated Tg values for most of the copolymers listed in Table XV seem to reflect this reasoning. Two of the copolymers, however, show differences of 17° (AS/AC-12/6) and 14°C (AS/AC-8/6) between the measured and calculated Tg's which may be an indication of preferential coupling. If AS/AC-8/6, for example, was actually a 16/12 its calculated Tg would be 166°C, very close to the measured value of 168°C. A high degree of preferential coupling would, of course, lead to microphase development as the block sizes increased. Why a limited amount of preferential coupling occured in only two of the single phase copolymers cannot be explained at the present time. It does appear, however, that coupling of the bisphenol-A terminated oligomers is random in most cases. Further work is needed to adequately describe the coupling of bisphenol-T and bisphenol-S polysulfone oligomers with bisphenol-A polycarbonate. The reactivities of the phenolic groups terminating these polysulfones should differ from those of bisphenol-A polycarbonate due to their greater acidity.

B. Microphase Separation. Strictly one-phase AS/AC copolymers are obtained at block lengths less than 10,000 g/mole whereas two phase materials are exclusively obtained at block lengths exceeding 20,000 g/mole. Microphase separation can be noted only in 50/50 by weight compositions in accordance with Krause's[57] theory which predicts that phase separation is thermodynamically favored at this composition. It

should be pointed out, however, that other compositions in which both block lengths were above the critical value of approximately 15,000 g/mole were not investigated.

A very significant finding of this research is the transition from single phase to two phase morphology exhibited by AS/AC-16/17 (50/50) upon annealing at high temperatures. Such behavior suggests the existence of a lower critical solution temperature (LCST) in single phase block copolymers whose segment lengths lie close to those required for microphase separation. The DSC curves in Figures 32 and 33 clearly indicate that microphase separation has both kinetic and thermodynamic origins. The separation takes place only at temperatures above the Tg of polysulfone, however, where the chains are mobile enough to migrate. Annealing at temperatures between the Tg's of polycarbonate and polysulfone does not induce microphase separation. Unlike the LCST behavior exhibited by low molecular weight mixtures, the formation of microphases is irreversible.

The ability of AS/AC-16/17 to exist as either a homogeneous or microheterogeneous material points out that these block lengths lie close to the critical values. A value of the critical interaction parameter for this system can be approximated from the equation given by Krause[57] below.

$$(X_{AB})_{cr} = \frac{zV_r}{(z-2)v_B V_A n_A}_c \left[-\ln(v_A)^{\nu A}(v_B)^{\nu B} + 2(m-1)\frac{\Delta S}{R} - \ln(m-1)\right]$$

The terms in the above expression were defined earlier. For AS/AC-16/17 the following can be assumed:

(a) $\langle M_n \rangle \cong 70{,}000$ so $m \cong 4$

(b) $z = 8$ such that $\Delta S/R \cong 1.0$

(c) $V_R = V_A$

(d) $v_A = v_{PC} = 0.50$ and $v_B = v_{PSf} = 0.50$

(e) n_A^c = # A segments in copolymer molecule = 134

Using the above assumptions, a value of $(X_{AB})_{cr}$ equal to 0.25 is obtained. This value of $(X_{AB})_{cr}$ for the polysulfone-polycarbonate system is much greater than that calculated by Krause[73] for the styrene-α-methylstyrene block copolymer where $(X_{AB})_{cr} \cong 0.003$. The critical block lengths for microphase separation in the latter system were estimated to be on the order of 10^6 g/mole for a triblock copolymer. The much larger value of $(X_{AB})_{cr}$ for the polysulfone-polycarbonate system is indicative of why relatively low block lengths (~15,000 g/mole) can precipitate microphase separation. It was noted earlier that blends of polysulfone and polycarbonate also exhibit two phase behavior at molecular weights as low as 5,000 g/mole. The solubility parameters of polysulfone ($\delta = 10.3$) and polycarbonate ($\delta = 9.6$) are similar but not close enough to predict miscibility except at very low molecular weights. It is interesting to note that the coefficients of thermal expansion of the two homopolymers ($\alpha_{PSF} = 5.2 \times 10^{-5}$ in./in./°C, $\alpha_{PC} = 6.6 \times 10^{-5}$ in./in./°C)[198] differ by approximately 20%. This large discrepancy must also contribute to the mutual incompatibility of polysulfone and polycarbonate if equation-of-state predictions[47] are correct.

Phase behavior in the TS/AS system is probably similar to that found for the AS/AC copolymers. The solubility parameter of bisphenol-T polysulfone lies close to that of the bisphenol-A polymer (10.3) when estimated by the method of group contributions due to Small.[41] Substitution of the sulfonyl group for the isopropylidene group raises the one dimensional solubility parameter of bisphenol-S polysulfone to about 12.6. Even though the coefficient of thermal expansion is nearly equal to that of polycarbonate (α_{PSF-S} = 5.5 x 10^{-5} in./in./°C)[198], the SS/AC block copolymers display heterogeneous behavior at block lengths as low as 5,000 g/mole. It is apparent that closely matched thermal expansion coefficients alone are insufficient to predict miscibility.

C. Effects of Microphase Separation. The phase distribution in the AS/AC and SS/AC copolymers remains unknown at this time. Suitable staining techniques for transmission electron microscopy do not exist for these materials. Their similar electron densities prevent unstained specimens from being examined also. Small angle X-ray studies kindly run by Professor Garth Wilkes on AS/AC-26/22 and SS/AC-10/10 showed no diffraction peaks whatsoever, apparently due to the similar atom densities of the components. It can be stated that the microphases must be smaller than the wavelength of visible light (4000-7000 Å) since the copolymers are transparent. However, since the components are present in equal amounts it is likely that the microphases form a continuous lamellar domain structure. Of course, this is pure speculation, but domains of this type are observed in styrene-diene block copolymers at the point of phase inversion[7].

Tensile tests run at low strain rates (5 cm/min) failed to differentiate between single and multiphase copolymers. Falling weight impact tests in which the strain rates were appreciably higher ($\sim 10^4$ cm/min) gave similar results. The yield stresses, yield elongations and impact strengths are intermediate to those of the homopolymers and increase with increasing polycarbonate content. This is not surprising when one considers that the mechanical properties of polysulfone and polycarbonate are nearly identical. Both are tough, ductile materials as are the copolymers. Although further work is needed to fully characterize the copolymers, it appears unlikely that any synergism in tensile or impact properties exists.

Microphase separation does play a role in governing the melt flow characteristics of the AS/AC block copolymers. Single phase materials display melt viscosities and thermal activation energies similar to those of the homopolymers, whereas the two-phase copolymers exhibit higher viscosities and activation energies. Similar behavior has been observed in styrene-diene,[35] and polysulfone-poly(dimethyl siloxane)[109] block copolymers.

The high melt viscosities and activation energies result from the need to break up the domain structure of the multiphase material. Segments of one polymer type must be pulled from their domains and dragged through the second polymer. The melt flow of the polysulfone-polycarbonate copolymers is complex. Further work is necessary to elucidate the effects of composition and block length on the rheology of both one and two-phase systems.

In polysulfone-polycarbonate block copolymer microphase separation appears to have no effect on the shapes or magnitudes of the low temperature (-100°C) β relaxations. Moreover, the thermal activation energies calculated for the copolymer transitions lie in the same range as those of the homopolymer, namely 8-11 Kcal/mole. The role of the β relaxations in governing impact strength has still not been resolved. All that can be said here is that the copolymers exhibit significant low temperature loss peaks and, like the homopolymers, display excellent toughness under impact conditions. Neither homo- or heterogeneity appear to affect the chain motions giving rise to β relaxations.

High temperature dynamic mechanical studies clearly indicate the effects of microphase separation. Drops in modulus accompanied by relaxation peaks occur at the Tg of each component. It is important to note that the glass transition due to polycarbonate segments always occurs at a temperature 7 to 18° higher than that of the corresponding polycarbonate oligomer, whereas that of the polysulfone blocks occur close to that of polysulfone homopolymer (190°C). Although some degree of mixing may occur, it is possible that such effects are due to the immobilization of the lower Tg material by the surrounding glassy matrix. The presence of polycarbonate some 40° above its normal Tg would not be expected to change the Tg of the polysulfone domains appreciably. Krause and Iskandar[197] have discussed similar behavior in styrene-dimethylsiloxane block copolymers and styrene-diene materials.

A third loss peak appears in the temperature range between 0 and 100°C for each of the two phase AS/AC copolymers studied. Since

similar transitions were not observed in any of the single-phase copolymers, it is suggested here that they arise from interfacial phenomena at the domain boundaries.[199] It is possible that the difference in thermal expansion of the two components results in frozen stresses at the domain interface as the molded specimens are cooled from the melt. Similar intermediate transitions have been observed in pure polycarbonate[136] and appear to result from the relaxation of residual stresses induced by molding or drawing of the material. No loss peaks have been observed for bisphenol-A polysulfone in the 0 to 100°C range.

Bisphenol-S polysulfone exhibits a small broad relaxation between 0 and 100°C.[98] The peak at ~70°C shown in Figure 26 for SS/AC-10/10 can, therefore, be attributed to the bisphenol-S polysulfone blocks.

Another aspect of the dynamic mechanical behavior of two phase copolymers needs further discussion. That is the apparent reversal in the magnitudes of the loss peaks obtained when the loss modulus (E") is plotted instead of tan δ as a function of temperature. Such behavior was pointed out in Figures 21 and 22 for the AS/AC-16/17 copolymer and Figures 25 and 26 for SS/AC-10/10. How can this transformation be rationalized?

Recall that tan δ may be expressed as

$$\tan \delta = E''/E'$$

where E' is the storage modulus. In materials such as AS/AC-16/17 where the weight and volume fractions of the components are nearly 0.5,

it is reasonable to assume that two continuous phases exist and that a simple rule of mixtures can be applied to describe E'. Thus, one may write

$$E' = V_{PC} E'_{PC} + V_{PSF} E'_{PSF}$$

where V designates the volume fraction of a particular component. A more complex expression can be written for E"[200] but will not be necessary for the following analysis. At 150°C, the Tg of polycarbonate, E''_{PC}, passes through a maximum while E''_{PSf} remains insignificant. Using the Rheovibron data in Figures 17 and 18 to calculate E'_{PC}, E'_{PSF}, E''_{PC} and E''_{PSF} one finds that at 150°C

$E'_{PC} = 1.8 \times 10^8$ dynes/cm^2

$E'_{PSF} = 1.4 \times 10^{10}$ dynes/cm^2

$E''_{PC} = 3.1 \times 10^8$ dynes/cm^2

$E''_{PSF} = 1.4 \times 10^7$ dynes/cm^2

Tan δ of the composite may be estimated as

$$\tan \delta(150^\circ C) \cong \frac{3.1 \times 10^8}{1.4 \times 10^{10}} \cong 0.022 .$$

At 190°C both E'_{PC} and E''_{PC} become relatively insignificant compared to E'_{PSF} and E''_{PSF} as shown below:

$E'_{PC} \cong 10^7$ dynes/cm^2

$E'_{PSF} = 3.3 \times 10^8$ dynes/cm^2

$E''_{PC} \cong 10^6$ dynes/cm^2

$E''_{PSF} = 5.4 \times 10^8$ dynes/cm^2

Tan δ is then calculated as

$$\tan \delta(190^{\circ}C) \cong \frac{5.4 \times 10^{8}}{3.3 \times 10^{8}} = 1.7 .$$

This analysis clearly shows that the magnitudes of tan δ peaks cannot be taken as measures of copolymer composition.

Microphase separation does not improve the resistance of the AS/AC copolymers to stress-cracking agents such as acetone even though the single and multiphase copolymers react differently to the same. Only the two-phase systems can be induced to crystallize by immersion in acetone. This finding is supported by a recent report[201] which indicates that the surfaces of the two-phase block copolymers are composed largely of polycarbonate, apparently due to its lower surface energy. Similar surface segregation was observed in polycarbonate-poly(dimethyl siloxane) block copolymers where the siloxane component appeared as the dominant surface specie.[201]

VI. Conclusions

From the results of this investigation, the following conclusions have been reached.

1. The interfacial technique, used in this research for coupling polysulfone and polycarbonate oligomers, yields block copolymers comprised of four number average blocks. The Tg values of single phase copolymers, as a function of composition, provide good evidence that coupling is random rather than preferential towards either of the components.
2. Strictly one phase AS/AC copolymers result when the block lengths are 10,000 g/mole or less. Strictly two phase copolymers are obtained when the block lengths are 20,000 g/mole or greater.
3. The critical block lengths for microphase separation in AS/AC block copolymers lie in the 15,000 range for 50/50 compositions. In such materials the phase nature depends upon the previous thermal history of the sample.
4. Microphase separation has both thermodynamic and kinetic origins. Behavior similar to the LCST exhibited by many homogeneous blends may be observed.
5. The tensile and impact properties of homogeneous and microheterogeneous polysulfone-polycarbonate block copolymers are intermediate to those of the homopolymers.

6. The polycarbonate segments of the two-phase block copolymers can be selectively crystallized unlike those of the purely homogeneous materials. Single phase block copolymers in which microphase separation can be thermally induced are also capable of partial crystallization. The environmental stress crack resistance of the copolymers is not enhanced by the presence of microphases since both components are susceptible to stress cracking agents.
7. Two phase AS/AC block copolymers retain their domain structure in the melt. Higher viscosities and thermal activation energies are observed for such copolymers.
8. The critical block molecular weight in SS/AC copolymers lies below 5,000 g/mole. TS/AC systems behave similarly to AS/AC copolymers due to the similar solubility parameters of the polysulfones in question.
9. The falling weight impact tester described in this thesis provides reliable and reproducible values of impact strength for both polymers and composite materials.
10. Strain rate effects become important when ductile polymers such as polysulfone and polycarbonate are impact tested. Lower fracture energies are observed with increasing projectile velocities. Brittle materials do not exhibit a marked strain rate dependence.

VII. Future Work

Many questions remain to be answered about the properties of polysulfone-polycarbonate block copolymers. The lack of published information dealing with ductile, amorphous block copolymers makes further studies especially significant. Future work should include the following:

1. Studies of the phase behavior of other poly(aryl ether)-polycarbonate block copolymers to better ascertain the effects of chemical structure and block length on microphase separation in these systems.
2. Studies of the kinetics of microphase separation. Since the rate of microphase separation can be controlled in these materials, useful thermodynamic quantities might be derived from microcalorimetry or rate studies at different temperatures.
3. Detailed characterization of the melt properties of these copolymers as a function of temperature, shear rate, and composition. The usefulness of many polymers is governed by their processability.
4. Studies of the effects of physical aging on the properties of single and multiphase block copolymers compared to those of the homopolymers. The two-phase materials may retain their ductility to a greater extent as the phase boundaries sharpen.
5. Crystallographic studies of the amorphous and solvent crystallized copolymers. The application of the various light, X-ray, and neutron scattering techniques available today would be useful in characterizing the morphology of the multiphase block copolymers.

6. Investigations of the mechanical properties of the copolymers as functions of temperature. The tensile and impact properties of the two-phase materials, between the Tg's of the components, should be similar to those of either thermoplastic elastomers or impact-modified thermoplastics.
7. Studies of the solution properties of the block copolymers.

One further extension of the present work involves the falling weight impact tester described in this dissertation. Since the manual data reduction becomes quite tedious, it is suggested that the device be completely interfaced with a suitable data storage system such as a simple tape cassette. The data from many experiments could be stored for future reference and conveniently integrated by computer rather than the graphic method currently in use.

References

1. Sperling, L. H., Ed., "Recent Advances in Polymer Blends, Grafts, and Blocks," Plenum, New York (1974).

2. Platyer, N.A.J., Ed., "Multicomponent Polymer Systems," Adv. Chem. Ser., 99 (1971).

3. Platzer, N.A.J., Ed., "Copolymers, Polyblends, and Composites," Adv. Chem. Ser., 142 (1975).

4. Klempner, D. and Frisch, K. C., Eds., "Polymer Alloys: Blends, Blocks, Grafts and Interpenetrating Networks," Plenum, New York (1977).

5. Cooper, S. L. and Estes, G. M., Eds., "Multiphase Polymers," Adv. Chem. Ser., 176 (1978).

6. Paul, D. R. and Barlow, J. W., in Reference 5, p. 315.

7. Molan, G. E., "Block Polymers," S. L. Aggarwal, Ed., Plenum, New York, 1970, p. 79.

8. Yee, A. F., Polym. Eng. Sci., 17, 213 (1977).

9. Saunders, K. J., "Organic Polymer Chemistry," Chapman and Hall, London, 1973, p. 30.

10. Saunders, K. J., Ibid, p. 31.

11. Kennedy, J. P., see Reference 1, p. 3.

12. Ceresa, R. J., Ed., "Block and Graft Copolymerization," Wiley, New York (1973).

13. Battaerd, H. and Tregear, G. W., "Graft Copolymers," Interscience, New York (1967).

14. Saunders, K. J., Ibid, p. 78.

15. Manson, J. A. and Sperling, L. H., "Polymer Blends and Composites," Plenum, New York, 1976, Chapter 3.

16. Saunders, K. J., Ibid, p. 81.

17. Noshay, A. and McGrath, J. E., "Block Copolymers: Overview and Critical Survey," Academic Press, Inc., New York (1977).

18. Allport, D. C. and Janes, W. H., Eds., "Block Copolymers," Applied Science Publishers, Ltd., Essex, England (1973).

19. Aggarwal, S. L., Ed., "Block Polymers," Plenum, New York (1970).

20. Burke, J. J. and Weiss, V., Eds., "Block and Graft Copolymers," Syracuse University Press, Syracuse, New York (1973).

21. Ceresa, R. J., "Block and Graft Copolymers," Butterworth, London (1962).

22. Szwarc, M., Levy, M., and Milkcovich, R., J. Am. Chem. Soc., 78, 2656 (1956).

23. Morton, M., in Reference 19, p. 1.

24. Janes, W. H., in Reference 18, p. 62.

25. Matzner, M., Robeson, L. M., Noshay, A., and McGrath, J. E., Encyclo. Polym. Sci. Technol. Supplement No. 2, p. 129, John Wiley and Sons, Inc., New York (1977).

26. Finaz, G., Gallot, Y., Parrod, J., and Rempp, P., J. Polym. Sci., 58, 1363 (1962).

27. Kato, K., Polym. Eng. Sci., 7, 38 (1967).

28. McIntyre, D. and Campos-Lopez, E., in Reference 19, p. 19.

29. Aggarwal, S. L., Polymer, 17, 938 (1976).

30. Zelinski, R. and Childers, C. W., Rubber Chem. Technol., 41, 161 (1968).

31. Milkovich, R. (to Shell Oil Co.), S. African Pat. 280,712 (1963).

32. Angelo, R. J., Ikeda, R. M., and Wallach, M. L., Am. Chem. Soc., Div. Org. Coat. Plast. Chem., Preprints, 34, 315 (1974).

33. Rosen, S. L., "Fundamental Principles of Polymeric Materials for Practicing Engineers," Barnes and Noble, Inc., New York (1971).

34. Kraus, G., Naylor, F. E., and Rollman, K. W., J. Polym. Sci., Part A-2, 9, 1839 (1971).

35. Arnold, K. R. and Meier, D. J., J. Appl. Polym. Sci., 14, 427 (1970).

36. Scott, R. L., J. Chem. Phys., 17, 279 (1949).

37. Flory, P. J., J. Chem. Phys., 10, 51 (1942).

38. Hildebrand, J. H. and Scott, R. L., "The Solubility of Nonelectrolytes," Reinhold, New York (1950).

39. Scott, R. L. and Magat, M., J. Polym. Sci., 4, 555 (1949).

40. Huglin, M. B. and Pass, D. J., J. Appl. Polym. Sci., 12, 473 (1968).

41. Small, P. A., J. Appl. Chem., 3, 71 (1953).

42. Hansen, C. M., J. Paint Technol., 39, 104 (1967).

43. Crowley, J. D., Teague, G. S., and Lowe, J. W., J. Paint Technol., 38, 269 (1966).

44. Shaw, M. T., J. Appl. Polym. Sci., 18, 449 (1974).

45. Flory, P. J., Orwoll, R. A., and Vrij, A., J. Amer. Chem. Soc., 86, 3515 (1964).

46. Flory, P. J., J. Amer. Chem. Soc., 87, 1833 (1965).

47. McMaster, L. P., Macromolecules, 6, 760 (1973).

48. McMaster, L. P. and Olabisi, O., Coat. Plast. Prep., 35, 322 (1975).

49. Olabisi, O., Macromolecules, 9, 316 (1975).

50. Paul, D. R. and Altamirano, J. O., in Reference 3, p. 371.

51. Wahrmund, D. C., Bernstein, R. E., Barlow, J. W., and Paul, D. R., Polym. Eng. Sci., 18, 677 (1978).

52. Bernstein, R. E., Paul, D. R., and Barlow, J. W., Polym. Eng. Sci., 18, 683 (1978).

53. Rowlinson, J. S., "Liquids and Liquid Mixtures," Academic, New York (1967).

54. Meier, D. J., J. Polym. Sci., Part C, 26, 81 (1969).

55. Meier, D. J., Polym. Preprints, 11, 400 (1970).

56. Meier, D. J., Polym. Preprints, 15, 171 (1974).

57. Krause, S., Macromolecules, 3, 84 (1970).

58. Krause, S., J. Polym. Sci., Part A-2, 7, 249 (1969).

59. Krause, S., in Reference 20, p. 143.

60. Leary, D. F. and Williams, M. C., Polym. Lett., 8, 335 (1970).

61. Leary, D. F. and Williams, M. C., J. Poly. Sci.: Polym. Phys. Ed., 11, 345 (1973).

62. Leary, D. F. and Williams, M. C., J. Polym. Sci.: Polym. Phys. Ed., 12, 265 (1974).

63. Helfand, E., in Reference 1, p. 141.

64. Helfand, E., Macromolecules, 8, 553 (1975).

65. LeGrand, D. G., Polym. Lett., 8, 195 (1970).

66. LeGrand, D. G., Polym. Prep., 11, 434 (1970).

67. Inoue, T., Soen, T., Hashimoto, T., and Kawai, H., J. Polym. Sci.: Part A-2, 7, 1283 (1969).

68. Inoue, T., et al., Macromolecules, 3, 87 (1970).

69. Soen, T., Inoue, T., Miyoshi, K., and Kawai, H., J. Polym. Sci.: Part A-2, 10, 101 (1972).

70. Uchida, T., Soen, T., Inoue, T., and Kawai, H., J. Polym. Sci.: Part A-2, 10, 1757 (1972).

71. Baer, M., J. Polym. Sci.: Part A, 2, 417 (1964).

72. Robeson, L. M., Matzner, M., Fetters, L. J., and McGrath, J. E., in Reference 1, p. 281.

73. Krause, S. and Dunn, D. J., Polym. Lett., 12, 591 (1974).

74. Krause, S., Dunn, D. J., Seyed-Mozzaffari, A., and Biswas, A. M., Macromolecules, 10, 786 (1977).

75. Beevers, R. B., Trans. Faraday Soc., 58, 1465 (1962).

76. Rempp, P., Polym. Preprints, 7, 141 (1966).

77. Tanaka, T., Kotaka, T., and Inagaki, H., Polym. J., 3, 338 (1972).

78. Kotaka, T., Tanaka, T., and Inagaki, H., Polym. J., 3, 327 (1972).

79. Kotaka, T., Ohnuma, H., and Inagaki, H., Polym. Preprints, 11, 660 (1970).

80. Dondos, A., Rempp, P., and Benoit, H. C., Polymer, 16, 97 (1972).

81. Hsiue, G., Yasukawa, T., and Murakami, K., Die Makromol. Chemie, 139, 285 (1970).

82. Perry, E., J. Appl. Polym. Sci., 8, 2605 (1964).

83. Bennet, J. G. and Cooper, G. D., Macromolecules, 3, 101 (1970).

84. Hay, A. S., J. Amer. Chem. Soc., 81, 6335 (1959).

85. Johnson, R. N., Farnham, A. G., Clendinning, R. A., Hale, W. F., and Merriam, C. N., J. Polym. Sci.: Part A-1, 5, 2375 (1967).

86. Rose, J. B., Polymer, 15, 456 (1974).

87. Jennings, B. E., Jones, M.E.B., and Rose, J. B., J. Polym. Sci.: Part C, 16, 17 (1967).

88. Robeson, L. M., Farnham, A. G., and McGrath, J. E., Appl. Polym. Symp., 26, 373 (1975).

89. Ivin, K. J. and Rose, J. B., in "Advances in Macromolecular Chemistry," W. M. Paiska, Ed., Academic Press, New York (1968), Vol. 7, p. 336.

90. Cohen, S. M. and Young, R. H., J. Polym. Sci.: Part A-1, 4, 722 (1966).

91. Cudby, M.E.A., Feasey, R. G., Jennings, B. E., Jones, M.E.B., and Rose, J. B., Polymer, 6, 589 (1965).

92. Hale, W. F., Farnham, A. G., Johnson, R. N., and Clendinning, R. A., J. Polym. Sci.: Part A-1, 5, 2399 (1967).

93. MacNulty, B. J., J. Polym. Sci.: Part A-1, 7, 3038 (1969).

94. McGrath, J. E., personal communication (1979).

95. Kambour, R. P., Romagosa, E. E., and Gruner, C. L., Macromolecules, 5, 335 (1972).

96. Baccaredda, M., Butta, E., Frosini, V., and De Petris, S., J. Polym. Sci.: Part A-2, 5, 1296 (1967).

97. Kurz, J. E., Woodbrey, J. C., and Ohta, M., J. Polym. Sci.: Part A-2, 8, 1175 (1970).

98. Chung, C. I. and Sauer, J. A., J. Polym. Sci.: Part A-2, 9, 1097 (1971).

99. Robeson, L. M. and Faucher, J. A., Polym. Lett., 7, 35 (1969).

100. Robeson, L. M., Polym. Eng. Sci., 9, 277 (1969).

101. Anon., Modern Plastics, 42, 87 (1965).

102. Lannon, D. A., in "Encyclopedia of Polymer Science and Technology," Vol. 7, Interscience, New York (1967), p. 620.

103. Mills, N. J., Neuin, A., and McAinsh, J., J. Macromol. Sci. - Phys., B4, 863 (1970).

104. Shaw, M. T., Polym. Eng. Sci., 18, 359 (1978).

105. Cogswell, F. N. and McGowan, J. C., Brit. Polym. J., 4, 183 (1972).

106. McGrath, J. E., Matzner, M., Robeson, L. M., and Barclay, R., J. Polym. Sci.: Polym. Symp., 60, 29 (1977).

107. McGrath, J. E., Robeson, L. M., and Matzner, M., in Reference 1, p. 195.

108. Noshay, A., Matzner, M., Merriam, C. N., J. Polym. Sci.: Part A-1, 9, 3147 (1971).

109. Noshay, A., Matzner, M., Barth, B. P., Walton, R. K., in "Toughness and Brittleness of Plastics," R. D. Deanin and A. M. Crugnola, Eds., Advances in Chemistry Series No. 154, Am. Chem. Soc., Wash. D.C. (1976), p. 302.

110. Robeson, L. M., Noshay, A., Matzner, M. and Merriam, C. N., Die Angew. Makromol. Chemie, 29/30, 47 (1973).

111. Kawakami, J., Kwiatkowski, G. T., Brode, G. L., and Bedwin, A. W., J. Polym. Sci.: Polym. Chem. Ed., 12, 565 (1974).

112. Kwiatkowski, G. T., Brode, G. L., Kawakami, J., and Bedwin, A. W., J. Polym. Sci.: Polym. Chem. Ed., 12, 589 (1974).

113. Schnell, H., Angew. Chem., 68, 633 (1956).

114. Schnell, H., "Chemistry and Physics of Polycarbonates," Interscience, New York (1964), p. 32.

115. Saunders, K. J., Ibid, p. 240.

116. Saunders, K. J., Ibid, p. 240.

117. Kazanjian, A. R., Polymer-Plastics Technol. Eng., 2, 123 (1973).

118. Bottenbruch, L., in "Encyclopedia of Polymer Science and Technology," Vol. 10, Interscience, New York (1969), p. 710.

119. Kunze, R. J., Metal Progr., 99, Aug. (1963).

120. Frank, W., Goddar, H., Stuart, H. A., Polym. Lett., 5, 711 (1967).

121. Siegman, A. and Geil, P. H., J. Macromol. Sci.-Phys., B4, 273 (1970).

122. Morgan, R. J. and O'Neal, J. E., J. Polym. Sci.: Polym. Phys. Ed., 1053 (1976).

123. Saunders, K. J., Ibid, p. 243.

124. Carr, S. H., Geil, P. H., and Baer, E., J. Macromol. Sci.-Phys., B2, 13 (1968).

125. MacNulty, B. J., Polymer, 9, 41 (1968).

126. Mercier, J. P., Groeninckx, G., and Lesne, M., J. Polym. Sci.: Part C, 16, 2059 (1967).

127. Gallez, F., Legras, R., and Mecier, J. P., Polym. Eng. Sci., 16, 276 (1976).

128. Kambour, R. P., Gruner, C. L., and Romagosa, E. E., Macromolecules, 7, 248 (1974).

129. Kambour, R. P., Polymer, 5, 143 (1964).

130. Miltz, J. D., Benedetto, A. T., and Petrie, S., J. Mats. Sci., 13, 2037 (1978).

131. Schnell, H., "Chemistry and Physics of Polycarbonates," Ibid, p. 128.

132. Peilstöcker, G., Kunstoffe, 51, 509 (1961).

133. Sacher, E., J. Macromol. Sci.-Phys., B10, 319 (1974).

134. Sacher, E., J. Macromol. Sci.-Phys., B11, 403 (1975).

135. Allen, G., Morley, D.C.W., and Williams, T., J. Mats. Sci., 8, 1449 (1973).

136. Watts, D. C. and Perry, E. P., Polymer, 19, 248 (1978).

137. Baumann, G. F. and Steingeiser, S., J. Polym. Sci.: Part A-1, 3395 (1963).

138. Merrill, S. H., J. Polym. Sci., 55, 343 (1961).

139. Berger, M. N., Boulton, J. K., and Brooks, B. W., J. Polym. Sci.: Part A-1, 7, 1339 (1969).

140. Goldberg, E. P., J. Polym. Sci.: Part C, No. 4, 707 (1964).

141. Vaughn, H. A., Polym. Lett., 7, 569 (1969).

142. Kambour, R. P., Polym. Lett., 7, 573 (1969).

143. Kambour, R. P., Polym. Preprints, 10, 885 (1969).

144. Beach, B. M., Kambour, R. P., Shultz, A. R., Polym. Lett., 12, 247 (1974).

145. Kambour, R. P., et al., in "Toughness and Brittleness of Plastics," Reference 109, p. 312.

146. Kambour, R. P., in Reference 19, p. 263.

147. Magila, T. L. and Le Grand, D. G., Polym. Eng. Sci., 10, 349 (1970).

148. LeGrand, D. G., Polym. Lett., 9, 145 (1971).

149. Union Carbide Corp., Neth. Appl. 6,604,731, Oct. 10 (1966). Chem. Abs. 66:95785j (1967).

150. Myers, F. S., Brittain, J. O., J. Appl. Polym. Sci., 17, 2715 (1973).

151. Owada, Y., Tsunemori, I., and Kinoshita, Y., to Kanegafuchi Chemical Industry Co., Ltd., Japan Kokai 75 59,472, May 22 (1975). Chem. Abs. 83:132687c (1975).

152. Itinskaya, G. P., et al., Plast. Massy, 11,59 (1975). Chem. Abs. 84:74939u (1976).

153. Binsack, R., Reese, E., and Wank, J., to Bayer A. G., Ger. Offen. 2,735,144, Feb. 15 (1979). Chem. Abs. 90:153065h (1979).

154. Burns, H., in "Encyclopedia of Polymer Science and Technology," Vol. 7, Interscience, New York (1967), p. 584.

155. Ward, I. M., "Mechanical Properties of Solid Polymers," John Wiley and Sons, Ltd., London (1971), p. 352.

156. Telfair, D. and Nason, H. K., Mod. Plast., 20, 85 (1943).

157. Ives, G. C., Mead, J. A., and Riley, M. M., "Handbook of Plastics Test Methods", Iliffe Books, London (1971).

158. Ritchie, P. D., "Physics of Plastics," Chapter 3, Iliffe Books, Ltd., London (1965).

159. Therberge, J. E. and Hall, N. T., Mod. Plast., 46, 114 (1969).

160. Cann, J. M., Brit. Plast., 36, 517 (1963).

161. Moritz, W. J., Mod. Plast., , 60 (1975).

162. Wolstenholme, W. E., J. Appl. Polym. Sci., 6, 332 (1962).

163. Wolstenholme, W. E., Pregun, S. E., and Stark, C. F., J. Appl. Polym. Sci., 8, 119 (1964).

164. Arends, C. B., J. Appl. Polym. Sci., 9, 3531 (1965).

165. Lubert, W., Rink, M., and Pauan, A., J. Appl. Polym. Sci., 20, 1107 (1976).

166. Rink, M., Ricco, T., Lubert, W., and Pauan, A., J. Appl. Polym. Sci., 22, 429 (1978).

167. Radon, J. C. and Turner, C. E., Eng. Fract. Mech., 1, 411 (1969).

168. Radon, J. C., Coll. Polym. Sci., 252, 117 (1974).

169. Radon, J. C., J. Appl. Polym. Sci., 22, 1569 (1978).

170. Fujioka, K., J. Appl. Polym. Sci., 13, 1421 (1969).

171. Cessna, L. C., Lehane, J. P., Ralston, R. H., and Prindle, T., Polym. Eng. Sci., 16, 419 (1976).

172. Gonzalez, H. and Stowell, W. J., J. Appl. Polym. Sci., 20, 1389 (1976).

173. Ward, T. C., Wnuk, A. J., Shchori, E., Viswanathan, R., and McGrath, J. E., in Reference 5, p. 293.

174. Wnuk, A. J., Davidson, T. F., and McGrath, J. E., J. Appl. Polym. Sci.: Appl. Polym. Symp., 34, 89 (1978).

175. Kucharsky, J. and Safarik, L., "Titrations in Nonaqueous Solvents," Elsevier Publishing Company, Amsterdam (1965).

176. Huber, W., "Titrations in Nonaqueous Solvents," Academic Press, New York (1967).

177. Gyenes, I., "Titrations in Nonaqueous Media," Van Nostrand Co., Inc., Princeton, New Jersey (1967).

178. Fritz, J. S., "Acid-Base Titrations in Nonaqueous Solvents," Allyn and Bacon, Inc., Boston (1973).

179. Moss, M. L., Elliot, J. H., and Hall, R. T., Anal. Chem., 20(8), 784 (1948).

180. Deal, V. Z. and Wyld, G.E.A., Anal. Chem., 27, 47 (1955).

181. Cundiff, R. H. and Markunas, P. C., Anal. Chem., 28(5), 792 (1956).

182. Price, G. C. and Whiting, M. C., Chem. and Ind., 19, 775 (1963).

183. Fritz, J. S. and Yamamura, S. S., Anal. Chem., 29(7), 1079 (1957).

184. Harlow, G. A., Noble, C. M., and Wyld, G. E., Anal. Chem., 28(5), 787 (1956).

185. Bruss, D. B. and Wyld, G.E.A., Anal. Chem., 29(2), 232 (1957).

186. Garmon, R. G., in "Polymer Molecular Weights, Part I", P. E. Slade, Ed., Marcel Dekker, Inc., New York, 1975, p. 31.

187. Shchori, E. and McGrath, J. E., J. Appl. Polym. Sci.: Appl. Polym. Symp., 34, 103 (1978).

188. Flory, P. J., "Principles of Polymer Chemistry," Cornell University Press, London (1953), pp. 269-73.

189. Flory, P. J., Ibid, pp. 610-612.

190. Dawkins, J. V., Maddock, J. W., and Neuin, A., Europ. Polym. J., 9, 327 (1973).

191. DSC-2 Operator's Manual, Perkin-Elmer Corp., Norwalk, Conn.

192. Koo, G. P., Plast. Eng., 30, 33 (1974).

193. Weissenberg, K., Proc. 1st Internat. Congr. Rheol., North Holland Public., 1949, p. 114.

194. "Piezo electric Accelerometer and Vibration Handbook," Bruel and Kjaer Instruments, Inc., Cleveland, Ohio (1976).

195. Collins, E. A., Bares, J., and Billmeyer, F. W., "Experiments in Polymer Science," John Wiley and Sons, New York (1973).

196. Fox, T. G., Bull. Amer. Phys. Soc., 2, 123 (1956).

197. Krause, S. and Iskandar, M., in Reference 5, p. 205.

198. "Modern Plastics Encyclopedia," Vol. 53, McGraw Hill, Inc., New York (1976).

199. Miyamoto, T., Kodama, K., and Shibayama, K., J. Poly. Sci.: Part A-2, 8, 2095 (1970).

200. Takayanagi, M., Harima, H., and Iwata, I., Mems. Fac. Eng., Kyushu Univ., 23, 1 (1963).

201. McGrath, J. E., Dwight, D. W., Riffle, J. S., Webster, D. C., and Davidson, T. F., Polym. Preprints, 20, 528 (1979).

The vita has been removed from the scanned document

Engineering Properties of Multiphase
Block Copolymers

by

Andrew J. Wnuk

(ABSTRACT)

Multiblock $\{A\text{-}B\}_n$ copolymers of bisphenol-A polycarbonate (I) and several poly(arylether sulfones) (II) have been investigated. The copolymers

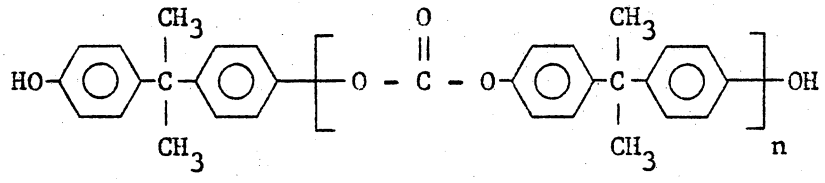

I

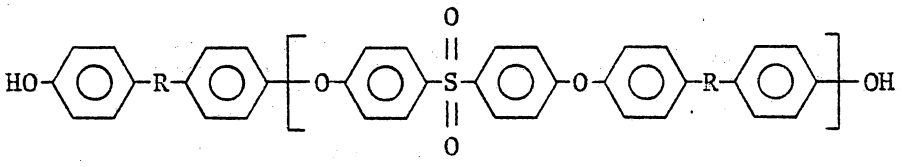

II

were prepared from hydroxyl terminated oligomers ($4{,}000 < \bar{M}_n < 30{,}000$) by an interfacial technique which utilized phosgene as the coupling agent. Characterization of the oligomers and copolymers included end

group analysis, membrane osmometry, and gel permeation chromatography.

One of the most interesting aspects of block copolymers is their ability to undergo microphase separation above a critical block length. Either one or two phase block copolymers can be prepared by controlling the molecular weights of the parent oligomers. In the bisphenol-A polycarbonate/bisphenol-A polysulfone system, for example, strictly one phase materials, with only one intermediate glass transition temperature, were obtained at block lengths of less than 10,000 g/mole. Two-phase copolymers resulted when blocks exceeding 20,000 g/mole were coupled. Copolymers comprised of intermediately sized blocks ($\bar{M}_n \cong 16{,}000$) could be obtained as either single or multiphase systems depending upon their previous thermal history. Homogeneous films, with a single intermediate Tg, were obtained via solution casting, whereas compression molding provided films exhibiting two Tg's. Subsequent DSC studies pointed out that microphase separation could be thermally, and irreversibly, induced by annealing above the Tg of the polysulfone blocks (190°C).

Since polycarbonate and polysulfone are leading examples of tough, amorphous thermoplastics, the effects of microphase separation on the tensile, impact, and melt flow properties of the copolymers were investigated. A novel falling weight impact tester was designed and constructed to meet the needs of this study. The device was fully instrumented to provide a deceleration-time plot of the impact process by means of an accelerometer mounted in the projectile. Fracture energies for commercial homopolymers and graphite reinforced composites, in

addition to polysulfone-polycarbonate block copolymers, were calculated from the impact curves.

Both the tensile and impact properties of the copolymers improved with increasing polycarbonate content. Both single and multiphase materials were ductile and transparent as opposed to physical blends of the two oligomers which were opaque and possessed poor mechanical properties. No differences due to microphase separation were observed in either the tensile or impact studies.

The homogeneous copolymers displayed melt viscosities and activation energies nearly equal to those of the homopolymers. Much greater viscosities and activation energies were exhibited by the phase separated materials indicating that the heterogeneity was retained in the melt.